BKM/F-632

TACOM REPORT NO. 13603

ADA279176

Advanced Diesel Electronic Fuel Injection and Turbocharging

N. John Beck

Robert Barkhimer

David Steinmeyer

John Kelly

BKM Inc.

December 1993

Contract DAAE07-90-C-R030

Prepared for

UNITED STATES ARMY
TANK - AUTOMOTIVE COMMAND
Warren, MI 48397-5000

DISCLAIMER NOTICE

THIS DOCUMENT IS BEST QUALITY AVAILABLE. THE COPY FURNISHED TO DTIC CONTAINED A SIGNIFICANT NUMBER OF COLOR PAGES WHICH DO NOT REPRODUCE LEGIBLY ON BLACK AND WHITE MICROFICHE.

REPORT DOCUMENTATION PAGE

Form Approved
OMB No. 0704-0188

1. AGENCY USE ONLY (*Leave blank*)

2. REPORT DATE
Dec. 1993

3. REPORT TYPE AND DATES COVERED
FINAL - JULY 1990 - DEC. 1993

4. TITLE AND SUBTITLE
Advanced Diesel Electronic Fuel Injection and Turbocharging

5. FUNDING NUMBERS
DAAE07-90-C-R030

6. AUTHOR(S)
N.J. Beck, R.L. Barkhimer, D.C. Steinmeyer, and J.E. Kelly

7. PERFORMING ORGANIZATION NAME(S) AND ADDRESS(ES)
BKM, Inc.
5141 Santa Fe Street
San Diego, CA 92109

8. PERFORMING ORGANIZATION REPORT NUMBER
F-632

9. SPONSORING/MONITORING AGENCY NAME(S) AND ADDRESS(ES)
US-Army Tank and Automotive Command
Warren, MI 48397-5000

10. SPONSORING/MONITORING AGENCY REPORT NUMBER
13603

11. SUPPLEMENTARY NOTES

12a. DISTRIBUTION/AVAILABILITY STATEMENT
Approved for public release
Distribution unlimited

12b. DISTRIBUTION CODE

13. ABSTRACT (*Maximum 200 words*)

The program investigated advanced diesel air charging and fuel injection systems to improve specific power, fuel economy, noise, exhaust emissions, and cold startability. The techniques explored included variable fuel injection rate shaping, variable injection timing, full-authority electronic engine control, turbo-compound cooling, regenerative air circulation as a cold start aid, and variable geometry turbocharging.

A Servojet electronic fuel injection system was designed and manufactured for the Cummins VTA-903 engine. A special Servojet twin turbocharger exhaust system was also installed.

A series of high speed combustion flame photos was taken using the single cylinder optical engine at Michigan Technological University. Various fuel injection rate shapes and nozzle configurations were evaluated. Single-cylinder bench tests were performed to evaluate regenerative inlet air heating techniques as an aid to cold starting.

An exhaust-driven axial cooling air fan was manufactured and tested on the VTA-903 engine.

14. SUBJECT TERMS
Electronic fuel injection, turbocharging, diesel combustion, cold starting, flame photography

15. NUMBER OF PAGES
226

16. PRICE CODE

17. SECURITY CLASSIFICATION OF REPORT	18. SECURITY CLASSIFICATION OF THIS PAGE	19. SECURITY CLASSIFICATION OF ABSTRACT	20. LIMITATION OF ABSTRACT
Unclassified	Unclassified	Unclassified	Unlimited

NSN 7540-01-280-5500

Standard Form 298 (Rev 2-89)
Prescribed by ANSI Std Z39-18
298-102

NOTICES

This report is not to be construed as an official Department of the Army position.

Mention of any trade names or manufacturers in this report shall not be construed as an official endorsement or approval of such products or companies by the U.S. Government.

Destroy this report when it is no longer needed. Do not return it to the originator.

Contents

List of Figures and Tables

Appendixes

Attachments

Video Tape: *VHS format tape of flame photographs described in Appendix F.*

1.0 Summary

This program has investigated advanced diesel air charging and fuel injection to improve specific power, fuel economy, exhaust emissions, and cold startability. The techniques explored include variable fuel injection rate shaping, turbo-compound cooling, regenerative recirculating cold start, variable injection timing, variable geometry turbocharging, and full-authority electronic engine control.

A Servojet electronic fuel injection system was designed and manufactured for the Cummins VTA-903 engine. This system consists of the unit injectors, fuel manifolds, electronic pressure regulator, high pressure fuel pump, electronic control unit, wiring harness, and engine sensors. Injector nozzle breakage and leakage problems were solved during bench tests. The performance and reliability of the electronic control unit and high pressure fuel pump were successfully demonstrated. Engine control and calibration software was written. This software was shown to be a powerful development tool.

In addition, Servojet twin turbochargers and a high efficiency exhaust system were installed. This system reduced the throttle response time in half compared to the stock single turbocharger.

A series of high speed combustion flame photos was taken using the single cylinder optical engine at Michigan Technological University. Various pre injection rate shapes and nozzle configurations were evaluated. The 8 hole x .006 In. diameter nozzle with pre injection demonstrated the best overall result. During several tests, there was visual evidence that cylinder wall wetting caused high smoke readings. Note that subsequent combustion system optimization work by a major diesel engine manufacturer (to compliment the spray characteristics of the Servojet fuel system) has resulted in drastic smoke reduction.

Single-cylinder bench tests were performed to evaluate regenerative inlet air heating techniques as an aid to cold starting. An inlet manifold air temperature rise of 42 degrees C above ambient was demonstrated during cranking.

An exhaust-driven axial cooling air fan was designed and a test prototype manufactured. Preliminary performance tests were conducted using the VTA-903. Fan airflow and efficiency were less than predicted and

matching of the prototype fan to the VTA-903 engine was not optimized. Preliminary tests indicate that further analysis of the complete engine and TCS combination should be performed. Improved fan manufacturing techniques and ducting design with reduced flow losses are needed to achieve better efficiency and reliability.

2.0 Introduction. This Small Business Innovation Research (SBIR) project, contract number DAAE07-90-C-R030 was awarded in July of 1990. Amendments were made to the original award/contract in October 1990, May 1991, January 1993, and August 1993.

The program objective, as described in the current contract revision, includes investigation of the practicality of unique combustion control techniques and how they apply to highly flexible and advanced air charging/fuel injection systems to improve specific power, smoke, fuel economy, heat rejection/cooling, noise, emissions, fuel tolerance, and cold startability.

The techniques explored include variable fuel injection rate shaping, turbo-compound cooling, regenerative recirculating cold start, variable injection timing, variable geometry turbocharging, and full-authority electronic engine control.

The engine used to test these various techniques was a Cummins VTA-903 rated at 500 brake horsepower (BHP) at 2600 RPM. The stock engine performance specifications are attached in Appendix D5.. A Servojet electronic fuel injection system was designed and manufactured for this engine. This fuel system was installed along with a special Servojet twin turbocharger exhaust system.

In addition to the VTA-903 performance tests, a series of combustion flame photos was taken using the single cylinder optical engine at Michigan Technological University (MTU). Various fuel injection rate shapes and nozzle configurations were photographed.

Bench tests were performed at BKM using one cylinder of a Perkins 4.236 engine to evaluate regenerative inlet air heating techniques as an aid to cold starting.

3.0 System Hardware Overview. The following sections of this report describe the design and operation of the Servojet system components and detail the test results. Refer to the Fuel Schematic diagram,

Appendix A5, and the Diesel Electronic Control System diagram, Appendix A6. The Servojet fuel injection system consists of the following components.

Fuel Pump - A high pressure (2000 PSI maximum) positive displacement axial piston pump, Servojet model RV-40 provides fuel at up to 2000 PSIG. This pump is sized to provide fuel for injection plus an excess capacity for the volume required for injector pressure intensification. The ratio of bypassed fuel to injected fuel is 24 to 1. This results in a ratio of injection pressure to rail pressure of approximately 16 to 1. Appendix D3 is a technical specification of the RV-40 pump. A pump installation drawing is shown in Appendix C1.

Electronic Pressure Regulator (EPR)- An electronically controlled pilot solenoid valve controls a high volume pressure relief valve that bleeds a portion of the pump output back to the pump supply side to regulate the fuel rail pressure at the injectors - thereby controlling fuel delivery to the engine. Refer to the EPR Assembly drawing in Appendix C2 and the *Parts List in* Appendix B6.

Fuel Manifold - The pressure controlled output from the EPR is routed to a manifold assembly that is mounted on the inboard side of each of the two modified valve covers. Excess fuel from the pressure intensifiers is returned from each manifold to the pump inlet. The rocker lever housing (valve cover) is modified to mate with the fuel manifold, sealing the area under each housing. The fuel injector control cartridges mount in the manifolds and high pressure tubes connect each control cartridge to the fuel injectors. The Manifold drawing is in Appendix C3 and the Rocker Lever Housing modifications are shown in Appendix C4.

Fuel Injectors - The Servojet fuel injector assemblies (Appendix C5) are mounted in the cylinder head in the stock mounting holes. The Control Cartridge (Appendix C6), containing the electro-mechanical High Speed Valve (HSV) and pressure intensifier section, is mounted in the fuel manifold. An HSV technical specification is included in Appendix D2.

Electronic Control Unit (ECU) - This microprocessor-based control computer receives inputs from the engine sensors and computes the appropriate injector and EPR control outputs. The ECU is mounted on the engine and cooled by passing low pressure fuel through drilled passages in the die cast ECU enclosure. Appendix D1 contains the ECU technical specification.

Engine Sensors - Crankshaft position, manifold pressure, and rail pressure sensors are engine-mounted. In addition, analog input commands for engine speed, injector timing, rail pressure, and governor mode are provided. Specification sheets for the engine sensors are contained in Appendix D4.

Wiring Harness - A prototype wiring harness interfaces all sensors inputs and solenoid outputs to the ECU. A remote signal breakout box was built to house the command input potentiometers and oscilloscope signal monitoring points. The potentiometers control injection timing, engine speed, rail pressure, and select the governing mode (constant speed or load). Schematic diagrams of the wiring harness and breakout box are included in Appendix A.

4.0 Fuel Injector Design and Calibration

4.1 Fuel Injector Design. The typical Servojet diesel fuel injector (Figure 1) is pressure metered - using an integral intensifier to increase the fuel rail pressure (500-1500 PSI) to the pressure required for injection (22,000 PSI). It is controlled by a 3-way solenoid valve that, when energized, admits fuel to the intensifier which multiplies the pressure of the fuel in the accumulator by the ratio of areas of the primary piston to the intensifier plunger. The bulk modulus of the fuel, contained in the accumulator, is utilized to store the hydraulic energy. Injection is initiated by de-energizing the solenoid valve, venting pressure in the intensifier and creating a pressure imbalance which causes the injector needle valve to lift and the pressurized fuel to discharge through the nozzle orifices. The needle closes when the accumulator pressure has dropped to the point where the needle spring force is greater. Since the fuel quantity per injection is directly related to the accumulator pressure, engine power is governed by regulating the rail pressure with the EPR. (Ref. 1)

Since it was not possible to fit the standard solenoid valve and spool valve into the existing injector mounting space in the VTA-903 cylinder head, a special 2-piece fuel injector was designed. A remote control cartridge, containing the solenoid and spool valves, is located outside the valve cover - mounted in a manifold (Figure 2) that is supplied with fuel by the EPR. Hard lines carry the fuel from the control cartridge, past the engine valve gear, to the injector assembly containing the intensifier, accumulator, rate shaping plate, and nozzle (Figure 3). Some

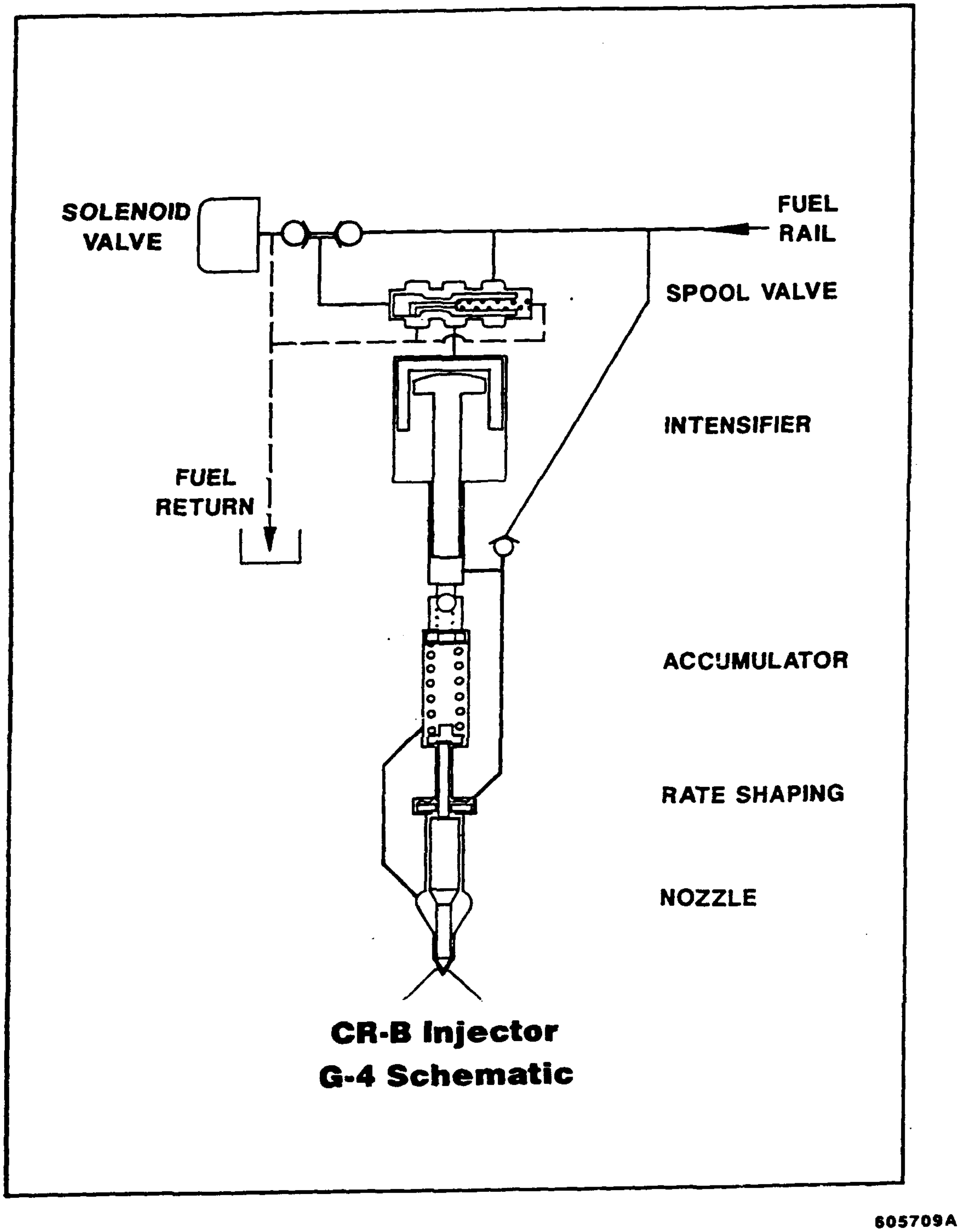

Figure 1 - Servojet CR-B Injector G-4 Schematic

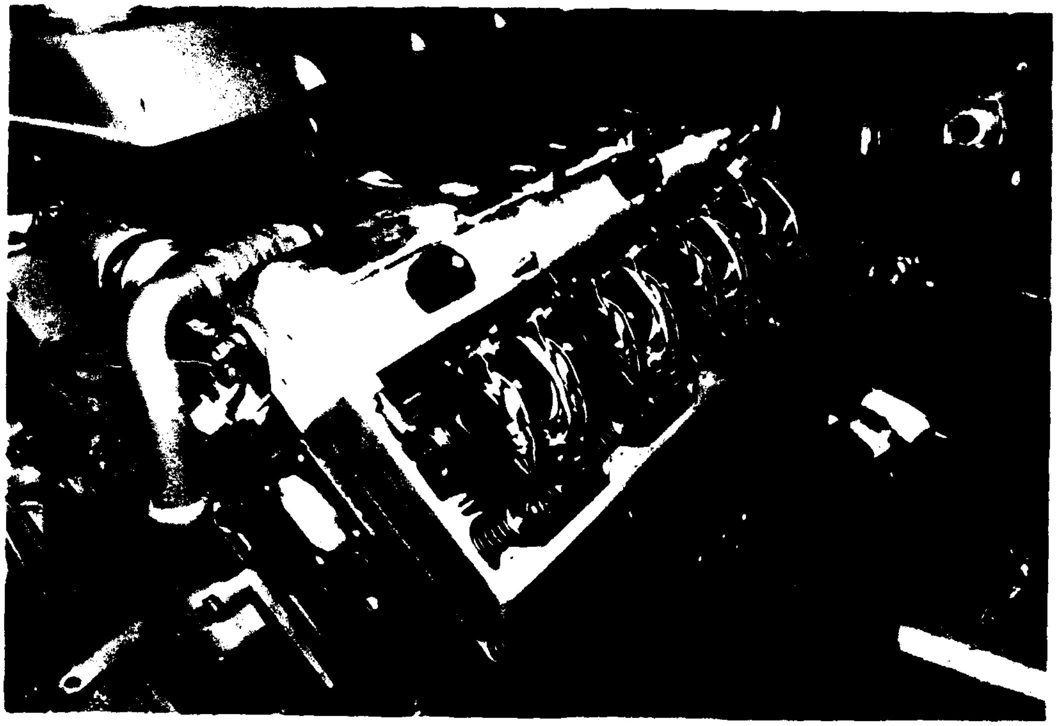

Figure 2 - Fuel Manifold Installation

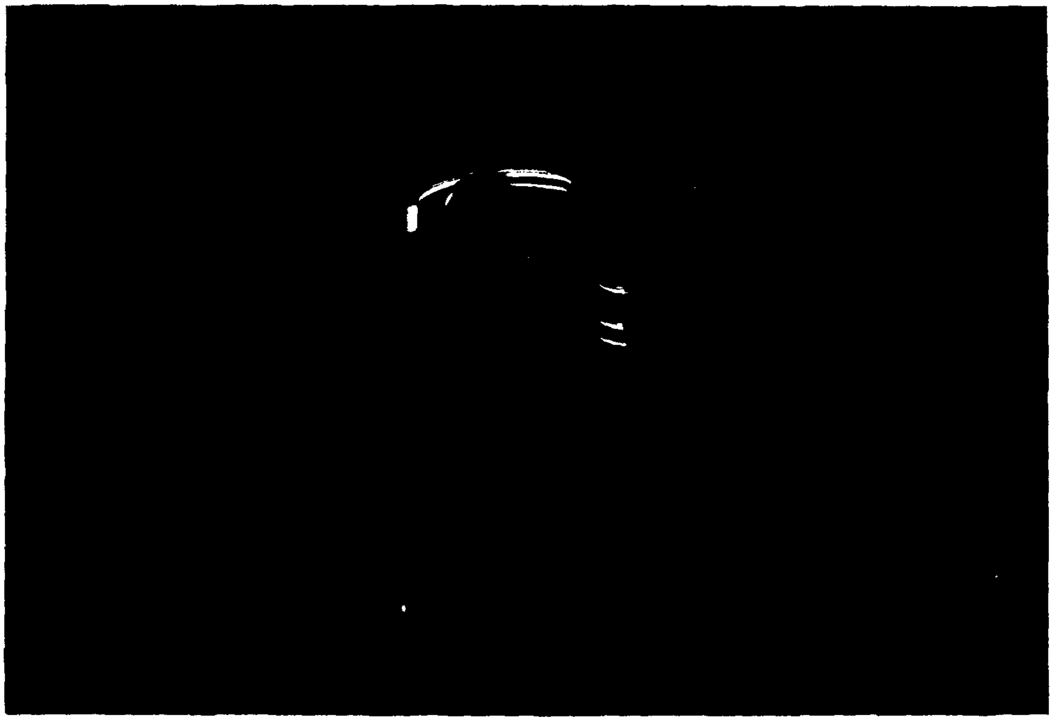

Figure 3 - Fuel Injector

modification to the cylinder head was required to install the injector. The major injector subassemblies are:

Injector Assembly	608400
Tube Assembly	608379
Control Cartridge Assy	608399
Fuel Manifold Assy	610107

A parts list for each of these assemblies is included in Appendix B. Copies of all engineering drawings are contained in Appendix C.

The injector nozzles used for engine testing were fabricated from heat treated 52100 tool steel and contained 8 x .010" diameter holes. A photograph of the combustion chamber, with the nozzle tip installed and wires inserted into the spray holes (to indicate the spray pattern), is shown in Figure 4.

Extensive refinement of the original injector design was done to achieve consistent and reliable operation. This development process is described in section 12.0.

4.2 Injector Calibration. The injectors were calibrated on a test bench to characterize fuel delivery (cubic mm per injection) and delay time (milliseconds between commanded injection and actual start of injection). Both of these key parameters are a function of rail pressure. Figure 5 shows the delivery curve for the 8 injectors. The minimum rail pressure was found to be approximately 500 PSI. Below this pressure, injection consistency is degraded. In order to extend the delivery curve somewhat below this level, additional calibration tests were conducted using reduced solenoid energize times (ET). By reducing the ET, the injector is fired before the accumulator can fully charge to the full rail pressure. However, acceptable injection quality is maintained even though the quantity injected is reduced. This is shown in Figure 6.

Injector delay times as a function of rail pressure and ET are shown in Figures 7 and 8. Note that the variation in delay time from injector to injector is approximately 1 mSec which is too large to be acceptable for a production fuel system. This is due to variation in mechanical characteristics in the prototype unit injectors. Although the system software takes injector delay difference into account, correcting the timing of each cylinder individually, production tolerances still need to be closer than in these prototypes. Subsequent development improvements

Figure 4 - Fuel Injector Spray Pattern

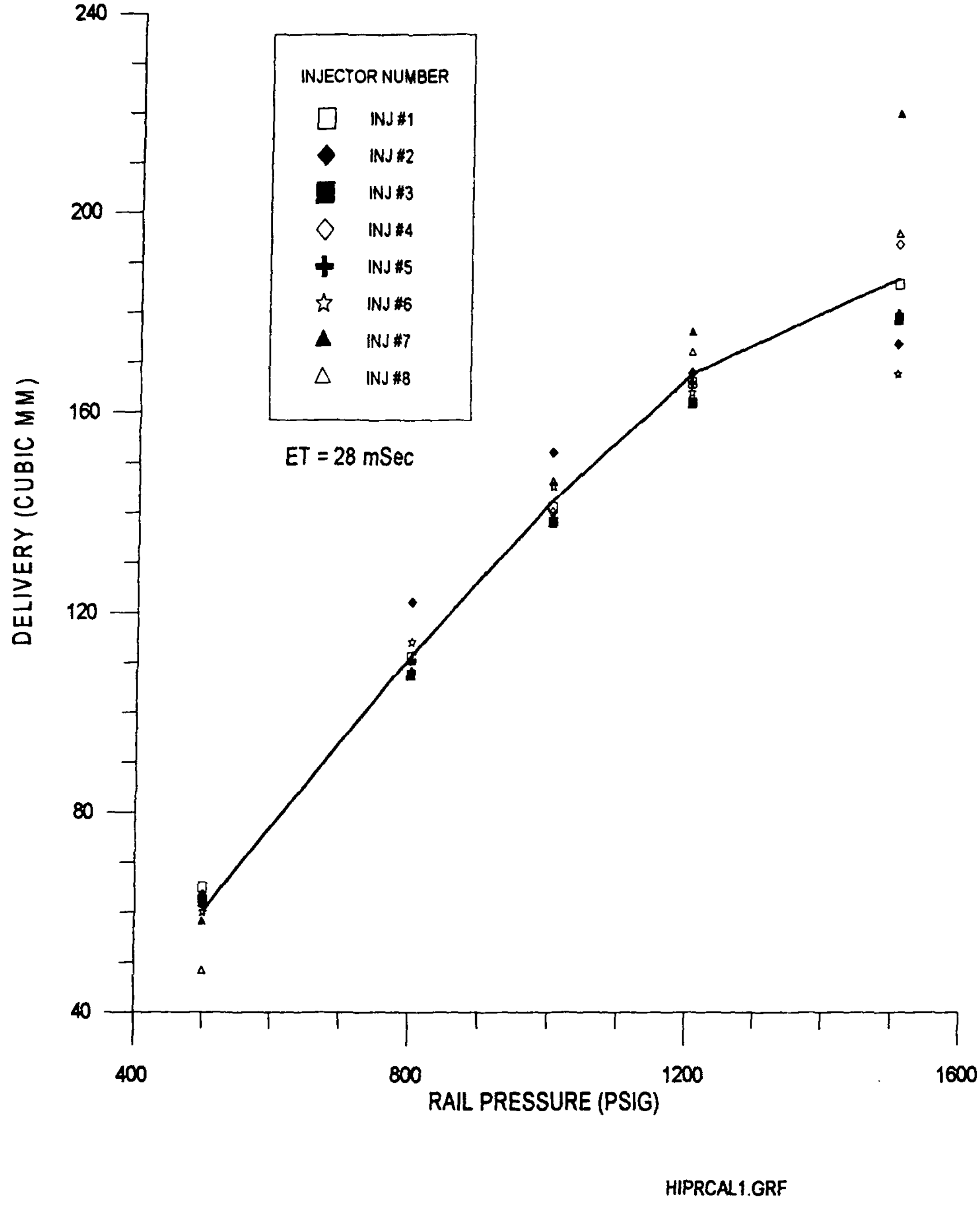

Figure 5 - Fuel Injector Delivery Vs Rail Pressure

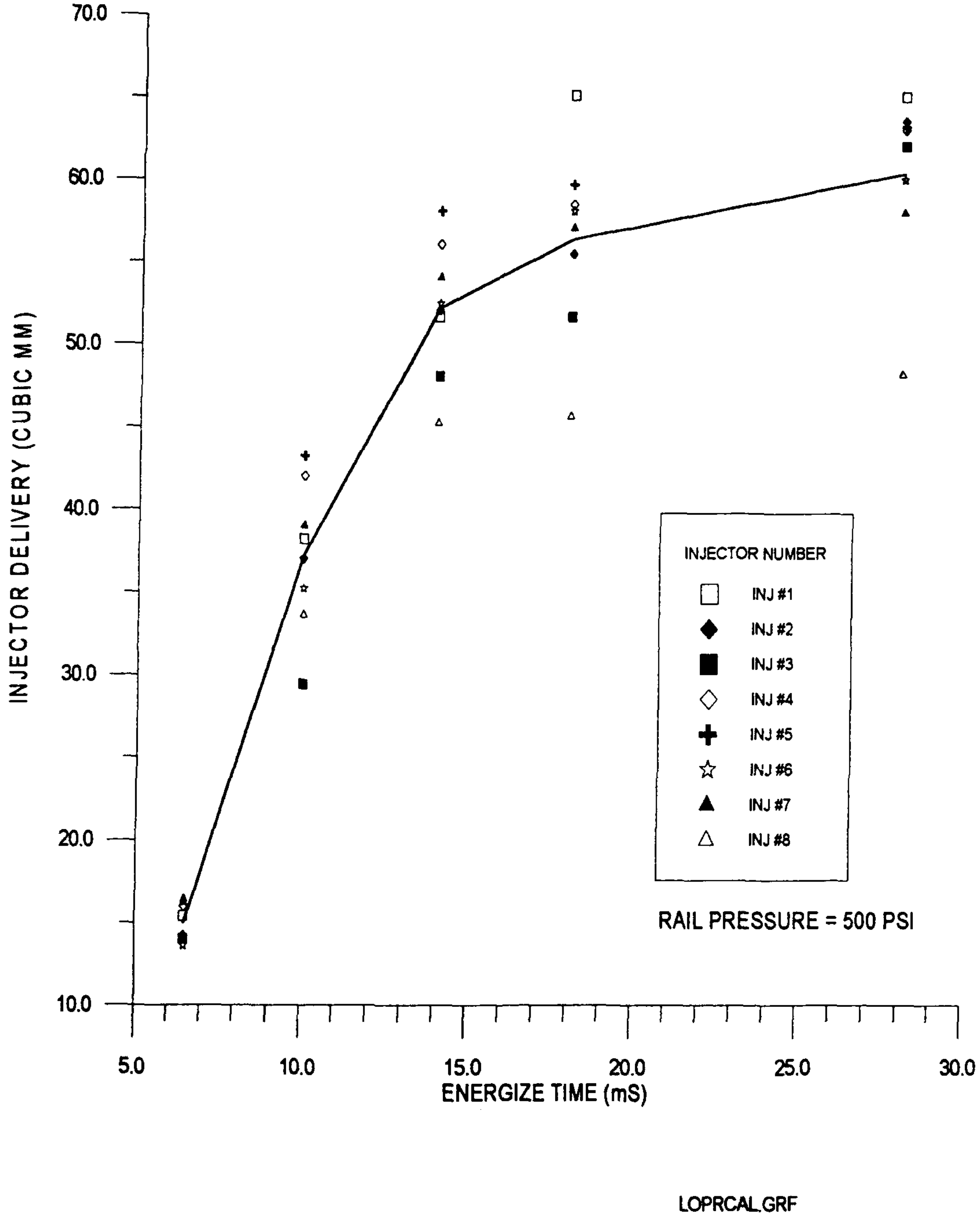

Figure 6 - Fuel Injector Delivery Vs Energize Time

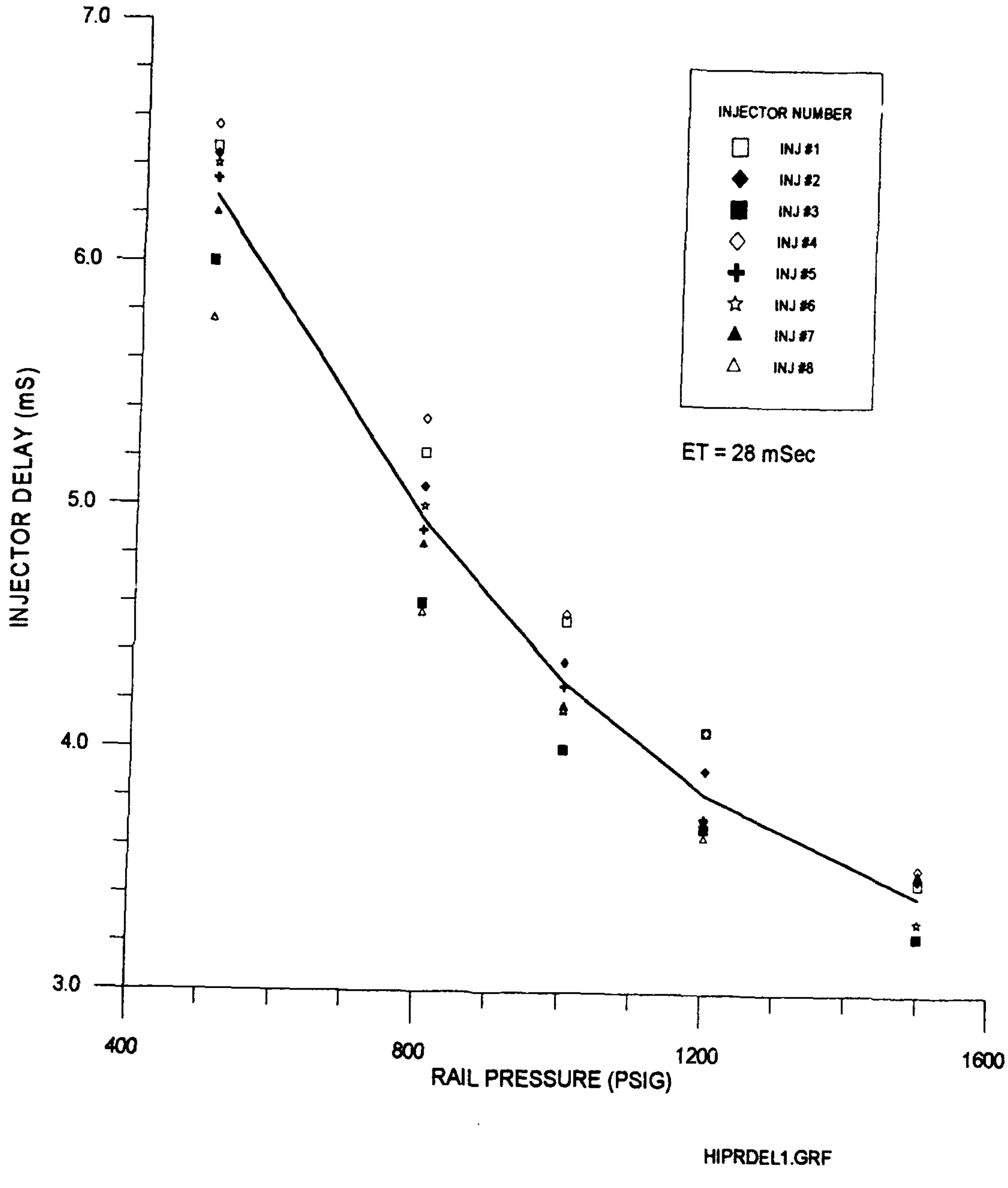

Figure 7 - Fuel Injector Delay Time Vs Rail Pressure

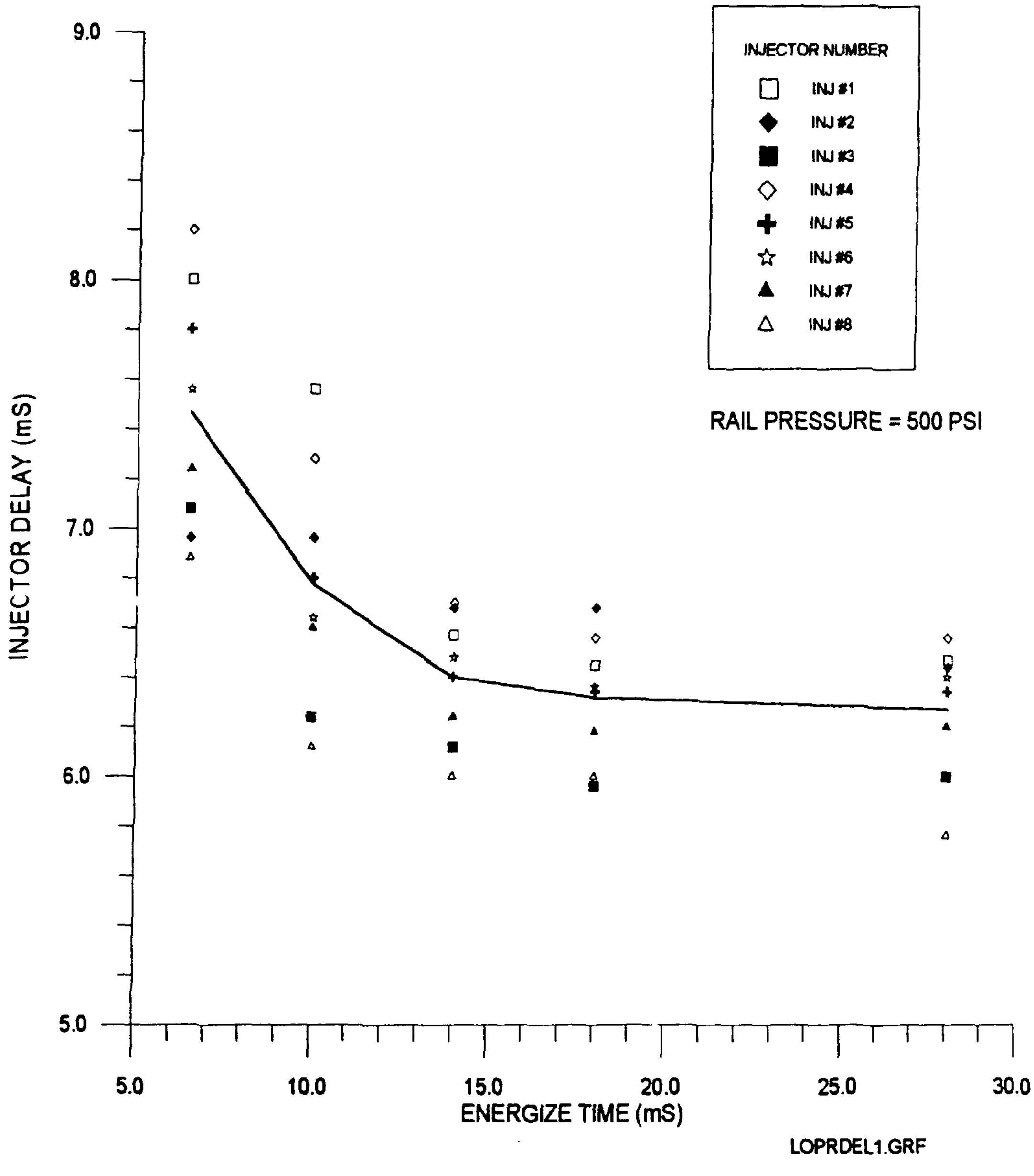

Figure 8 - Fuel Injector Delay Time Vs Energize Time

to the solenoid valve design have alleviated this discrepancy in fuel systems designed for production release.

5.0 Fuel System Design and Installation

5.1 Fuel Pump. The fuel pump selected for the VTA-903 is the Servojet RV-40, part number 608344. This axial piston pump is a standard commercial part designed by BKM and manufactured by Servojet Products International.

5.2 Gearbox. A special gearbox assembly (See Figure 9 and drawing 608212 - Appendix C8) was designed and manufactured to drive the RV-40 pump plus the Hall effect crankshaft position / timing mask.

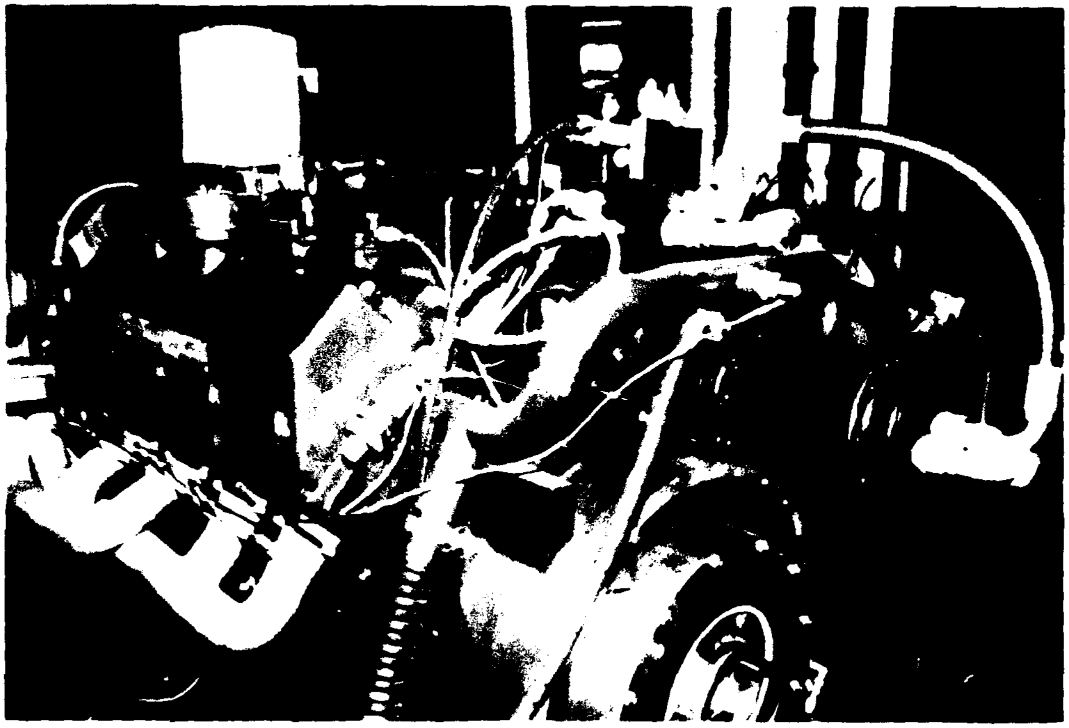

Figure 9 - Fuel Pump Drive and EPR Installation

5.3 EPR. The EPR Assembly (608398 - Appendix C2) and twin fuel manifolds (608353 - Appendix C3) were designed and manufactured for this project. The EPR regulates the fuel rail pressure by bleeding a portion of the RV-40 pump outlet flow. A Servojet Proportional HSV (PHSV) is driven by a pulse width modulated driver in the ECU. This PHSV acts as a pilot to control a high volume pressure relief valve which bleeds the pump outlet as required to maintain the necessary rail pressure. The EPR assembly also contains outlet ports for the rail pressure transducer and a mechanical pressure gauge.

5.4 Fuel Manifold. The fuel manifold, part number 608353 (Appendix C3), distributes the fuel output from the EPR to the individual injector control cartridges and from the cartridges to the injectors. It acts as a mounting structure for the injector control cartridges and helps to seal the modified rocker lever housing.

6.0 Turbocharger and Exhaust System

6.1 Turbocharger Design. The VTA-903 was originally equipped with a single AiResearch turbocharger part number 3032046. This was replaced with twin Servojet WS-90 VAT - Variable Area Turbochargers (Figures 10, 11, & 12) and the corresponding exhaust manifolds (Figure 13). The performance objectives with this exhaust system were to:

1) improve throttle response by reducing turbocharger rotating inertia

2) increase volumetric efficiency by conserving exhaust energy with shorter, more direct entry to the turbos

3) better utilizing exhaust pulse energy by careful pairing of manifold branches

4) evaluate the benefits of a 2-position exhaust diverter valve on the turbocharger inlet. This valve directs exhaust into both inlets or the axial inlet only

The WS-90 VAT has several unique design features that result in high efficiency. These include:

- The exhaust turbine is a combined axial-radial design with high efficiency and increased flow capacity. The axial-radial exhaust housing is cast in two sections. One directs the exhaust gas predominantly in the direction of the turbine axis. The second section directs exhaust gas inward radially toward the outer circumference of the turbine. The split housing permits the exhaust gas to be directed into either or both sections thereby adjusting turbine speed and acceleration characteristics to match engine speed and load.

- The WS turbocharger utilizes a full floating ball bearing which has all of the advantages of the conventional floating bushing, but decreases the mechanical parasitic losses from 4% to 1% with accompanying improvement in acceleration and combined efficiency. The advantages of the floating ball bearing are lower brake specific fuel consumption (BSFC), faster acceleration, lower exhaust emissions, and reduced sensitivity to starting and stopping distress.

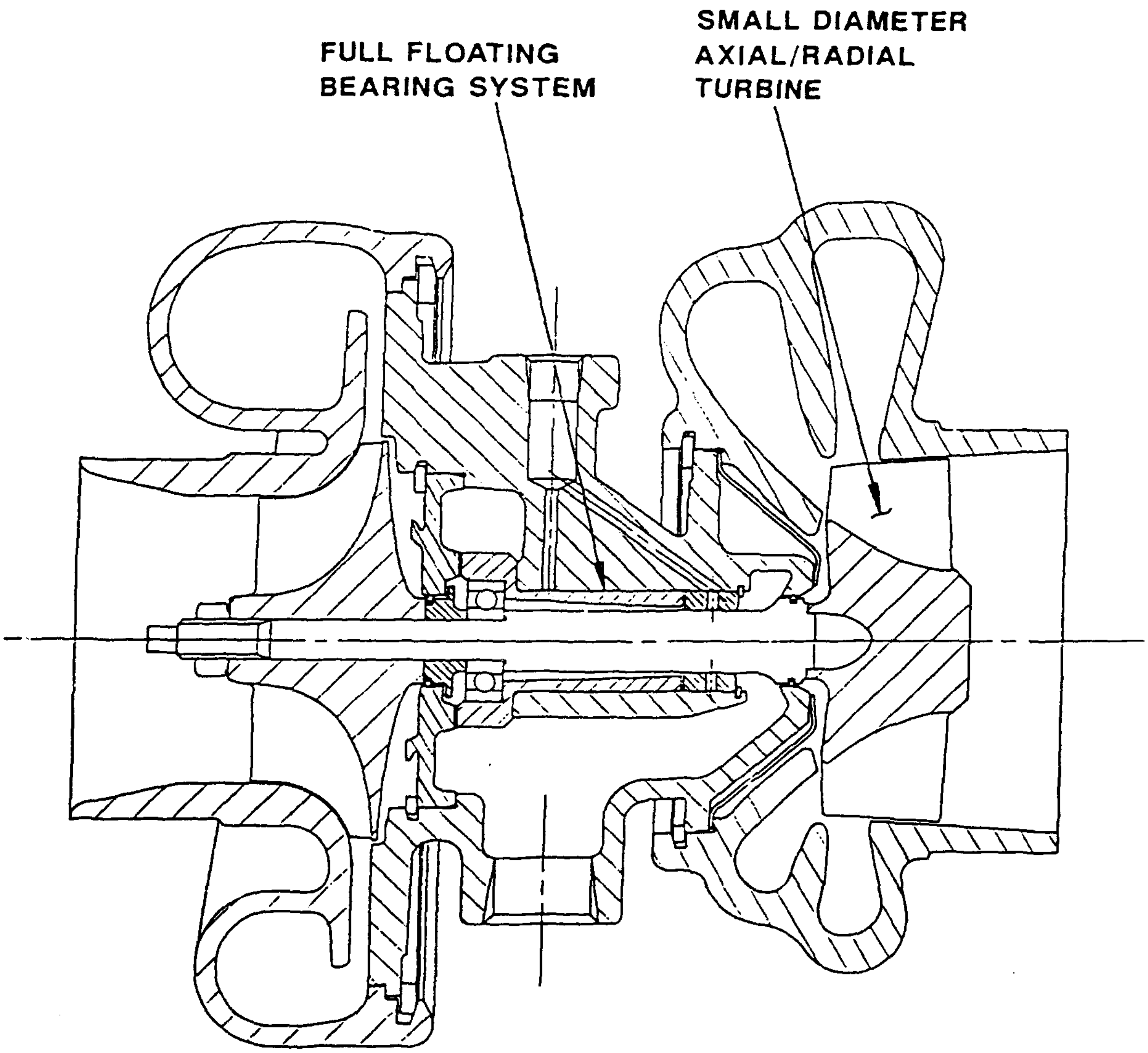

Figure 10 - Servojet WS-90 Turbocharger

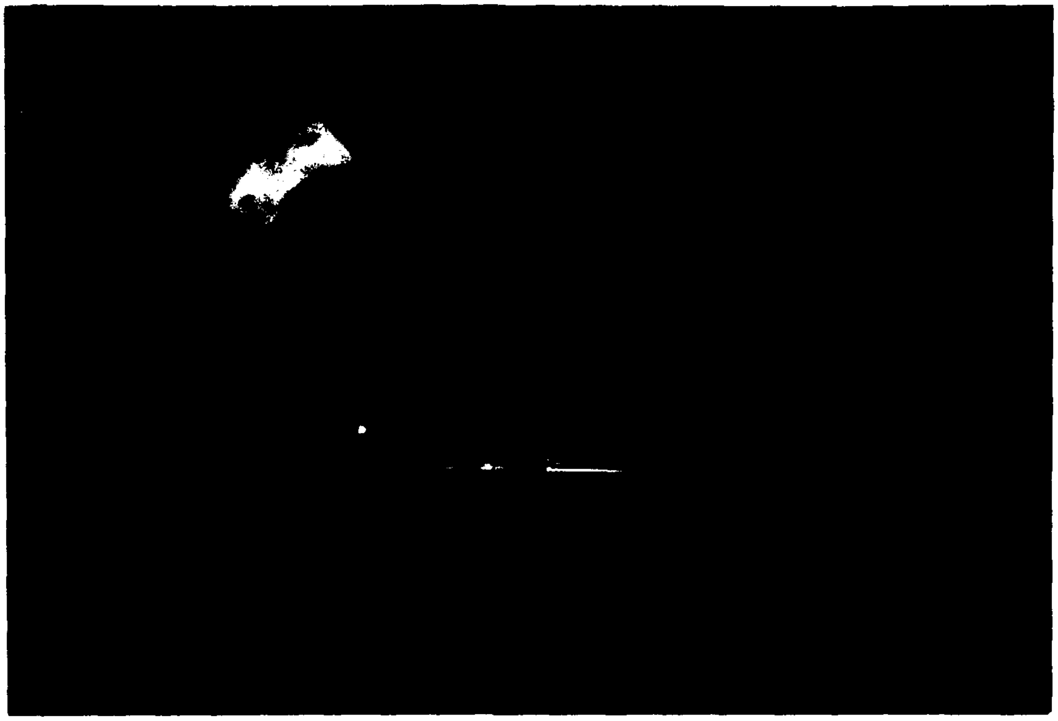

Figure 11 - WS-90 Turbocharger

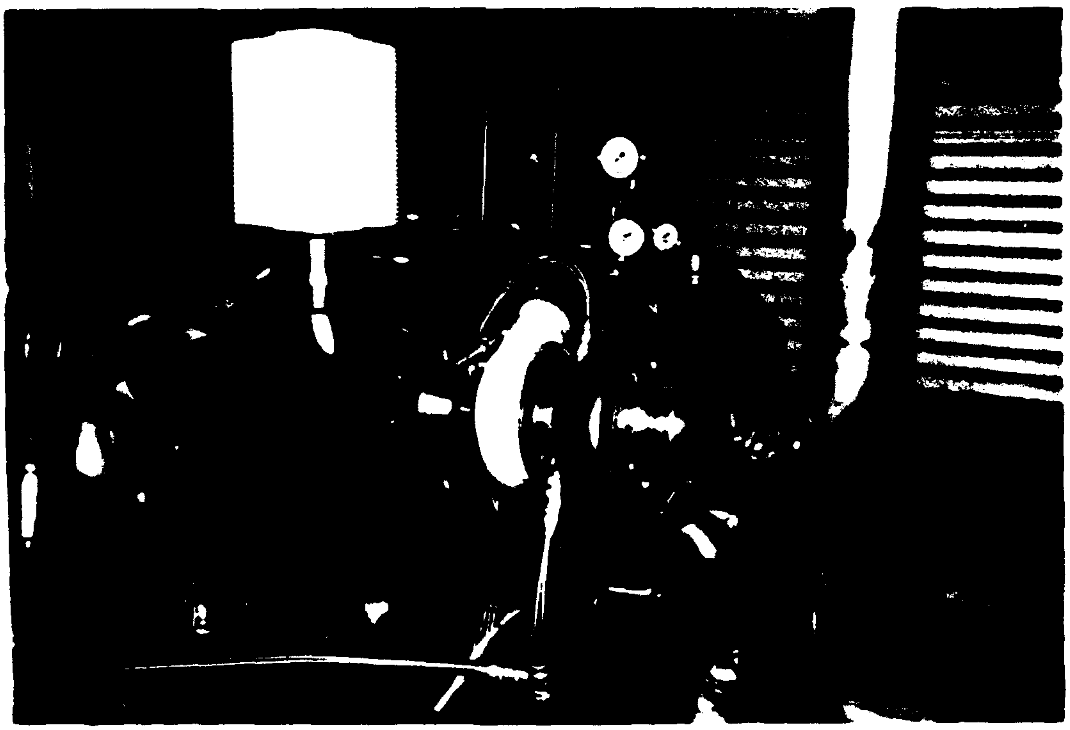

Figure 12 - WS-90 Turbocharger Installation

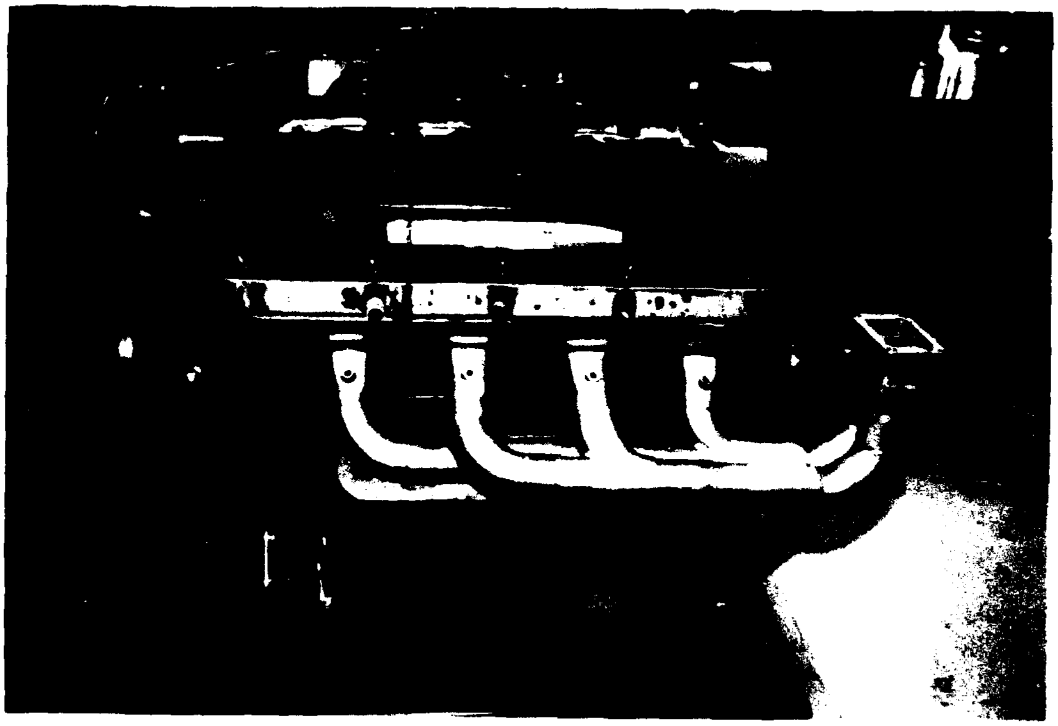

Figure 13 - Exhaust Manifold with Diverter Valve

- *The variable area turbine feature* is a simple, low cost and commercially practical two step device. The WS-VAT provides faster acceleration, lower exhaust emissions and increased engine breaking torque.

- The centrifugal compressor design is the latest state-of-the-art with a broad flow range and a high peak efficiency of 78% - typical of modern centrifugal compressors of this size.

- The WS-90 turbocharger has been demonstrated in commercial operation in a class 8 diesel truck with very favorable results including improved acceleration and reduced fuel consumption.

In November of 1990, BKM issued interim report F-521 titled " TACOM TURBOCHARGER DEVELOPMENT AND TEST PROGRAM" under contract number DAAE07-87-C-R106 . This report includes all turbocharger design data, including turbocharger mapping. A copy of F-521 is included as Appendix H.

6.2 Exhaust system. A stainless steel tube exhaust manifold was fabricated to enhance the efficiency of the twin WS-90 turbochargers. The exhaust manifolds were made in a 4-into-2 configuration on each engine bank (see Figure 13). The paired cylinders were chosen to result in even exhaust pulses at each collector tube. An exhaust diverter valve assembly (Figure 14), part number 60804, was placed at the exit of the collector tube pair on each bank. A manual push-pull cable actuates the diverter valve which determines the exhaust path into the turbocharger inlet. With the valve open, each manifold collector is routed into one of the turbocharger inlets - axial and radial. When the diverter valve is closed, the radial turbocharger inlet is fully blocked off and exhaust from both collector tubes flows into the axial inlet only.

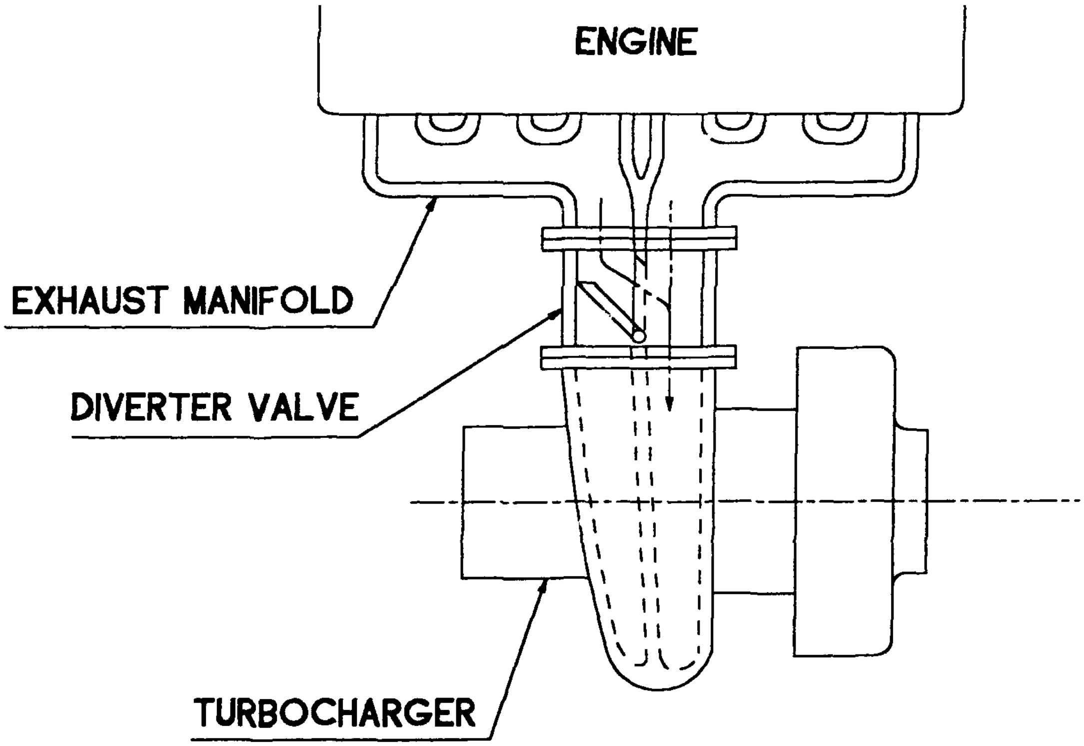

Figure 14 - Exhaust Diverter Valve Installation

7.0 Electronic Control System

Early in this project, it was intended to use a Servojet SE-4D electronic controller which is based on the production Ford EEC-IV ECU. BKM modifies the SE-4D hardware and writes application-specific control software. This custom control unit is packaged in an instrument enclosure containing the necessary solenoid drivers and command signal potentiometers, resulting in the SE-4D. However, prior to the start of engine tests, a BKM-designed and manufactured ECU became available and the decision was made to use it instead.

The BKM ECU has several advantages over the EEC-IV in this application:

- All injector drivers are contained within the ECU
- Engine mounting and fuel cooling capability
- User friendly calibration and diagnostics via IBM-compatible personal computer (IBM-PC)

7.1 Electronic Control Unit (ECU) The ECU is described in Appendix D1. It was mounted on the top of the aftercooler on rubber vibration isolators and cooled with low pressure fuel from the inlet side of the mechanical pump.

7.2 Control Software. The engine control software is based on existing diesel engine programs and modified to map the time delay of each fuel injector individually rather than using an average delay curve as is the normal practice. This compensates for the relatively wide variation in delay times experienced with these prototype injectors (see section 4.2 and Figure 7). Calibration data for the injectors, EPR, and engine sensors is incorporated into the software.

The fuel quantity is calculated as a function of engine RPM and the throttle command input. A manifold pressure sensor input is used to limit smoke by limiting the fuel quantity as a function of boost pressure.

Governing modes - The ECU governs the engine in two modes

- The LOAD MODE (MIN/MAX) governor maintains engine power by changing rail pressure directly in response to a command potentiometer. The engine speed varies between programmed idle and overspeed RPM limits as a function of the applied engine load.

- The SPEED MODE (ALL SPEED) governor holds a fixed engine RPM as the load changes by adjusting rail pressure (and therefore engine power) as required.

7.3 Calibration Software. An IBM-PC is interfaced to the ECU over a 2-wire serial (RS-232C) link to transfer data between the PC and the ECU. Calibration look-up tables and engine control parameters can be displayed, modified, and saved to disk files while the engine is running. This menu-driven software, BKMPANEL, allows the development engineer to quickly evaluate the effect of calibration changes on the engine.

7.4 Wiring Harness. The wiring harness (Appendix A1) connects the ECU to the other electro-mechanical components. A signal breakout box (Appendix A2) is inserted between the harness and the ECU for development testing only. This box taps into the ECU input and output signals and connects the ECU to a remote Control Panel (Appendix A4) via a pair of Interface Cables (Appendix A3). The Control Panel contains several potentiometers that gave the operator manual control of engine speed (in the speed governing mode), rail pressure (in the load governing mode), injection timing, and a mode select switch to place the engine in SPEED or LOAD control mode. An additional CAL(ibration) mode allows the injectors to be fired without an input from the engine mounted crankshaft position (PIP) sensor. In the CAL mode, the Speed command potentiometer controls the frequency of injection. The CAL mode is used only for troubleshooting or injector calibration.

Several other key ECU signals are brought out to the Control Panel so that they can be monitored on an oscilloscope if desired. These signals include the (8) injector solenoid voltages, (8) injector logic signals, the PIP input, EPR rail pressure transducer input, and the EPR solenoid voltage.

7.5 Sensors. The following sensors are installed on the VTA-903. Sensor specifications are contained in Appendix D4.

Crankshaft position (PIP)
Manifold Air Pressure (MAP)
Air Charge Temperature (ACT)
Rail Pressure (RPX)

8.0 Cold Start Aids

Several techniques for improving the cold startability and initial engine warm-up time were investigated. In general, the aim of these techniques was to take advantage of the compression heating effect to warm the inlet air charge - using either the engine pistons or the turbocharger compressor.

The first test of charge air heating was performed on both the twin turbo VTA-903 and a 6-cylinder Cummins NTC-400 engine using a single WS-90 turbocharger. Turbine inlet sliders with drilled impulse nozzles (10x.06", 60x.06", and 30x.125") were installed in the turbocharger (Figure 15). The engine was cranked without starting and also run at idle while the resulting manifold pressures were measured. It was concluded that this technique may be used to improve throttle response and warm up times, but would not be effective as a starting aid since the increase in manifold pressure and temperature at minimum engine RPM (600) is very small - only 1 degree F and 0.5 In.Hg. At a fast idle speed (1200 RPM), the temperature rise is 22 degrees F and manifold pressure increases by 3.95 In.Hg . The full test reports TR-018, TR-019 and TR-026 are contained in Appendix E1.

A more promising cold start technique was investigated that takes advantage of regenerative heating of the inlet air charge. With this technique, the engine is cranked for several seconds without injection of fuel while the exhaust valve is kept closed and the inlet valve is cracked open a small amount during the compression stroke. As the piston compresses and heats the air in the cylinder, the heated air bleeds back into the inlet manifold. Each successive cycle adds heat to the manifold air until a predetermined temperature threshold is reached. At that point, the valves are returned to normal operation and fuel is injected at the normal time. Since the manifold air is significantly warmer than the ambient air temperature, combustion is achieved more easily.

In order to test the effectiveness of regenerative inlet air heating as an aid to cold starting, a simulation test was conducted at BKM. This test did not attempt to start an engine but simply to quantify the amount of manifold temperature rise that could be achieved.

A Perkins 4.236 diesel engine, configured as a single cylinder research engine, was the test subject (Figure 16). Various combinations of inlet and exhaust valve settings were tested. The test indicated that regenerative inlet air heating has potential as a practical cold starting aid. The maximum manifold air temperature rise, after 30 seconds of cranking, was 42 degrees C above ambient (21°C) with the exhaust valve mechanism disabled and the inlet valve held open .010 In.. A graph of manifold temperature vs time is shown in Figure 17. The full results of this test are presented in Appendix E2. A similar cranking test was performed on the VTA-903 engine in which the inlet valve lash was set to a negative .010"

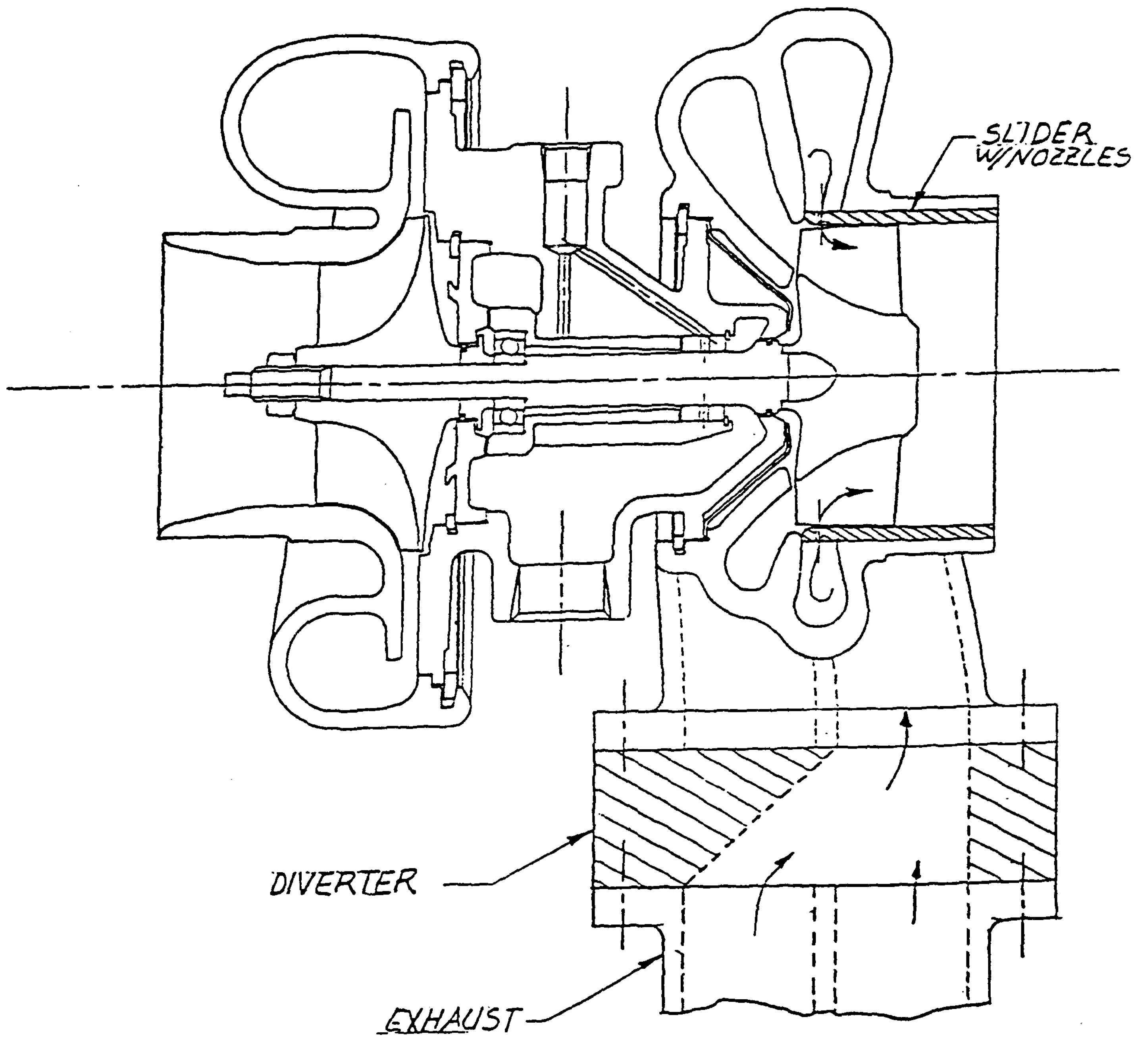

Figure 15 - Exhaust Slider Installation

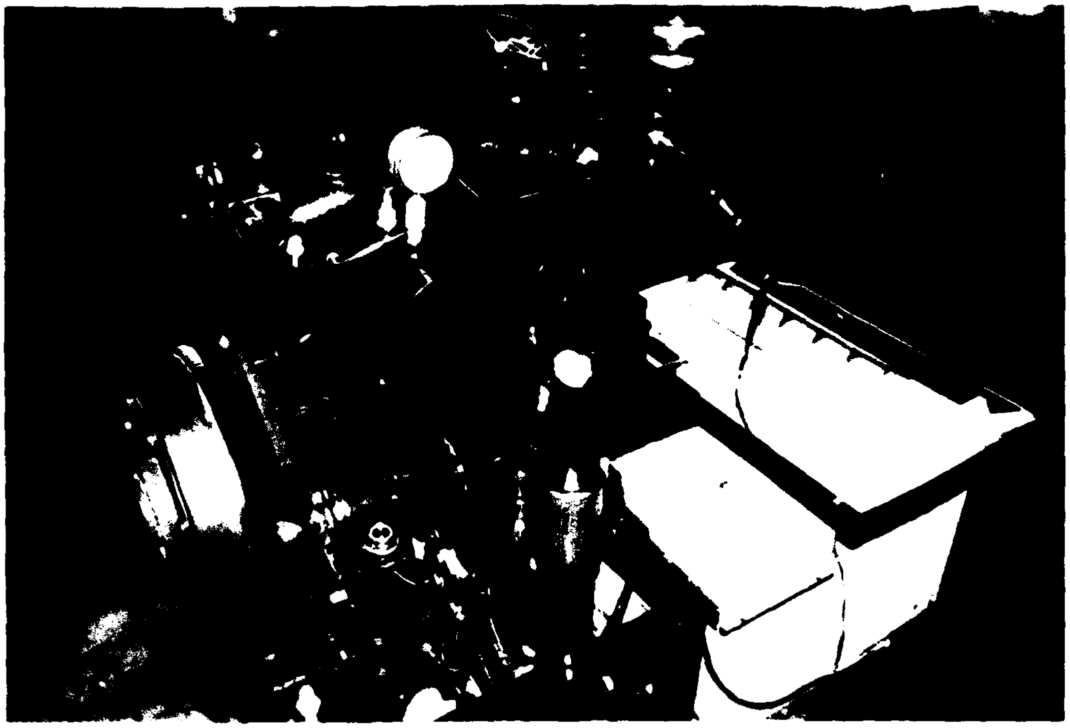

Figure 16 - Cold Start Bench Test

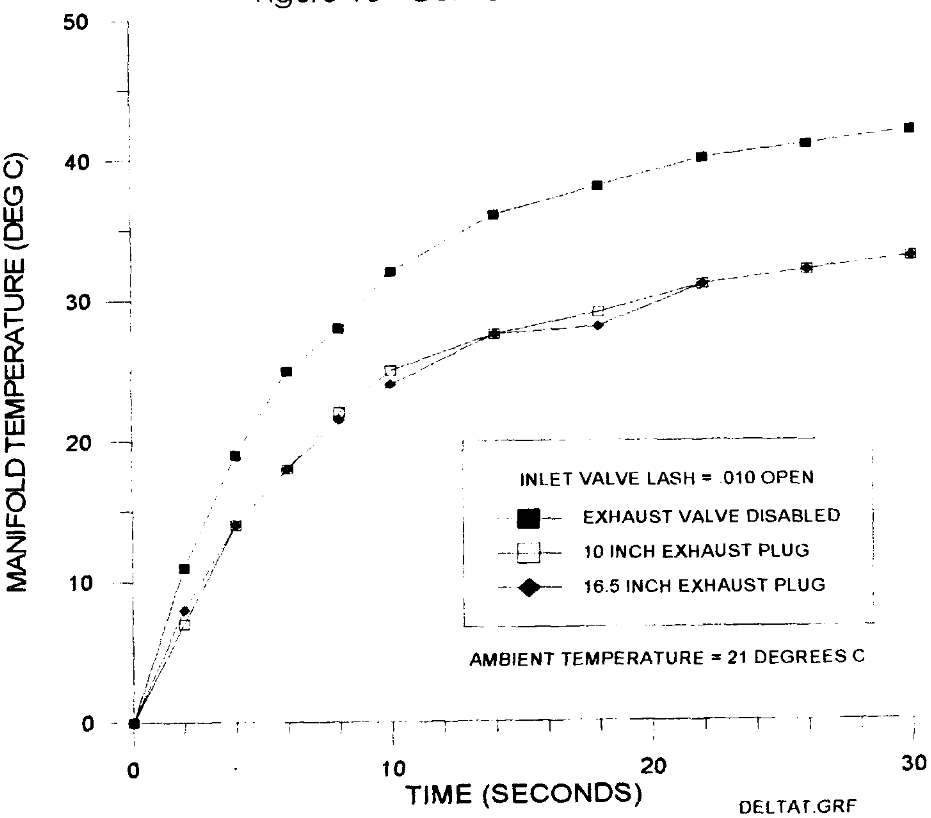

Figure 17 - Temperature Rise Above Ambient

and the exhaust valve function was not changed. Under these conditions, a manifold temperature rise of approximately 15 degrees C was observed. It is evident from the bench test that the VTA-903 temperature rise would be increased if, in addition to the negative inlet lash, the exhaust valves were disabled during cranking. A follow-up test program is needed to evaluate this technique on a functioning engine.

9.0 Engine tests (BKM & Golden West College)

The fuel injection and turbocharger hardware described above was installed on the Cummins VTA-90 engine. Initial system checkout was done at BKM with the engine running unloaded - see Figure 18. The purpose was to verify starting and to evaluate idle quality prior to performing full power dynamometer tests.

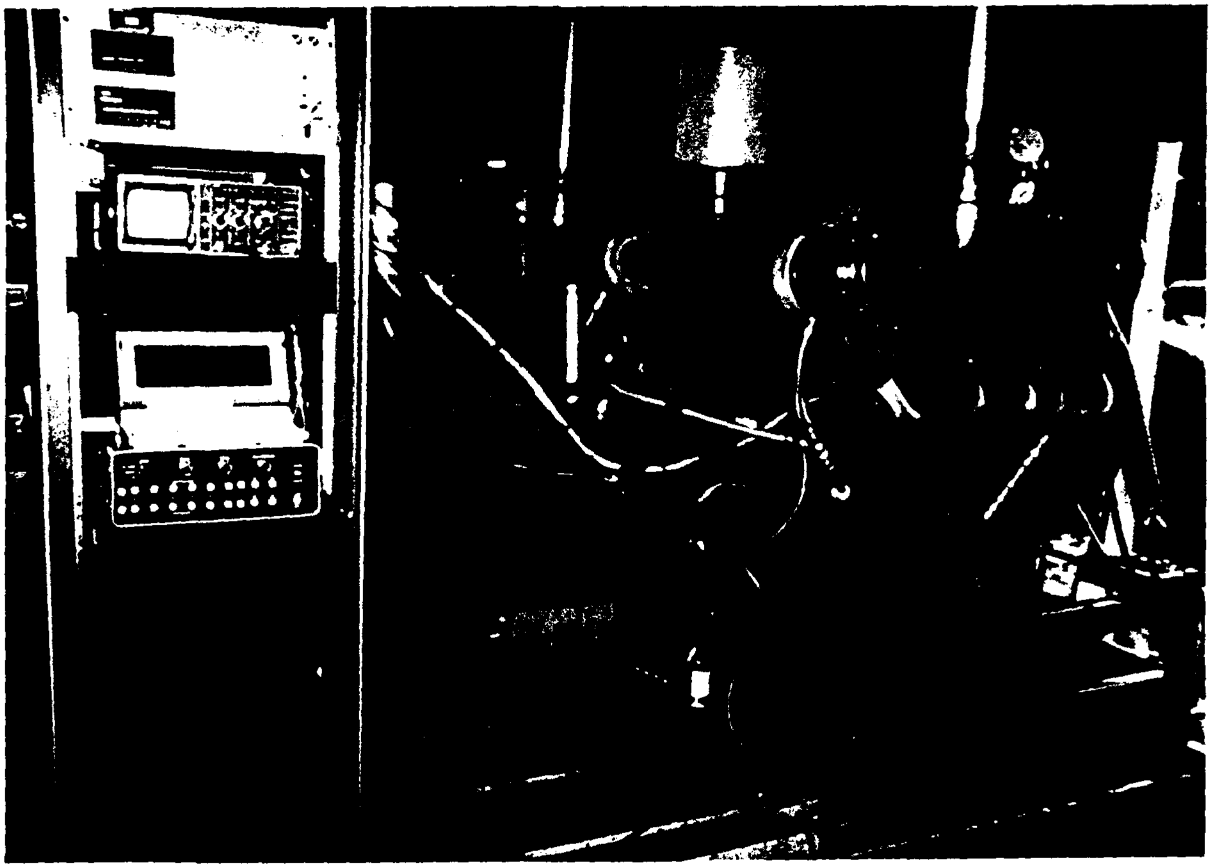

Figure 18 - VTA-903 Test Stand (BKM)

Following the unloaded checkout, the engine was transported to Golden West College (GWC) in Huntington Beach, CA for full power dynamometer tests. The GWC test cell contains a Clayton water brake dynamometer and Digilog data acquisition system.

9.1 System Checkout (BKM).

Startability and idle quality were the first characteristics to be evaluated. Although the engine started easily, marginal injector spray quality and HSV instability at the idle rail pressure (480 PSI) resulted in occasional misfires and erratic injection timing. This marginal spray quality is typical of this injector type when the rail pressure approaches the needle closing pressure. When that occurs, the needle fails to lift completely and throttling of the fuel charge occurs across the needle seat rather than the spray orifices. This throttling reduces the injection pressure resulting in poor atomization, i.e. larger droplet size and less spray penetration. If the rail pressure is reduced further, the injector eventually does not fire. Each injector has a slightly different closing pressure and therefore will stop firing at a different rail pressure. Future fuel injector designs for this engine should allow consistent operation down to 450 PSI rail. As a short term solution to this problem, the *two stage* injector calibration technique, described in section 4.2, was incorporated into the software which extended the minimum fuel delivery range and improved the idle quality.

It was discovered that injection delay times in the engine were somewhat different from delay times measured on the calibration bench. This is believed to be the result of dynamic rail pressure differences between the bench and the engine. Since the delay is a function of rail pressure, standing waves that are present in the engine installation (but not on the bench) will effect timing. As a result, cylinder-to-cylinder injection timing is spread over a wide range with some too advanced and some too retarded. Each injector was instrumented with a strain gauge to measure instantaneous accumulator pressure and thereby determine actual injection timing. The ECU software was then modified to allow timing adjustment of each cylinder independently. Originally, the timing was determined using an average delay function for all eight injectors. Software control of injector-to-injector timing was a more cost-effective solution than reducing the standing wave amplitude through hydraulic methods which would have required extensive bench testing. In developing a commercial version of this system, it would be advantageous to solve the hydraulic instability problem instead.

Another control strategy that was evaluated in an attempt to improve idle quality was skip-fire. Four of the eight fuel injectors were disabled by disconnecting the solenoid electrical connectors. The engine was idled on the remaining four cylinders which each had to produce higher power than usual to make up for the power lost to the inactive cylinders. Since the four active cylinders were each required to inject more fuel per cycle, they operated further above the minimum rail pressure and therefore were less likely to misfire. Although the engine idled smoothly on four cylinders, the idle quality was not much improved compared to eight cylinders. The change in power per cylinder, at idle, between eight and four active cylinders was not enough to result in a large enough change in rail pressure to make a noticeable difference.

9.2 Engine Test Results (GWC).

All dynamometer tests were conducted with the Servojet fuel system installed. The engine was tested with the following turbocharger configurations.

- Stock Single turbocharger and stock exhaust manifolds
- Twin WS-90 turbos, fabricated exhaust manifold - both turbo inlets
- Twin WS-90 turbos, fabricated exhaust manifold - radial turbo inlet
- Twin WS-90 turbos, fabricated exhaust manifold - axial turbo inlet

The test results with these four configurations are plotted together with the manufacturers published performance data in Figure 19. Turbocharger compressor outlet and turbine inlet pressures are plotted in Figure 20. Figure 21 shows the pressure differential (boost minus exhaust). Figure 22 is total engine inlet airflow (pounds per second). Figure 23 shows exhaust smoke, and Figure 24 is a chart of throttle response times from idle to 2200 RPM. All of the above data is at maximum power.

The throttle response test simulated vehicle acceleration, from off-idle to near maximum engine RPM, on the water brake dynamometer. The dyno load control (water flow) was set to hold the engine at 2200 RPM when full power was commanded. With this load setting maintained, the engine speed command was reduced to 1200 RPM. At this engine speed, the dyno loading was minimal. A mode input to the ECU was then switched which instantaneously commanded maximum fuel. The engine quickly accelerated up to the previously set maximum speed.

The time between the maximum fuel command and attainment of the preset maximum RPM was measured. The resulting times in Figure 24 are the average of at least four runs in each configuration. As shown, the twin WS-90 turbochargers (with blocked inlets) accelerated in less than half the time of the stock single turbocharger.

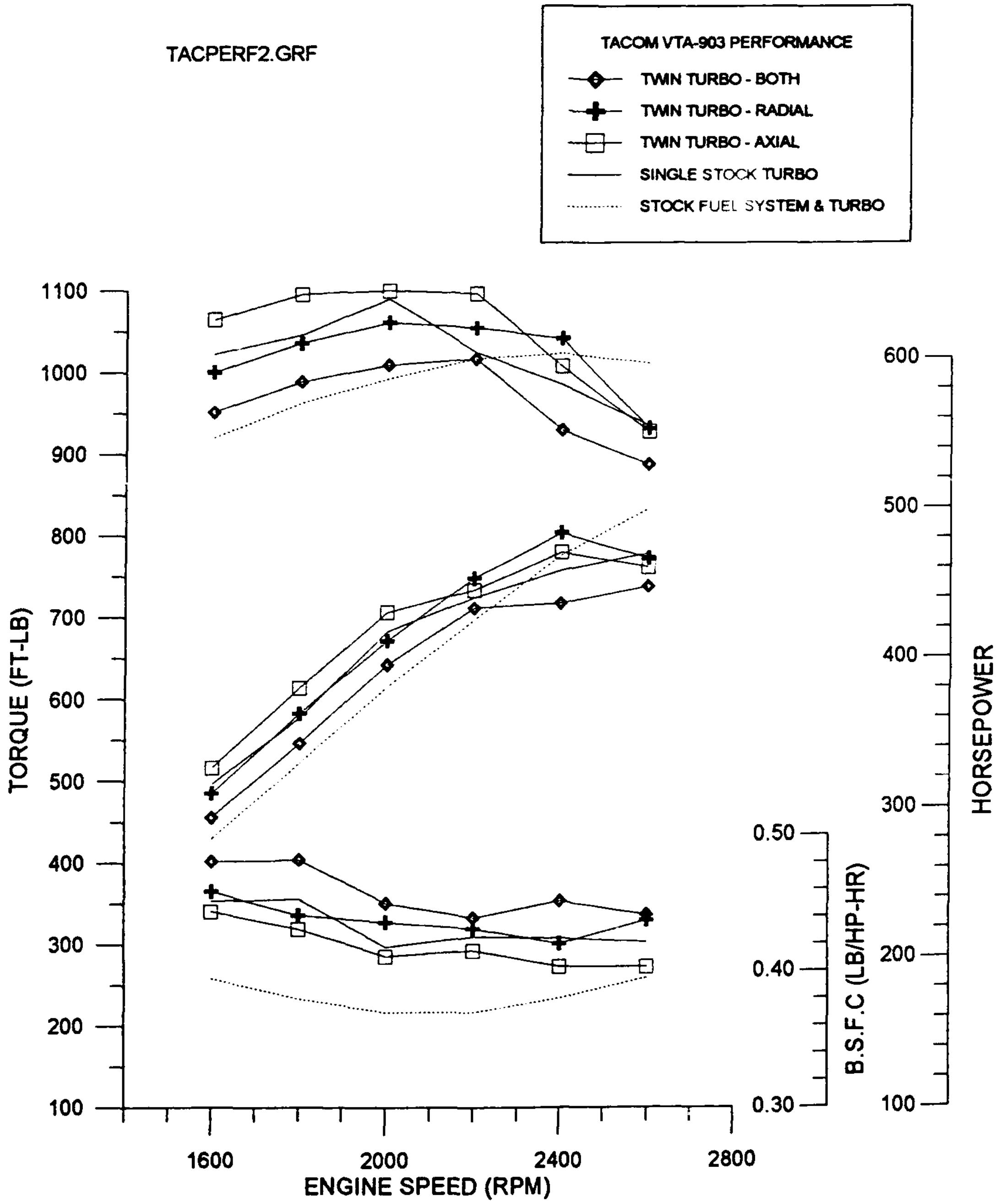

Figure 19 - Engine Performance Vs RPM

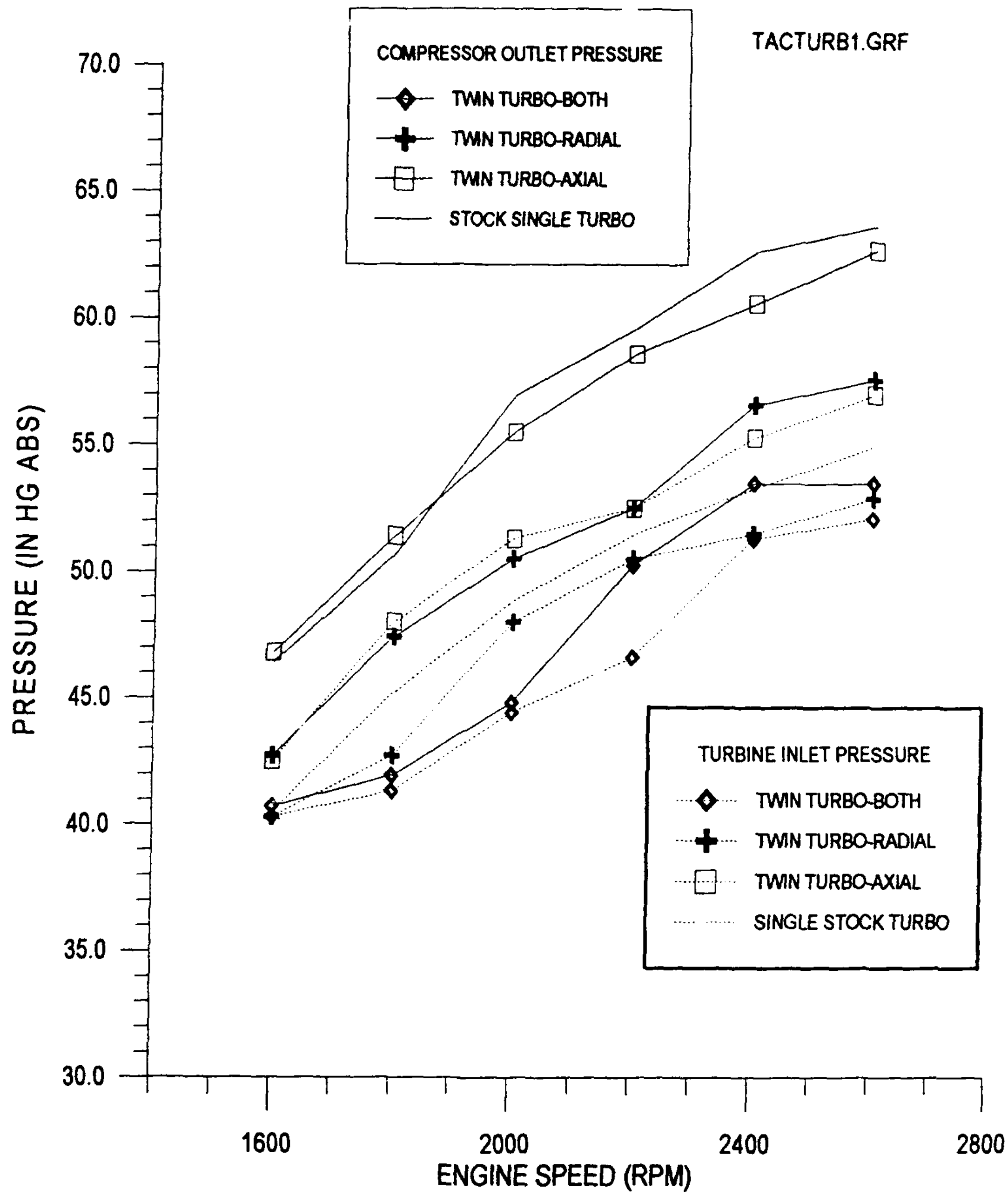

Figure 20 - Turbocharger Inlet and Outlet Pressures Vs RPM

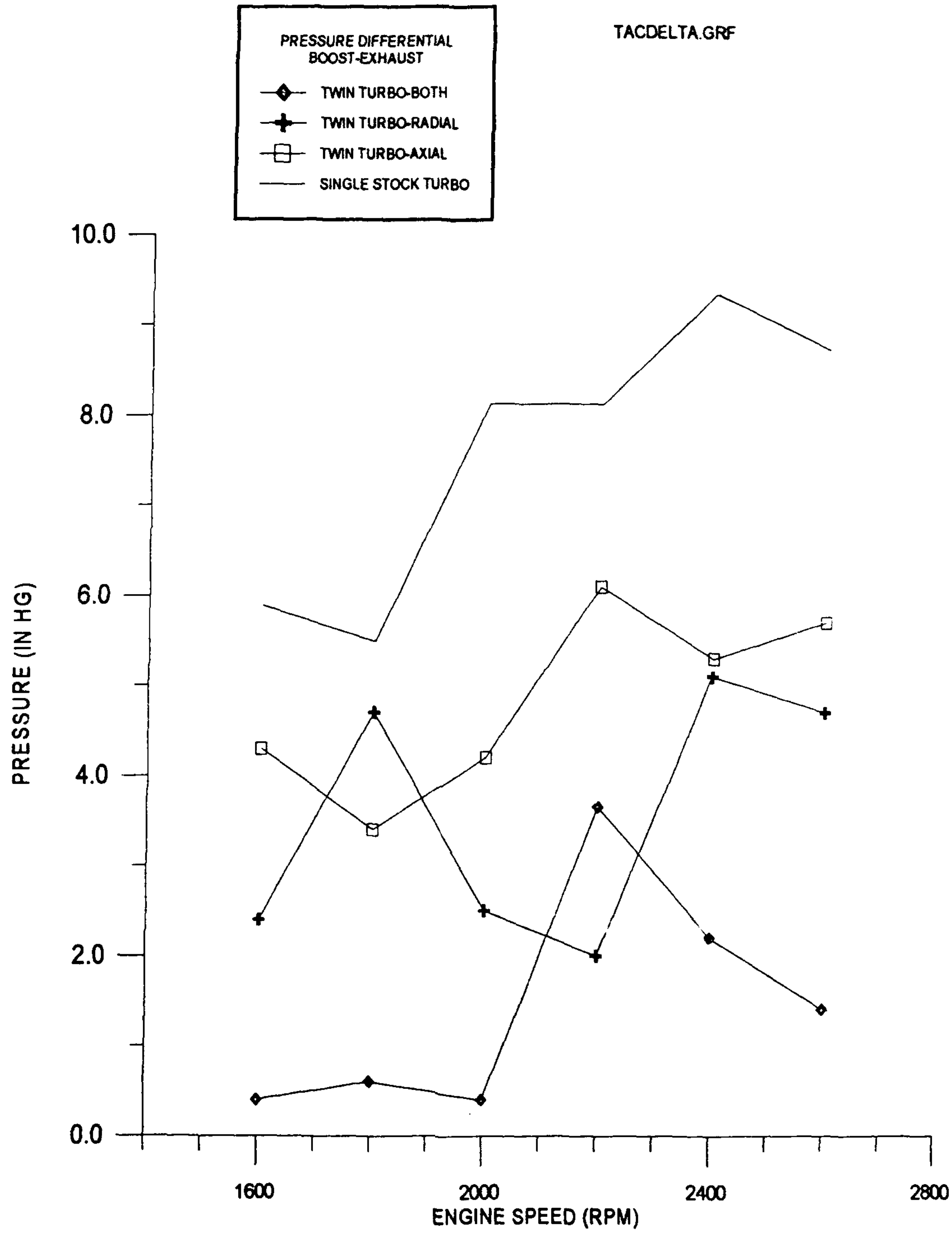

Figure 21- Turbocharger Pressure Differential Vs RPM

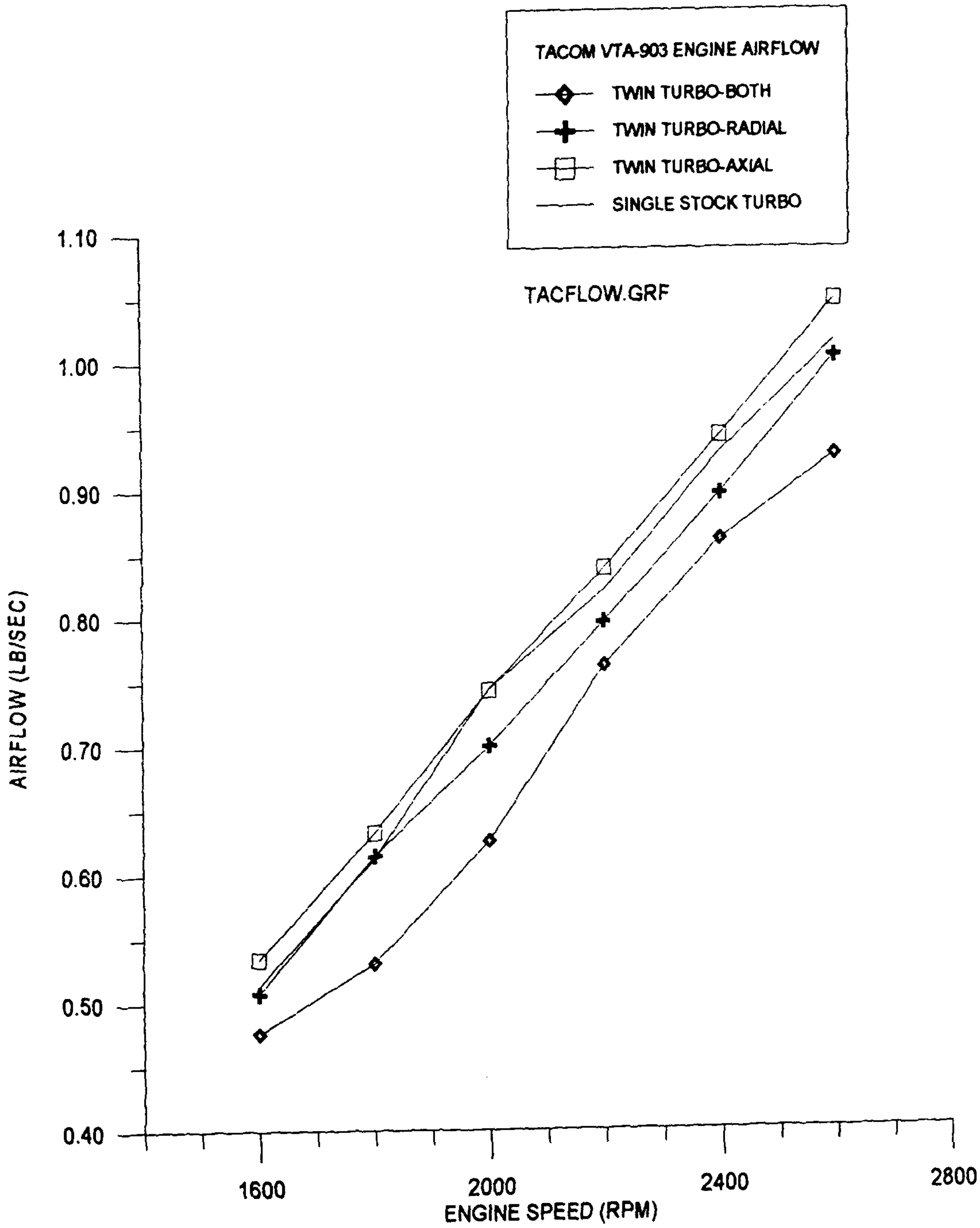

Figure 22 - Engine Airflow Vs RPM

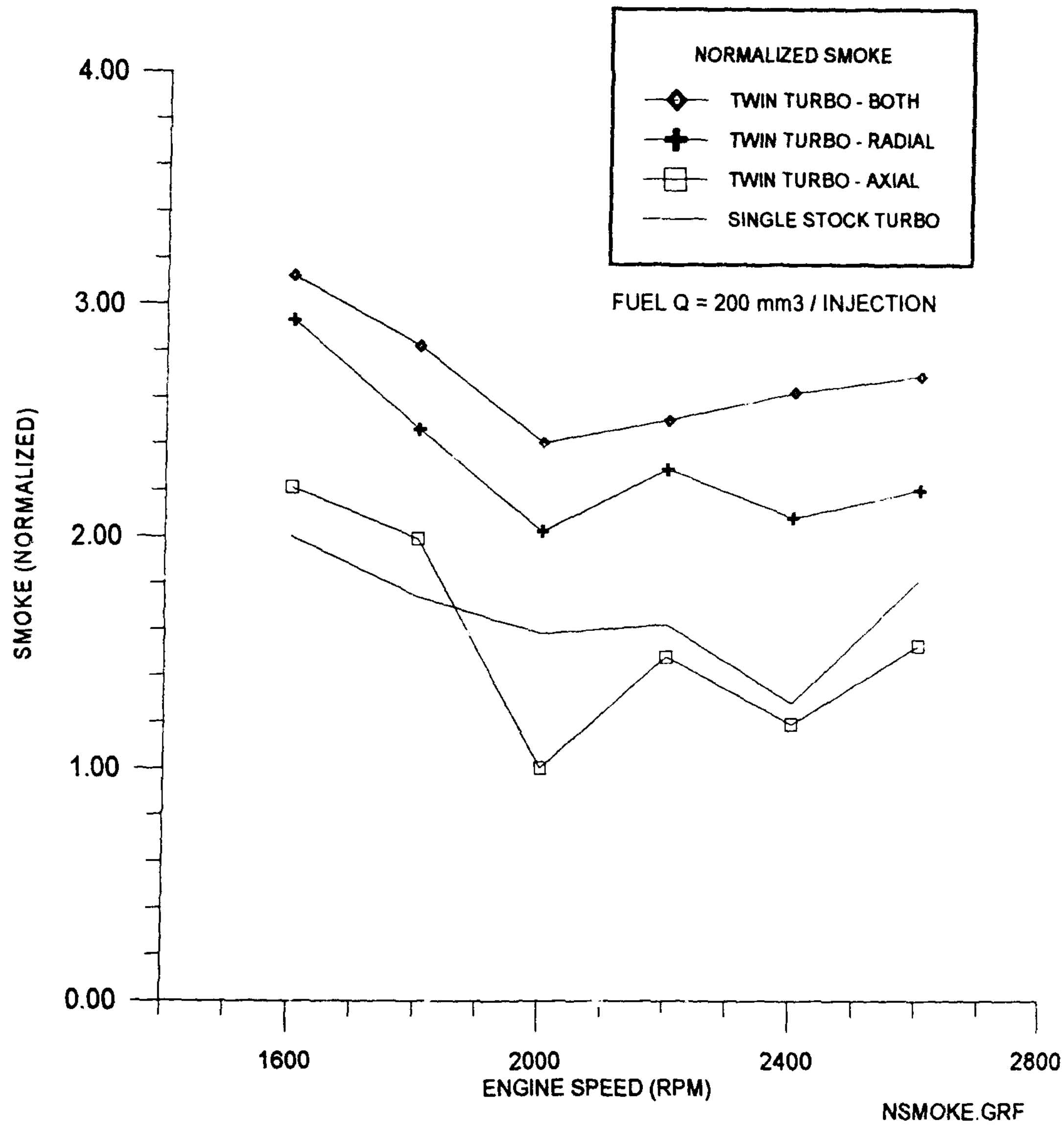

Figure 23 - Normalized Smoke Vs RPM

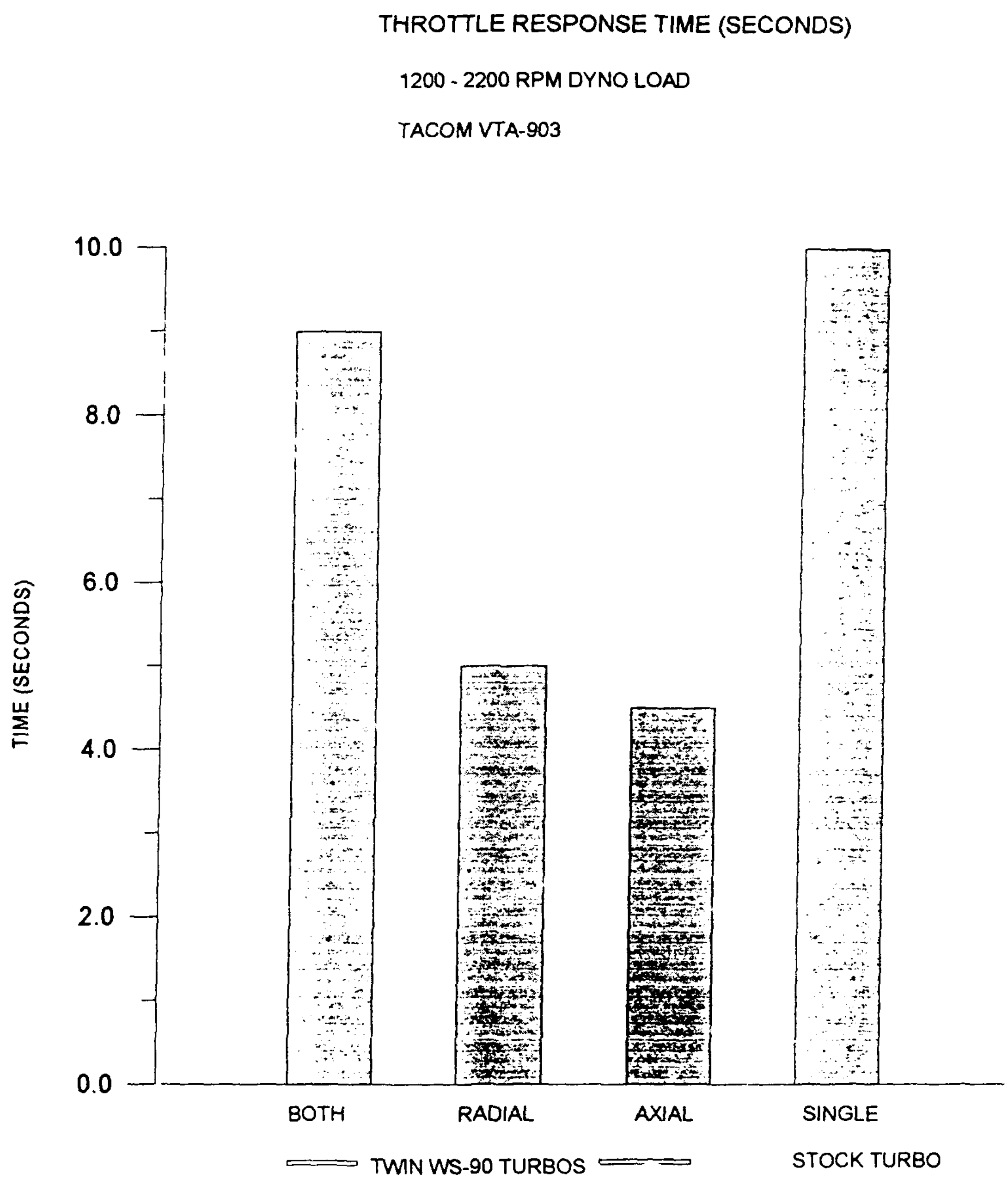

Figure 24 - Throttle Response Time

10.0 High Speed Combustion photography (MTU)

Dr. Duane Abata of Michigan Technological University (MTU) was subcontracted to perform a series of combustion flame photography tests (Ref. 2) on a Servojet fuel injection system. The purpose was to evaluate and compare the combustion resulting from the use of various injector nozzle configurations (no. and diameter of holes)and rate shapes. Each nozzle was tested with two rate shapes - one where the full fuel charge is injected immediately at a high initial rate and the other where a small percentage of fuel is pre injected at a low rate immediately prior to the higher rate main charge. The pre injection percentage is controlled by calibration of the rate shaping section of the nozzle assembly (Figure 1).

A combustion analyzer was used to measure cylinder pressure and heat release during the filming. A high speed camera, installed in an instrumented single-cylinder research engine, filmed the combustion events. These films were transferred to VHS videotape for viewing. The video tape is included as part of this report. Details of the test procedure and the resulting data are contained in the MTU test report (Appendix F).

10.1 Injector Configuration and Calibration. Six unique injector configurations were tested. The nozzle hole combinations and the percentage of pre injection are listed below.

Nozzle Configuration (No. holes x dia. - In.)	Pre Injection Quantity (%)
8 x .006"	0 & 15
7 x .007	0 & 15
6 x .006	0 & 10

RUN NO.	INJECT S/N	HOLE CONFIG # X DIA	PRE-INJ %	FUEL Q mm3	INJECT DELAY mS	DUR mS	RAIL PRESS PSI	START OF INJ DEG	START COMB DEG	NORM SMOKE
1	303	8X.006	0	34	2.53	1.77	800	5	-4	1.60
2	303	8X.006	0	46	2.06	2.07	1150	3	-3	1.73
3	304	7X.007	0	35	2.77	1.55	800	4	-4	1.44
4	304	7X.007	0	53	1.73	1.94	1500	9	0	1.31
5	303	6X.006	10	32	2.92	2.92	800	3	-8	1.13
6	303	6X.006	10	51	2.26	2.49	1500	5	-3	1.69
7	304	7X.007	15	30	2.40	1.90	800	2	0	1.23
8	304	7X.007	15	52	1.90	2.00	1500	3	-4	1.44
9	304	8X.006	15	29	2.64	2.02	800	10	3	1.15
10	304	8X.006	15	52	2.05	2.31	1500	12	5	1.42
11	303	6X.006	0	31	3.13	1.87	800	-	-	1.00
12	303	6X.006	0	50	2.37	2.19	1500	-	-	1.25

TABLE 1- Flame Photo Calibration Data

Each of the six combinations of nozzle and rate shape were tested at two injection quantities representing approximately 100% and 50% of maximum fuel delivery. Table 1 presents the calibration data and the injection rate traces are presented in Figure 25. Note the difference in rate traces with and without pre injection. The injector energize time was 15 mSec in all cases.

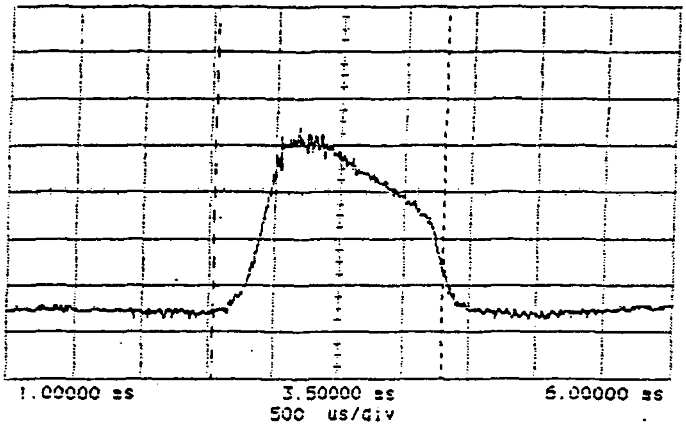

Run 1- 8X.006, 800psi
0% pre-injection

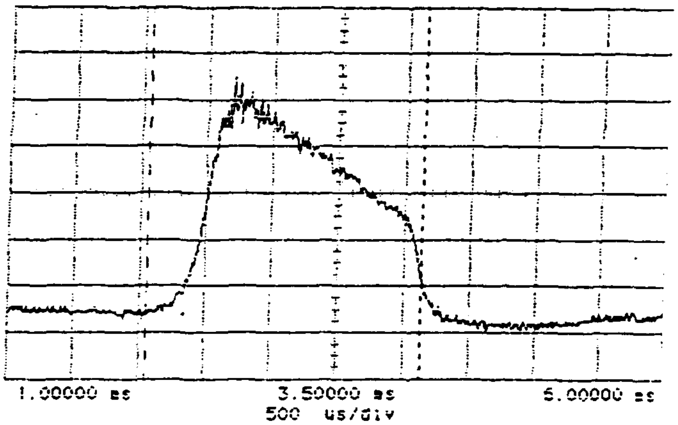

Run 2 - 8X.006, 1150psi
0% pre-injection

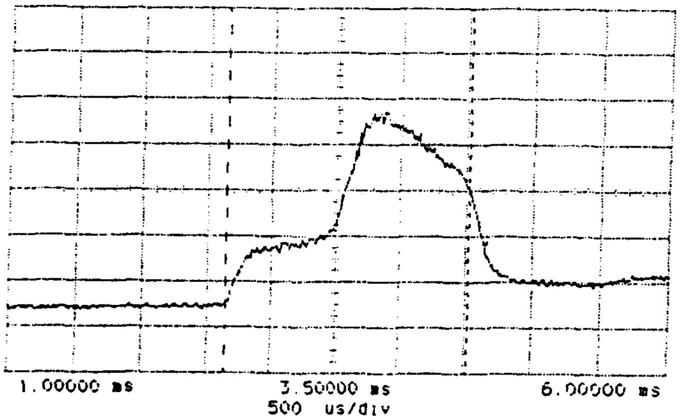

Run 9- 8X.006, 800psi
15% pre-injection

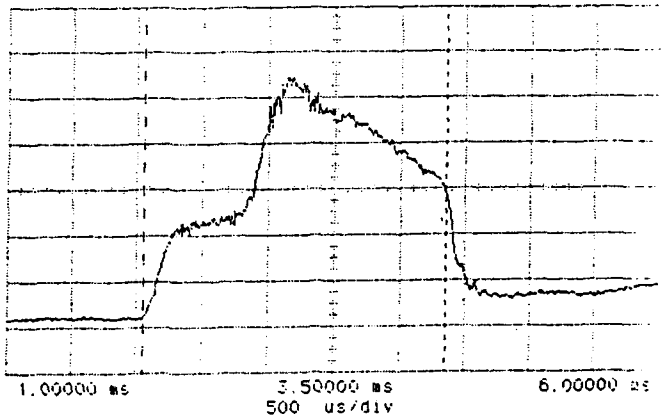

Run 10 - 8X.006, 1500psi
15% pre-injection

Figure 25 - Injection Rate Traces

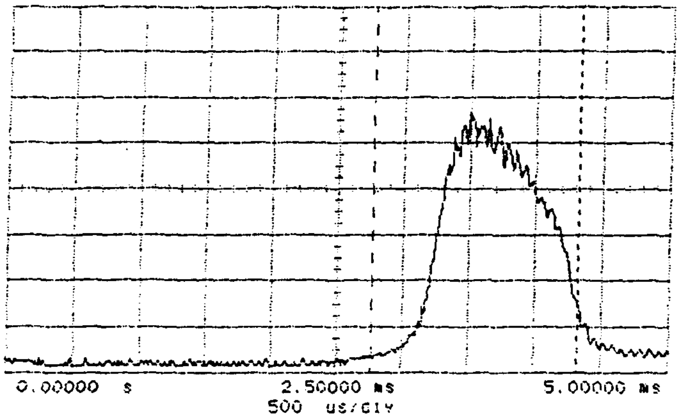

Run 3- 7X.007, 800psi
0% pre-injection

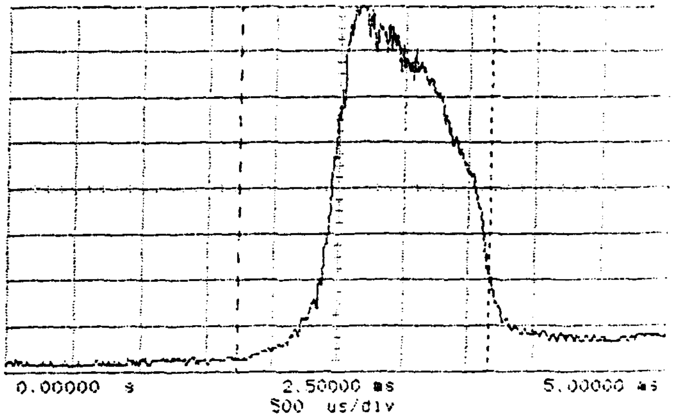

Run 4 - 7X.007, 1500psi
0% pre-injection

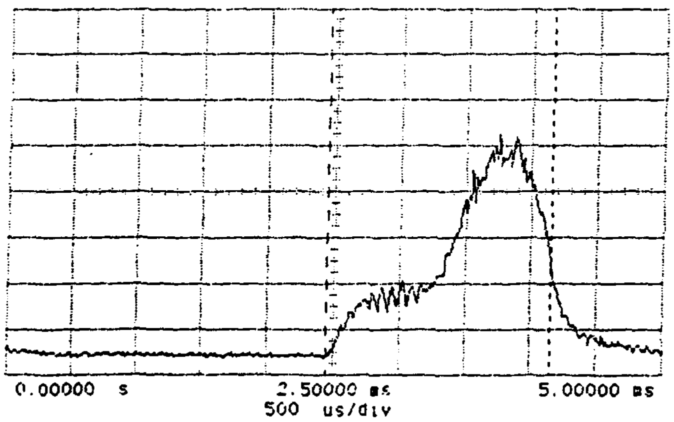

Run 7 - 7X.007, 800psi
15% pre-injection

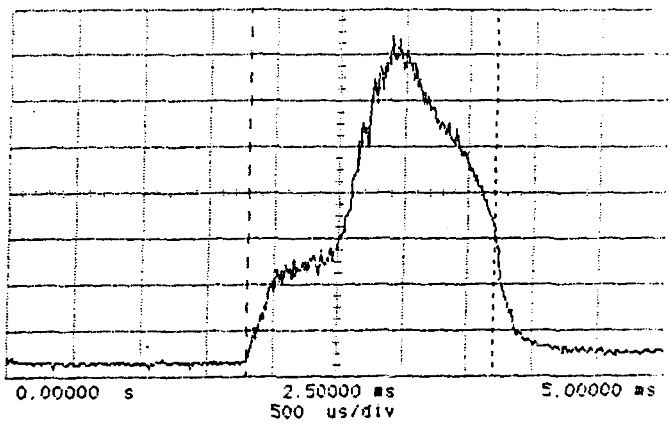

Run 8 - 7X.007, 1500psi
15% pre-injection

Figure 25 - Injection Rate Traces

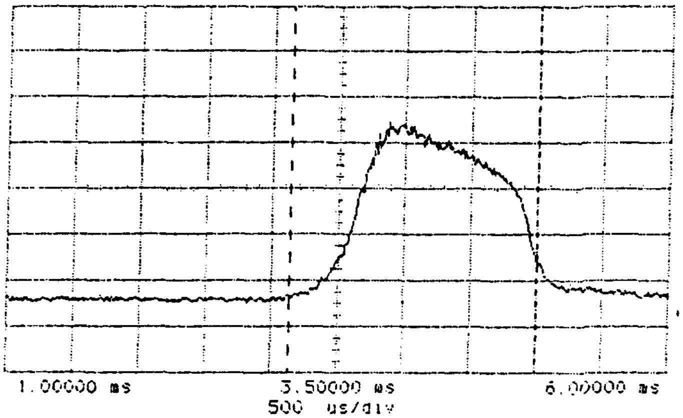

Run 11 - 6X.006, 800psi
0% pre-injection

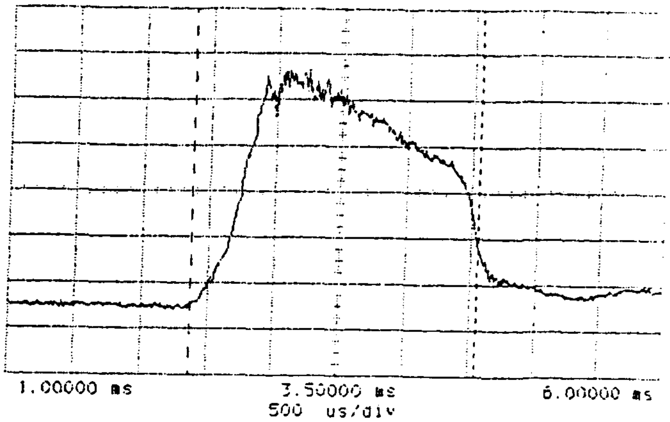

Run 12 - 6X.006, 1500psi
0% pre-injection

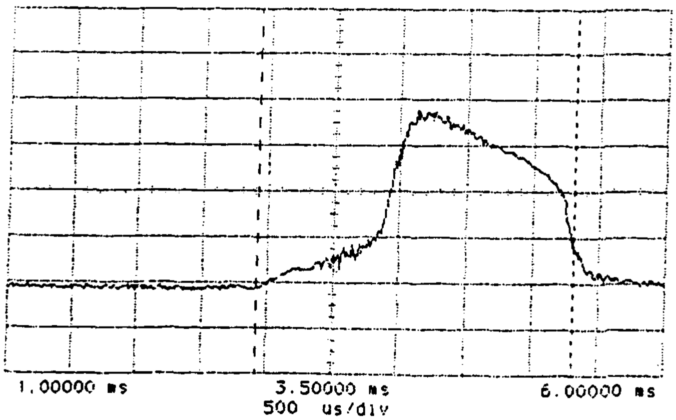

Run 5- 6X.006, 800psi
10% pre-injection

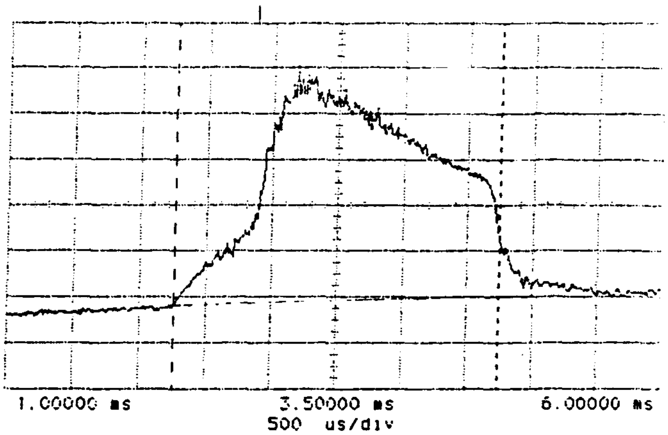

Run 6 - 6X.006, 1500psi
10% pre-injection

Figure 25 - Injection Rate Traces

10.2 Analysis of Flame Photography Test Results.

The rail pressure, injection timing, and normalized smoke data for each run is listed in Table 1. Normalized smoke is used instead of an absolute value because baseline data for the optical engine with standard mechanical injectors was unavailable.

The 8x.006 nozzle configuration with pre injection (runs 9 and 10) demonstrated the best overall result for the following reasons.

- It had the highest peak cylinder pressures, 7.67 MPa at 800 PSI rail and 9.05 MPa at 1500 PSI rail.
- The peak rate of heat release for this nozzle, 164 kJ at 800 PSI rail and 409 kJ at 1500 PSI rail, was even with the other injectors.
- The cumulative heat release curves show a value of 1.3 MJ at 800 PSI and 1.18 MJ at 1500 PSI.

Several nozzle combinations produced relatively high smoke readings. This can be explained by the fact that combustion begins at the cylinder walls. Some fuel appears to have been deposited on the walls and not burned completely. This will result in larger carbon particles flowing out the exhaust. If no wall wetting had occurred, the smoke readings would be lower. There was no clear correlation between nozzle configuration or pre injection and smoke readings.

The complete test report is included in Appendix F. Refer also to the VHS format video tape included with this report.

11.0 Turbocompound Cooling System

11.1 TCS Design. In response to interest expressed by TACOM personnel, BKM agreed to design and conduct preliminary "proof of concept" tests on an exhaust driven engine cooling fan called the Turbocompound Cooling System (TCS). The objective of the TCS concept is to utilize wasted exhaust energy to spin a radiator cooling fan rather than driving the fan directly via the engine crankshaft. This will, in theory, increase the mechanical efficiency of the engine. As a secondary benefit, replacing the engine driven fan with the TCS allows the cooling radiator to be placed remotely. By eliminating the need to place the mechanically-driven fan and radiator at the front of the vehicle, designers have more flexibility and can place greater emphasis on low-drag aerodynamic designs or other packaging considerations.

The TCS prototype test unit was based on the existing Servojet turbocharger design. The WS-90 exhaust turbine wheel was retained. To this was added a new exhaust housing with integral wastegate mounting bosses and ducting (Figure 26), and a new axial fan (Figure 27) and housing (Figure 28). External air and exhaust ducting was designed and built to allow performance tests (Figure 29).

Manufacture of the high speed axial fan presented a technical challenge. A computerized stereo lithography process was used to generate a master model of the fan which was then used to cast the finished part. Although this process was less expensive than more traditional modeling techniques or NC machining, the dimensional accuracy of the model, and therefore the finished fan blades, was less than expected. In particular, the resulting blade thickness is outside the design tolerance. Since the blade profile is critical to the aerodynamic performance of the fan, this variation was expected to reduce fan efficiency and could potentially affect the vibration characteristics.

11.2 TCS engine tests: The TCS fan instrumented for temperature and pressure, as indicated in Figure 30, was tested at Golden West College using the VTA-903 engine exhaust to power the TCS turbine (Figures 31 through 34). The VTA-903 had the stock single turbocharger installed during this test. The exhaust outlet from the engine turbocharger was ducted into the TCS turbine inlet. The TCS fan outlet air passed through a diffuser, a plenum chamber, and an adjustable orifice to simulate a heat exchanger which then discharged into the dynamometer test cell. Airflow measurement nozzles (1 to 4 depending on flow rate) were attached to the fan inlet duct. The pressure drop across the nozzles was used to calculate volumetric airflow. The TCS Figure 35 shows the TCS airflow and exhaust back pressure for fan speeds from 5000 to 17700 RPM with a 100 square In. exit opening area. Drawing 614036 (Appendix C6) details the test installation. The full test report (MR-941) is presented in Appendix G.

Figure 26 - TCS Turbine Housing and Wastegate

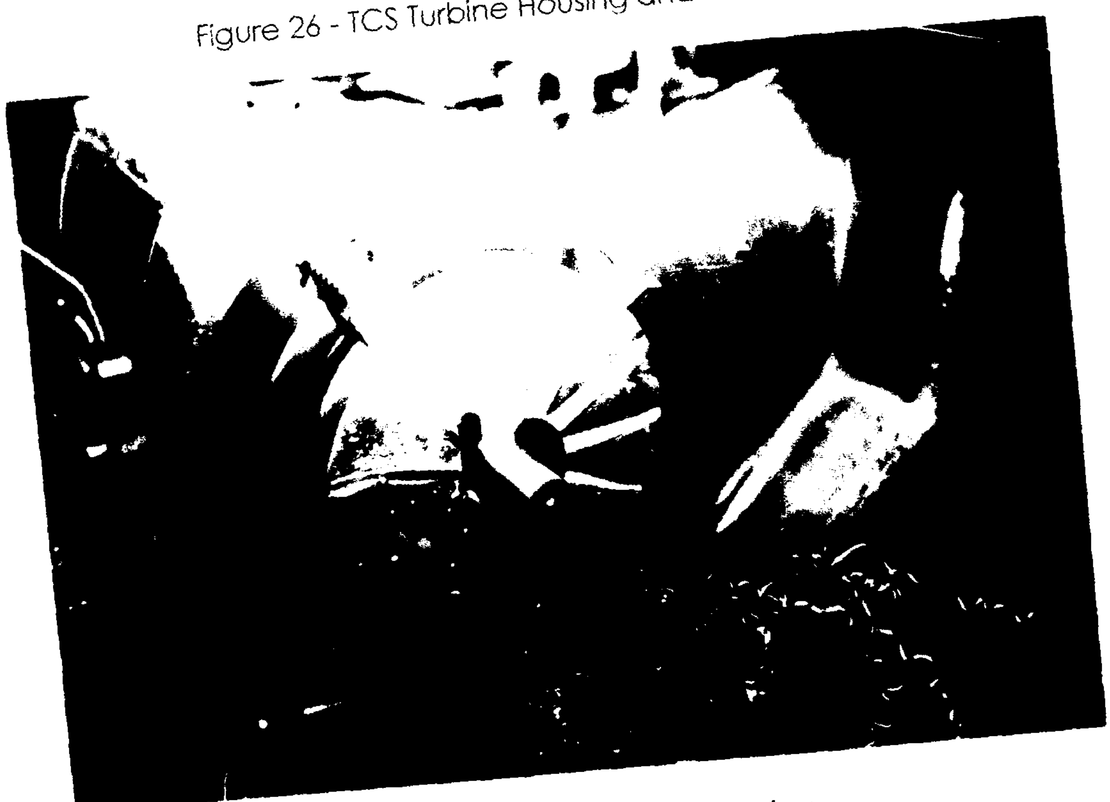

Figure 27 - TCS Fan Machining

Figure 28 - TCS Fan Housing

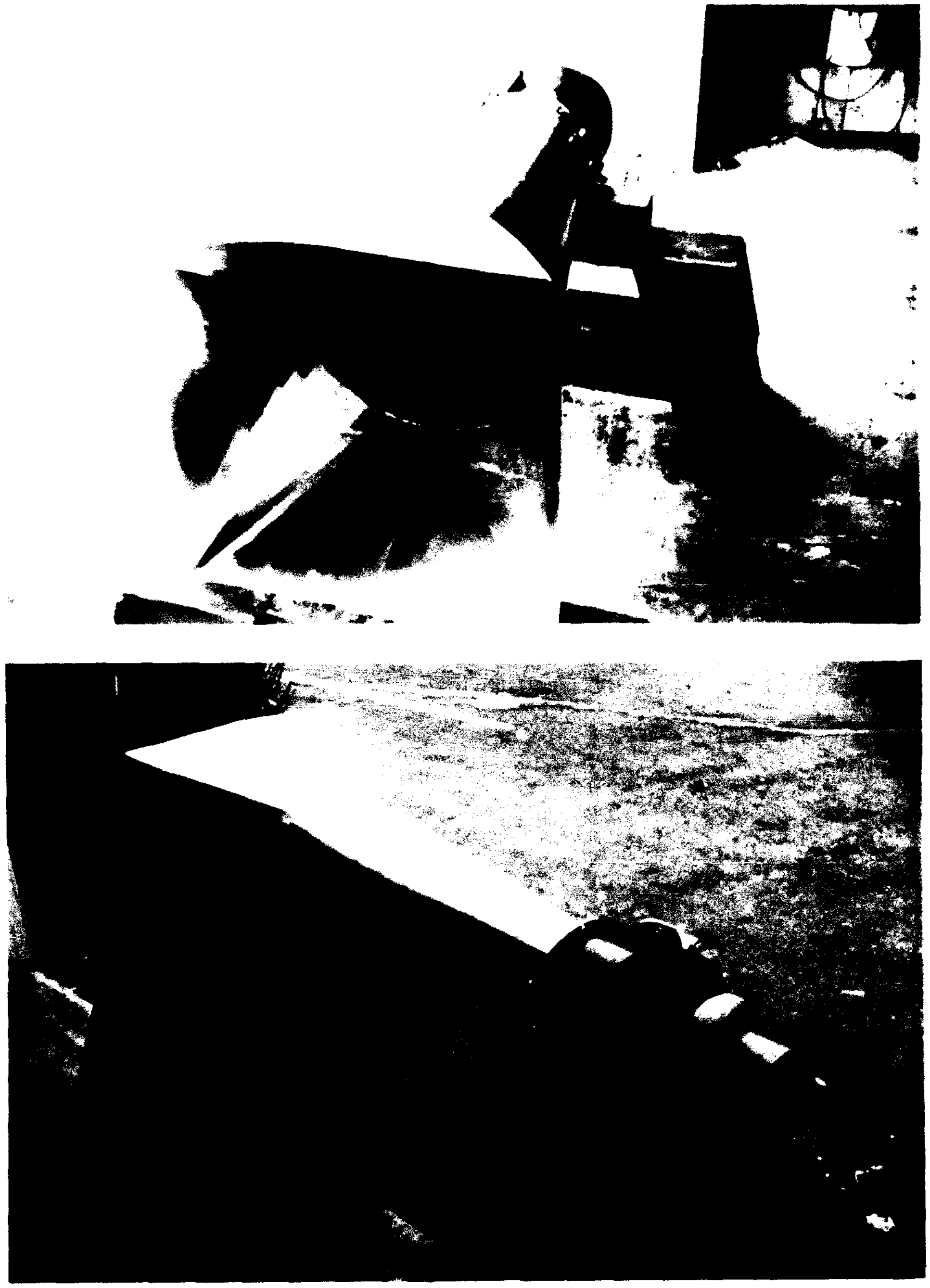

Figure 29 - TCS Diffuser Assembly

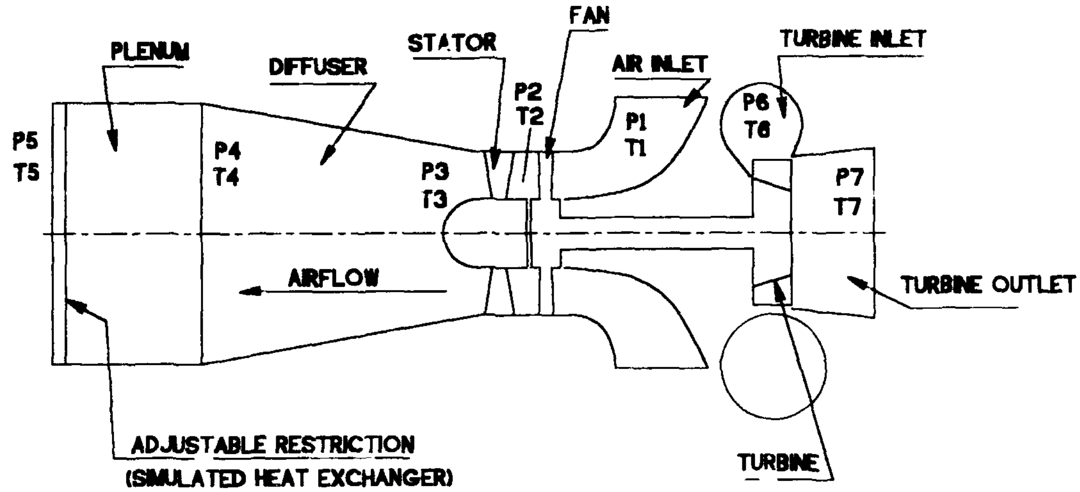

Figure 30 - TCS instrumentation points

Figure 31 - Golden West Dynamometer

Figure 32 - TCS Test

Figure 33 - TCS Test

Figure 34 - TCS Test

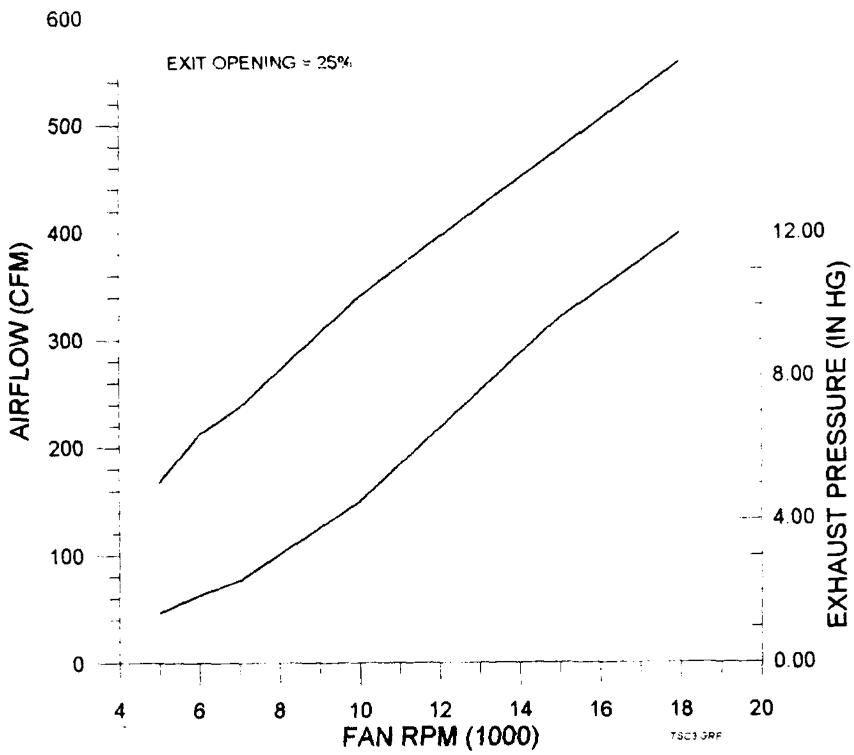

Figure 35 - TCS Airflow and Exhaust Backpressure

11.3 *TCS conclusions:*

- The prototype was built and successfully demonstrated to be a viable concept for future combat vehicles.
- Prototype fan airflow and efficiency are less than predicted. A hot bench test program should be performed to characterize the fan performance under controlled conditions.
- Matching of the prototype TCS fan to the VTA-903 engine is not optimized. Future TCS engine tests should be performed after an analysis of the complete engine and TCS system is made.
- Fan blade modeling and casting techniques need to be improved. Higher accuracy tooling is necessary to achieve better efficiency and reliability.
- TCS durability and burst tests should be included in a future development program.
- The TCS design should be reviewed to improve the ease of assembly.
- The TCS air ducting design should be improved to minimize flow losses

12.0 Technical problems Encountered and Solutions:

During the course of this program, various technical problems were encountered and solved. This section describes those experiences.

12.1 Injector nozzle failures: During early bench calibration tests, several injector nozzle failures were experienced when run at rail pressures above 800 PSI. In each case, the tip of the nozzle broke out in line with the drilled holes (Figures 36, and 37). The failures were originally attributed to the nozzle material (52100) and heat treat. A new set of nozzles were machined by BKM using an OEM material (GM 7520 Semi-Stainless) and then heat treated by Diesel Technology Corporation (Detroit Diesel). This increased the failure point to 1200 PSI but did not entirely solve the problem. Following a design review of the nozzle and a detailed inspection of the failed parts, the cracks were found to be originating at the machined radius immediately above the needle seat. Various machining modifications were incorporated to improve stress concentration and eliminate tool marks in that area. The final design was

Figure 36 - Injector Nozzle Failures

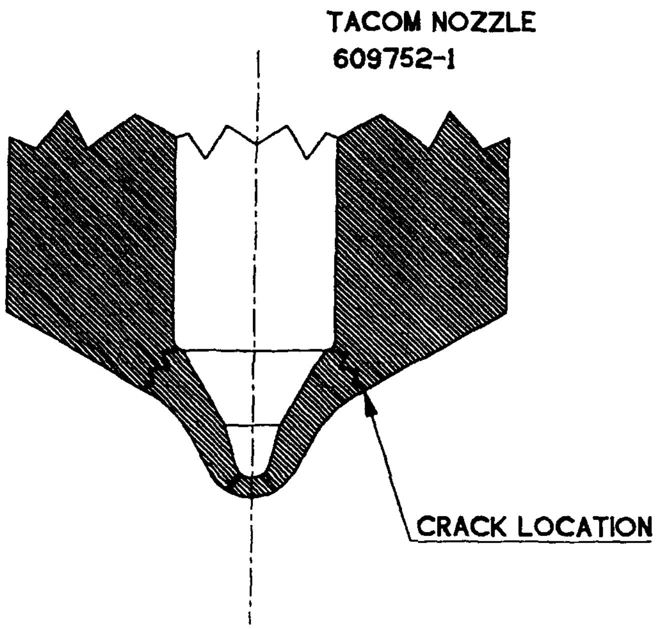

Figure 37 Injector Nozzle Cross Sectional Drawing

bench tested for 160 hours (10 million cycles) at full rail pressure (1500 PSI) without failure. A revised set of injector nozzles were manufactured, calibrated, and installed in the VTA-903 engine. No further nozzle failures occurred during the remainder of this project.

12.2 Injector leakage: Internal sealing of the unit injector depends partially on the creation of high unit pressures between two lapped mating surfaces in the injector body (see section B-B in drawing 608400, Appendix C5). A large nut clamps the intensifier body to the intermediate body at this mating surface. It was found that the nut threads failed before the torque required to maintain an adequate clamping force was reached. The solution was to reduce the mating surface area by removing material between the fluid passages and dowel pin holes . This resulted in an increased clamping pressure at a reduced nut torque and eliminated the leakage.

12.3 Injector hold-down clamp breakage: The stock Cummins injector clamps, which had to be modified for injector clearance, broke upon installation in the engine. Strength tests were performed on a previous revision of this clamp early in the design process, however, it was found that the currently available production version does not have adequate strength when modified. This problem was solved by machining a set of clamps from 4140 steel. No further failures were experienced.

12.4 Fuel Contamination: On numerous occasions, small metal shavings in the EPR caused the high pressure relief valve to stick open. This resulted in a loss of rail pressure. In addition to EPR contamination, debris also caused several injectors to fail. The source of these shavings was not conclusively determined but "last chance" filters installed in fuel rail lines (EPR outlets) and a filter at the EPR inlet solved the problem.

12.5 High smoke levels: During engine tests and flame photo runs, the smoke meter readings were higher than expected. The high smoke is caused by cylinder wall fuel impingement as seen in the flame photos. Additional research is needed to optimize the combustion chamber shape, air swirl pattern, and injection spray characteristics to eliminate wall wetting and reduce smoke. Recent success in a production engine development program indicates that dramatic smoke reduction is possible with combustion system optimization.

12.6 Low boost: Initial engine performance tests indicated a lower than expected boost pressure with the twin WS-90 turbochargers installed. Several possible explanations for this were explored. Analysis indicated that the problem was a combination of incorrect matching of the turbocharger to the engine and a loss of exhaust efficiency from the original exhaust manifold design.

The WS-90 turbochargers were designed to be manufactured with either a 3.40 or a 4.00 square in. turbine inlet area. The optimum area for the VTA-903 twin turbo configuration is 3.40 However, only the 4.00 version was available for this test. This caused the boost pressure to be lower than desired. This was verified during the engine tests by closing either the axial or radial half of the turbine which effectively reduced the inlet area. When one half was closed, the boost pressure increased to normal levels as expected. For future engine tests, turbochargers with the appropriate inlet area should be built and installed.

The exhaust manifold was originally designed with a "stuffing plate" that was intended to fill a dead space in the exhaust port ceiling. The original manifold flange opening was also found to be smaller than the cylinder head port opening, further restricting exhaust flow. To improve exhaust efficiency, the stuffing plate was removed and the flange opening was increased to match the port.

Back to back tests conducted with the stock single turbocharger installed confirmed that the reduced boost was not due to the fuel system.

12.7 Rail pressure surges: During the engine tests, occasional transient rail pressure surges were observed. Typically, these were brief (approximately 100-200 mSec) increases in rail pressure. The transient pressure change was as much as 100 PSI. At the conclusion of the test program, it had not yet been determined if this was due to hardware - such as a sticking EPR - or if a random software bug was commanding the event. The transient was brief enough and infrequent enough that it did not affect the test data, however it should be investigated if this fuel system is the subject of further tests.

13.0 Conclusions and recommendations

13.1 Project Achievements:

This project has achieved the following:

Remote control cartridge injector designed - A separate injector control cartridge was engine tested for the first time. This design allows installation of the Servojet injector in cylinder heads like the VTA-903 where space is limited or the environmental conditions (temperature and oil splash) could adversely affect the solenoid valve.

Injector design improvement - Through extensive bench and engine testing of the fuel injectors a better understanding was gained of the factors that influence performance and reliability. This knowledge will improve all future diesel injector designs.

Demonstrated diesel electronic control - Continuous operator control of all engine control parameters including timing (Figure 38), governor mode, idle speed, sensor calibration, and fuel delivery curves.

Electronic control unit reliability demonstrated - This application marked the first engine-mounted ECU installation. Although a preliminary shock and vibration bench test was performed on this ECU design, reliability under actual engine vibration and temperature conditions was previously unproved. No failures of the control unit were experience during engine testing.

A. Advanced Timing
SOI = 5 degrees BTDC

800 RPM, Cylinder #4,
20 cubic mm per injection

Upper Trace: Accumulator Pressure from Strain Gauge

Lower Trace: Cylinder Pressure

B. Standard Timing
SOI = TDC

C. Retarded Timing
SOI = 5 degrees ATDC

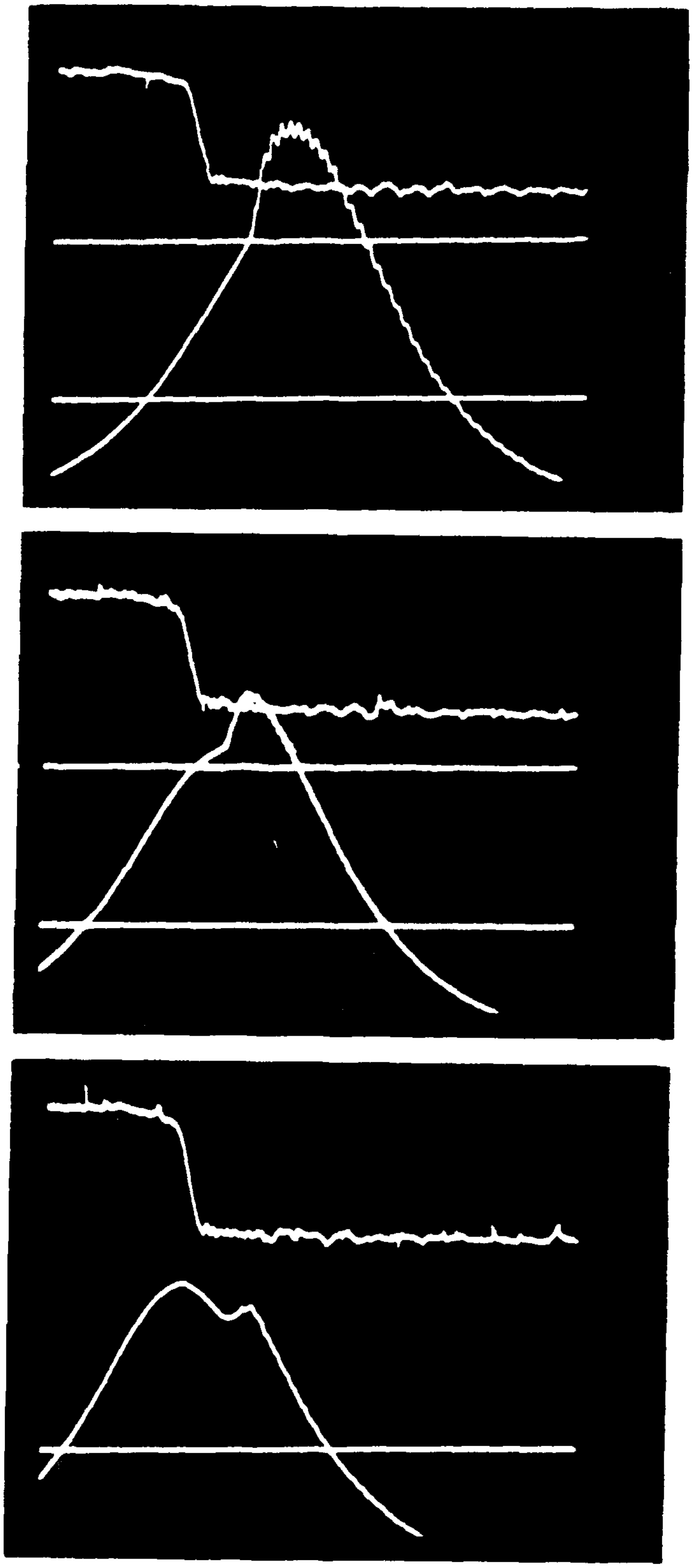

Figure 38 - Effect of Injection Timing on Cylinder Pressure

RV-40 pump and gear drive reliability demonstrated - This project saw the first use of the RV-40 fuel pump on an engine. The pump gear drive assembly was designed and built for this program Both performed flawlessly.

WS-90 Variable Area Turbocharger tested - This component, designed and manufactured under a previous TACOM contract, exhibited good performance with no failures. The VAT control concept was shown to be a practical way to modify turbine inlet area and the resulting gas velocity on a running engine.

Improved throttle response demonstrated - The WS-90 turbochargers reduced the throttle response time in half compared to the stock single turbocharger.

Demonstrated engine power equal to or higher than stock - The engine output with the Servojet fuel system easily matched stock levels except at the maximum tested speed (2600 RPM) where the injected fuel quantity was slightly low. With an improved injector spray pattern to eliminate the smoke-producing wall wetting, the power levels are expected to increase without the need to increase the fuel quantity. The BSFC at peak power should show a corresponding improvement.

Combustion flame photography test conducted - A better understanding of in-cylinder injection spray patterns and the effect of rate shaping on flame initiation and burning has been gained. High smoke levels experienced during VTA-903 engine tests were duplicated in the optical engine and attributed to cylinder wall wetting.

Turbocompound cooling fan concept demonstrated - A prototype exhaust driven fan was designed and built to prove the concept. Preliminary engine tests were conducted that indicate that this approach to engine cooling is feasible. However, the fan and turbine design need to be refined and better matched to this engine.

Regenerative heating cold start technique - A non-running bench test of compression heating demonstrated a significant charge air temperature rise (42 degrees C above ambient) in the inlet manifold of a single cylinder engine. This concept is worthy of further study using both bench tests and running engines to quantify the temperature rise that can be achieved.

13.2 Recommended system development: The subject Servojet engine control system successfully demonstrated that electronic control of diesel fuel injection is a powerful engine development tool. This prototype hardware generally performed up to expectations, however, lessons learned during this program indicate that improvements should be made in the following areas to bring reliability and performance to a production level and realize a significant improvement over existing fuel systems.

1. Improve injector reliability and minimize delay variation between iniectors. This can be achieved with careful selection of materials and attention to machining and assembly tolerances.

2. Match turbocharger to engine. A pair of the smaller 3.40 square In. inlet area WS-90 turbochargers should be built and installed on the VTA-903. This will result in higher boost and better throttle response compared to the 4.00 square In. version. An improved dual-range version of the WS-90, which has increased low speed torque, should also be tested.

3. Software calibration and strategy refinement. Dynamometer engine mapping should continue to optimize the fuel delivery curve over the entire engine operating range. The current software look up tables are a close approximation but there is room for improvement. Future vehicle drivability tests will also influence the software calibration.

4. Eliminate rail pressure surges. The source of these pressure surges should be investigated and corrected.

13.3 Recommended additional research: It is recommend that a single cylinder research engine, with the same bore and stroke as the VTA-903, be equipped with a Servojet fuel system and used to explore the effect that injection spray pattern, rate shapes, combustion chamber shape, and swirl have on power, fuel efficiency, and exhaust emissions - especially smoke. Various injector nozzles and rate shapes should be engine tested with a variety of piston bowl shapes. It is clear that optimum results cannot be achieved by simply bolting the Servojet fuel injectors into an engine with a combustion system that was optimized for another fuel system.

Single cylinder research should also be done to achieve a practical regenerative cold start system on a running engine. Design, fabricate, and test a prototype control system to disable the inlet and exhaust valves during cranking. An electro-hydraulic system, controlled by the ECU, is recommended.

Once a practical cold start system is demonstrated and the combustion chamber has been optimized, a Servojet second generation VTA-903 fuel and exhaust systems should be built and installed. These systems will incorporate all the lessons learned during this project regarding system design, performance, and reliability. Dynamometer performance tests and vehicle drivability and durability tests would then demonstrate the full potential of the Servojet system.

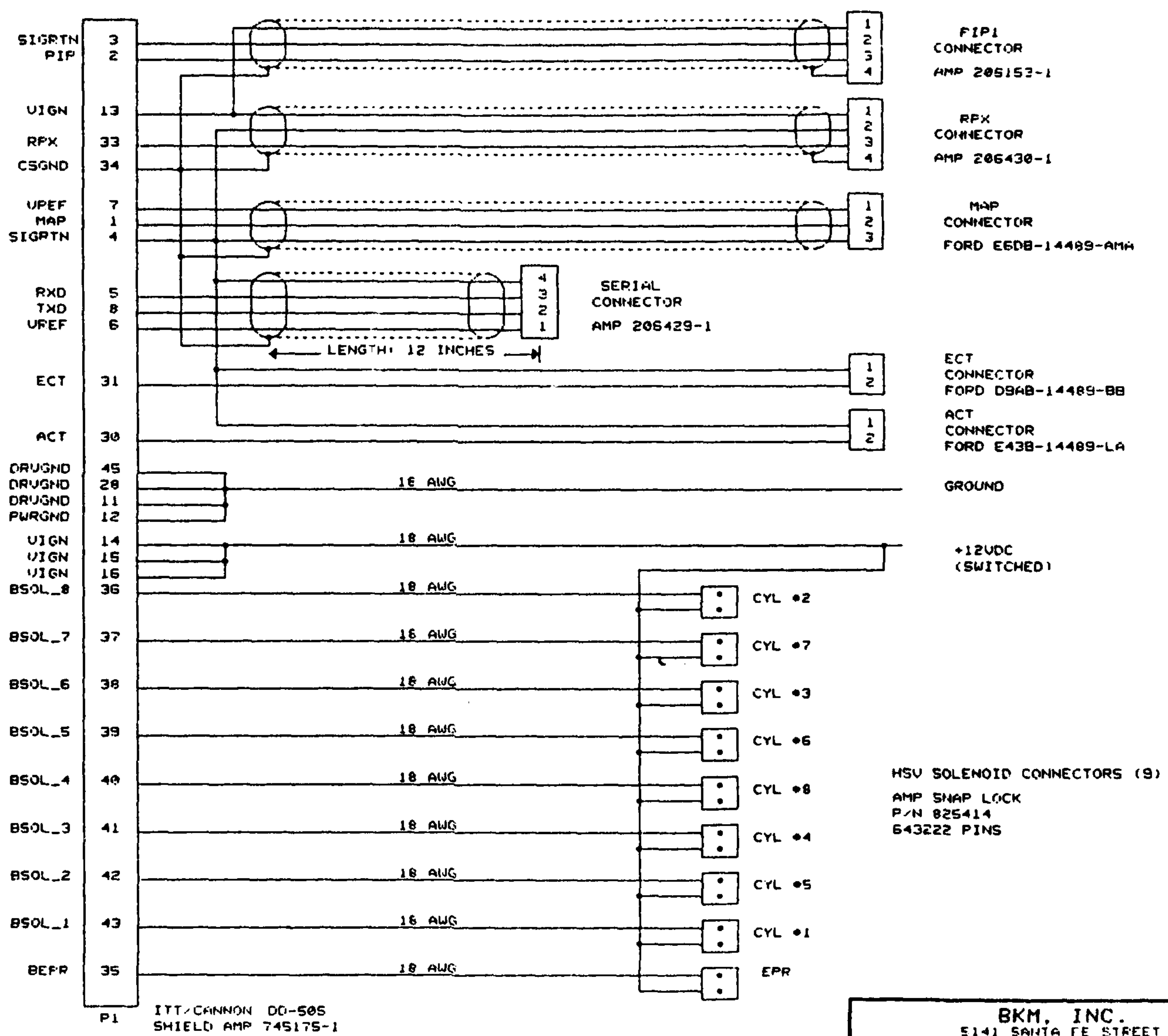

NOTES:

1. LENGTH: 6 FEET
2. ALL WIRES 22 AWG, 105 DEG C. PVC INSULATED
   EXCEPT 18 AWG POWER AND SOLENOID LEADS
3. INSTALL ROUND CONVOLUTED CONDUIT OVER WIRING HARNESS

DRAWN:	DCS
CHECKED:	
APPROVED:	

BKM, INC.
5141 SANTA FE STREET
SAN DIEGO, CA. 92109

WIRING HARNESS, ECU

D	607095 (TACCABLE.P01)	REV	0
DATE:	9/28/93	SHEET	1 OF 1

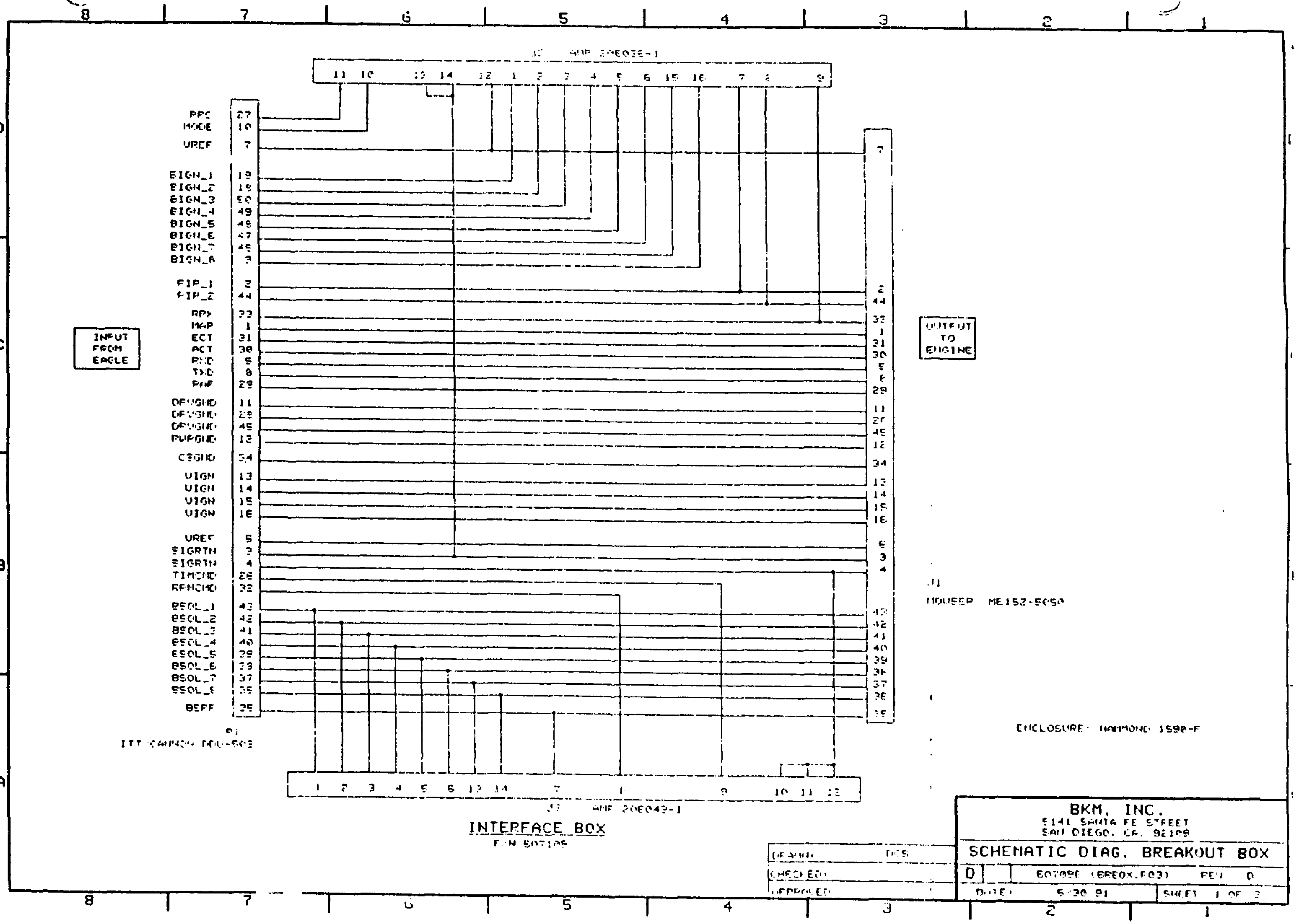

J2 AMP 206036-1
INPUT FROM EAGLE
PPC
MODE
VREF
BIGN_1
BIGN_2
BIGN_3
BIGN_4
BIGN_5
BIGN_6
BIGN_7
BIGN_8
PIP_1
PIP_2
RPX
MAP
ECT
ACT
RXD
TXD
PNF
DRVGND
DRVGND
DRVGND
PWPGND
CSGND
VIGN
VIGN
VIGN
VIGN
VREF
SIGRTN
SIGRTN
TIMCMD
RFNCMD
BSOL_1
BSOL_2
BSOL_3
BSOL_4
BSOL_5
BSOL_6
BSOL_7
BSOL_8
BEFF
P1
ITT/CANNON DDU-50S
OUTPUT TO ENGINE
J1
MOUSER ME152-5050
ENCLOSURE: HAMMOND 1590-F
J3 AMP 206043-1
INTERFACE BOX
P/N 507105
BKM, INC.
5141 SANTA FE STREET
SAN DIEGO, CA. 92109
SCHEMATIC DIAG. BREAKOUT BOX
D
507090 (BREOX.F03)
REV 0
DATE: 5/30/91
SHEET 1 OF 2
DRAWN DCS
CHECKED
APPROVED

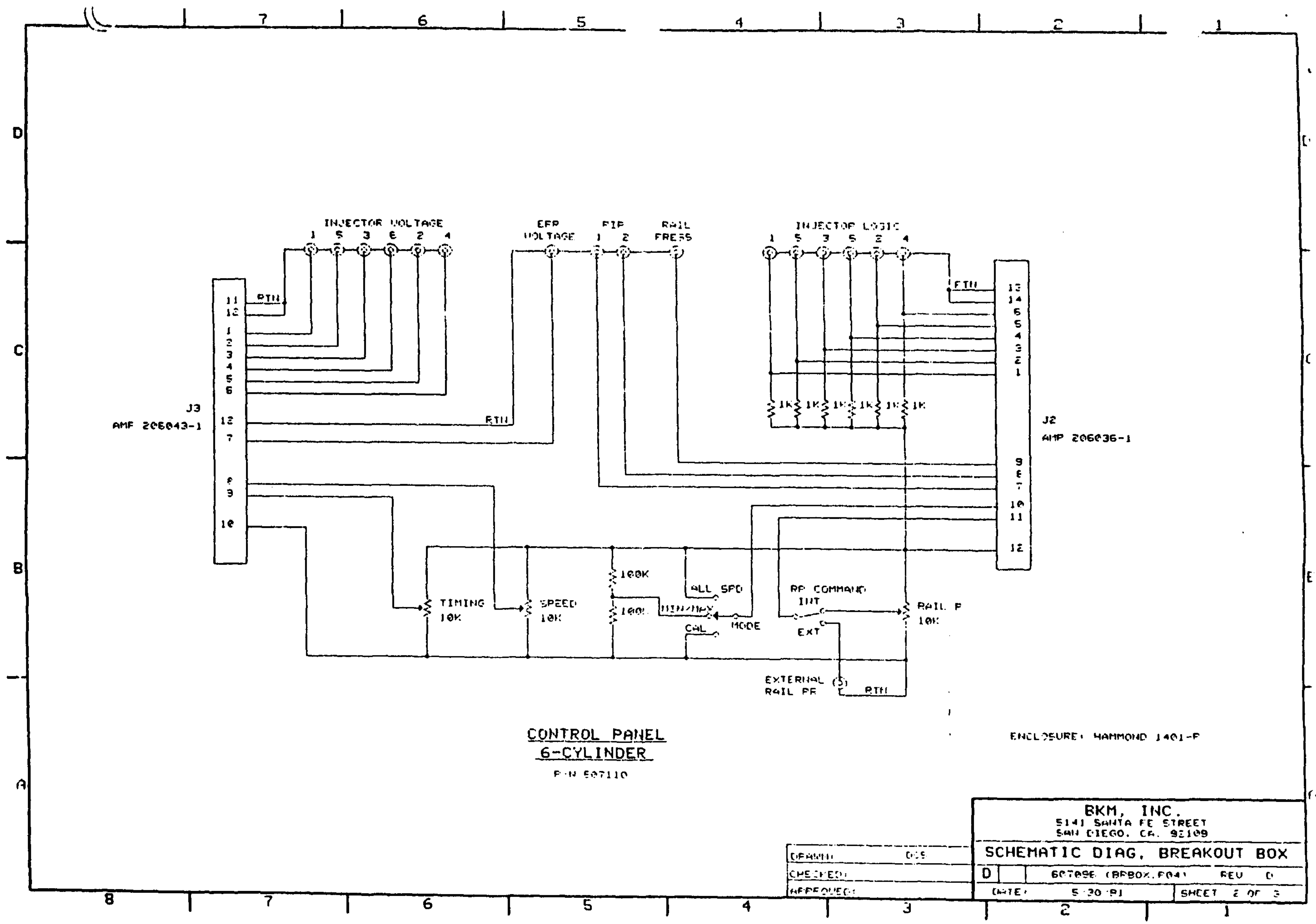
INJECTOR VOLTAGE
1 5 3 6 2 4
EFP VOLTAGE
PIP 1 2
RAIL PRESS
INJECTOR LOGIC
1 5 3 6 2 4
RTN
J3
AMP 206043-1
J2
AMP 206036-1
1K
100K
ALL SPD
MIN/MAX
CAL
MODE
RP COMMAND
INT
EXT
TIMING 10K
SPEED 10K
RAIL P 10K
EXTERNAL RAIL PR
CONTROL PANEL
6-CYLINDER
P/N 507110
ENCLOSURE: HAMMOND 1401-P
BKM, INC.
5141 SANTA FE STREET
SAN DIEGO, CA. 92109
SCHEMATIC DIAG, BREAKOUT BOX
D
607096 (BRBOX.P04)
REV 0
DRAWN: DCS
CHECKED:
APPROVED:
DATE: 5-20-91
SHEET 2 OF 3

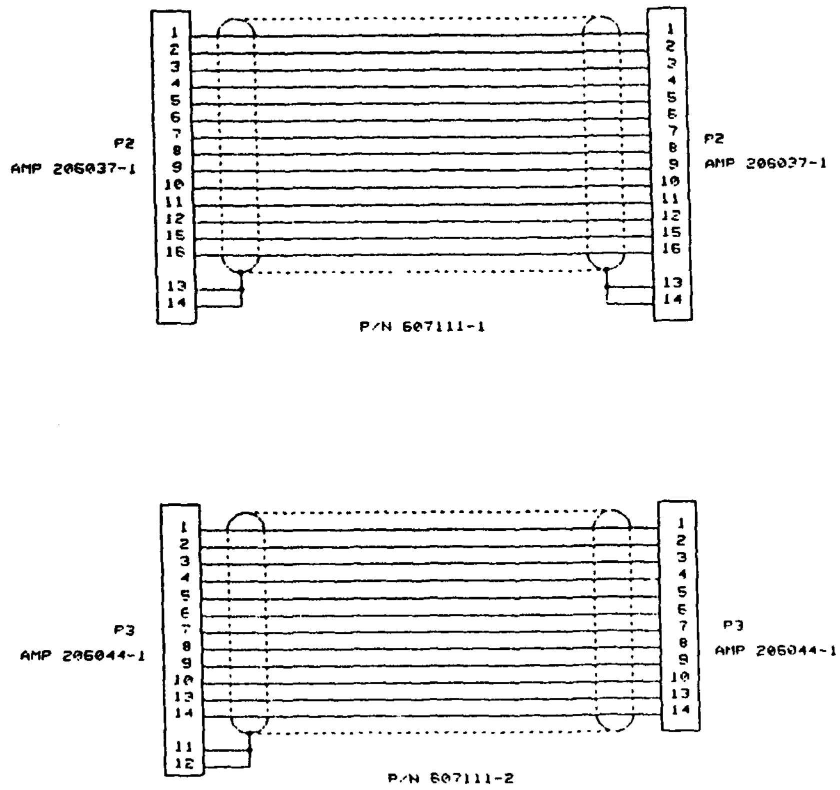

WIRE TYPE: 22 AWG SHIELDED CABLE

INTERCONNECT CABLES

DRAWN:	DCS
CHECKED:	
APPROVED:	

BKM, INC.
5141 SANTA FE STREET
SAN DIEGO, CA. 92109

SCHEMATIC DIAG, BREAKOUT BOX

D | 607096 (BRBOX.P0S) | REV C

DATE: 5/30/91 | SHEET 3 OF 3

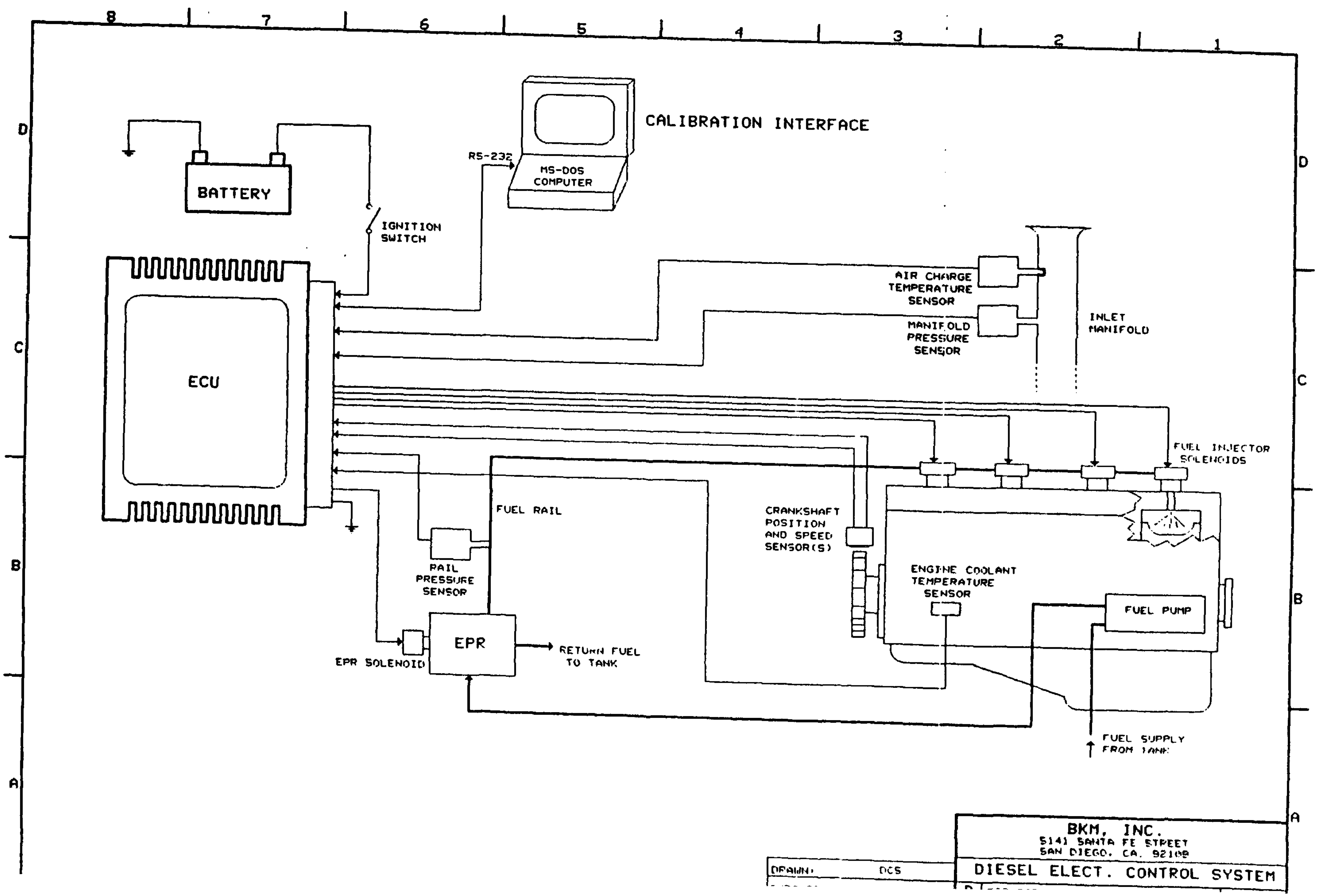

CALIBRATION INTERFACE
RS-232
MS-DOS COMPUTER
BATTERY
IGNITION SWITCH
ECU
AIR CHARGE TEMPERATURE SENSOR
MANIFOLD PRESSURE SENSOR
INLET MANIFOLD
FUEL INJECTOR SOLENOIDS
FUEL RAIL
CRANKSHAFT POSITION AND SPEED SENSOR(S)
ENGINE COOLANT TEMPERATURE SENSOR
FUEL PUMP
RAIL PRESSURE SENSOR
EPR
EPR SOLENOID
RETURN FUEL TO TANK
FUEL SUPPLY FROM TANK
BKM, INC.
5141 SANTA FE STREET
SAN DIEGO, CA. 92109
DIESEL ELECT. CONTROL SYSTEM
DRAWN: DCS

130894

(1)

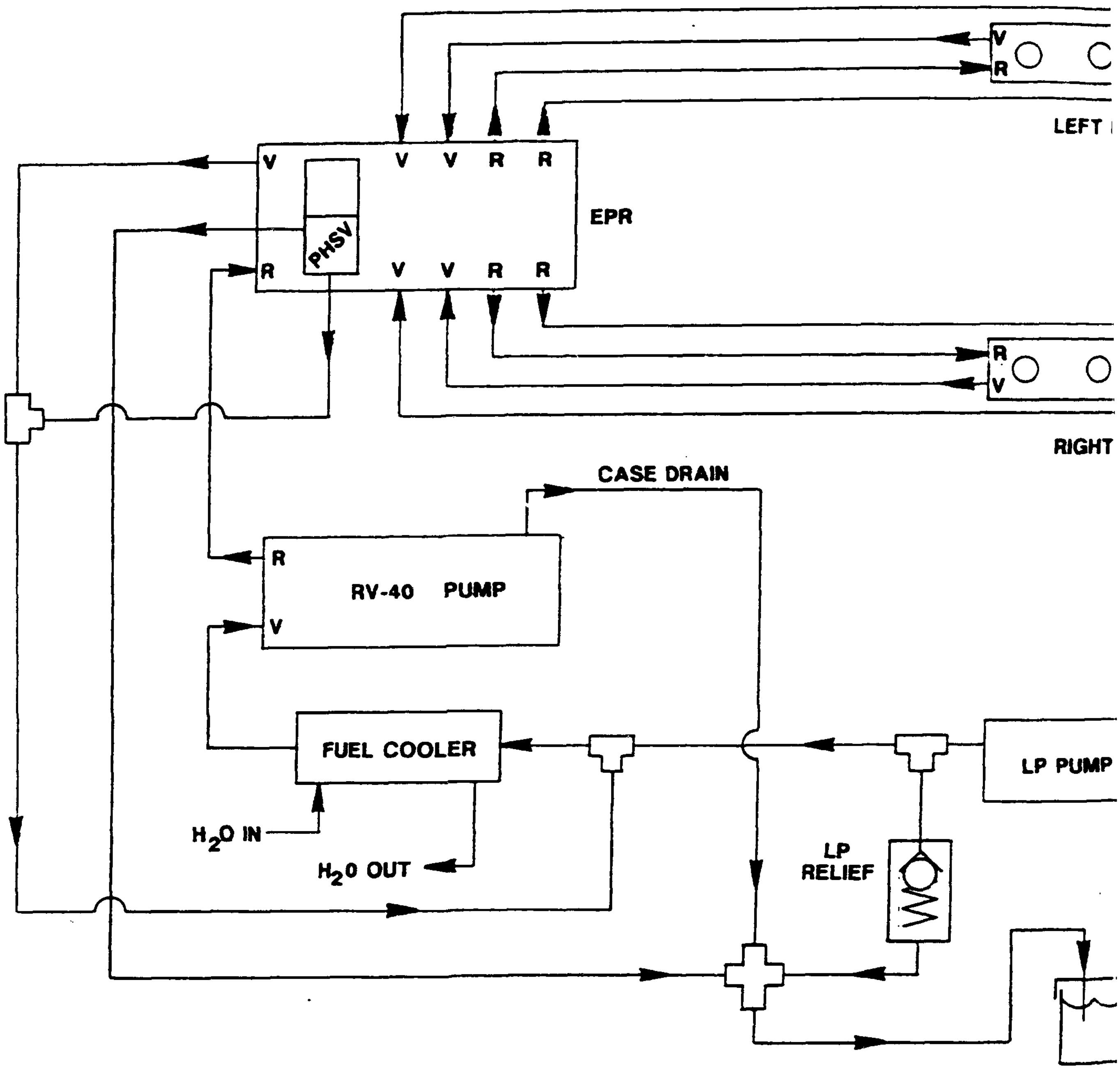

			UNLESS OTHERWISE SPECIFIED TOLERANCES ON THREE PLACES DECIMALS ±.005 · TWO PLACES DECIMALS ±.01 · ANGLES ±1/2
			DO NOT SCALE DRAWING
			MATERIAL
25138			FINISH
PROJECT USED ON	NEXT ASSEM.	QTY. REQ'D.	

FORM 92 REV D

REVISIONS		
LTR	ZONE	DESCRIPTION

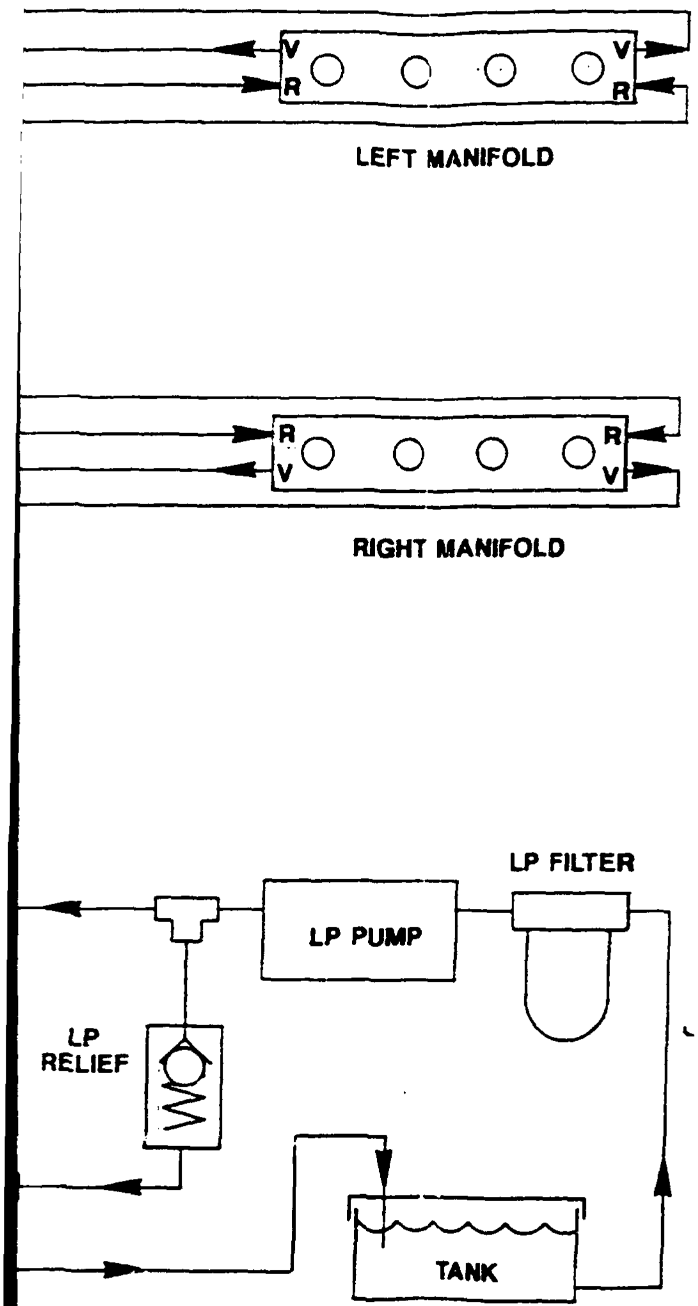

UNLESS OTHERWISE SPECIFIED
TOLERANCES ON

THREE PLACES DECIMALS	TWO PLACES DECIMALS	ANGLES
±.005	±.01	±1/2°

DO NOT SCALE DRAWING

MATERIAL

FINISH

BKM, Inc.
5141 Santa Fe Street
San Diego, CA 92109

DRAWN	S. DODGE	10-1-90
CHECKED	D. STEINMEYER	10-9-90
ENGINEER		
APPROVED		

TITLE

FUEL SCHEMAT

SIZE: B

DRAWING: 6101

SCALE: NONE

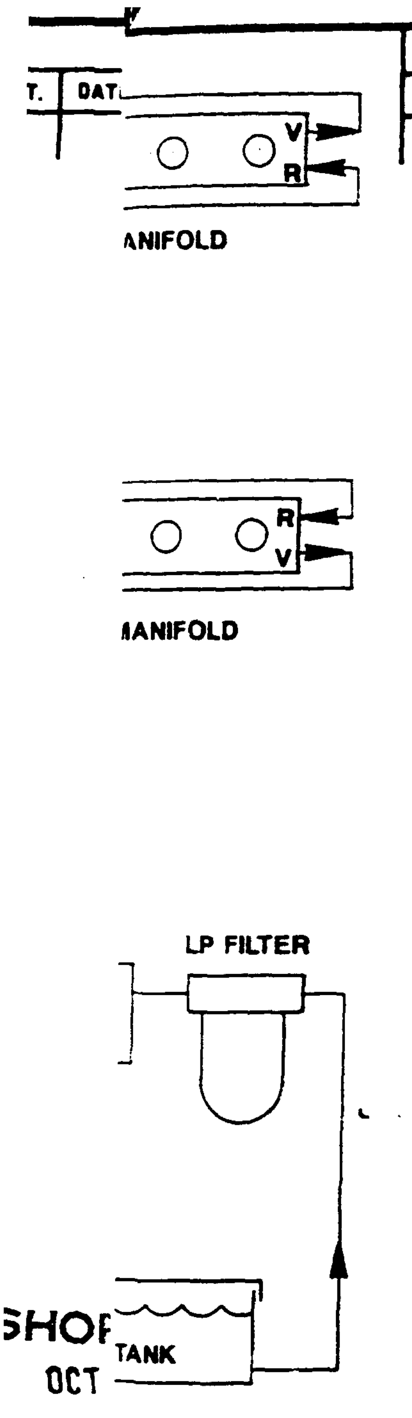

REVISIONS						
LTR	ZONE	DESCRIPTION	DRFT.	DATE	CHK'D	APPD.

SHOP COPY
OCT 0 9 1990

BKM, Inc.
5141 Santa Fe Street
San Diego, CA 92109

TITLE

FUEL SCHEMATIC

DRAWN	S. DODGE	10-1-90
CHECKED	D. STEINMEYER	10-9-90
ENGINEER		
APPROVED		

SIZE	DRAWING NO.	LTR
B	610106	—

SCALE NONE | SHEET 1 OF 1

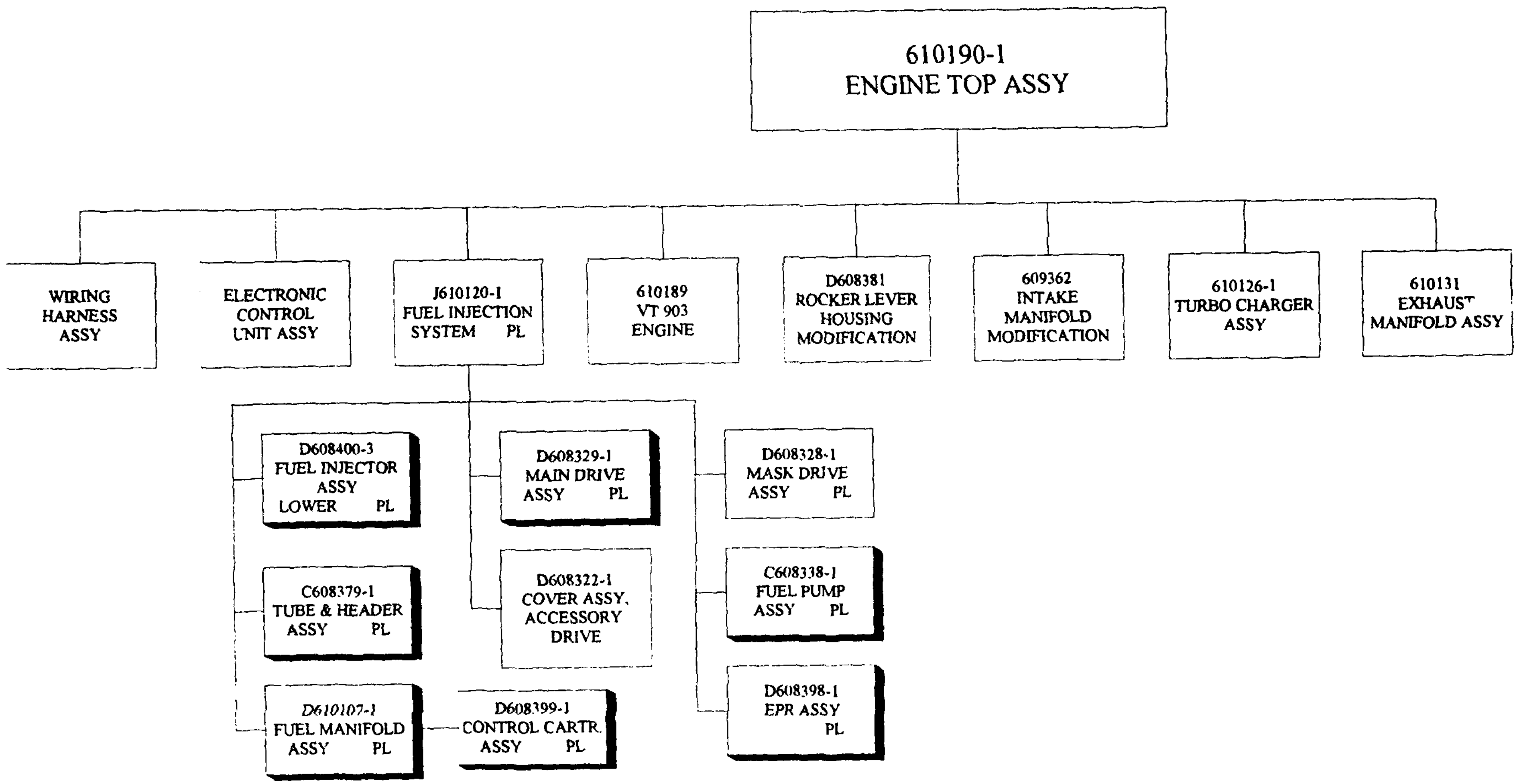

610190-1
ENGINE TOP ASSY
WIRING HARNESS ASSY
ELECTRONIC CONTROL UNIT ASSY
J610120-1 FUEL INJECTION SYSTEM PL
610189 VT 903 ENGINE
D608381 ROCKER LEVER HOUSING MODIFICATION
609362 INTAKE MANIFOLD MODIFICATION
610126-1 TURBO CHARGER ASSY
610131 EXHAUST MANIFOLD ASSY
D608400-3 FUEL INJECTOR ASSY LOWER PL
C608379-1 TUBE & HEADER ASSY PL
D610107-1 FUEL MANIFOLD ASSY PL
D608399-1 CONTROL CARTR. ASSY PL
D608329-1 MAIN DRIVE ASSY PL
D608322-1 COVER ASSY, ACCESSORY DRIVE
D608328-1 MASK DRIVE ASSY PL
C608338-1 FUEL PUMP ASSY PL
D608398-1 EPR ASSY PL

PARTS LIST NUMBER:PL610190

PARTS LIST TITLE: ENGINE TOP ASSEMBLY
PROJECT NUMBER: 25138
INITIAL RELEASE: 12-13-90
REVISION LTR:
REVISION DATE:
ENGINE USAGE: VT903
FILE NAME: TACENG01.XSS

ITEM NO	PART NUMBER	REV	NOMENCLATURE	QTY -1	MATERIAL TYPE-ALLOY
1	610190-1		ENGINE ASSEMBLY	-	
2	J610120-1		.FUEL INJECTION SYSTEM	1	
3	610189-1		.ENGINE	1	VT-903
4	610124-1		.TRANSDUCER INSTL.-C.P.	1	
5	610125-1		.FLYWHEEL MODIFICATION	1	
6	610129-1		.ENGINE OIL FILTER INSTL.	1	
7	610130-1		.AIR INTAKE INSTL.	1	
8	610127-1		.ENGINE COOLANT PLUMBING	1	
9	610132-1		.TIMING SENSORS INSTL.	1	
10	610133-1		.TEST SENSORS INSTL.	1	
11	610126-1		.TURBOCHARGER ASSY.	1	
12	610131-1		.EXHAUST MANIFOLD ASSY		
13			.TURBO SUPPORTS		
14	610155-1		.EXHAUST ADAPTER		
15			.ELEC. CONTROLLER ASSY		
16			.WIRING HARTNESS ASSY		
17			.INJECTOR BORE MOD.		
18			.RCKR.LEVER HSG.MOD.		
19			.INTAKE MANIFOLD MOD.		
20			.PLUG-FOLLOWER BORE		
ITEM NO	PART NUMBER	REV	NOMENCLATURE	QTY -1	MATERIAL TYPE-ALLOY

PARTS LIST NUMBER: PL610190

PARTS LIST TITLE: ENGINE TOP ASSEMBLY
PROJECT NUMBER: 25138
INITIAL RELEASE: 12-13-90
REVISION LTR:
REVISION DATE:
ENGINE USAGE: VT903
FILE NAME: TACENG02.XSS

ITEM NO	PART NUMBER	REV	NOMENCLATURE	QTY -1	MATERIAL TYPE-ALLOY
21	608851-1	-	.BUSHING-ROCKER ARM	1	
22					
23					
24					
25					
26					
27					
28					
29					
30					
31					
32					
33					
34					
35					
36					
37					
38					
39					
40					
ITEM NO	PART NUMBER	REV	NOMENCLATURE	QTY -1	MATERIAL TYPE-ALLOY

PARTS LIST NUMBER:PL610120

PARTS LIST TITLE: TACOM II FUEL INJECTION SYSTEM
PROJECT NUMBER: 25138
INITIAL RELEASE: 12-6-90
REVISION LTR:
REVISION DATE:
ENGINE USAGE: VT903
FILE NAME: TACFIS01.XSS

ITEM NO	PART NUMBER	REV	NOMENCLATURE	QTY -1	MATERIAL TYPE-ALLOY
1	J610120-1	-	FUEL INJECTION SYSTEM	1	
2	D608400-3	A	.FUEL INJECTOR ASSY(LWR)	8	
3	B610160-1	-	.CLAMP - INJ. HOLDDOWN	8	M/F CUMMINS P/N:
4	D900301-34	-	.SHCS - INJ. CLAMP	8	3/8-16UNC x 2.25
5	D901002-11	-	.SPACER - INJ. CLAMP	8	3/8
6	C608379-1	-	.TUBE & HEADER ASSY	8	
7	D900301-11	-	.SHCS-INJ.	48	#10-32UNF-2A x 5
8	D900501-1	-	.LOCKWASHER-INJ.	48	#10
9	D900301-33	-	.SHCS-CART.	32	1/4-28UNF-2A x 3
10	D900501-2	-	.LOCKWASHER-CART.	32	1/4
11	D900201-54	-	.O-RING - INJ.	8	3-911 (N552-90)
12	D900202-8	-	.O-RING - CART.	24	2-011 (V884-75)
13	D900201-57	-	.O-RING - INJ.	16	2-008 (N552-90)
14	D610107-1	-	.FUEL MANIFOLD ASSY	2	
15	D900301-21	-	.SHCS-MAN. ATTACH	10	3/8-16UNC x 3 LO
16	D900501-6	-	.LOCKWASHER	18	3/8 HI-COLLAR
17	D900301-26	-	.SHCS-VALVE COVER	7	3/8-16UNC x 1.5
18	D901002-12	-	.SPACER	8	3/8
19	D901402-12	-	.NUT-HEX	1	3/8-16UNC
20	D902701-1	-	.STUD	1	3/8-16UNC x 1.5
ITEM NO	PART NUMBER	REV	NOMENCLATURE	QTY -1	MATERIAL TYPE-ALLOY

PARTS LIST TITLE: TACOM II FUEL INJECTION SYSTEM
PROJECT NUMBER: 25138
INITIAL RELEASE: 12-13-90
REVISION LTR:
REVISION DATE:
ENGINE USAGE: VT903
FILE NAME: TACFIS02.XSS

ITEM NO	PART NUMBER	REV	NOMENCLATURE	QTY -1	MATERIAL TYPE-ALLOY
21					
22	D608329-1	-	.MAIN DRIVE ASSEMBLY	1	
23	D900301-35	-	.SHCS	3	3/8-16 UNC x 3.50
24	D900301-36	-	.SHCS	1	3/8-16 UNC x 3.75
25					
26	D608328-1	-	.MASK DRIVE ASSEMBLY	1	
27	D900301-37	-	.SHCS	3	10-24 UNC x .875
28		-			
29	C608338-1	-	FUEL .PUMP ASSEMBLY	1	
30	D900302-15	-	.SHCS	3	M10x1.5x40.0
31					
32	610194-1	-	.COVER ASSY-ACCESS.DRIVE	1	
33	D608322-1	-	..COVER	1	
34	A903701-1	-	..HELICOIL	4	
35	610188-1	-	..PLUG	1	
36	610187-1	-	.GASKET	1	
37					
38					
39					
40					
ITEM NO	PART NUMBER	REV	NOMENCLATURE	QTY -1	MATERIAL TYPE-ALLOY

PARTS LIST NUMBER: PL610120

PARTS LIST TITLE: TACOM II FUEL INJECTION SYSTEM
PROJECT NUMBER: 25138
INITIAL RELEASE: 12-12-90
REVISION LTR:
REVISION DATE:
ENGINE USAGE: VT903
FILE NAME: TACFIS03.XSS

ITEM NO	PART NUMBER	REV	NOMENCLATURE	QTY -1	MATERIAL TYPE-ALLOY
41	D608398-1	-	.EPR ASSY	1	
42	610191-1	-	.BLOCK-MTG.	1	
43	610192-1	-	.PLATE-MTG	1	
44	D900309-4		.SCREW-HEX CAP	4	3/8-16 UNC x 1.
45	D900501-10		.LOCKWASHER	4	3/8 REGULAR
46	D900301-34		.SHCS	2	3/8-16 UNC x 2.25
47					
48					
49					
50	D900601-4	-	.ACCUMULATOR	2	
51	90	-	.CLAMP	2	
52	D900417-	-	.FITTING-ADAPTER	2	
53	90	-	.STUD	2	
54	90	-	.NUT	2	
55	90	-	.LOCKWASHER	2	
56					
57	90	-	.FUEL FILTER (LP)	1	
58	90	-	.BRACKET	1	
59	610	-	.SHIM	1	
60	D900	-	.FITTING	1	
ITEM NO	PART NUMBER	REV	NOMENCLATURE	QTY -1	MATERIAL TYPE-ALLOY

PARTS LIST NUMBER: PL610120

PARTS LIST TITLE: TACOM II FUEL INJECTION SYSTEM
PROJECT NUMBER: 25138
INITIAL RELEASE: 12-12-90
REVISION LTR:
REVISION DATE:
ENGINE USAGE: VT903
FILE NAME: TACFIS04.XSS

ITEM NO	PART NUMBER	REV	NOMENCLATURE
***			REFERENCE DRAWING LIST
***			
***	D609910		L/O VT903 INJECTOR SLEEVE
***	C608357		DESIGN L/O - TUBING
***	C610136		CARTRIDGE INSERTION L/O (MANIFOLD)
***	C608572		INJ.& MAN. INSTALLED L/O
***	D608391		INJ.& MAN.ARRANGEMENT L/O
***	B610106		FUEL SCHEMATIC
***	C608809		INJ.BORE MODIFICATION (VT-903)
***	D608212		GEARBOX LAYOUT (MASK & FUEL PUMP)
***			
***			
***			
***			
***			
***			
***			
***			
***			
***			

ITEM NO	PART NUMBER	REV	NOMENCLATURE	QTY -1	MATERIAL TYPE-ALLOY

PARTS LIST NUMBER: PL608400

PARTS LIST TITLE: TACOM INJECTOR ASSY. (G-4)
PROJECT NUMBER: 25138
INITIAL RELEASE: 11-26-90
REVISION LTR:
REVISION DATE:
ENGINE USAGE: VT903
FILE NAME: TACINJ01.XSS

ITEM NO	PART NUMBER	REV	NOMENCLATURE	QTY -3	MATERIAL TYPE-ALLOY
1	D608400-3	B	INJECTOR ASSEMBLY (LWR.)	-	
2	D608366-1	C	.BODY-INTENSIFIER	1	STEEL-8620
3	C608373-1	-	.CAP-PLUNGER	1	O-1 DRILL ROD
4	C608365-1	-	.PLUNGER-INTENSIFIER	1	M-2 DRILL BLAN
5	D900103-6	-	.SPRING-PISTON RETURN	1	MUSIC WIRE
6	C608363-1	A	.NUT-INTENSIFIER	1	STRESSPROOF
7	D900902-25	-	.DOWEL-UPPER	2	M-2 DRILL BLAN
8	D900101-50	-	.SPRING-NEEDLE	1	MUSIC WIRE
9	D608362-1	A	.NUT-TIP	1	STRESSPROOF
10	D900103-2	-	.SPRING-RATE SHAPE	1	MUSIC WIRE
11	C900802-5	A	.BALL-C.V.	2	STAINLESS
12	D900101-13	-	.SPRING-C.V.	2	MUSIC WIRE
13	C608367-1	A	.SEAT-SPRING	2	O-1 DRILL ROD
14	C901001-4	-	.SHIM	A/R	STEEL
15	C608388-1	-	.FILLER	1	O-1 DRILL ROD
16	C601329-30	N	.PISTON-PRIMARY	1	STEEL-52100
17	B608018-4	C	.SEAT-SPRING	1	O-1 DRILL ROD
18	D609698-1	-	.BODY-ACCUMULATOR	1	STEEL-8620
19	C609753-1	-	.ADAPTER-NEEDLE/SPRING	1	O-1 DRILL ROD
20	B609769-1	-	.PLUNGER-SEPARATOR	1	M-2 DRILL BLAN
ITEM NO	PART NUMBER	REV	NOMENCLATURE	QTY -3	MATERIAL TYPE-ALLOY

PARTS LIST NUMBER: PL608400

PARTS LIST TITLE: TACOM INJECTOR ASSY. (G-4)
PROJECT NUMBER: 25138
INITIAL RELEASE: 11-26-90
REVISION LTR:
REVISION DATE:
ENGINE USAGE: VT903
FILE NAME: TACINJ02.XSS

ITEM NO	PART NUMBER	REV	NOMENCLATURE	QTY -3	MATERIAL TYPE-ALLOY
21	C609745-1	-	.PLATE-RATE SHAPE	1	STEEL-8620
22	C610135-1	-	.NOZZLE ASSY	1	(MINI-SAC)
23	C608359-3	A	..NEEDLE VALVE	1	M-2 DRILL BLANK
24	D609532-2	-	..NOZZLE-DRILLED	1	M/F 609752-1
25	D609752-1	-	...NOZZLE-BLANK	1	STEEL-52100
26	D609749-1	-	.ADAPTER-TIP/ACCUMULATOR	1	STEEL-8620
27	D900902-26	-	.DOWEL-LOWER	2	M-2 DRILL BLANK
28					
29					
30					
31					
32					
33					
34					
***			REFERENCE DRAWINGS		
***					
***	D608390	-	TIP LAYOUT		
***	C609076	-	LAPPING TOOL ASSY		
***					
***					
ITEM NO	PART NUMBER	REV	NOMENCLATURE	QTY -3	MATERIAL TYPE-ALLOY

PARTS LIST NUMBER: PL608398

PARTS LIST TITLE: ELECTRONIC PRESSURE REGULATOR ASSY
PROJECT NUMBER: 25138
INITIAL RELEASE: 12-5-90
REVISION LTR:
REVISION DATE:
ENGINE USAGE: VT903
FILE NAME: TACEPRA1.XSS

ITEM NO	PART NUMBER	REV	NOMENCLATURE	QTY -1	MATERIAL TYPE-ALLOY
1	D608398-1	-	EPR ASSEMBLY	-	
2	D608395-1	B	.MANIFOLD	1	6061-T6 ALUM
3	B610153-1	-	.FITTING-FILTER	4	M/F 900401-9
4	D900401-9	-	..FITTING	4	STEEL
5	A902107-1	-	.FILTER SCREEN	4	STAINLESS
6	D900401-2	-	.FITTING-VENT	2	
7	D900401-10	-	.FITTING-RAIL/VENT	2	
8	D900410-3	-	.FITTING-ELBOW	2	
9	D900402-3	-	.ADAPTER-GAGE	1	
10	D608396-1	-	.BLOCK-SUN VALVE	1	6061-T6 ALUM
11	C900701-2	-	.SUN VALVE	1	
12	B900708-1	-	.VALVE-PHSV	1	(2 WAY)
13	D900401-3	-	.FITTING	1	
14	A900425-3	-	.CAP	1	
15	D900403-3	-	.PLUG	1	
16	D900403-4	-	.PLUG	1	
17	D900201-53	-	.O-RING	1	2-020
18	D900201-44	-	.O-RING	1	2-018
19	D900301-31	-	.SCREW-SHCS	6	1/4-20UNC-2A
20	C903601-2	-	.GAGE	1	
ITEM NO	PART NUMBER	REV	NOMENCLATURE	QTY -1	MATERIAL TYPE-ALLOY

PARTS LIST NUMBER: PL608398

PARTS LIST TITLE: ELECTRONIC PRESSURE REGULATOR ASSY
PROJECT NUMBER: 25138
INITIAL RELEASE: 12-5-90
REVISION LTR:
REVISION DATE:
ENGINE USAGE: VT903
FILE NAME: TACEPRA2.XSS

ITEM NO	PART NUMBER	REV	NOMENCLATURE	QTY -1	MATERIAL TYPE-ALLOY
21	A900424-1	-	.TEE-FEMALE PIPE	1	
22	D900501-2	-	.LOCKWASHER	6	1/4" HI-COLLAR
23	D900401-11	-	.FITTING	1	#6-4
24	A900423-1	-	.PIPE ADAPTER/REDUCER	1	
25	A901310-1	-	.THERMOCOUPLE ASSY.	1	
26	A900422-1	-	.PIPE NIPPLE	1	
27					
28					
29					
30					
***					
***			REFERENCE DRAWINGS		
***					
***					
***					
***	D608627		TACOM EPR LAYOUT		(PRELIMINARY)
***	D608637		L/O EPR & MANIFOLD		
***	608587		SUN VALVE DRILL (TD-2A)		994-002-001
***	608588		SUN VALVE REAMER (TR-2A)		995-002-001
***					
ITEM NO	PART NUMBER	REV	NOMENCLATURE	QTY -1	MATERIAL TYPE-ALLOY

PARTS LIST NUMBER: PL610107

PARTS LIST TITLE: FUEL MANIFOLD ASSY
PROJECT NUMBER: 25138
INITIAL RELEASE: 12-13-90
REVISION LTR:
REVISION DATE:
ENGINE USAGE: VT903
FILE NAME: TACMAN01.XSS

ITEM NO	PART NUMBER	REV	NOMENCLATURE	QTY -1	MATERIAL TYPE-ALLOY
1	D610107-1	-	FUEL MANIFOLD ASSY.	-	
2	D608399-1	-	.CONTROL CARTRIDGE ASSY.	4	
3	J608353-1	-	.MANIFOLD (4 CYL.)	1	ALUM.-6061-T6
4	D900301-8	-	.SHCS-CARTRIDGE ATTACH.	8	1/4-20UNC x 1
5	D900401-1	-	.FITTING-STRAIGHT	1	STEEL
6	D900410-3	-	.FITTING-ELBOW (90 DEG)	2	STEEL
7	D900421-1	-	.FITTING-TEE	1	STEEL
8	D900501-2	-	.LOCKWASHER	8	1/4" HI-COLLAR
9		-			
10		-			
11					
12					
13					
14					
15					
16					
17					
18					
19					
20					
ITEM NO	PART NUMBER	REV	NOMENCLATURE	QTY -1	MATERIAL TYPE-ALLOY

PARTS LIST NUMBER: PL608399

PARTS LIST TITLE: CONTROL CARTRIDGE ASSY
PROJECT NUMBER: 25138
INITIAL RELEASE: 12-13-90
REVISION LTR:
REVISION DATE:
ENGINE USAGE: VT903
FILE NAME: TACCCA01.XSS

ITEM NO	PART NUMBER	REV	NOMENCLATURE	QTY -1	MATERIAL TYPE-ALLOY
1	608399-1	-	CONTROL CARTRIDGE ASSY.	-	
2	608355-1	-	.BODY-CONTROL CARTRIDGE	1	
3	604779-1	-	.PISTON-S.S.CONTROL	1	
4	A900705-1	-	.VALVE-H.S. (3WNC)	1	
5	D900201-58	-	.O-RING (TOP)	1	APPLE-NITRILE
6	D900201-11	-	.O-RING (MID)	1	APPLE-NITRILE
7	D900202-9	-	.O-RING (BOT)	1	APPLE-VITON
8	D900101-18	-	.SPRING	1	C0180-022-0310M
9	608517-1	-	.RETAINER-S.S.SEAT	1	
10	D900802-4	-	.BALL	1	STAINLESS
11	608394-1	-	.GUIDE,SPRING	1	
12	D900202-8	-	.O-RING	2	
13	601331-4	-	.PIN-S.S.SEPARATOR	1	M-2 DRILL BLANK
14	608354-1	-	.SEAT-SECOND STAGE	1	
15	D900802-7	-	.BALL	1	STAINLESS
16	608377-1	-	.SLEEVE-S.S.PISTON	1	
17	D901101-9	-	.PLUG (LEE)	1	PLGA0930020
18	D900101-19	-	.SPRING	1	
19	608375-1	-	.PLUG-SPRING RETAINER	1	
20	608374-1		.SPRING GUIDE-C.V.	1	
ITEM NO	PART NUMBER	REV	NOMENCLATURE	QTY -1	MATERIAL TYPE-ALLOY

PARTS LIST NUMBER: PL608399

PARTS LIST TITLE: CONTROL CARTRIDGE ASSY
PROJECT NUMBER: 25138
INITIAL RELEASE: 12-13-90
REVISION LTR:
REVISION DATE:
ENGINE USAGE: VT903
FILE NAME: TACCCA02.XSS

ITEM NO	PART NUMBER	REV	NOMENCLATURE	QTY -1	MATERIAL TYPE-ALLOY
21	D900802-5	-	.BALL	1	STAINLESS
22	C608376-1	-	.SEAT-CHECK VALVE	1	O-1 DRILL ROD
23					
24					
25					
26					
27					
28					
29					
30					
31					
32					
33					
34					
35					
36					
37					
38					
39					
40					
ITEM NO	PART NUMBER	REV	NOMENCLATURE	QTY -1	MATERIAL TYPE-ALLOY

PARTS LIST NUMBER: [illegible] PAGE [illegible]

PARTS LIST TITLE: TUBE & HEADER ASSY.
PROJECT NUMBER: 25[illegible]8
INITIAL RELEASE: 11-26-90
REVISION LTR:
REVISION DATE:
ENGINE USAGE: VT9[illegible]
FILE NAME: TACTUBO1.[illegible]

ITEM NO	PART NUMBER	REV	NOMENCLATURE	QTY -1	MATERIAL TYPE-ALLOY
1	D608379-1	-	TUBE & HEADER ASSY.	-	
2	D608372-1		.HEADER-INJ.	1	STEEL-[illegible]
3	D608369-1	-	.HEADER-MAN.	1	STEEL-[illegible]
4	D610166-1		.TUBE-SUPPLY	1	STEEL
5	D610167-1		.TUBE-CONTROL	1	STEEL
6	D610168-1		.TUBE-VENT	1	STEEL
[illegible]					
8					
[illegible]					
10					
11					
12					
13					
14					
15					
16					
17					
18					
	REFERENCE DRAWINGS				
***	D608380		BRAZING FIXTURE		
ITEM NO	PART NUMBER	REV	NOMENCLATURE	QTY -1	MATERIAL TYPE-ALLOY

PARTS LIST NUMBER: PL608329

PARTS LIST TITLE: MAIN DRIVE ASSEMBLY
PROJECT NUMBER: 25138
INITIAL RELEASE: 12-13-90
REVISION LTR:
REVISION DATE:
ENGINE USAGE: VT903
FILE NAME: TACMDA01.XSS

ITEM NO	PART NUMBER	REV	NOMENCLATURE	QTY -1	MATERIAL TYPE-ALLOY
1	D608329-1	-	MAIN DRIVE ASSY	-	
2	C608337-1	-	.DRIVE GEAR ASSEMBLY	1	
3	D608332-1	-	..GEAR-CRANKSHAFT	1	
4	C902501-3	-	..KEY-WOODRUFF	1	
5	C608326-1	-	..HUB-DRIVE GEAR	1	
6	C902501-4	-	.KEY-WOODRUFF	2	
7	B608843-1	-	.RETAINER-BEARING	1	
8	C608330-3	-	.SPACER	1	
9	C608330-2	-	.SPACER	1	
10	B900506-1	-	.LOCKWASHER	1	
11	B901405-1	-	.LOCKNUT	1	
12	C608335-1	B	.GEAR-DRIVEN	1	
13	A903002-2	-	.BEARING	2	
14	B900506-2	-	.LOCKWASHER	1	
15	B901405-2	-	.LOCKNUT	1	
16	E608321-1	A	.GEARBOX HOUSING	1	
17	C608327-1	A	.SHAFT-MAIN DRIVE	1	
18	D900301-5	-	.SHCS	4	
19					
20					
ITEM NO	PART NUMBER	REV	NOMENCLATURE	QTY -1	MATERIAL TYPE-ALLOY

PARTS LIST NUMBER: PL608328

PARTS LIST TITLE: MASK DRIVE ASSY
PROJECT NUMBER: 25138
INITIAL RELEASE: 12-14-90
REVISION LTR:
REVISION DATE:
ENGINE USAGE: VT903
FILE NAME: TACMSK01.XSS

ITEM NO	PART NUMBER	REV	NOMENCLATURE	QTY -1	MATERIAL TYPE-ALLOY
1	D608328-1	-	MASK DRIVE ASSEMBLY	-	
2	D608323-1	A	.HOUSING-MASK	1	ALUM.
3	C608324-1	-	.SHAFT-MASK DRIVE	1	1215 STEEL
4	C608334-1	B	.GEAR-MASK DRIVE	1	
5	C608397-1	-	.MASK ASSY	1	
6	B608408-1	-	..MASK-MOD	1	
7	608329-1	-	...MASK	1	
8	C608325-1	-	..HUB-MASK	1	1215 STEEL
9	D900301-17	-	..SHCS	2	
10	D606556-2	B	.COVER-HALL EFFECT	1	ALUM.
11	608330-1	-	.SPACER	1	
12	608019-1	-	.CLAMP-H.E.COVER	3	
13	608350-1	-	.RING-SEAL	1	
14	901202-3	-	.RETAINING RING	1	
15	903002-1	-	.BEARING	2	
16	901701-2	-	.SEAL	1	
17	900201-9	-	.O-RING	1	
18	902501-5	-	.KEY-WOODRUFF	2	
19	900504-6	-	.WASHER-FLAT	1	
20	901402-5	-	.NUT		
ITEM NO	PART NUMBER	REV	NOMENCLATURE	QTY -1	MATERIAL TYPE-ALLOY

PARTS LIST NUMBER: PL608338

PARTS LIST TITLE: FUEL PUMP ASSY.
PROJECT NUMBER: 25138
INITIAL RELEASE: 1-22-91
REVISION LTR:
REVISION DATE:
ENGINE USAGE: VT903
FILE NAME: TACPMP01.XSS

ITEM NO	PART NUMBER	REV	NOMENCLATURE	QTY -1	MATERIAL TYPE-ALLOY
1	C609338-1	-	PUMP ASSEMBLY	1	
2	C608344-1	-	.PUMP (RV-40) MODIFIED	1	M/F 000-3500-1
3	C608336-1	B	.GEAR	1	
4	B608333-1	-	.WASHER	1	1215 STEEL
5	C902502-2	-	.KEY-WOODRUFF	1	
6	D901401-3	-	.NUT	1	
7	D900201-1	-	.O-RING	1	
8					
9					
10					
11					
12					
13					
14					
15					
16					
17					
18					
19					
20					
ITEM NO	PART NUMBER	REV	NOMENCLATURE	QTY -1	MATERIAL TYPE-ALLOY

PARTS LIST NUMBER:PL610154

PARTS LIST TITLE: ACCUMULATOR INSTL. - RAIL PRESS.
PROJECT NUMBER: 25138
INITIAL RELEASE: 10-23-90
REVISION LTR:
REVISION DATE:
ENGINE USAGE: VT903
FILE NAME: TACCUM01.XSS

ITEM NO	PART NUMBER	REV	NOMENCLATURE	QTY -1	MATERIAL TYPE-ALLOY
1	610154-1		ACCUMULATOR INSTL	-	
2	900601-4		.ACCUMULATOR	2	
3	610		.BRACKET	2	
4	D900417		.FITTING-ADAPTER	2	
5	90		.SCREW	2	
6					
7					
8					
9					
10					
11					
12					
13					
14					
15					
16					
17					
18					
19					
20					
ITEM NO	PART NUMBER	REV	NOMENCLATURE	QTY -1	MATERIAL TYPE-ALLOY

PARTS LIST TITLE: EXHAUST MANIFOLD ASSY
PROJECT NUMBER: 25138
INITIAL RELEASE:
REVISION LTR:
REVISION DATE:
ENGINE USAGE: VT903
FILE NAME: TACEXM01.X88

ITEM NO	PART NUMBER	REV	NOMENCLATURE	QTY -1	REMARKS
1	610131-1		EXHAUST MANIFOLD ASSY		
2	608041		DIVERTER VALVE ASSY	2	2 PER ENGINE
3	608040		BUSHING	4	
4	608037		VALVE BODY	2	
5	608038		FLANGE	2	
6	608039		DIVERTER	2	
7	608161		FLANGE (TURB. IN)	2	
8	608162		EXH.FLANGE	8	
9					
10					
11					
12					
13			2"SS ELBOW SCH.10S		
14			2"SS SCH.10S PIPE		
15					
16					
17					
18					
19					
20					
ITEM NO	PART NUMBER	REV	NOMENCLATURE	QTY -1	MATERIAL TYPE-ALLOY

ALL FULL SIZE DRAWINGS INCLUDED IN APPENDIX C ARE ATTACHED TO THIS REPORT IN A SEPARATE ENVELOPE

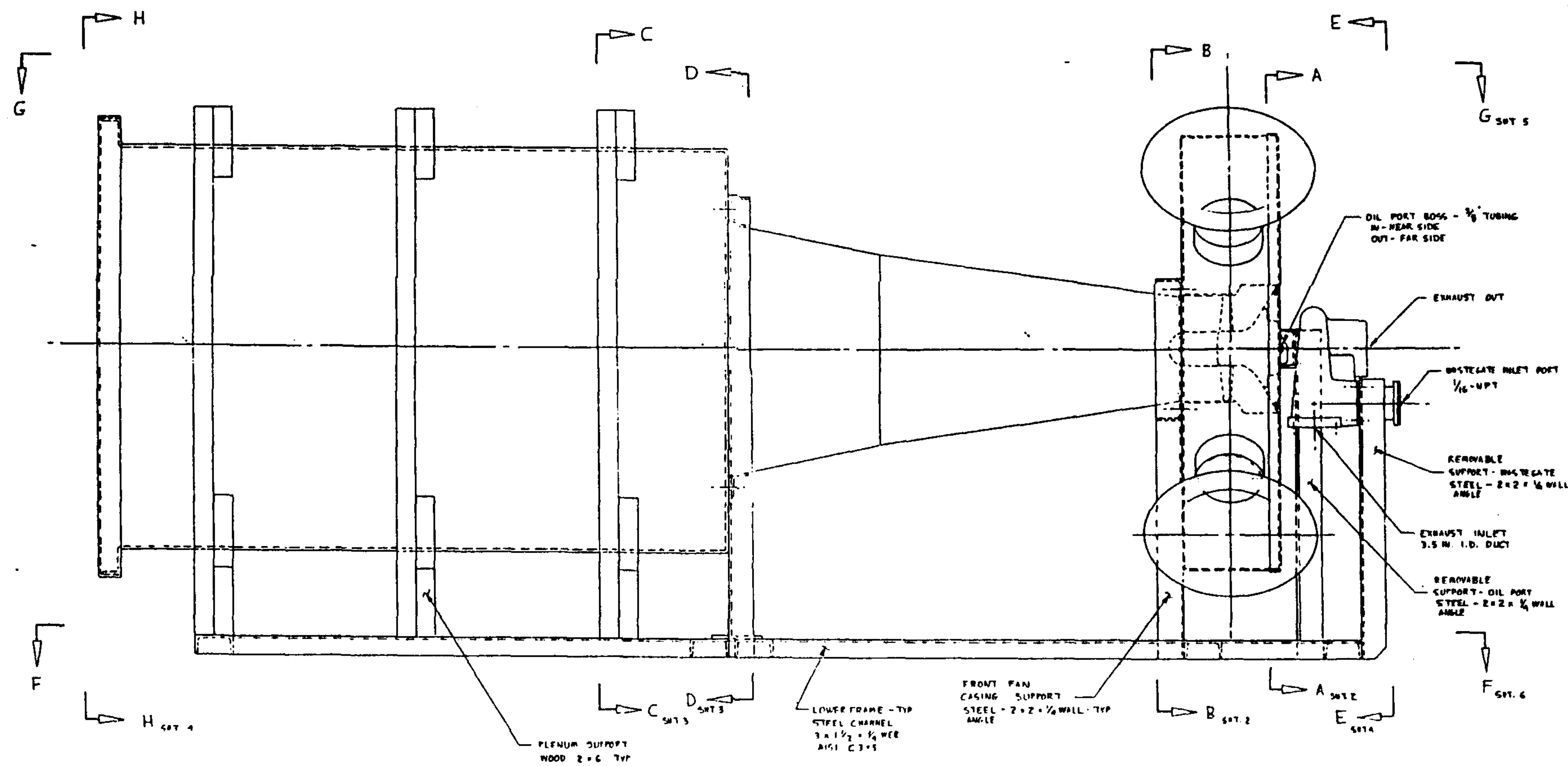

TEST ARRANGEMENT
AXIAL FAN

DRAWN	M. A. CALKINS
SIZE	D
DRAWING NO.	614036
SCALE	1/8
PROJECT	25145

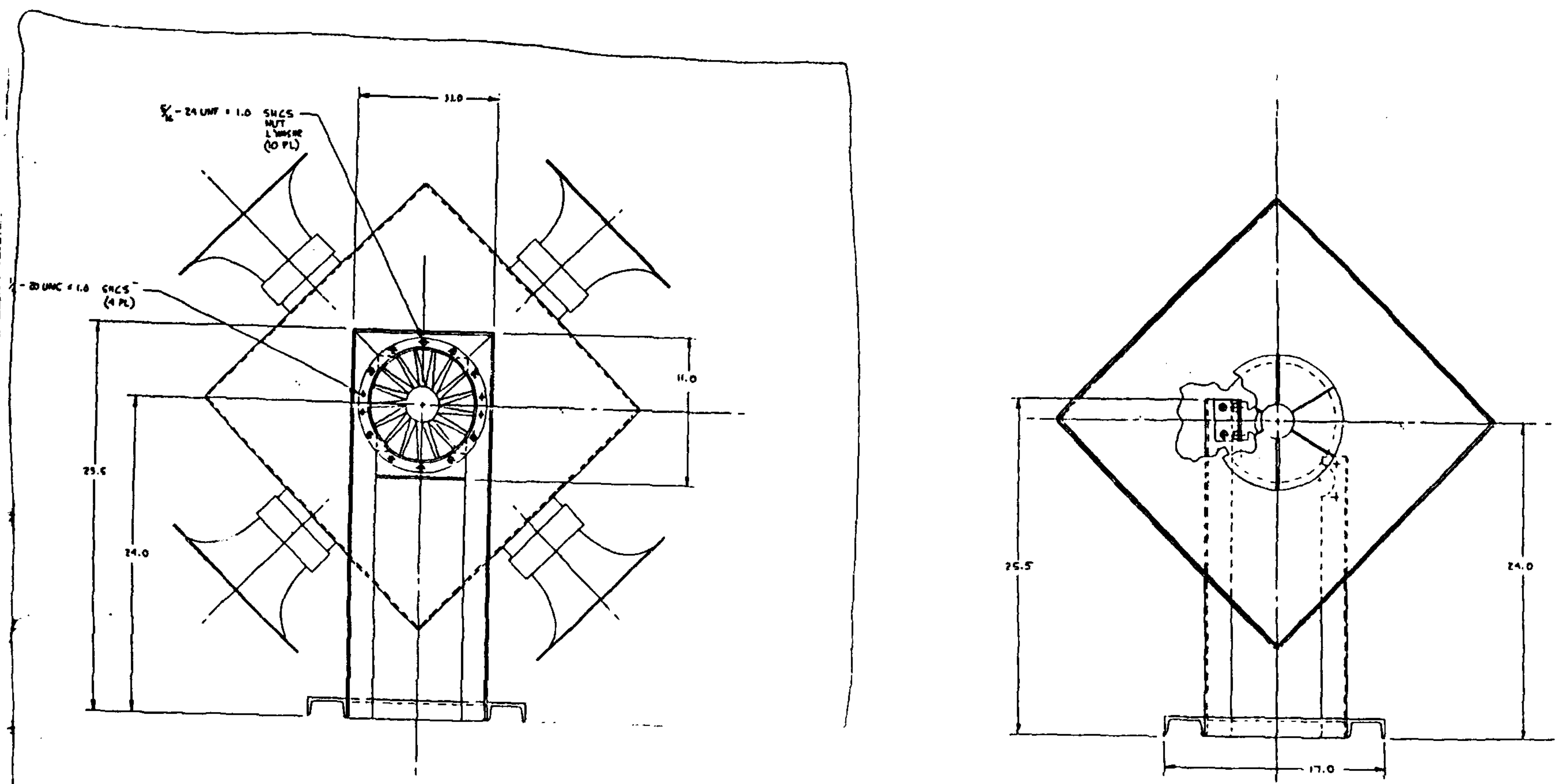

SECTION B-B

SECTION A-A

TEST ARRANGEMENT

AXIAL FAN

D 614036

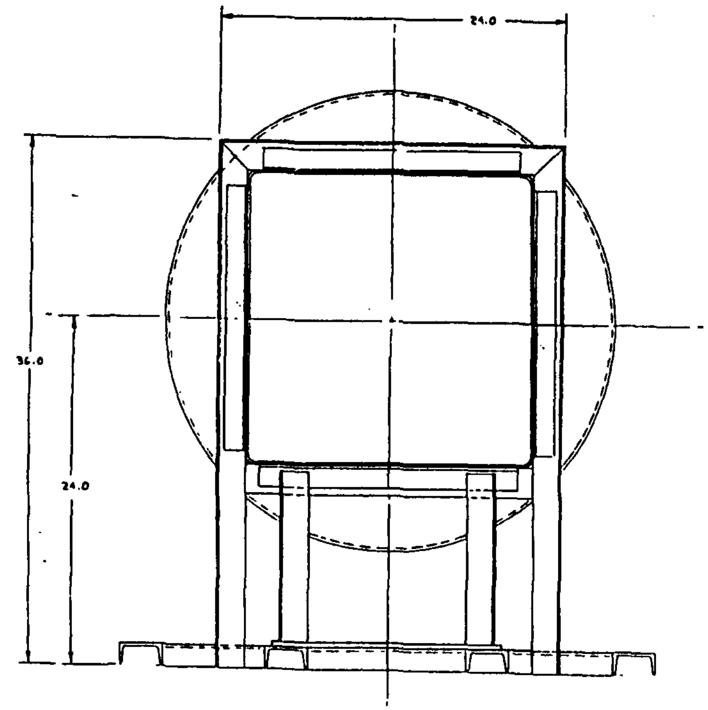

SECTION D-D

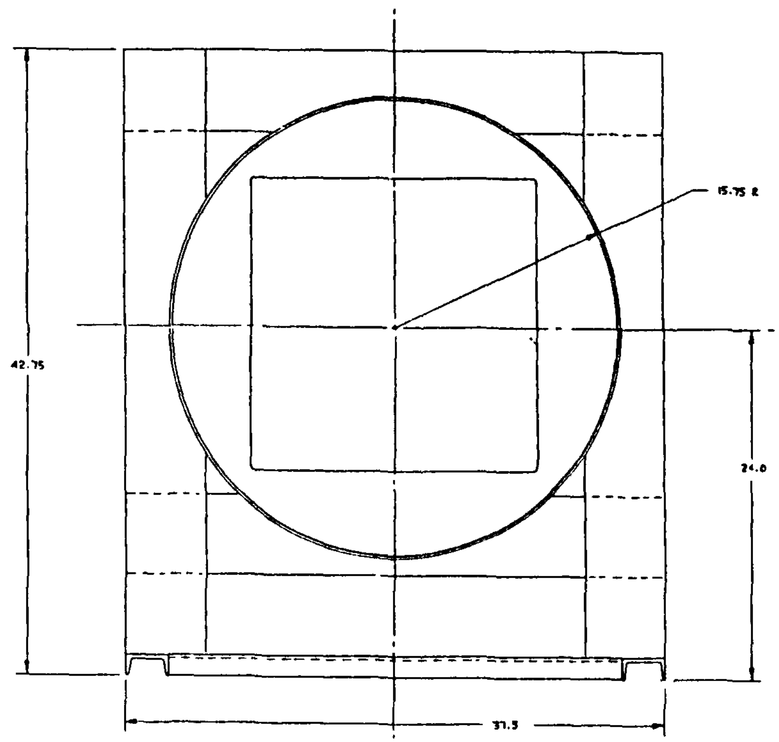

SECTION C-C

TEST ARRANGEMENT
AXIAL FAN

SIZE	DRAWING NO	REV
D	G14036	-

SCALE 1/4 SHEET 3

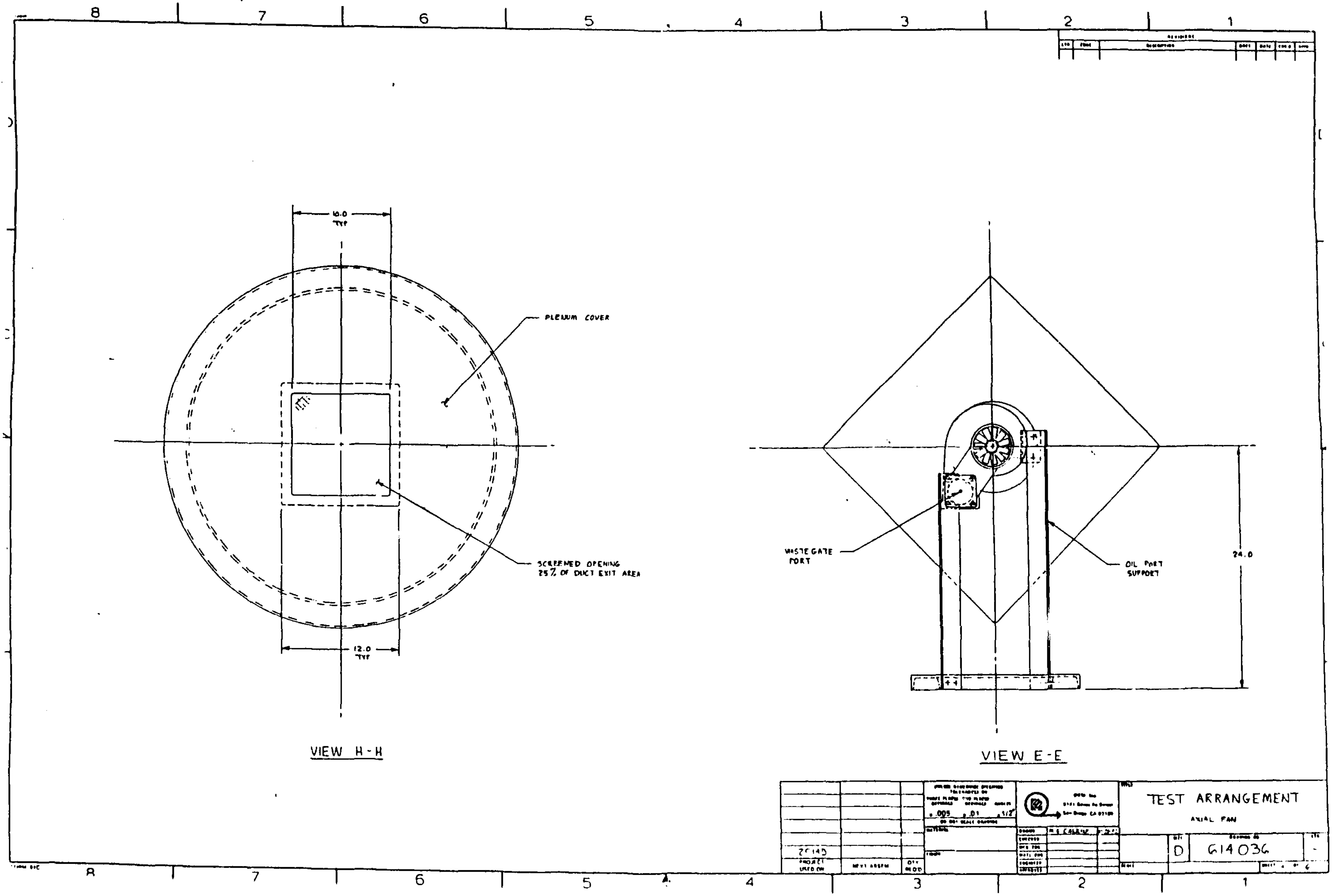
PLENUM COVER
SCREENED OPENING
25% OF DUCT EXIT AREA
10.0 TYP
12.0 TYP
VIEW H-H
WASTE GATE PORT
OIL PORT SUPPORT
24.0
VIEW E-E
TEST ARRANGEMENT
AXIAL FAN
D
614036
.005
.01
1/2°
2C145
PROJECT
USED ON
NEXT ASSEM
QTY
REQD

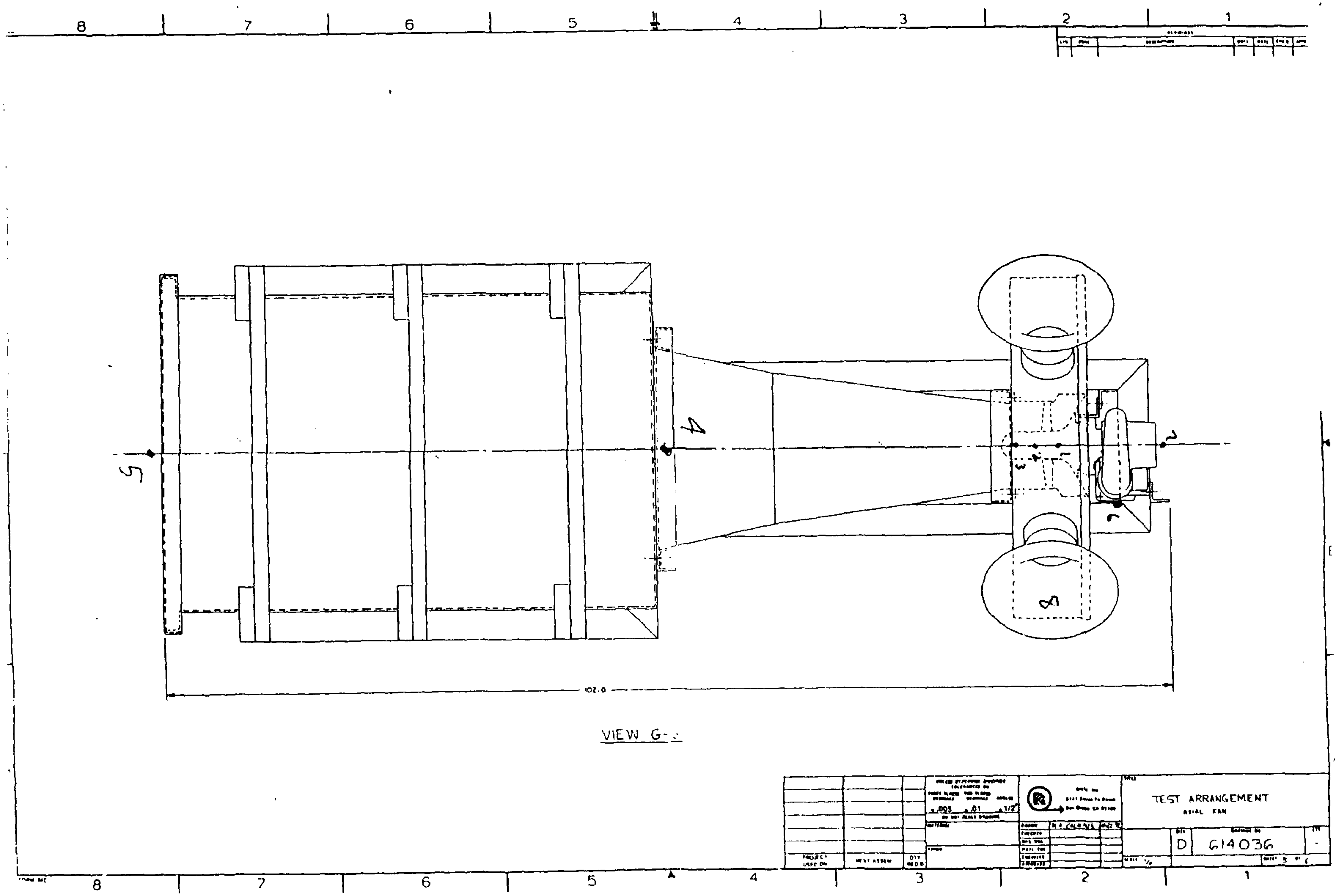
102.0
VIEW G-
TEST ARRANGEMENT
AXIAL FAN
D
G14036
1
2
3
4
5
6
7
8

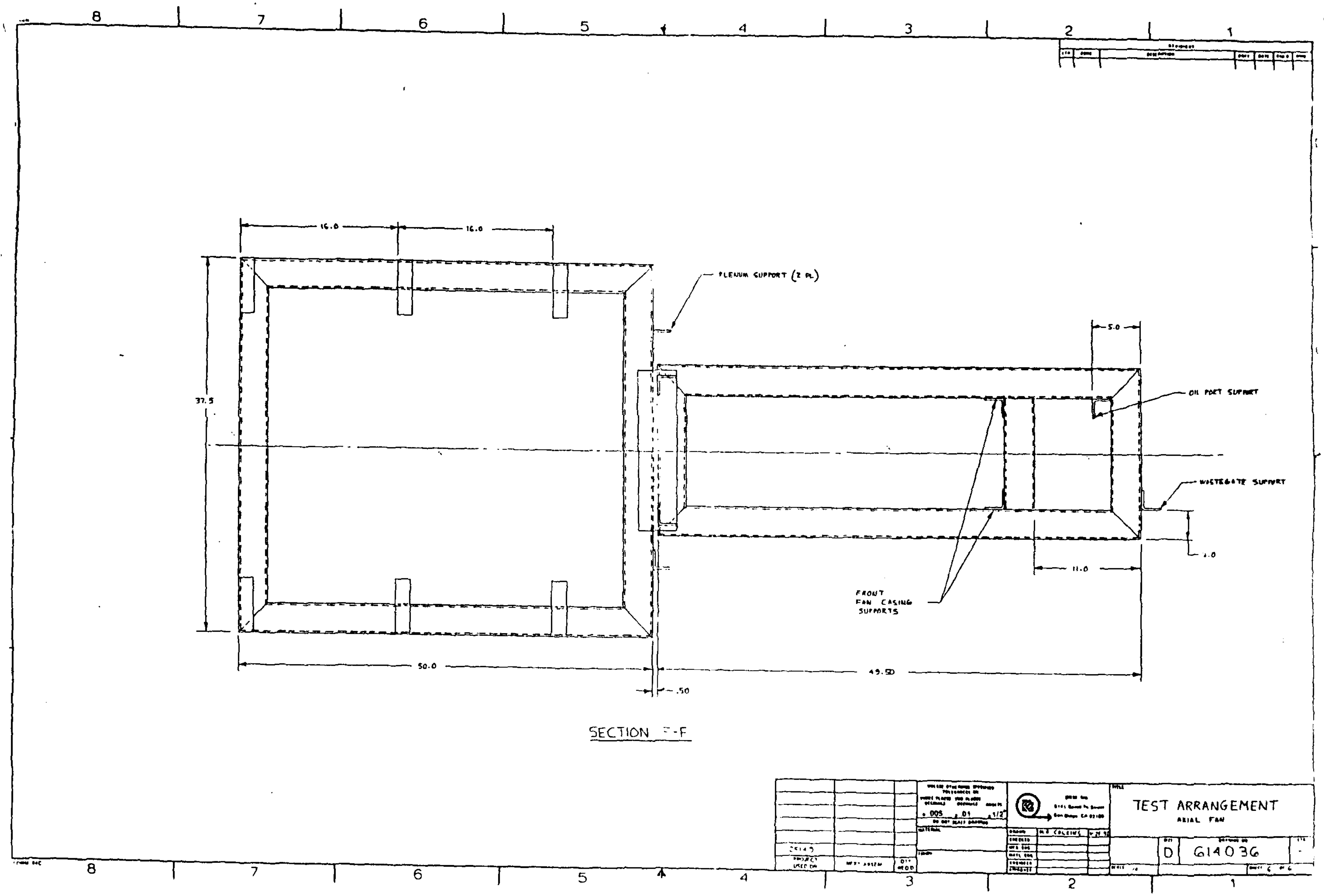

16.0
16.0
37.5
PLENUM SUPPORT (2 PL)
5.0
OIL PORT SUPPORT
WASTEGATE SUPPORT
1.0
11.0
FRONT
FAN CASING
SUPPORTS
50.0
49.50
.50
SECTION F-F
TEST ARRANGEMENT
AXIAL FAN
D
G14036

BKM, INC. 5141 SANTA FE STREET SAN DIEGO, CA 92109	DEVICE SPECIFICATION ELECTRONIC CONTROL UNIT	TS- 122-B DATE: 9/13/93 PAGE 1 OF 3

Engine Control System Overview:

The Engine Control System (ECS) consists of the following hardware items:

Electronic Control Unit (ECU)
Fuel Rail Pressure Transducer (RPX)
Engine Coolant Temperature Sensor (ECT)
Air Charge Temperature Sensor (ACT)
Manifold Air Pressure Sensor (MAP)
Crankshaft Position Input Pulse Sensor (PIP)
Other engine sensors, as required
Wiring harness assembly

The ECU reads engine operating parameters from the sensors and outputs signals to the fuel injectors in response to those parameters as determined by the control software. Depending on the engine type and the specific fuel used other outputs - such as ignition, idle speed contol, fuel pressure control, etc. - may also be generated by the ECU.

The ECU is capable of controlling a wide variety of engine types from 1 to 8 cylinders. The maximum speed capability depends on number of cylinders and the complexity of the control software.

Various engine control software strategies are currently available. The most common strategies may be broadly classified as follows:

Injection & Ignition Timing
Starting
Idle Control
Torque Shaping
Fuel / Air Ratio Control
Speed Governing
Fuel Pressure Regulation
Altitude Compensation

Generic control software may be customized to satisfy the specific requirement of each engine application.

A separate piece of support equipment, the Calibration Interface, connects to the ECU and permits control calibration parameters to be displayed or modified during engine operation. This unit is used by application engineers and consists of an MS-DOS personal computer, a serial interface adapter, and PC software. Once the calibration data is correct, a new EPROM may be programmed and installed into the ECU.

BKM, INC. 5141 SANTA FE STREET SAN DIEGO, CA 92109	DEVICE SPECIFICATION	TS- 122-B DATE: 9/13/93 PAGE 2 OF 3

ECU Specifications:

Microprocessors:	8097 or 80C196 main processor (CPU) 80C51 or 87C51 output multiplexer (MUX)
Clock Frequency:	12.00 MHz CPU (optional 16.00 MHz) 16.00 MHz MUX
Memory:	32 kByte strategy EPROM or ROM 32 kByte Static RAM 8 kByte MUX ROM or EPROM 128 Byte serial EEPROM (2 KByte optional)
Analog Inputs:	8 Channels, 0-5 volt, 10 bit resolution A/D conversion time, 22 mSec Typical inputs include: throttle position, temperatures, pressures.
Digital Inputs:	3 high-speed inputs, TTL voltage levels Typcial digital input: Crankshaft position
Outputs:	8 Injector solenoid drivers (4 Amps peak, 1 Amp holding current) 1 electronic pressure regulator solenoid driver (4A/1A) 8 high speed logic (400 mA current sink, 40V maximum) 5 low speed logic (400 mA current sink, 40V maximum) 1 regulated sensor excitation (+5.0 Volt DC, 500 mA) 1 Bipolar stepper motor driver (500mA maximum)
Power Requirement:	Supply Voltage: 8.0 to 16.0 Volts DC continuous Load dump and transient protection Supply Current: 250 mA standby plus up to 1.0 amp average current draw per solenoid driver.

Environmental:	Storage Temperature:	-40 to +105 C
	Operating (air-cooled):	-20 to +60 C
	Operating (fuel-cooled):	-20 to +105 C
	Altitude (operating):	SL to 3700 meters
	Mechanical Shock:	50 g peak, 10 mS duration
	Mechanical Vibration:	4 g at 5 to 200 Hz
	Humiditiy:	98%
	Material Compatibility:	SAE J1211
	EMI:	SAE J1113
Weight:	68 oz.	

BKM, INC. 5141 SANTA FE STREET SAN DIEGO, CA 92109	DEVICE SPECIFICATION	TS- 122-B DATE: 9/13/93 PAGE 3 OF 3

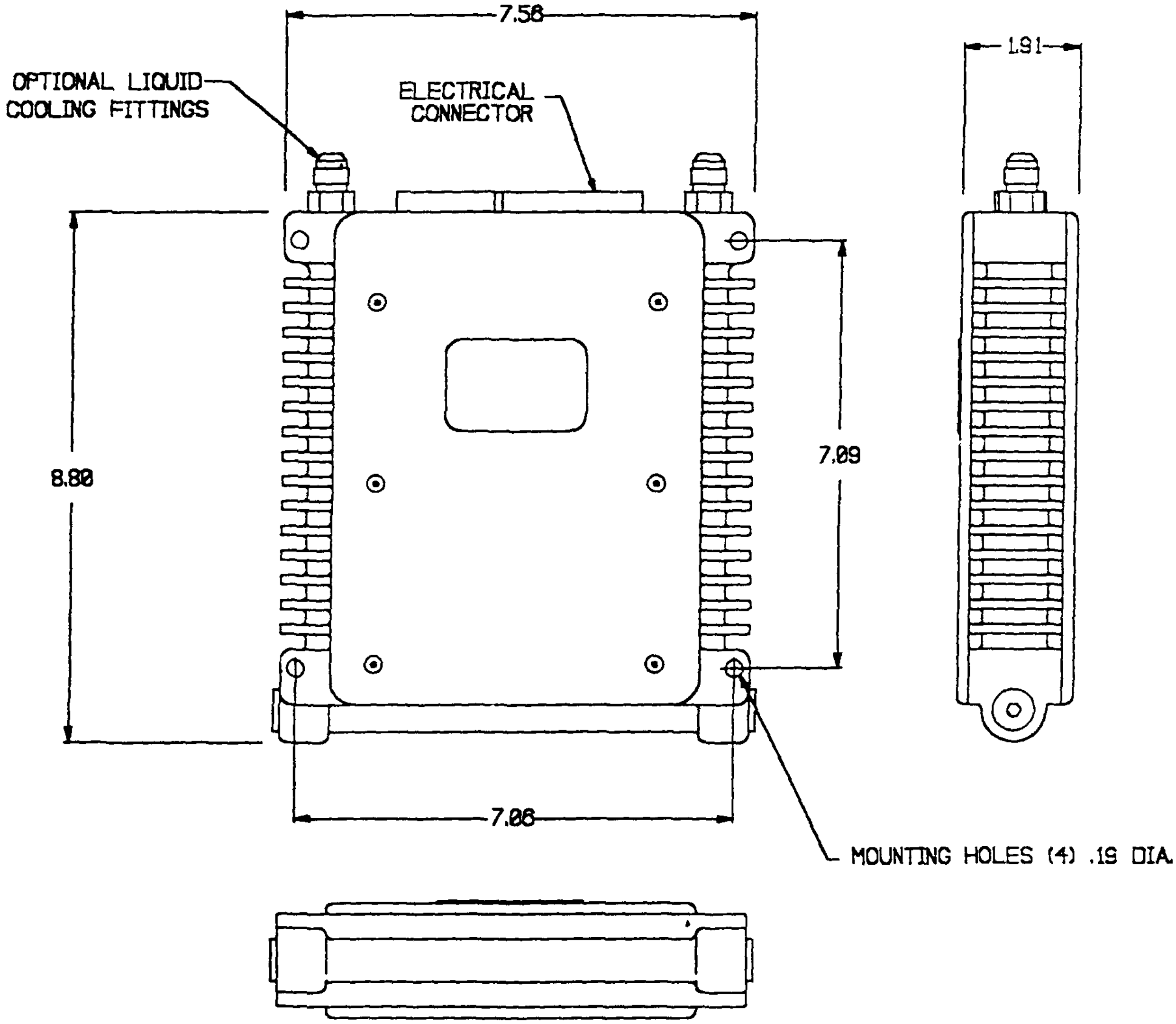

ECU INSTALLATION

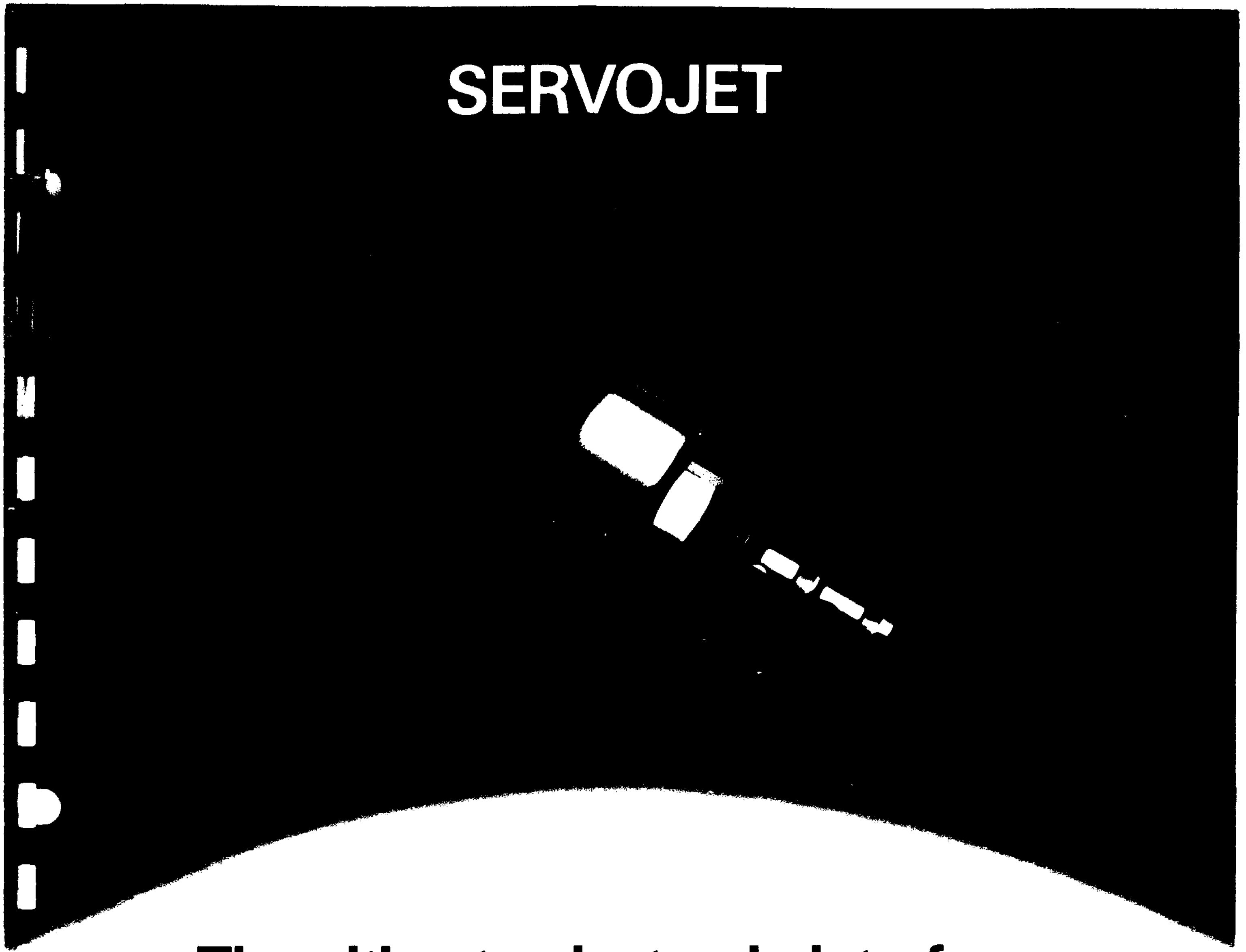

The ultimate electronic interface you need to cut cost and increase performance.

The HSV 3000 is a high speed solenoid valve designed for digital control of pressure or flow.

HSV 3000 - HIGH SPEED SOLENOID VALVE
Control Flow or Pressure with Pulse Width Modulation
Operation up to 200 Hz
Proven lifespan over 1 billion cycles
Excellent for a wide range of hydraulic and pneumatic control applications.

Order Information Sheet

HSV-3000 SERIES SOLENOID VALVES

Patents Issued and Pending

To order valves: Select assembly type, material and coil type

- Select number for valve type and pressure desired.
- 2W = Two Way; 3W = Three Way;
- NC = Normally Closed; NO = Normally Open

ASSEMBLY NO.

[illegible]	[illegible] / 30	750 / 50	1000 / 70	1500 / 100	3000 / 200
[illegible]	GROUP 1		GROUP 3		GROUP 5
[illegible]	3020	3050	3070	3100	3200
[illegible]	3021	3051	3071	3101	3201
[illegible]	GROUP 2		GROUP 4		GROUP 6
[illegible]	3022	3052	3072	3102	3202
[illegible]	3023	3053	3073	3103	3203

- Select material required. S = Stainless; C = Carbon Steel

COIL NO.

- Select coil type required.

[illegible]	[illegible]		12" METAL LEADS 20 GA. TEFLON INSULATION	
[illegible]	12VDC	[illegible]	12VDC	24VDC
[illegible]	1	3	5	7
[illegible] DUTY	2	4	6	8

Example: To order a 2 way, normally closed, stainless valve rated 750 psi with a 24 volt rapid response coil, the HSV model No. would be:

HSV MODEL NO.

3051S3

- 3 — Coil No.
- S = Stainless Steel
- 3051 — Assembly Type

Orders and/or inquiries should be made to:

SERVOJET PRODUCTS INTERNATIONAL
5141 Santa Fe St. • San Diego, CA 92109
(619) 259-6545 • TLX 4991588 BKMSD • FAX (619) 259-6681

BKM, Inc. ADVANCED PRODUCTS	SPECIFICATION SUMMARY RV-40 PUMP	TS-076 11/17/88 RLB Page 6 of 7

RV-40	S.I. UNITS		IN-LB UNITS
GENERAL			
NO. OF CYLINDERS		7	
RATED RPM		1850 RPM	
RATED DELIVERY PRESSURE	10,345 kPa		1,500 psi
MAXIMUM DELIVERY PRESSURE	13,790 kPa		2,000 psi
SUPPLY PRESSURE	100-170 kPa		14-25 psi
B-10 LIFE @ 8620 kPa (1250 psi) hours/rpm		10,000/1,300	
DISPLACEMENT/REV. (Theor.)	40.025 cc		2.442 in^3
RATED DELIVERY	74,046 cc/min 74 L/min		4.519 in^3/min 19.56 gpm
MEDIA		Diesel Lube oil	
PISTON			
DIAMETER	20.5 mm		0.807 in.
PITCH CIRCLE	81.5 mm		3.209 in.
SWASH PLATE		12°	
STROKE	17.323 mm		0.682 in.
RING VALVE			
HOUSING BORE DIAMETER	49.248 mm		1.9383 in.
ECCENTRICITY	10.95 mm		0.4311 in.
FACE O.D.	60.77 mm		2.3925 in.
FACE I.D.	32.36 mm		1.274 in.
CYLINDER BLOCK			
PORT PITCH DIAMETER	41.10 mm		1.6181 in.
PORT DIAMETER	13.95 mm		0.5492 in.
INPUT SHAFT		SAE 32-2	
MOUNTING FLANGE		SAE 127-2	
ENVELOPE			
LENGTH	278 mm		10.945 in.
DIAMETER	156 mm		6.142 in.
WEIGHT	17.8 kg		39.2 lbs.

BKM, Inc. 5141 Santa Fe Street, San Diego, CA 92109	ENGINEERING SPECIFICATION	NO. E-31	
		SHEET 2 OF 2	REVISION
	PREPARED BY M. Vanderslice / DATE 7-28-87	APPROVED BY	DATE

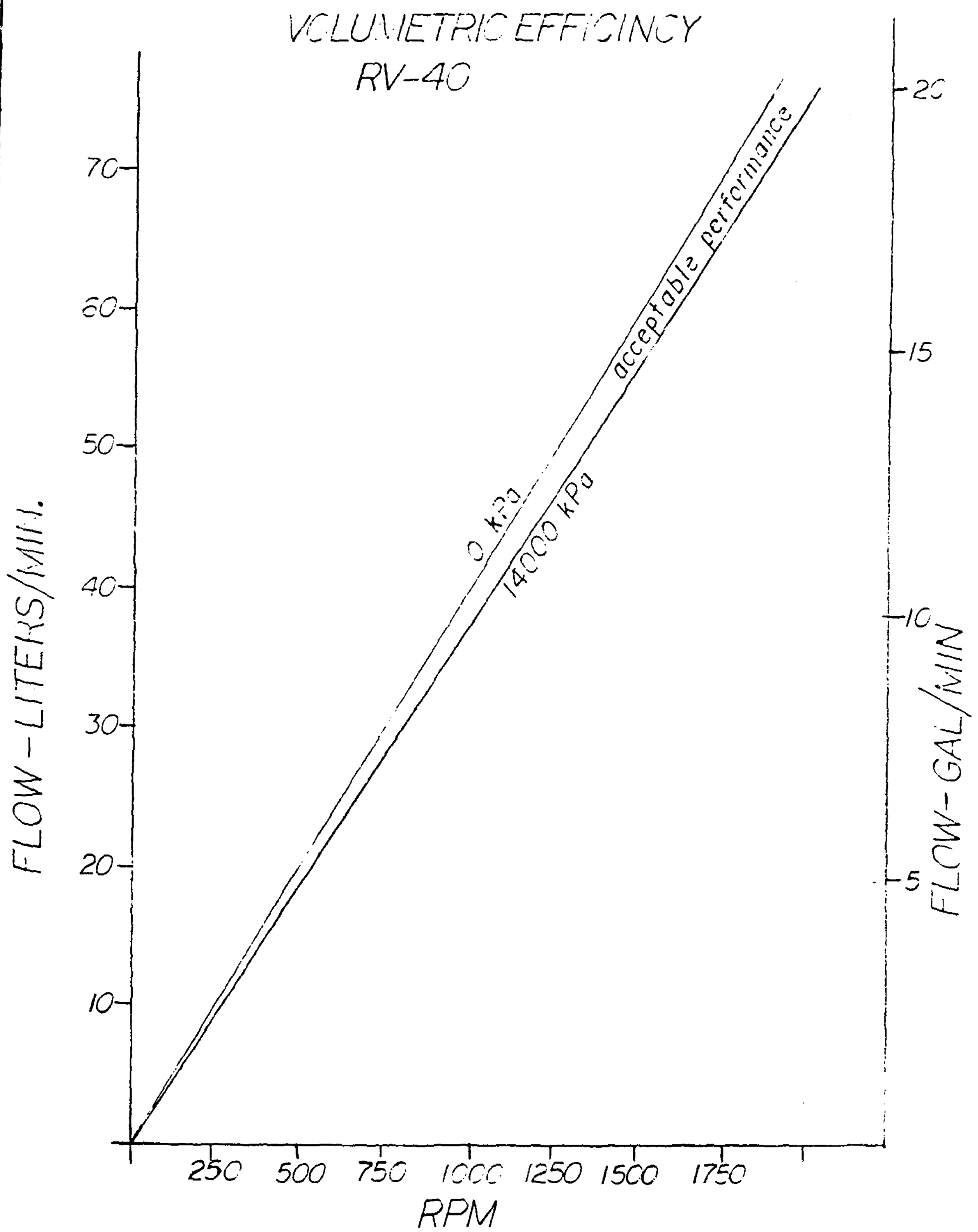

FORM 78

REVISIONS

LTR	ZONE	DESCRIPTION	DRFT	DATE	CHK'D	APPD.
A	—	13° 36' WAS 7° 30'; E.O.	ARR	2-28-91	MRC 3-16-91	WM

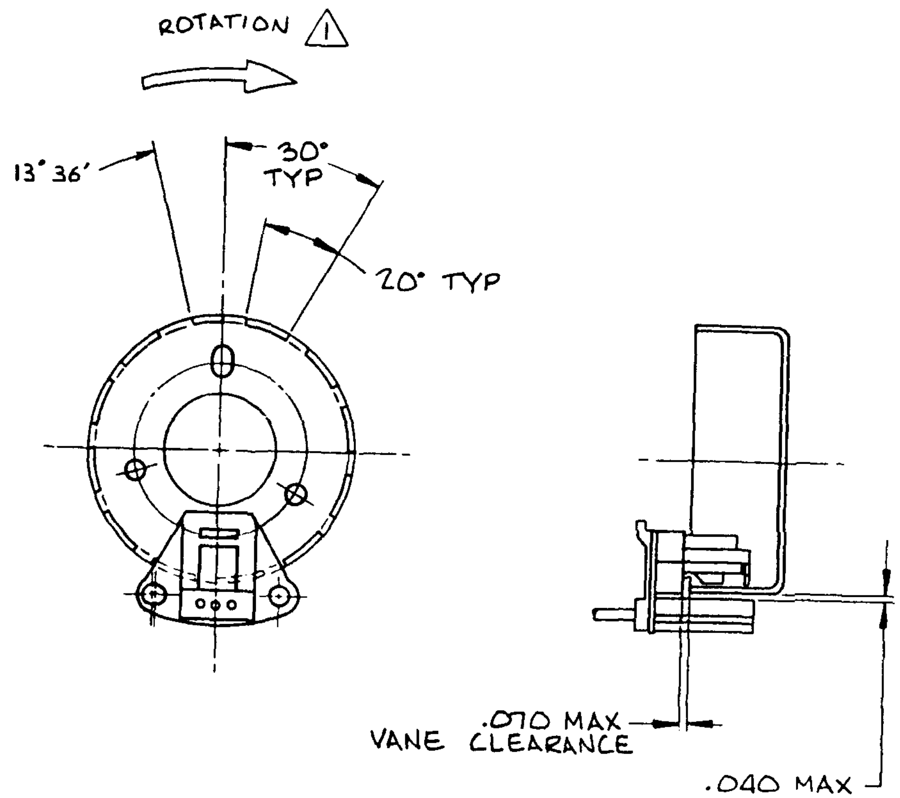

NOTES:

1. ROTATION: CW SHOWN
MASK P/N 608743-1
FOR CCW ROTATION USE
MASK P/N 608743-2

THIRD ANGLE PROJECTION

UNLESS OTHERWISE SPECIFIED TOLERANCES ON	
THREE PLACES DECIMALS ± .010 · TWO PLACES DECIMALS ± .03 · ANGLES ± 2°	
DO NOT SCALE DRAWING	
MATERIAL	
FINISH	

BKM, Inc.
5141 Santa Fe Street
San Diego CA 92109

DRAWN	N. POWERS	4-5-89
CHECKED		
ENGINEER	[illegible]	4/6/89
APPROVED	[illegible]	3/30/91

TITLE

SENSOR/MASK
INSTALLATION DRAWING

SIZE	DRAWING NO.	LTR
B	608950	A

SCALE FULL | PROJECT NO. 70065 | SHEET 1 OF 1

FORM 92 REV C

Model K1 Pressure Transmitter

ASHCROFT

PERFORMANCE CHARACTERISTICS

Standard Ranges (PSI):

0/15*	0/500	0/10,000
0/30*	0/750	0/15,000
0/60	0/1,000	0/20,000
0/100	0/2,000	0/30 and Vac.*
0/150	0/3,000	0/45 and Vac.*
0/200	0/5,000	0/60 and Vac*
0/300	0/7,500	

*1% Accuracy ranges only

Accuracy Class (F.S.)

	0.5%	1.0%
Non-lin.(Term. Pt.)*	±0.4	±0.7
(B.F.S.L.)*	±0.25	±0.4
Hysteresis	±0.15	±0.2
Non-Repeatability	±0.05	±0.07

*Including hysteresis

Durability:
10^8 cycles 0/100%F.S. with no performance loss

Overpressure: (F.S.)

	0/15-0/2000	0/3000-0/5000	0/7500-20,000
Proof	200%	150%	120%
Burst	800%	300%	150%

Response time:
Less than 1ms

ENVIRONMENTAL EFFECTS

Humidity:
No performance effect at 95% relative humidity-noncondensing.

Position Effect:
Less than 0.01% F.S.

TEMPERATURE :

Storage	-65/+250°F
Operating	-20/+180°F
Compensated	-20/+160°F

Thermal Coefficie (68°F ref.)

Standard:

	0.5%	1%
Zero	±0.028% F.S./°F	±0.04%F.S./°F
Span	±0.028	±0.04

Optional:

Zero	±0.014	N/A
Span	±0.014	N/A

0/60 psi range available in ±0.5% accuracy class with ±0.04% F.S./°F thermal coefficients. Multiply thermal coefficients by 2 on 0/30 psi range and by 3 on 0/15 psi range.

VIBRATION
Less than ±0.1% F.S. effect for 0-2000 Hz at 20 g's in any axis.

SHOCK
Less than ±0.05% F.S. effect for 100 g's, 20 ms shock in any axis.

ELECTRICAL

Output Signal:
4-20 mA (2 wire)
0-5 VDC (4 wire)*
1-5 VDC (3 wire)
1-6 VDC (3 wire)
0-10 VDC (4 wire)*
*Signal and power commons (neg) must be electrically isolated from each other.

Power Requirements:
10-30 VDC Unregulated, except 12-30 VDC for 0-10 VDC output
Reverse polarity protected

Supply Current:
Less than 3. mA for voltage output.

Output Impedance:
100 ohms

Circuit to Case Insulation Resistance:
100 M ohms @ 50 VDC

PHYSICAL
Weight: 2 oz. (approx. without cable)

MATERIALS
Case:
300 series stainless steel

Cable:
36" braided shield, PVC sheathing

Diaphragm:
17-4 PH stainless steel

Standard Process Connections:
(316 stainless steel)
1/8 NPT male or female
1/4 NPT male or female
1/4 SAE-J-514 (male)
1/4 AMINCO (female) required for pressures over 10,000 psi.

Calibration report is standard with 0.5% and optional with 1% accuracy units. Consult factory on other pressure, temperature or product packaging variations available.

Load Limitations 4-20mA Output Only

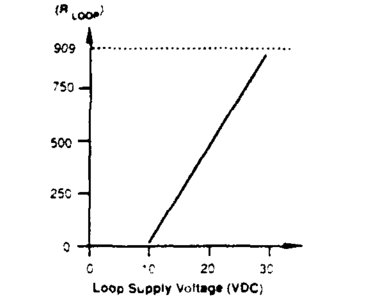

V_{min} = 10V+ [(.022A*(R $_{LOOP}$)]
*includes a 10% safety factor

Dimensions

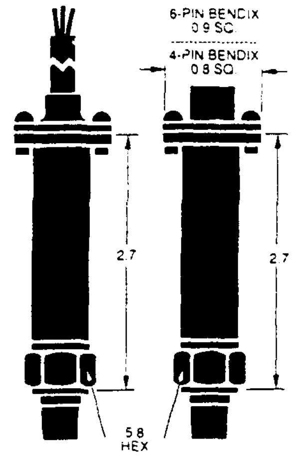

DRESSER INDUSTRIES DRESSER
INSTRUMENT DIVISION
STRATFORD, CT 06497

How To Order

ASH - K 1 - ☐ - ☐☐☐ - ☐ - ☐ - ☐☐☐ - ☐☐ - ☐☐ - ☐☐☐☐☐

Model Configuration
(K1)

Measurement Type
(G) Gauge
(S) Sealed

Accuracy %F.S.
(050) 0.5
(100) 1.0

Compensated Range
(D)-20/+160°F

Thermal Error
(3) .014%F.S./°F
(5) .028
(7) .040

Pressure Connection
(MO1) 1/8NPT-M
(FO1) 1/8NPT-F
(MO2) 1/4NPT-M
(F02) 1/4NPT-F
(MRW) 7/16-20 SAE-J-514
(F09) AMINCO 9/16-18 Female

Output Signal
(05) 0/5VDC
(15) 1/5 VDC
(42) 4/20 mA
(16) 1/6 VDC
(01) 0/10 VDC

Electrical Termination
(F2) 36"cable, braided shield, PVC sheathing
(B4) Bendix 4-pin# PTO2A-8-4P*
(B6) Bendix 6-pin# PTO2A-10-6P*
(B8)WP Bendix 4-pin# PTO2H-8-4P*
(B9)WP Bendix 6-pin# PTO2H-10-6P*
(J1) J Style connector (same as on K5 model, with mating connector and 36" cable)
(C1) 1/2 NPT-M Conduit

Pressure Range
(100) 100 PSI
(20000) 20000 PSI

* mating connector available as accessory

5/90 15M

MOTOROLA INC.

Automotive and Industrial Electronics Group

SENSOR PRODUCTS

SILICON CAPACITIVE PRESSURE TRANSDUCER

DATA SHEET

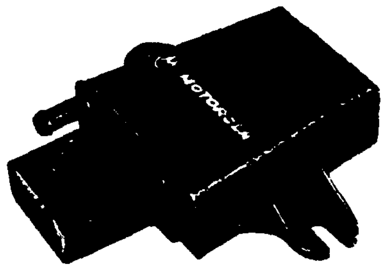

Motorola AIEG's silicon capacitive absolute pressure (SCAP) transducers provide a digital frequency output that is proportional to absolute pressure. Two plates of a variable capacitor are formed by mounting a silicon diaphragm on a metallized glass substrate. The measurement effect is produced when applied pressure creates a deflection of the silicon diaphragm resulting in a change in capacitance. This semiconductor sensor is mounted on a hybrid substrate containing both signal conditioning and temperature compensation circuitry to produce a reliable and durable solid state pressure transducer. The transducers are available as submodules consisting of the substrate only, or as fully packaged, environmentally protected modules.

OPERATING CHARACTERISTICS

Pressure Range:	1.7 to 15.2 psia (12 to 105 kPa) 2.5 to 29.0 psia (17 to 200 kPa)
Temperature Range:	−22 to 212°F (−30 to 100°C)
Supply Voltage:	V_S = 5.0 ± 0.25 VDC
Input Current:	1.5mA typical 7.5mA maximum
EMI Protection:	200 V/m (1 MHz – 1 GHz)

TRANSFER CURVE

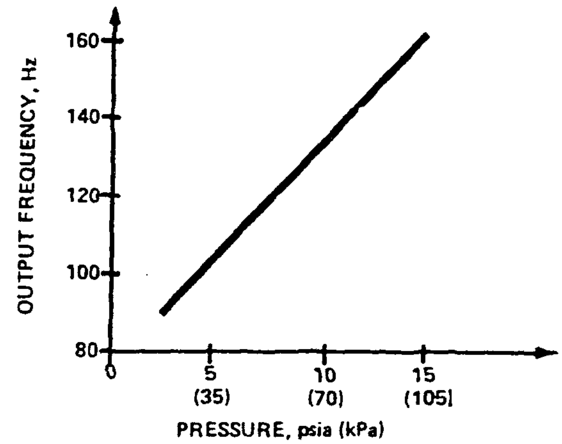

ACCURACY

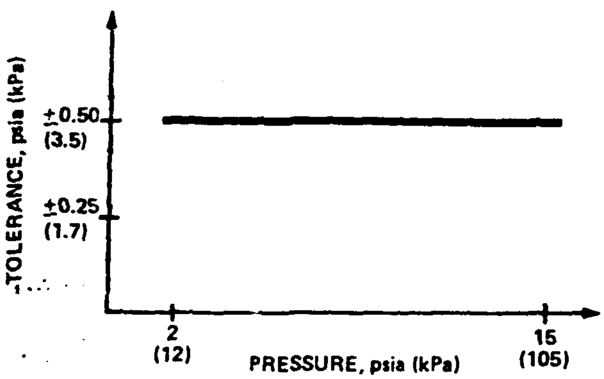

NOTE: Includes all error sources, except linearity. Assumes 5 volt supply.

LINEARITY ERROR

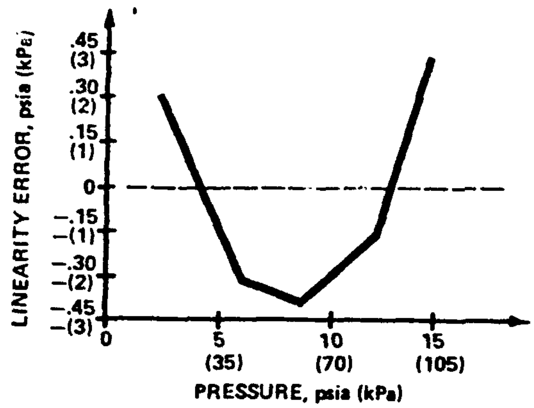

NOTE: Linearity error is repeatable and is calculated by subtracting nominal values from best fit straight line values.

MOTOROLA INC.

Automotive and Industrial Electronics Group

SENSOR PRODUCTS

PHYSICAL DIMENSIONS

DIMENSIONS	INCHES	MILLIMETERS
A	2.36	60.0
B	1.28	32.5
C	0.25	6.4
D	0.20	5.0
E	3.30	83.8
F	4.13	105.0
G	0.75	19.0
H	0.20	5.0
I	0.89	22.7
J	3.91	99.4
K	1.16	29.4
L	0.61	15.6

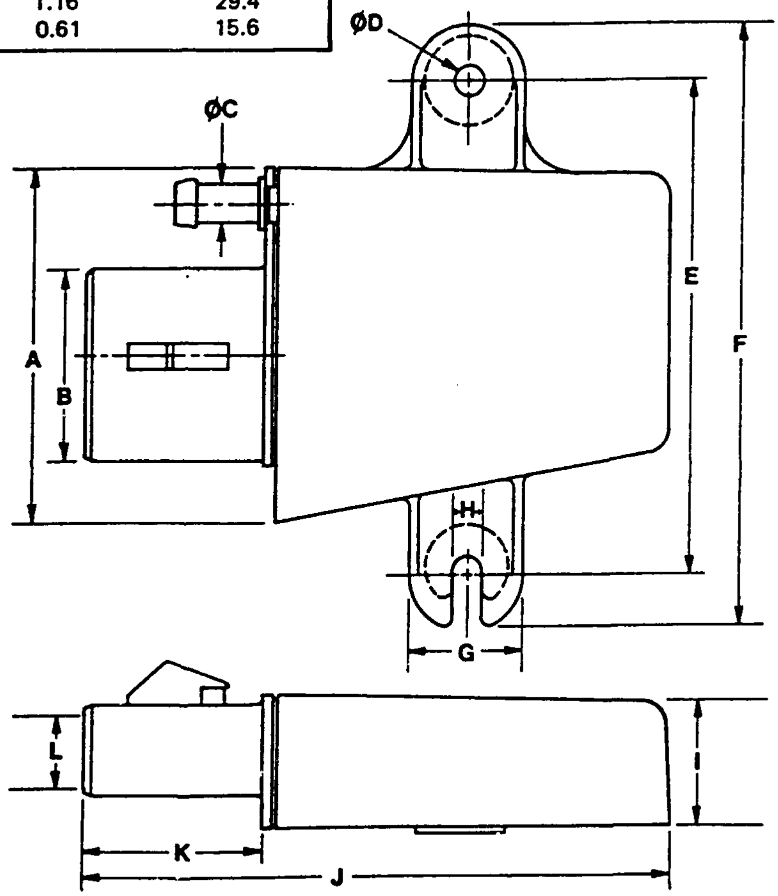

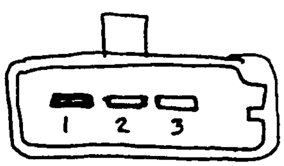

1 V+ (5 VDC)
2 OUTPUT
3 GROUND (⏚)

Sensor Products
1299 East Algonquin Road
Schaumburg, Illinois 60196
(312) 580-5475
Telex: 4990036 MOT APD

Motorola is an Equal Employment Opportunity/ Affirmative Action Employer

U.S. Sales Offices

Dearborn, Michigan
(313) 271-5500

Schaumburg, Illinois
(312) 576-2755

International Operations

Frankfurt, West Germany
(49-69) 66408-0
Telex: 176997188 AIEGD

Stotfold, Hertfordshire, U.K.
(44-462) 730661
Telex: 82437 MOTSTF G

Paris, France
(33-1) 47043635
Telex: MOTOFRA 630 193 F

Willowdale, Ontario, Canada
(416) 499-1441
Telex: 6986637 CDNMOTAIEG TOR

MAPCAL.XLS

File= NEWMAP. BIN

BKM, INC.

MAP TRANSDUCER CALIBRATION REPORT

PROJECT: TACOM
PROJECT NO.: 25138
DATE: 4/16/93

MAKE: FORD
PART NO: E43F 9F479 B2A
S/N:

VACUUM (IN HG-G)	PRESSURE (kPa-ABS)	FREQ (Hz)
-25.6	14.9	114.3
-19.9	34.3	122.5
-15.1	50.6	129.7
-10.0	67.9	137.7
-5.0	84.8	145.8
0.0	101.8	154.4
4.0	115.4	161.3
12.9	145.6	178.0
20.0	169.7	193.3

CALIBRATION BY: VLD
BAROMETER: 30.00 IN HG
TEMPERATURE: 70 DEG F
ECU S/N:

LTR	ZONE	DESCRIPTION	DRFT	DATE	CHK'D	APPD
REVISIONS						
A	–	ADDED INSTL. DIMS & NOTE 2	SLD	9.11.91		

AIR CHARGE TEMPERATURE SENSOR (ACT)

The ACT sensor consists of a disk thermistor with soldered leads and a protective plastic coating. It measures the temperature of the air entering the engine. The thermistor resistance is nonlinear and inversely proportional to temperature.

Size	61.3mm long
Weight	46 grams
Thread	3/8 — 18 PTF-SPL
Hex Size	25mm
Operating Temperature	-40°C to 125°C
Output	1k to 885k ohms
Output at 25°C	30k ohms
Temperature Coefficient	Negative
Accuracy	±3°C

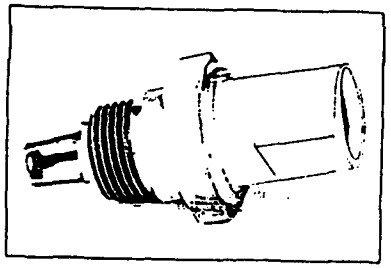

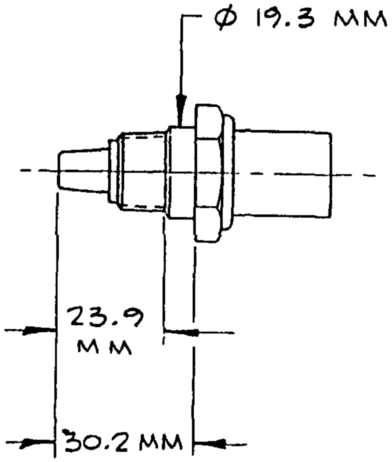

* ALT. SOURCE : NAPA/ECHLIN TS 5200

NOTES:

1. VENDOR: FORD ELECTRONICS & REFRIGERATION CO. (FERCO)
LANSDALE, PENN 19446
CONTACT : JOE SKOCZYINSKI
(215) 362-3140
2. SEE BKM DWG # 901810 FOR MATING CONNECTOR

SOURCE CONTROL DRAWING

DASH NO.	BODY MATERIAL	VENDOR PART NO.	FIRST USAGE
-3	BRASS	F2DZ ~~E1AZ~~-12A697-A*	70099
-2	PLASTIC	E7AF-12A697-AA	70072
-1	BRASS	E4AF-12A697-AA	70072

UNLESS OTHERWISE SPECIFIED TOLERANCES ON

THREE PLACES DECIMALS	TWO PLACES DECIMALS	ANGLES
± .010	± .03	± 2°

DO NOT SCALE DRAWING

MATERIAL

FINISH

BKM, Inc.
5141 Santa Fe Street
San Diego, CA 92109

DRAWN	S. DODGE	7.25.89
CHECKED	VCS	7.12.91
ENGINEER		
APPROVED		

TITLE: AIR CHARGE TEMP. SENSOR

SIZE: B | DRAWING NO. 901303 | LTR: A

SCALE NONE | PROJECT NO. SEE TAB | SHEET 1 OF 1

FORM 92 REV C

REVISIONS						
LTR	ZONE	DESCRIPTION	DRFT	DATE	CHK'D	APPD
A	—	ADDED INSTL. DIMS & NOTE 2	SLD	9-11-91		

ENGINE COOLANT TEMPERATURE SENSOR (ECT)

The ECT sensor consists of a disk thermistor with soldered leads and a protective plastic coating. It measures the engine coolant temperature. The thermistor resistance is nonlinear and inversely proportional to temperature.

Size	56.8mm long
Weight	42 grams
Thread	3/8 — 18 NPTF
Hex Size	25mm
Operating Temperature	-40°C to 125°C
Output	1k to 885k ohms
Output at 25°C	30k ohms
Temperature Coefficient	Negative
Accuracy	±3°C

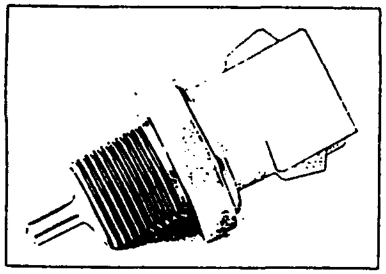

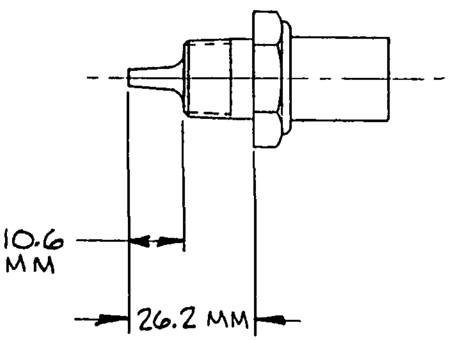

* ALT. SOURCE: NAPA/ECHLIN TS 4005 (BRASS)

NOTES:

1. VENDOR: FORD ELECTRONICS & REFRIGERATION CO. (FERCO) LANSDALE, PENN 19446 CONTACT: JOE SKOCZYNSKI (215) 362-3140
2. SEE BKM DWG # 901809 FOR MATING CONNECTOR

SOURCE CONTROL DRAWING

DASH NO.	BODY MATERIAL	VENDOR PART NO.
-3	BRASS	F2AZ ~~E1AZ~~-12A648-A
-2	PLASTIC	E6DF-12A648-AA
-1	BRASS	E4AF-12A648-AA

UNLESS OTHERWISE SPECIFIED TOLERANCES ON
THREE PLACES DECIMALS ±.010 | TWO PLACES DECIMALS ±.03 | ANGLES ±2°
DO NOT SCALE DRAWING
MATERIAL
FINISH

BKM, Inc.
5141 Santa Fe Street
San Diego CA 92109

DRAWN	S. DODGE	7-26-89
CHECKED	DCS	9-12-91
ENGINEER		
APPROVED		

TITLE: ENGINE COOLANT TEMP. SENSOR

SIZE: B | DRAWING NO. 901302 | LTR: A
SCALE: NONE | PROJECT NO. 70072 | SHEET 1 OF 1

FORM 92 REV C

DCS.

CUMMINS ENGINE COMPANY, INC. Columbus, Indiana 47201 MILITARY PERFORMANCE CURVE	BASIC ENGINE MODEL: VTA-903-T		CURVE NUMBER: RC-3914-A	
	ENGINE FAMILY:	CPL CODE: 0383	DATE: 4/12/79	BY: M.L.S.

DISPLACEMENT: 903 in^3 (14.8 litre) ASPIRATION: TURBOCHARGED & AFTERCOOLED RATING: HP (kW) @ RPM

BORE: 5.5 in (140 mm) STROKE: 4.75 in (121 mm) NO. OF CYLINDERS: 8

EMISSION CONTROL: AFC FUEL SYSTEM: PT 500 (373) @ 2600

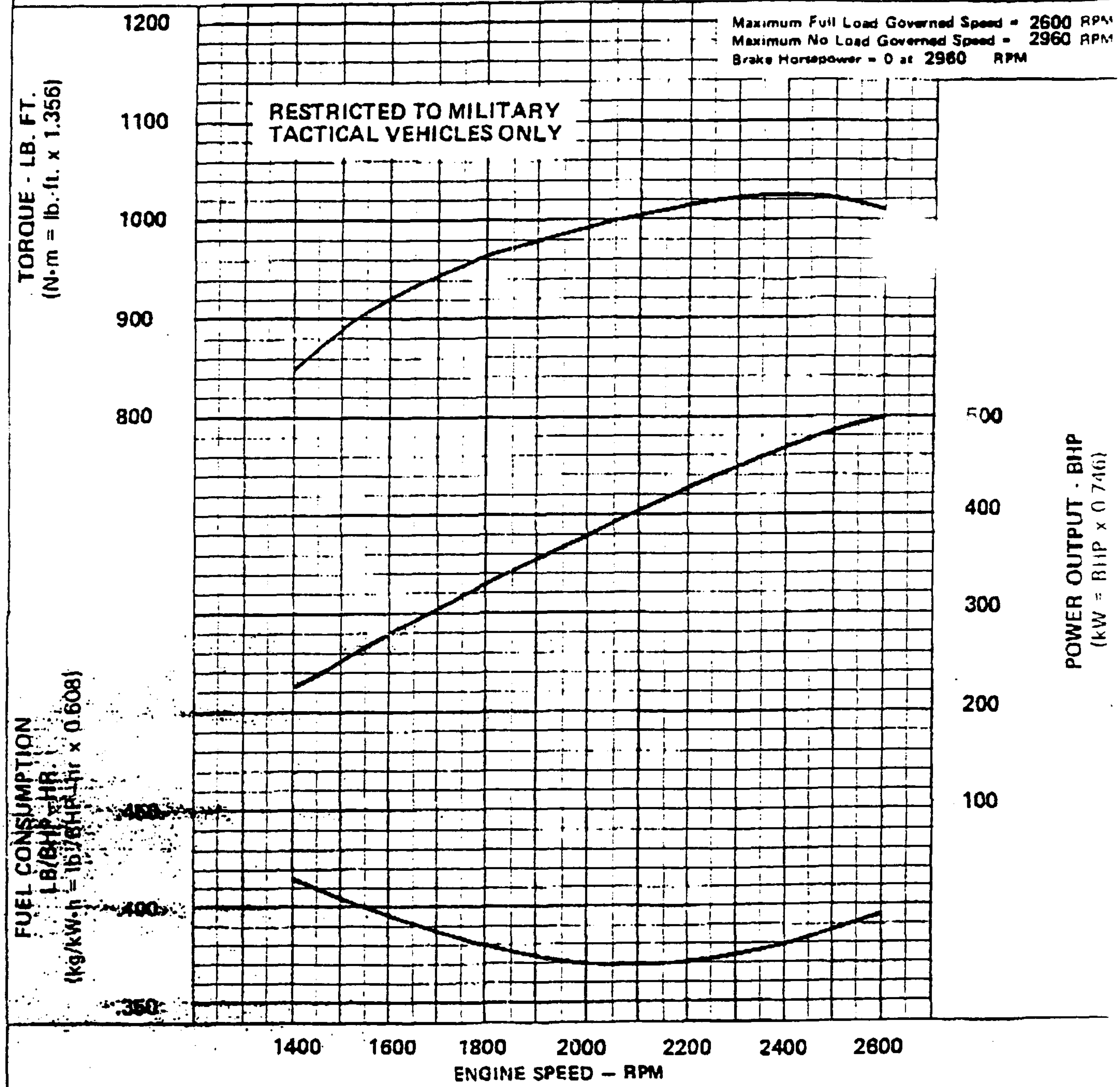

[illegible] represent engine performance capabilities at SAE standard J816b conditions of 500 ft. (150m) altitude (29.00" Hg [illegible]), 85°F (29°C) air intake temperature, and 0.38" Hg (9.6mm Hg) water vapor pressure with No. 2 diesel fuel.

STANDARDS DEPT. CERTIFIED WITHIN 5%: S. L. Gaal CHIEF ENGINEER

FORM 2714 Rev. 11-75

Military Engine Model: VTA-903-T **Date:** April, 1979 **Data Sheet:** DS-3914

CPL: 0383

General Engine Data

Reference Installation Drawing	3016663
Maximum Output (500 ft. & 85°F [150m & 29°C])—BHP (kW)	500 (373)
Speed @ Maximum Output—RPM	2600
Type	4 Cycle; 90° Vee; 8 Cylinder
Aspiration	Turbocharged & Aftercooled
Bore—in. (mm) x Stroke—in. (mm)	5.5 (140) X 4.75 (121)
Displacement—$in.^3$ (litre)	903 (14.8)
Compression Ratio	15.5:1
Dry Weight (with standard accessories)—lb. (kg)	2460 (1110)
Wet Weight (with standard accessories)—lb. (kg)	2580 (1170)
C.G. Distance from Front Face of Block—in. (mm)	
C.G. Distance above Crank Centerline—in. (mm)	
Moment of Inertia about Crank Centerline*—$lbm.-ft^2$ ($kg{\cdot}m^2$)	16.3 (.68)

*Standard Engine Less Flywheel

Engine Mounting

Maximum Allowable Bending Moment at Rear Face of Block—lb.-ft. (N-m)	1000 (1 350)
Moment of Inertia about Roll Axis—in.-lbf.-$sec.^2$ ($kg{\cdot}m^2$)	

Exhaust System

Maximum Allowable Back Pressure—in. Hg (mm Hg)	3.0 (76)
Exhaust Pipe Size Normally Acceptable—in. (mm) dia.	5.0 (125)

Air Induction System

Maximum Allowable Intake Restriction—Clean Element—in. H_2O (mm H_2O)	15 (380)
—Dirty Element—in. H_2O (mm H_2O)	25 (630)
Minimum Allowable Dirt Holding Capacity—g/CFM ($g{\cdot}litre^{-1}{\cdot}s$)	25 (53)

Cooling System

Coolant Capacity (engine only)—U.S. qt. (litre)	36 (34)
Standard Thermostat—(modulating)—Range—°F (°C)	170—185 (77—85)
Maximum Coolant Pressure (exclusive of pressure cap)—PSI (kPa)	35 (241)
Minimum Allowable Pressure Cap—PSI (kPa)	7 (50)
Maximum Allowable Top Tank Temperature—°F (°C)	210 (99)
Minimum Recommended Top Tank Temperature—°F (°C)	160 (70)
Minimum Fill Rate—U.S. GPM (litre/min)	5 (20)
Maximum Initial Fill Time—min	5
Minimum Coolant Expansion Space—% of System Capacity	5
Maximum Allowable Deaeration Time—min	25
Drawdown* Must Exceed the Volume Not Filled at Initial Fill	
Minimum Allowable Drawdown*— U.S. qt (litre)	13 (12)

*Drawdown does not include expansion space. It is suggested that initial design be at least 10% of system capacity.

Lubrication System

Oil Pressure @ Idle—PSI (kPa)	5—25 (34—172)
@ Rated Speed—PSI (kPa)	30—55 (210—380)
Oil Flow @ Maximum Rated Speed (nominal)—U.S. GPM (litre/min)	36 (136)
Flow Required for By-Pass Filter at No Load Governed Speed—U.S. GPM (litre/min)	***
By-Pass Filter Size—$in.^3$ (litre)	***
By-Pass Filter Capacity—U.S. gal. (litre)	***
Oil Capacity of Standard Pan (High-Low)—U.S. gal. (litre)	4.5—3.5 (17—13)
Total System Capacity of Standard Engine —U.S. gal. (litre)	6.5 (25)
Angularity of Standard Pan—Front Down	55°
—Front Up	35°
—Side to Side	30°

***BY-PASS FILTER NOT REQUIRED ON TACTICAL VEHICLES

Fuel System

Maximum Fuel Consumption @ Rated HP & Speed—lb./hr. (kg/h)	199 (90)
—U.S. GPH (litre/h)	28 (106)
Maximum Fuel Flow to Pump @ Rated HP & Speed—lb./hr. (kg/h)	930 (422)
—U.S. GPH (litre/h)	131 (496)
ıximum Allowable Restriction to Pump—Clean Filter—in. Hg (mm Hg)	4.0 (100)
—Dirty Filter—in. Hg (mm Hg)	8.0 (200)
Maximum Allowable Return Line Restriction—in. Hg (mm Hg)	4.0 (100)

Electrical System

Minimum Recommended Battery Capacity	0°F CCA
Cold Soak @ 32°F (0°C) and Above — 12 volt Starter	1280
— 24 volt Starter	640
Cold Soak @ 0°F to 32°F (-18°C to 0°C) — 12 volt Starter	1800
— 24 volt Starter	900
Maximum Allowable Resistance of Starting Circuit —	
With 12 volt Starter—Ohms	0.00075
With 24 volt Starter—Ohms	0.002

Performance Data

All data is based on the engine operating with fuel system, water pump, lubricating oil pump, air cleaner, and muffler; *not included are alternator, compressor, fan, optional equipment and driven components.* Data is based on operation under SAE standard J816b conditions of 500 feet (150m) altitude (29.00 in. (736mm) Hg dry barometer), 85°F. (29°C) intake air temperature and 0.38 in. (9.6mm) Hg water vapor pressure, using No. 2 diesel or a fuel corresponding to ASTM D2. **All data is subject to change without notice.**

Performance Curve	RC—3914—A
Brake Mean Effective Pressure @ Rated Power—PSI (kPa)	169 (1 165)
@ 1800 — —PSI (kPa)	161 (1 110)
Piston Speed @ 2600 RPM—ft./min. (m/s)	2060 (10.5)
Friction Horsepower @ 2600 RPM (kW)	95 (71)
@ 1800 RPM (kW)	50 (37)
Idle Speed—RPM	800
Maximum No Load Governed Speed—RPM	2980
Maximum Overspeed Capability—RPM	3300
ɾrque Available at Clutch Engagement (800 RPM)—lb.-ft. (N-m)	600 (814)
Minimum Recommended Combined Converter and Hydraulic Stall Speed—RPM	2600
Thrust Bearing Load Limit—Maximum Intermittent—lb. (N)	2500 (11 000)
—Maximum Continuous—lb. (N)	1250 (5 500)

Chart Below Reflects Data Based on Following Variables at Conditions of Rated Power:

Coolant Temperature—°F (°C)	185 (85)	Air Intake Restriction—in. H_2O (mm H_2O)	10 (250)
Water Inlet Pressure—PSI (kPa)	7 (50)	Air Intake Temperature—°F (°C)	85 (29)
Block Pressure—PSI (kPa)	30 (207)	Exhaust Restriction—in. Hg (mm Hg)	2.0 (50)

Engine Ratings	Output BHP (kW)	Speed RPM	Torque Lb-Ft (N-m)	Air Flow CFM (litre/s)	Exhaust Gas CFM (litre/s)	Exhaust Gas Temp. °F (°C)	Water Flow U.S. GPM (litre/s)	Heat Rejection, BTU/Min. (kW)
Full Power	500 (373)	2600	1010 (1370)	1100 (519)	3050 (1439)	1050 (566)	127 150 (8.0)	14,000 (246)
Check Point	330 (246)	1800	963 (1306)	600 (283)	1680 (793)	1060 (571)	88 104 (5.6)	9,000 (158)

NOTE: *This engine is restricted in its application to:* Military Tactical Vehicles Only.

**—Radiator coolant flow is approximately 5% less with a continuous deaerating system.

Engine Model: VTA—903—T
Data Sheet No: DS—3914
Date: April, 1979
Bulletin No:

Test Report TR-018
Subject: Preliminary Test of WS-90 Turbo Boost System
Date: 12-11-1990

1. Objective

As part of the TACOM Cold Start project, a modification of the variable area tail pipe slider installed on a WS-90 turbocharger may present an opportunity to enhance starting as well as serve the main purpose of fast warm up and boost at idle. The objective of this test was to determine the effectiveness of a number of nozzles incorporated in the slider to spin the turbo to a speed sufficient to develop a PR of approximately 1.1.

2. Procedure

For the purposes of this test, 10 nozzles of .0625 diameter were drilled around the periphery of the slider at an angle of 30 degrees from the tangent in line with the radial volute. The WS-90 was installed on a Cummins NTC-400 with a diverter block installed between the exhaust manifold and the turbo to divert all exhaust to the radial volute, at the same time effectively blocking and isolating the axial volute, Fig. 1. Pressure and temperature sensors were installed in the intake as well as the exhaust manifolds with a mechanical tachometer used to measure engine cranking speed. The fuel supply pump was de-activated to prevent the engine from starting.

3. Results and conclusions

At a cranking speed of 180 RPM, the exhaust back pressure was measured at 12 PSIG and turbine speed was estimated at approximately 2000 RPM. At this low cranking speed and correspondingly low gas volume pumped into the exhaust manifold, the smallest leaks will have a large effect on manifold pressure. Leaks can exist at manifold gaskets, turbo flanges and between the slider and turbo housing. The low turbine power developed at this low pressure was too small to have any measureable effect on intake manifold pressure or temperature.

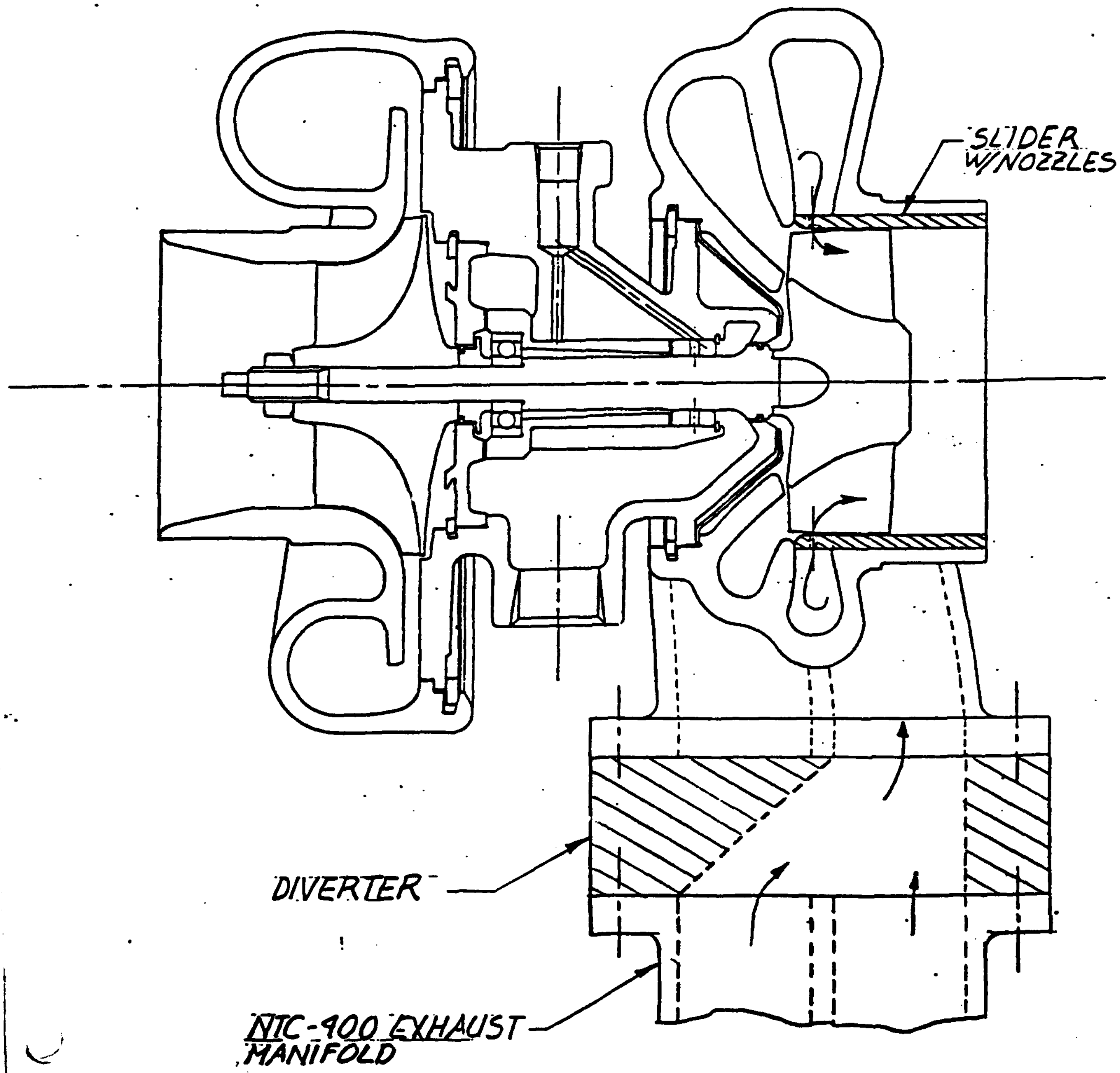

FIG. 1

BKM. INC TEST REPORT

TR- 019

STATEMENT OF PROBLEM:

Test Revised Configuration of Slider drilling. Is boost pressure at low idle adequate?

REFERENCES: (Part designation, correspondance, lit. reference, etc.)

TACOM Turbo. Slider drilled with 60 Holes, .06 Dia. Tested at U. of Nebraska on NTC400 Cummins engine. Diverter plate installed (see DIAGRAM)

ASSUMPTIONS:

TARGET Manif. Pressure is 6.0 "Hg (gauge) At 600 RPM low idle.

RESULTS-SUMMARY:

See Attached data The MAP achieved was 2.6" Hg - Approximately half of the target value. It is felt that a smaller number of larger holes will work better. The turbo will be returned to BKM and a bench test performed to optimize hole configuration before the next engine test.

Prepared by: DCS
Date: 12/27/90
No. of Sheets: 2

Checked by: Jurgen Antman
Date: 1-8-91

Approved by:
Date:

BKM FORM #123

Univ. of Neb.
Cold Start Turbo test.
60 Holes x .060 ø
Cummins NT400 Dual Fuel Engine.

DATE: 12/21/90
ENGINE: 91 NTC400
TEST: IDLE TESTING OF STP TURBO

TIME	ENGINE SPEED rpm	TURBO CONFIG.	INTAKE MANIFOLD PRESSURE in Hg	INTAKE MANIFOLD TEMP. deg F	EXHAUST PRESSURE psi	EXHAUST TEMP. deg F	TURBO SPEED rpm	COOLANT TEMP. deg F
TART-UP WITH DYNO CONNECTED -- MANOMETER OFF SCALE								
10:05	NA	STC	NA	59	>30	400	NA	61
TART-UP WITH DYNO DISCONNECTED - MANOMETER OFF SCALE								
10:12	NA	STC	1.5	62	>30	380	NA	61
TART-UP AND RAN WITH DYNO CONNECTED WITH GAUGE MEASURING EXHAUST PRESSURE								
10:24	740	STC	3 1.5/	83	45	434	NOTE 1	61
10:27	720	STC	2.6 [illegible]	58	42	557	NOTE 2	61

UT DOWN AT 10:28 BECAUSE BACKPRESSURE WAS ABOVE SPECIFIED VALUE

TES
URBO SPEED APPEARED TO BE ABOUT 4000 RPM, BUT SPEED WAS CHANGING QUICKLY
ARD TO MEASURE, BUT STROBE MARK WAS STEADY AT 1280 RPM (COULD BE MULTIPLE)

BKM, INC. TEST REPORT

TR-026

STATEMENT OF OBJECTIVE: To test the performance of the Stage I turbocharger configuration (impulse nozzle inlet) on the VTA-903. The engine will be run without load from low idle speed (600 RPM) up to the speed at which the turbine inlet pressure ratio is 2.0. Turbine and compressor inlet and outlet temperatures and pressures will be recorded. Turbine speed data will also be taken.

REFERENCES: (Test equipment) Cummins VTA-903 engine with Servojet injection system and twin WS-90 TACOM turbochargers.

The impulse nozzles (30 hole x .125 dia.) were drilled into the turbine slider rings and inserted into the Stage II position. An exhaust diverter valve and a special block-off plate were installed to totally seal the axial exhaust inlet - simulating the Stage I configuration. See figure 1.

ASSUMPTIONS: Based on earlier bench testing, a target point for combined efficiency vs boost pressure was calculated (figure 2). A compressor pressure ratio of approximately 1.2 was expected at a turbine pressure ratio of 2.0.

RESULTS: As plotted in figure 2, the resulting combined efficiency was slightly below the target point. The compressor ratio was 1.18 at a turbine pressure ratio of 2.01. Exhaust pressure, boost pressure, and turbine speed vs engine RPM are plotted in figures 3-6.

Prepared by: D. Steinmeyer
Date: 5/29/91

TEST DATA

Stage III Baseline data without impulse nozzles or diverter valve.

ENGINE RPM	Pc(out) "Hg ga	Pt(in) "Hg ga	Tt(in) Deg F	Tt(out) Deg F	Tc(out) Deg F	TURBINE RPM
600	0.0	0.3	196	160	71	4150
800	0.0	0.5	214	175	71	5900
1000	0.1	0.85	234	195	72	9100
1200	0.25	1.3	247	218	73	11300
1400	0.35	1.7	269	239	75	13800

Stage I data with 30 x .125" impulse nozzles and diverter valve.

ENGINE RPM	Pc(out) "Hg ga	Pt(in) "Hg ga	Tt(in) Deg F	Tt(out) Deg F	Tc(out) Deg F	TURBINE RPM
600	0.5	5.0	215	172	72	10750
800	1.2	9.4	257	207	76	16400
1000	2.35	16.1	301	245	84	22600
1040						25000
1200	4.2	26.4	364	297	95	25K+
1280	5.4	30.4				25K+

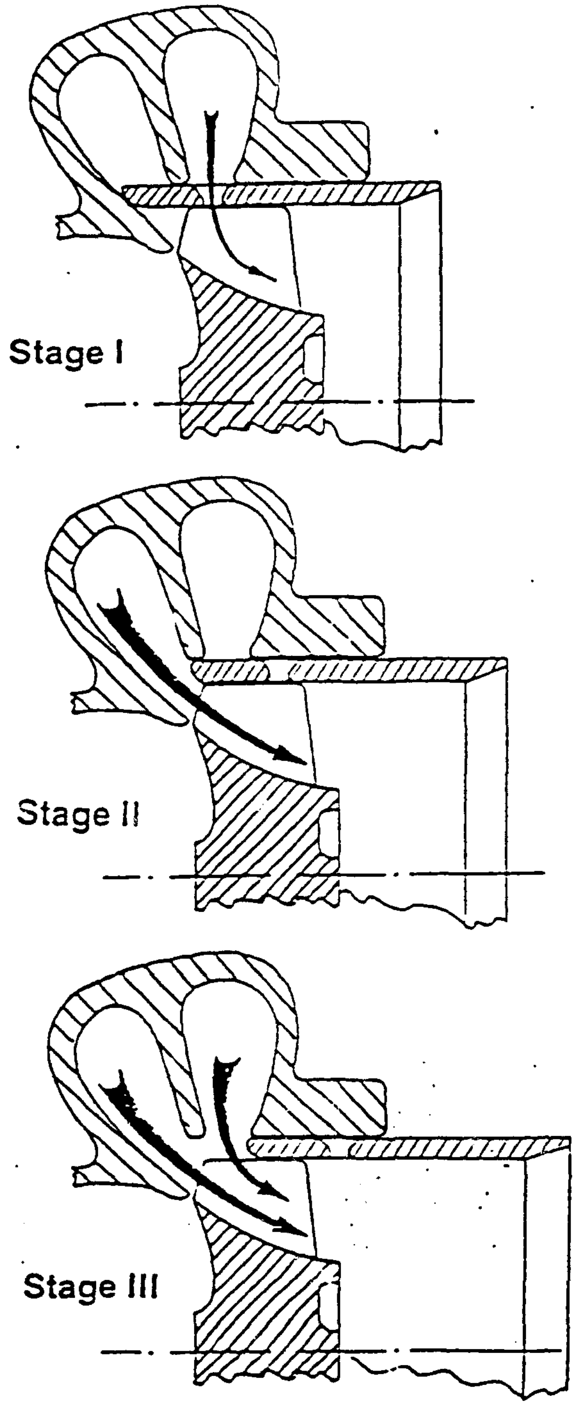

Figure 1 Three Stage Operation

FIGURE 2

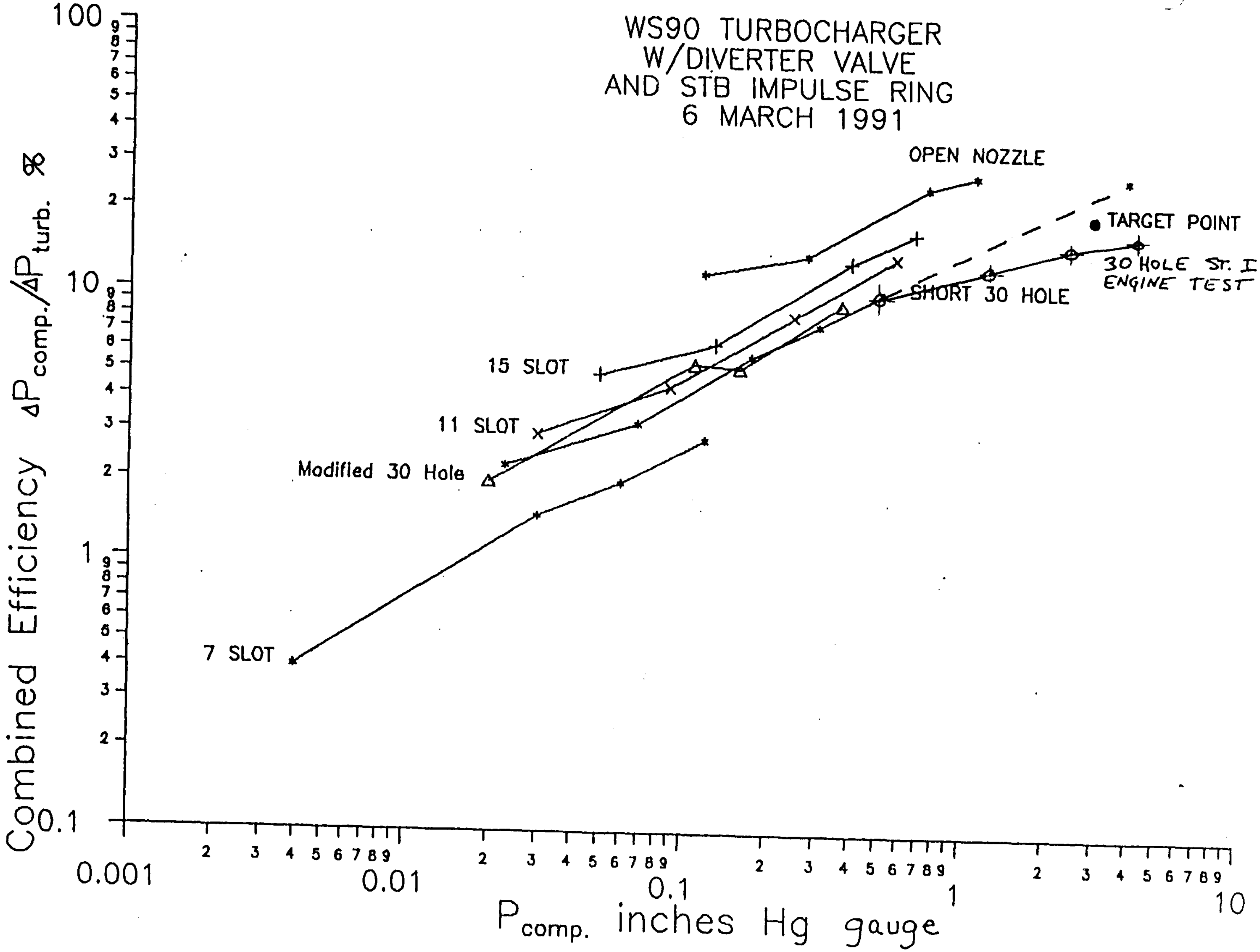

WS90 TURBOCHARGER
W/DIVERTER VALVE
AND STB IMPULSE RING
6 MARCH 1991
OPEN NOZZLE
TARGET POINT
30 HOLE St. I
ENGINE TEST
SHORT 30 HOLE
15 SLOT
11 SLOT
Modified 30 Hole
7 SLOT
Combined Efficiency ΔPcomp./ΔPturb. %
Pcomp. inches Hg gauge
100
10
1
0.1
0.001
0.01
0.1
1
10

FIGURE 3

TACOM TURBO BASELINE
MAY 23, 1991
VTA-903

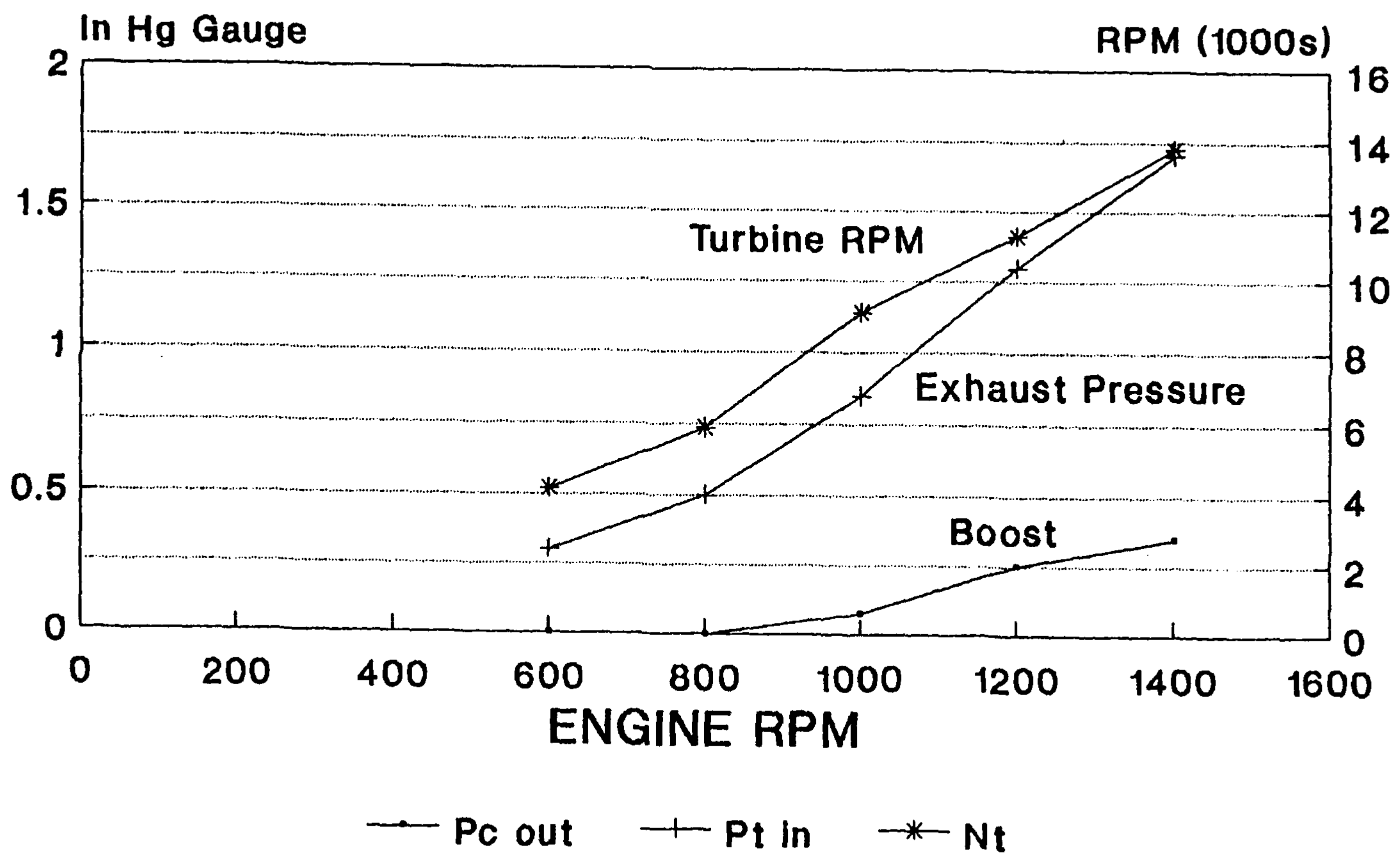

FIGURE 4

TACOM TURBO RING 30 X .125
MAY 24, 1991
VTA-903

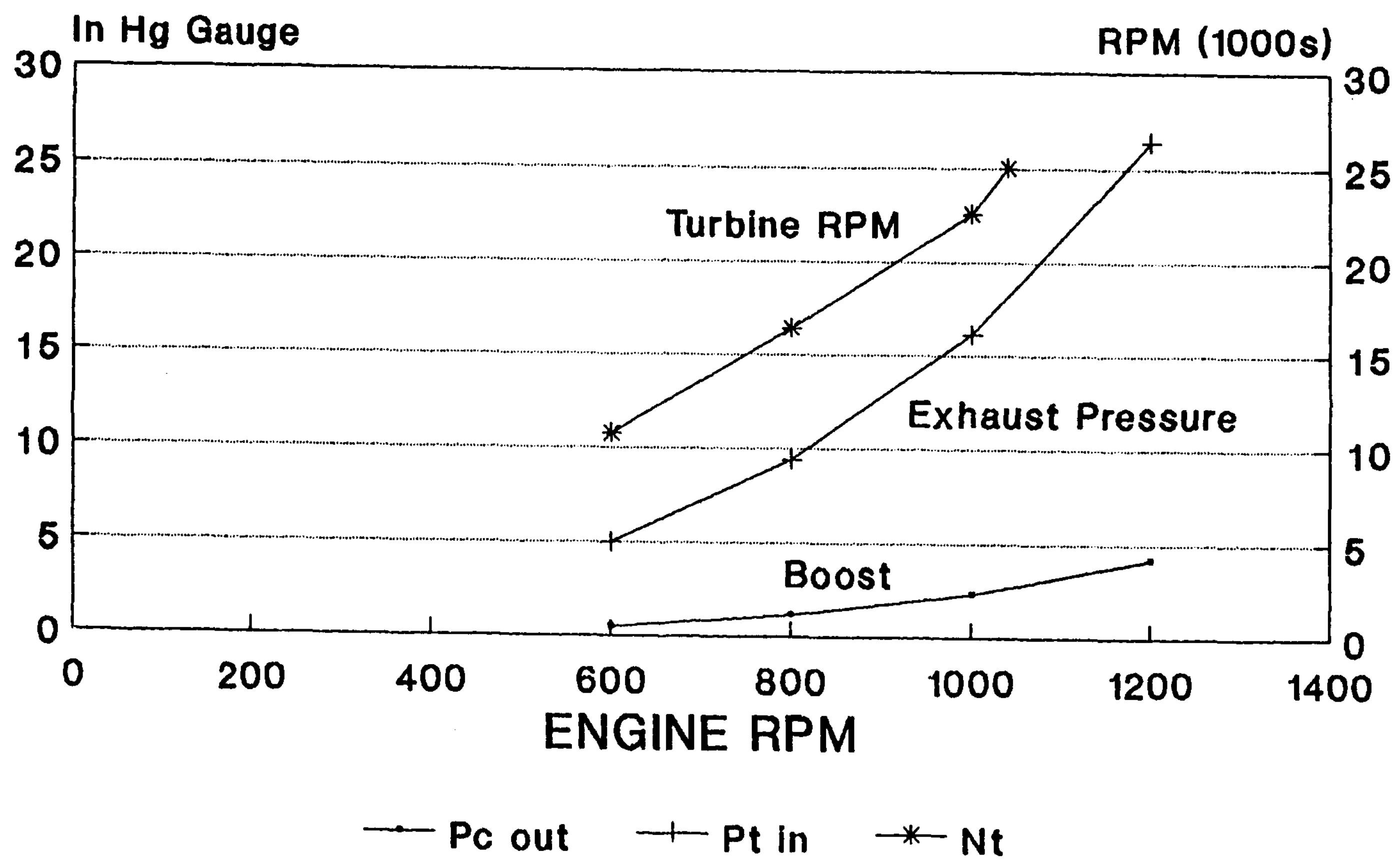

FIGURE 5

TURBOCHARGER PERFORMANCE
STAGE I vs STAGE III
VTA-903

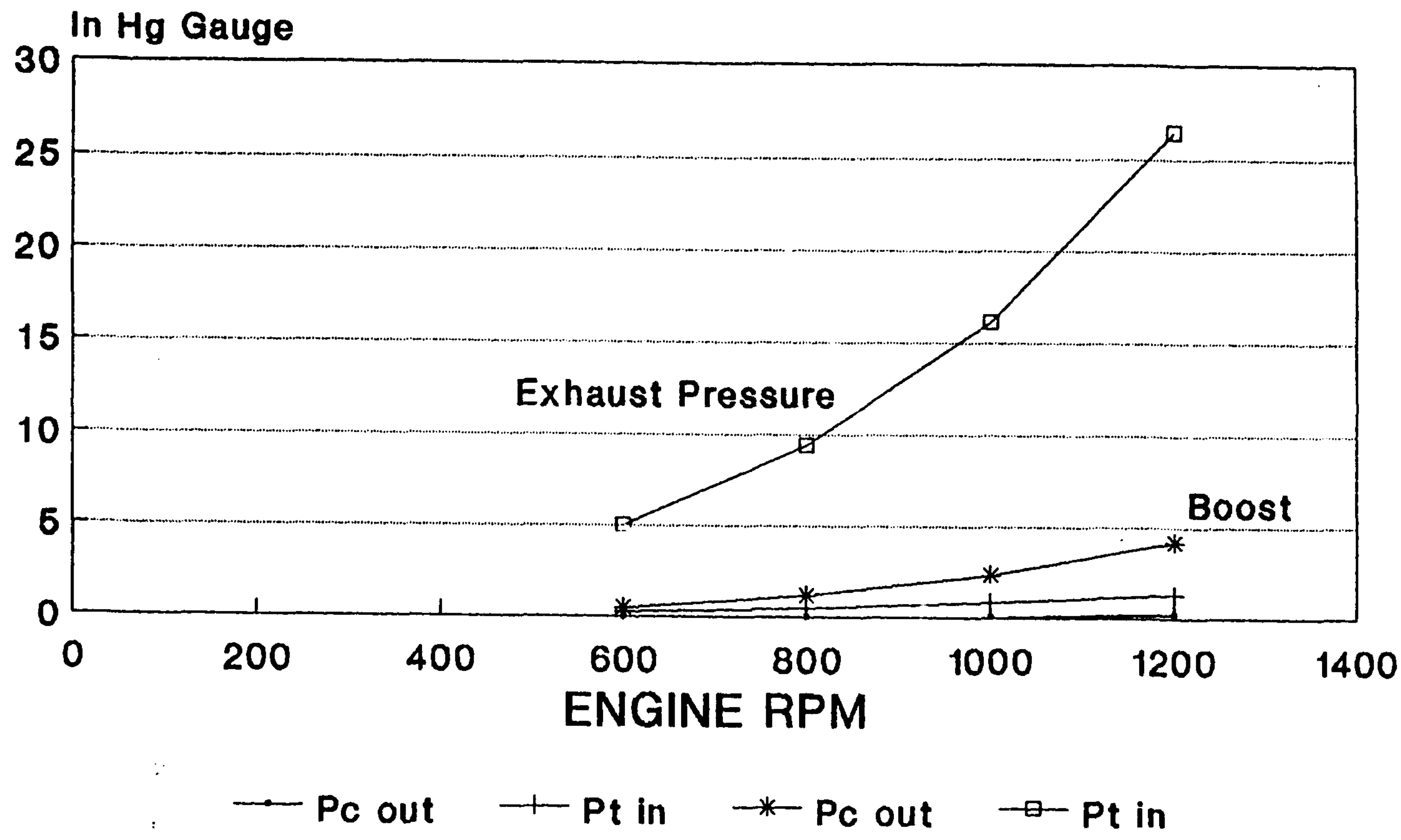

FIGURE 6

TURBINE SPEED
STAGE I vs STAGE III
VTA-903

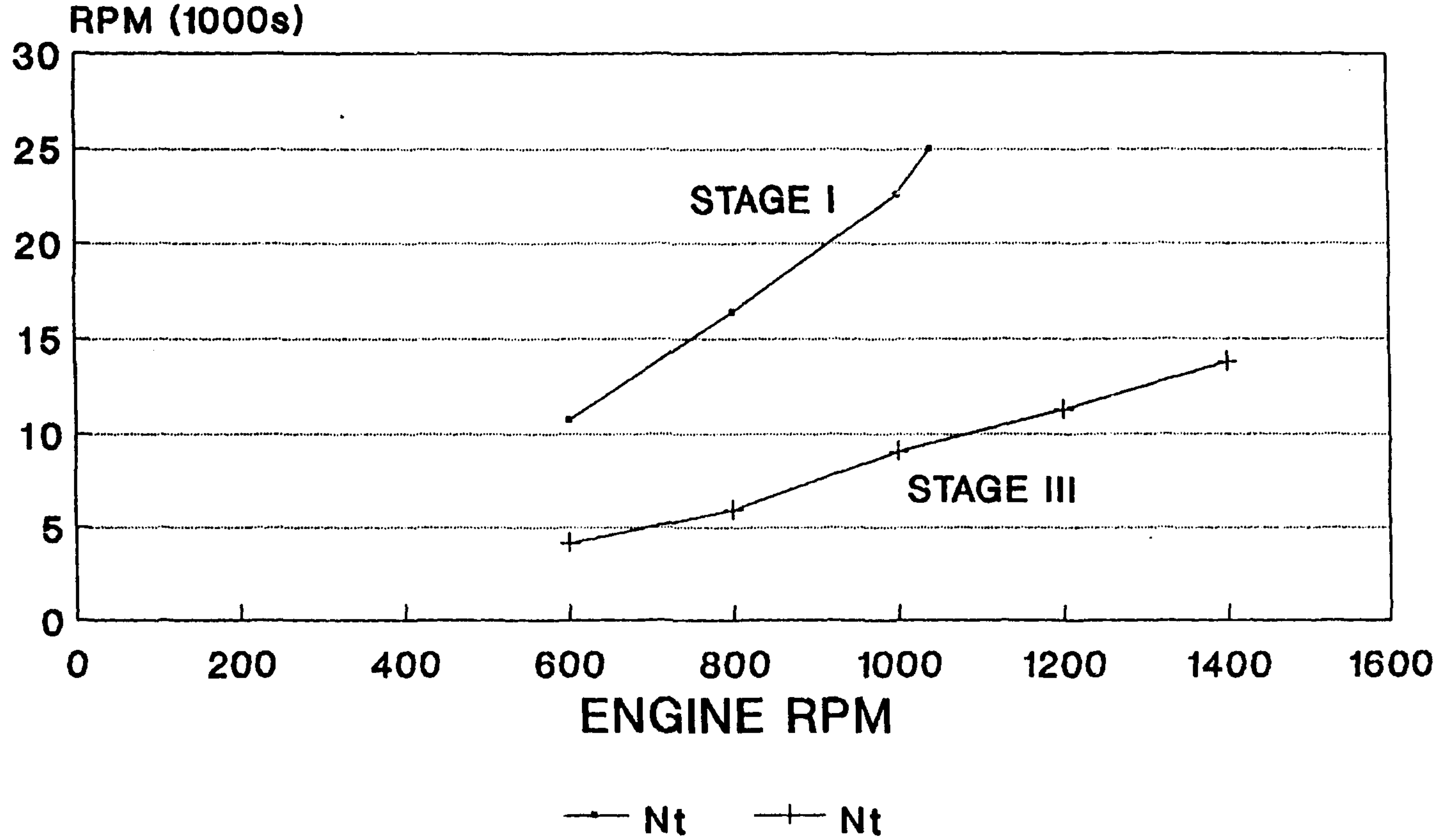

TR-021
January 24, 1991
Prepared by: D. Steinmeyer

Objective: To quantify the temperature rise in the inlet manifold of a diesel engine while cranking with various inlet and exhaust valve lash configurations and various exhaust restrictions. The maximum manifold air temperature is desired as an aid to cold starting. No attempt was made to actually start the test engine.

The technique proposed includes: 1) blocking off the exhaust manifold and allowing the compressed exhaust air to blow back into the cylinder and 2) holding the inlet valve open a small amount so that the heated compressed air can escape into the inlet manifold during the compression stroke.

References: A Perkins 4.236 diesel engine, configured as a single cylinder research engine, was the test subject. The bore diameter is 3.875 inches, stroke is 5.00 inches, and the compression ratio is 16.0 to 1. Only the #4 piston and rod were installed. The exhaust manifold was removed and replaced with a closed-end tube, 16.5 inches in length and 3.0 inches in diameter. This exhaust tube was shortened to 10.0 inches during the test. Since the engine has siamesed exhaust ports, the adjacent #3 exhaust valve was clamped shut to prevent exhaust pressure from escaping.

The engine was lubricated with an external electric pump. The electric starter was used to crank the engine. Each test was 30 seconds in duration.

An Analog Devices microMac 5000 data acquisition system was used to collect four channels of temperature data at 2 second intervals. Inlet manifold temperature was measured in 2 locations - immediately upstream (1.5 inches) from the #4 inlet port, and at the manifold entrance (19 inches upstream). A standard Perkins air cleaner was installed on the open end of the manifold. Exhaust tube temperature was taken 5 inches downstream from the port. Ambient air temperature was also recorded. J-type thermocouple sensors (1/16" diameter) were used. All temperature data has been normalized to show the increase over the starting ambient temperature.

Cylinder and exhaust pressures were recorded on mechanical gauges and total engine revolutions were recorded during each test on a digital counter.

Results: The most effective inlet air heating occurred when the exhaust valve was disabled (by removing the pushrod) and the inlet valve held open 0.010 inch. This results in a compression stroke which leaks hot air into the inlet manifold during each engine revolution. Figure 1 shows the manifold temperature vs time under these conditions (#8) and also with normal exhaust valve operation and the 16.5 inch and 10.0 inch exhaust plugs (#3 and #11).

Various inlet valve lash settings were evaluated with -0.010 inch being the optimum for this engine. Figure 2 shows the temperature rise at .005, .010, and .015 inch. Openings of .008 and .012 were also tested and exhibited a smaller temperature rise than the .010 setting.

Several tests with the exhaust and inlet valves held open a small amount were tested as shown in figure 3. None of these combinations were as effective as a completely disabled exhaust in heating the inlet air.

Finally, a set of baseline tests, with a fully open exhaust pipe and various inlet lash settings, were conducted. The results of these tests are presented in figure 4.

The starter current draw was also measured during the final baseline test to determine the electrical power input during cranking. We found that with standard inlet and exhaust lash and an open exhaust pipe, the starter drew 1920 Watts. Assuming a starter efficiency of 40%, this equals 1.02 HP or 0.72 BTU. At the optimum configuration for maximum inlet air heating (-.010 inlet lash and the exhaust disabled), the starter drew 2100 Watts, an increase of about 9%.

Recommendations: The feasibility of using compression heating to raise inlet manifold temperatures has been demonstrated.

The next step should be to design and test the practical application of this concept to a running multi-cylinder engine. The temperature distribution within the inlet manifold should be measured during cranking and the transition to running.

Such a test is outside the scope of the current SBIR project but could be run by TACOM at its cold-start facility or elsewhere as the subject of a future project.

Test Summary:

Test No.	In Lash*	Ex Lash*	Revs	Cyl Pres	Ex Pres	Comments
1	+0.010"	+0.018"	134	425psi	40psi	16.5x3 ex
2	-0.005	+0.018	160	260	5	"
3	-0.010	+0.018	160	130	2	"
4	-0.020	+0.018	170	27	.5	"
5	-0.015	+0.018	168	43	1	"
6	+0.010	-	137	435	-	exh disabled
7	-0.005	-	153	270	-	"
8	-0.010	-	154	90	-	"
9	-0.015	-	163	20	-	"
10	+0.010	+0.018	139	450	40	10x3 exh
11	-0.010	+0.018	162	75	1	"
12	-0.008	-	144	155	-	exh disabled
13	-0.010	-	149	60	-	"
14	-0.012	-	156	40	-	"
15	-0.010	-0.005	161	35	1	10x3 exh
16	-0.010	-0.010	168	15	.5	"
17	-0.005	-0.005	162	150	1	"
18	-0.010	-	149	50	-	exh disabled
19	-0.010	+0.018	159	70	-	open exhaust
20	+0.010	+0.018	163	450	-	"

* A (+) lash indicates standard running clearance and a (-) lash indicates that the valve is held open the amount indicated off the seat.

FIGURE 1 1/14/91

TEMPERATURE RISE ABOVE AMBIENT

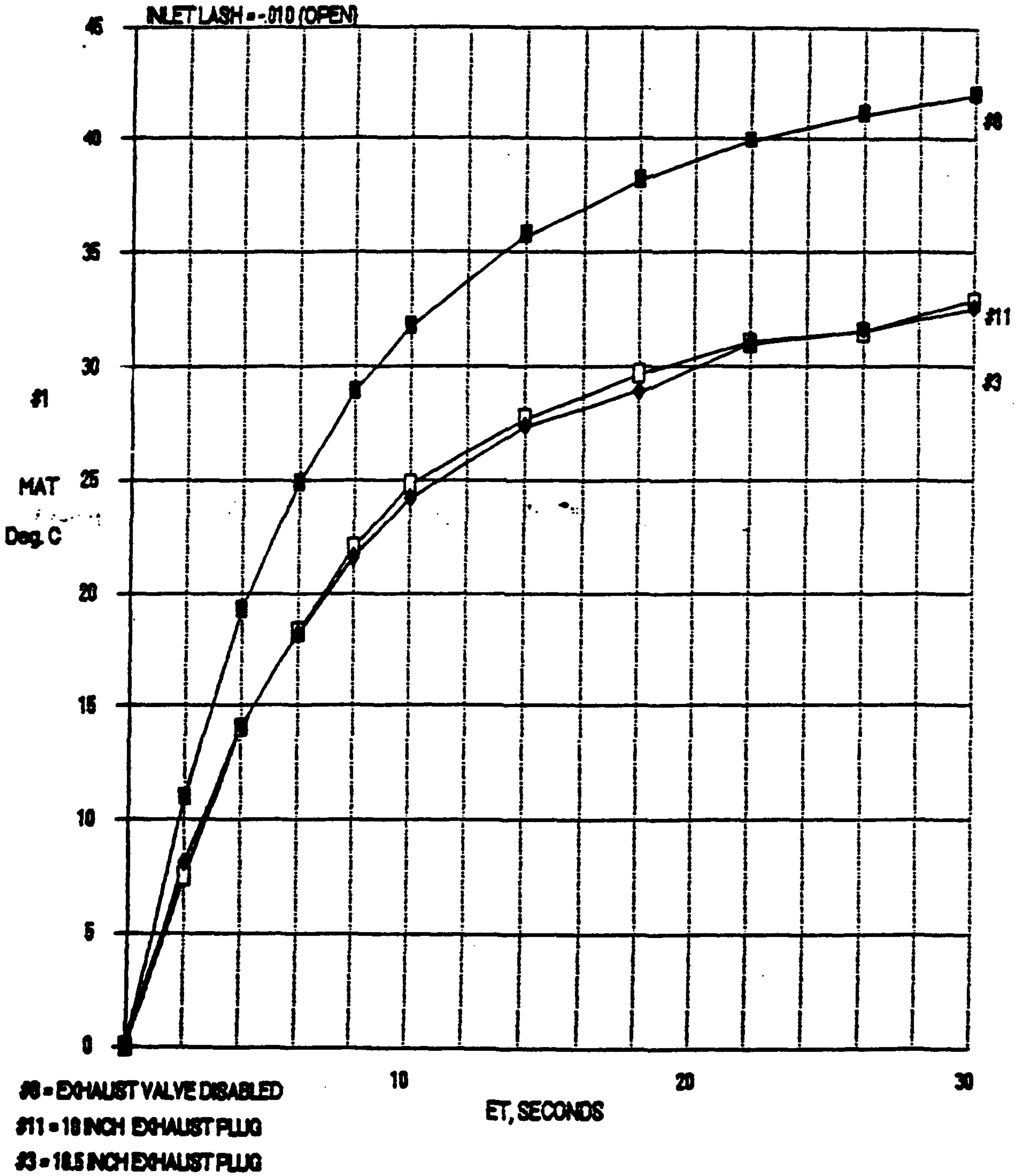

FIGURE 2 1/14/91

TEMPERATURE RISE ABOVE AMBIENT

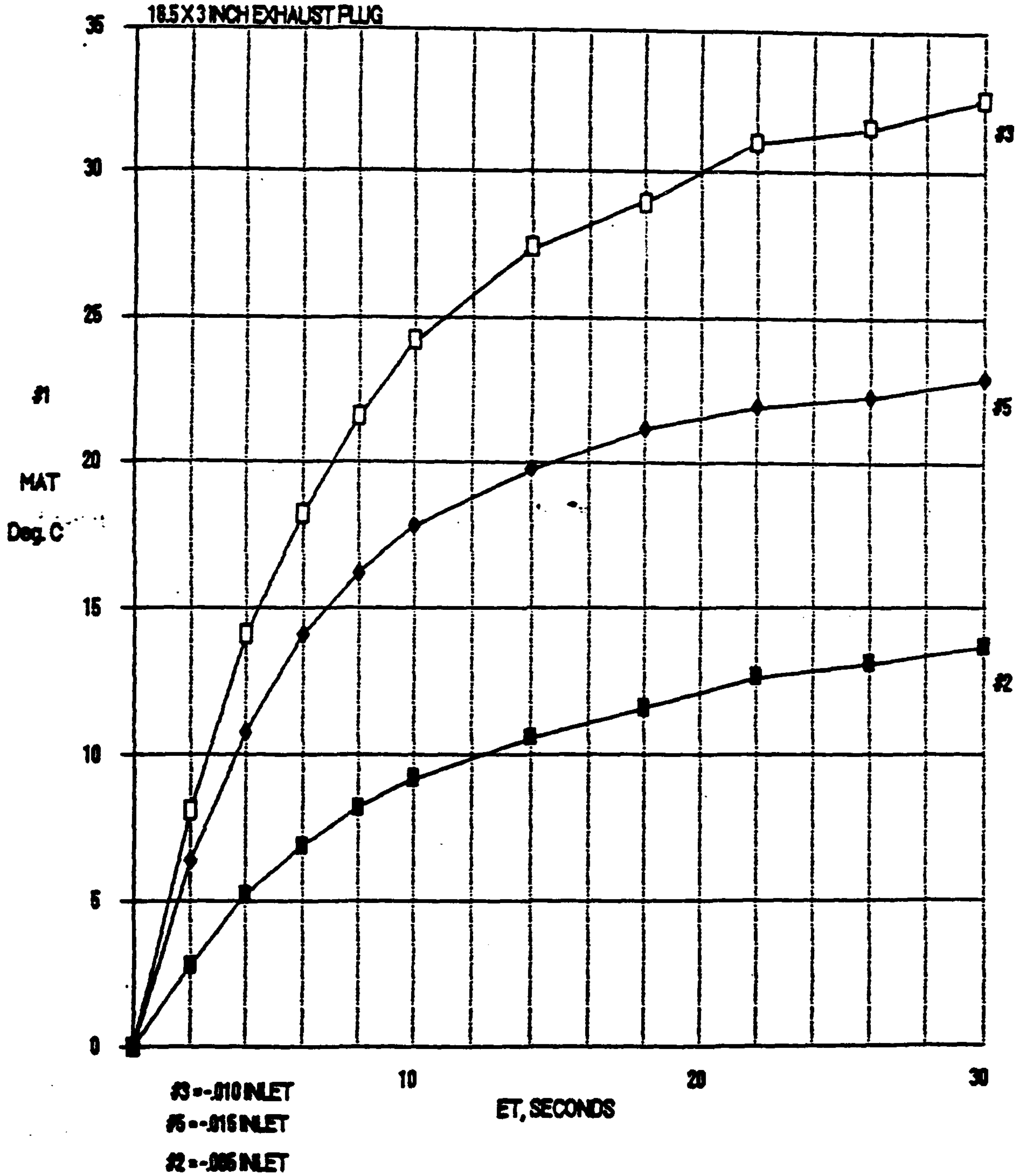

FIGURE 3 1/16/91

TEMPERATURE RISE ABOVE AMBIENT

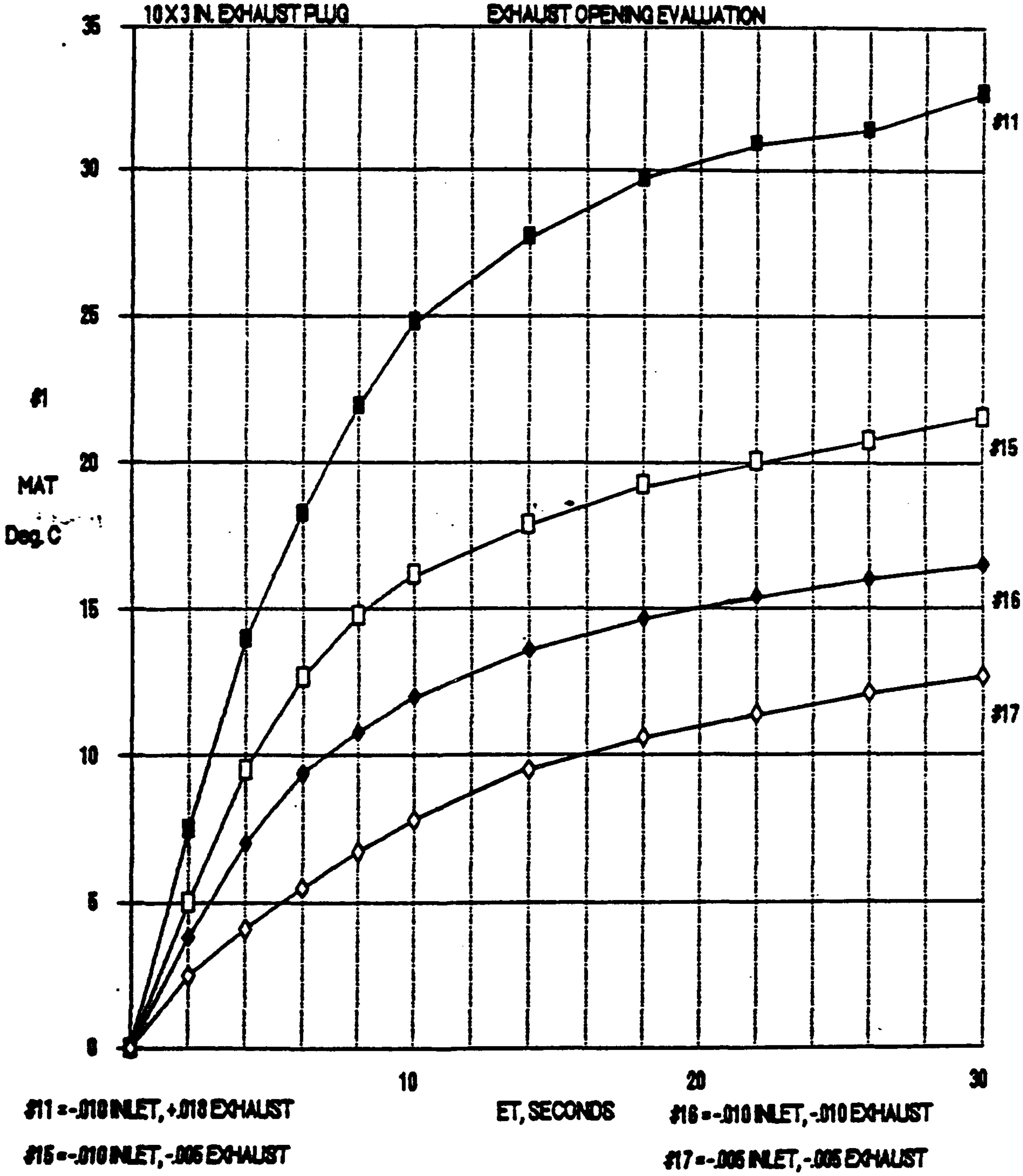

FIGURE 4 1/22/91

TEMPERATURE RISE ABOVE AMBIENT

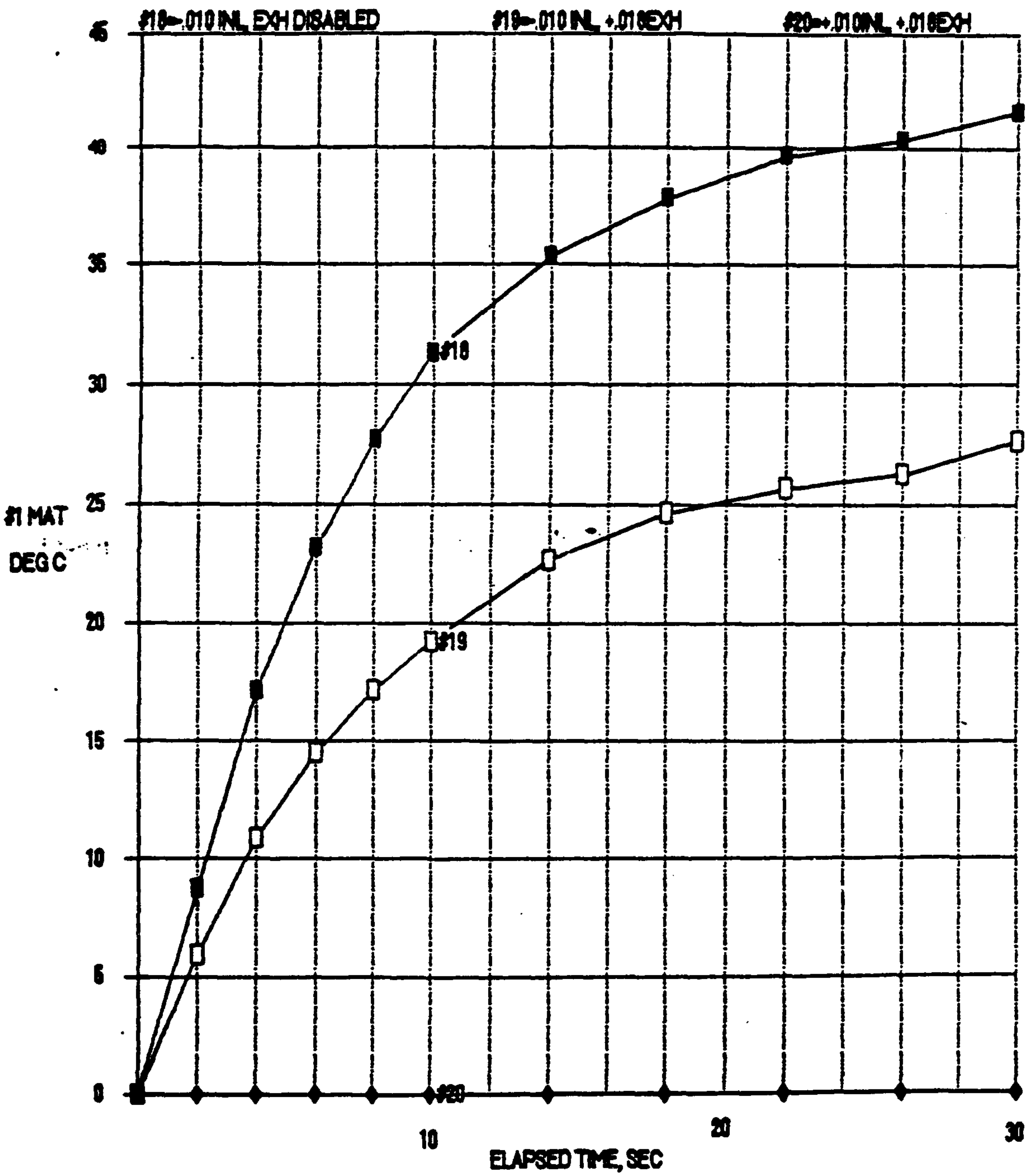

BKM, Inc. 5141 Santa Fe Street, San Diego, CA 92109	TACOM COLD-START CRANKING TEST		NO TR-021 SHEET ___ OF ___
	PREPARED BY	DATE 1/24/91	APPROVED BY

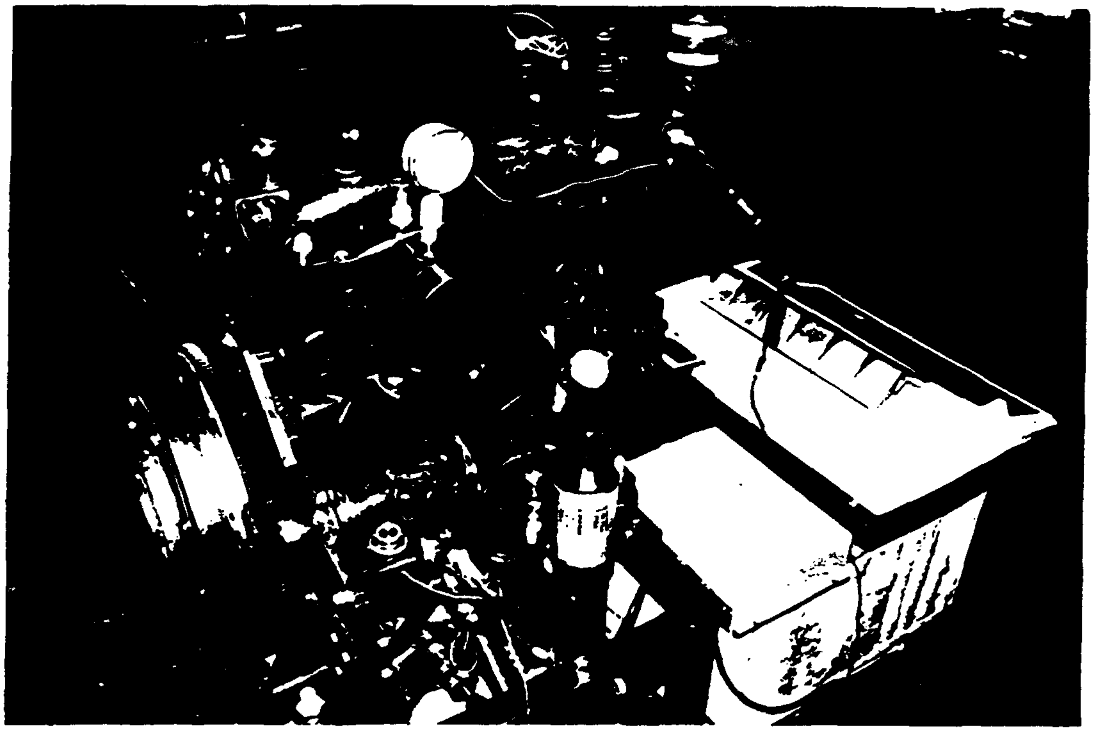

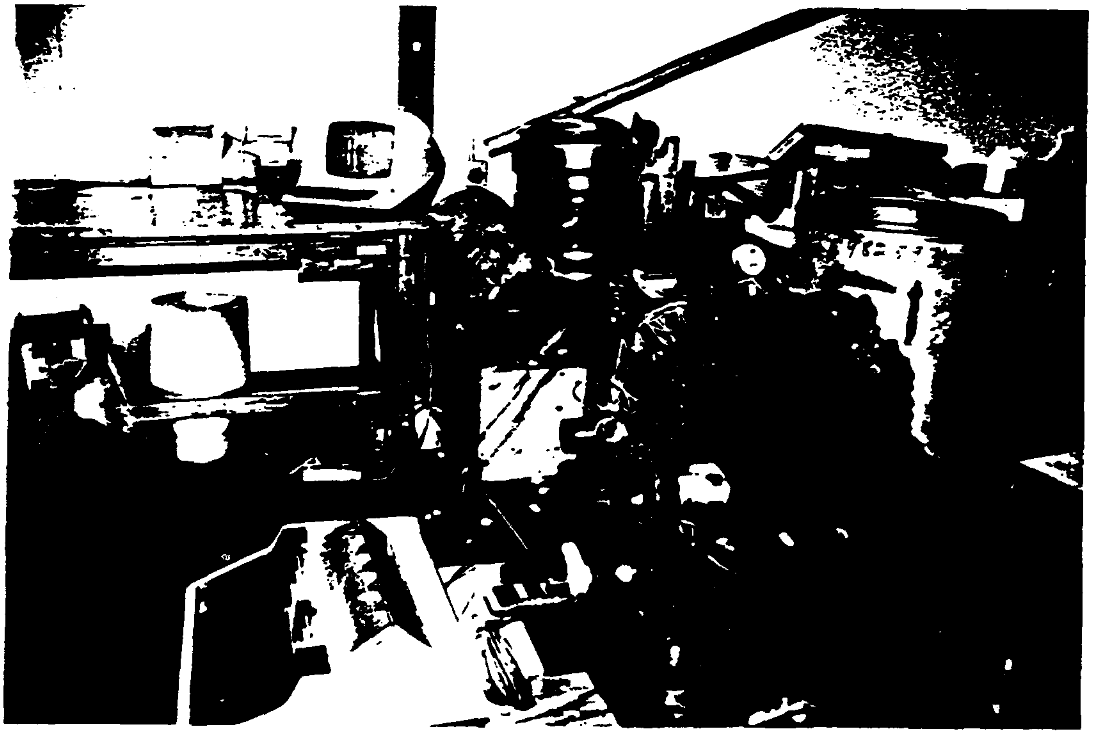

Analysis of a High Pressure Injection System

~Final Report~

Submitted to:

BKM, Inc.
San Diego, California

Submitted By:

Dr. Duane Abata

Mr. Roderick Strong

Department of Mechanical Engineering - Engineering Mechanics

College of Engineering

Houghton, Michigan

June 28, 1993

Analysis of a High Pressure Injection System

Contents

List of Figures, Tables and Photographs

Analysis of a High Pressure Injection System

Executive Summary

This final report represents the results of an investigation of a high pressure injection system operated with six different injectors/nozzle configurations. The purpose of the investigation was to obtain high speed photographs of the injection process, and analyze the effects of nozzle configurations on the cylinder pressure and heat release during the combustion process within the cylinder.

Injecting fuel into the cylinder head at higher pressure results in a finer fuel mist which facilitates mixing. It is believed that better mixture of air and fuel improves ignition and combustion. This is countered with the fact that higher injection pressures may cause fuel wall wetting and increase smoke in the exhaust. Hopefully, the results of this investigation will lead to a better understanding of these interacting phenomena.

The injectors were tested at a nominal rail pressure of 800 and 1500 pounds per square inch (psi) The engine used was a modified three cylinder, two-stroke 353 Detroit Diesel engine. One cylinder was modified to allow viewing and high speed filming of the combustion process. This was achieved by extending the cylinder and placing a clear round quartz crystal in the piston head. Engine speed was approximately 900 rpm. Instantaneous cylinder pressure was obtained with an in-cylinder pressure transducer together with a Hall effect sensor to locate crank angle position and recorded data with a data acquisition system. The data was then transferred into the DAYDISP computer program and manipulated to extract the information desired for the tests. The information was then exported to Lotus 123 and further manipulated to produce the graphs included in this report.

The major observation that emerges from the analysis of these tests is that the injector with a nozzle configuration of 8 x 0.006 and 0.002 inch prelift, showed the best overall results. While all injectors produced relatively high smoke levels, the 8 x .006 nozzle without prelift displayed the highest smokemeter readings and the 6 x .006 nozzle the lowest. The high overall smoke can be explained by the fact that combustion begins at the cylinder walls. Some fuel may have been deposited on the walls, and not have been ignited or burned completely. This incomplete burning will result in larger carbon particles reaching the exhaust ports and flowing through the exhaust system. If the wall wetting was eliminated, the smokemeter readings would be more in line with those of other injectors used on this engine.

The 8 x 0.006 nozzle with 0.002 prelift was judged to be the best overall choice for the following reasons: (1) This injector produces the highest cylinder pressures, 7.67 MPa at 800 psi and 9.05 MPa at 1500 psi; (2) The rate of heat release is roughly 163.89 kJ at 800 psi and 409 kJ at 1500 psi. These values are nearly even with the rest of the injectors; (3) The cumulative heat release curves show a value of 1.3 MJ at 800 psi and an average value of 1.18 MJ at 1500 psi.

The recommendation reached is that testing should be continued using the 8 x .006 nozzle, with prelift, in a fully operational engine. This injector should also be tested in an experimental vehicle under actual road and load conditions.

1. INTRODUCTION

This report discusses the effects of nozzle configuration of a high pressure diesel injector on heat release and cylinder pressure in a diesel engine modified for optical access. With this setup, it was possible to observe ignition and subsequent combustion and complement heat release calculations in the investigation of this high pressure injection system. This work represents a continuing study into the diesel injection process utilizing visual aids, such as high speed photography. Previous work is reported in the literature (1-4).

The high pressure injection system investigated in this study produces fuel sprays in the range of 15,000 to 20,000 psi, or about double the pressures produced by a typical unit injector. This system is especially effective at lower speeds where typical unit injectors have very low injection pressure capability. A brief description of this system is included in the Experimental Setup section of this report.

Better atomization of fuel occurs by injecting diesel fuel at high pressure. The atomization of the fuel is also influenced by the hole configuration, i.e., number of holes and diameter. The increased atomization of the diesel fuel facilitates the ignition combustion process. Since the droplet sizes are smaller than in a regular diesel injection system, the probability for complete combustion rises considerably. Less fuel will "wet" the cylinder walls or be lost in the crevices of the piston and its rings.

The objective of this study experimentally investigates the ignition and combustion characteristics of the high pressure injection system with both high speed photography and conventional heat release calculations. Six different nozzle configurations were investigated at approximately 900 rpm and two loads resulting in twelve experiments. Heat release calculations, based upon cylinder pressure data, are based upon Heywood (5), and are integral to the data acquisition system manufactured by DAYDISP (6). The results of these experiments will aid in the development of efficient high pressure diesel injection engines for military and transportation uses.

2. EXPERIMENTAL SETUP

The engine used in the study was a modified Detroit Diesel Allison (DDA) 3-53 (Model 5033-8300). The engine is a three-cylinder, two-stroke direct injected diesel engine with angled intake ports and four exhaust valves per cylinder providing moderate swirl with "through" scavenging. A detailed presentation covering the modification of the engine for optical access is given in Reference 1. A schematic of the modified engine is shown in Figure 1. Specifications of the engine, as supplied by Detroit Diesel, are given in Table 1.

The injection system consists of the following components: (1) SE-4D Electronics Engine Controller (EEC), (2) Servojet fuel supply module, (3) Hall effect transducer, (4) rail pressure solenoid, (5) 12 volt/10 amp power supply, and (6) electronic injector.

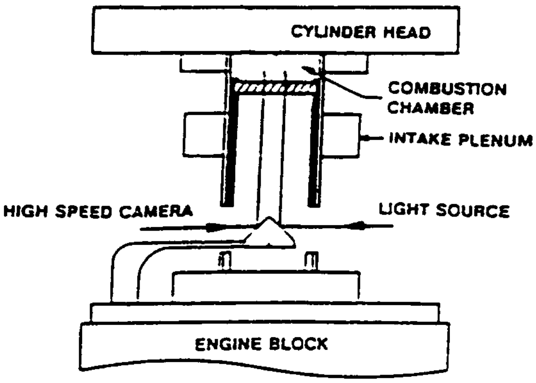

Figure 1. Modified Diesel Engine

Detroit Diesel Model #	5033-8200
Engine Type	2 cycle
Combustion Type	Direct Injection
No. of Cylinders	3
Displacement	159 in^3
Bore	3.875 in.
Stroke	4.50 in.
Aspiration	Blower, turbocharger
Normal Coolant Temp.	180F
Compression Ratio	18.7:1
Combustion chamber	Mexican Hat Open
Injector (5A60)	8 Hole
Nozzle Opening Pres.	3500 psig
Airbox Pressure	37 in. Hg.

Table 1. Engine Specifications

The EEC allows manual control of the injector without interfering with any of the other components. From the EEC, energize time, frequency, and injection count are displayed. The fuel supply module contains the hydraulic pump, electronic pressure regulator (EPR), and fuel temperature controller. This apparatus allows the fuel to be supplied to the fuel injector at the desired pressure. The Hall effect transducer is used to sense engine position for injection timing and engine speed. The EPR controls the fuel pressure delivered to the injector. (The nominal injected quantity was $34mm^3$ per injection at a rail pressure of 800 psi and $54mm^3$ at 1500 psi.)

The injectors evaluated in this study are electronically controlled via the EEC unit. Within the injector body, a solenoid controls the opening and closing of the needle valve that allows fuel to be injected. All nozzles tested had a spray cone angle of 165 degrees. The nozzle had either six, seven, or eight holes with a diameter of 0.006 or 0.007 inches. Some of the injectors had rate shaping or a prelift, which is indicated in the accompanying data.

In-cylinder pressure was measured using a Kistler Model 601 piezoelectric pressure transducer. The signal was sent to an IBM PC-based oscilloscope using a Rapid Systems R1005 Digital Oscilloscope interface.

The high speed camera used in this study was a HYCAM model 41-0004. Actual film speeds of up to 10,000 frames per second are made possible through the use of high speed rotating prisms used in the design of the camera. The film used was 250 ft. rolls of 16mm high speed Kodak Ektachrome (color) video news film. Approximately ten engine cycles were recorded on each 250 ft. roll of film. Photography lasted about three seconds at maximum film speeds of 5,000 to 8,000 frames per second.

3. RESULTS AND DISCUSSION

Experimental Results from High Speed Photography. Six different injector and/or nozzle configurations were evaluated at two loads (34mm^3 and 54mm^3 of fuel delivery) resulting in twelve experimental runs. Speed was held constant at approximately 900 rpm for all tests. Intake plenum pressure was held at approximately 1.8 to 2.0 psi for all tests. Results and discussion of these runs are given in this section on the following pages.

The followng nozzle combinations were tested:

Run No.	S/N	Hole Configuration	% Rate Shaping
1, 2	303	8 x 0.006"	0
3, 4	304	7 x 0.007"	0
5, 6	303	6 x 0.006"	10
7, 8	304	7 x 0.007"	15
9, 10	304	8 x 0.006"	15
11, 12	303	6 x 0.006"	0

Run: 1
Nozzle Model: 303
Rate Shaping: 0%
Nozzle Configuration: 8 - 0.006
Rail Pressure: 800 psi
Fuel Delivery: 34 mm^3

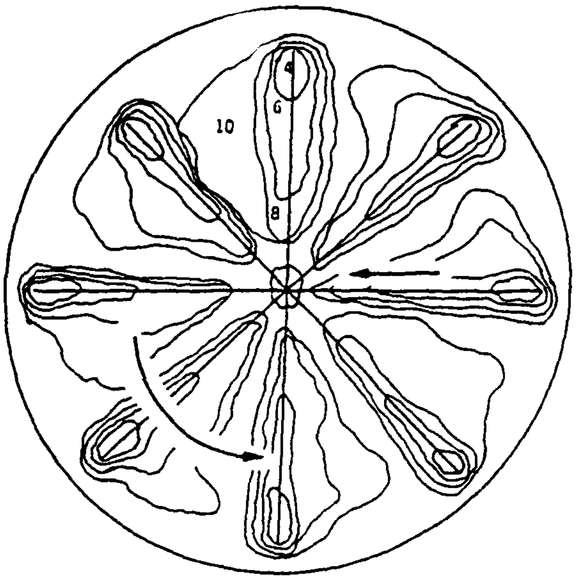

In Run 1, shown at the right, ignition begins at the end of the fuel spray lobe at approximately 4 degrees after top dead center, and then burns inward and spreads throughout the chamber because of the existing swirl. This is typical of diesel combustion observed with lower pressure injection systems although the rate of burn is somewhat higher and ignition appears to be initiated from a single source at each fuel lobe rather than multi-point ignition typical of lower pressure injection systems.

Run: 2
Nozzle Model: 303
Rate Shaping: 0%
Nozzle Configuration: 8 - 0.006
Rail Pressure: 1150 psi
Fuel Delivery: 46mm^3

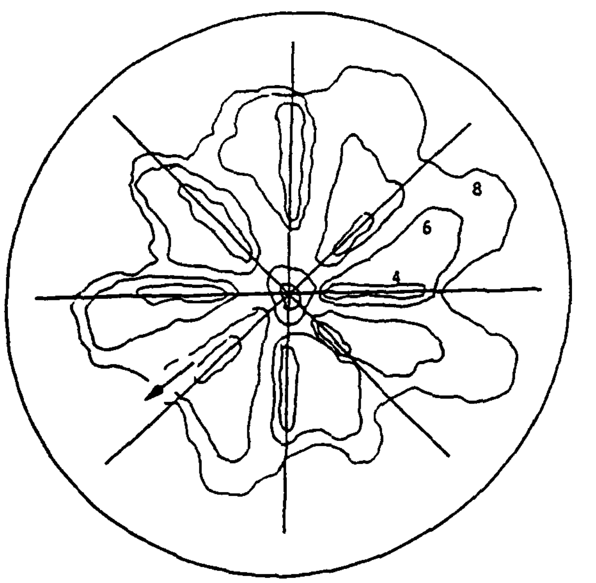

Run 2 is the higher load condition of Run 1. Here ignition occurs within the access of the fuel spray lobe at 4 degrees after top dead center and burns outward as expected. Swirl has a much lesser effect, or at least it is not observed probably because the very rapid rate of combustion. Flame spreads from the initial ignition points approximately 4 degrees after top dead center to throughout the chamber at 8 degrees after top dead center. Flame movement appears to be outward, as opposed to Run 1 where flame movement was inward.

Run:	**3**
Nozzle Model:	304
Rate Shaping:	0%
Nozzle Configuration:	7 - 0.007
Rail Pressure:	800 psi
Fuel Delivery:	34 mm^3

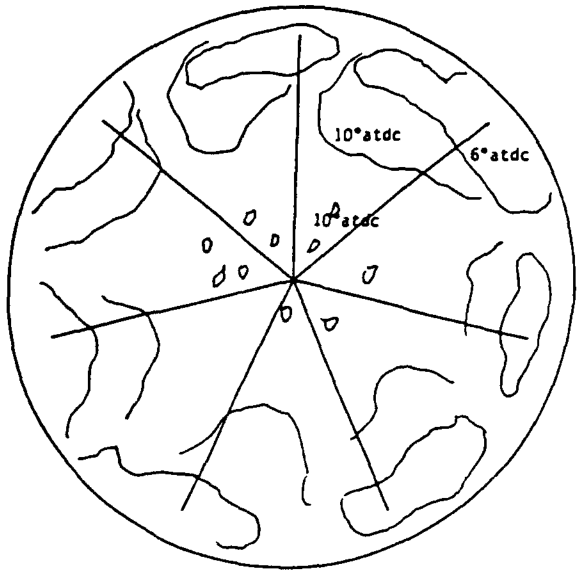

With Run 3 shown at the right, ignition appears to initiate at the walls of the combustion chamber. Spray is visible at 3 degrees btdc. Combustion becomes visible from the circumference of the chamber at approximately 6 degrees atdc and then burns inward. At approximately 8-10 degrees atdc at the center of the chamber, perhaps due to nozzle dripping following the injection event.

Run:	**4**
Nozzle Model:	304
Rate Shaping:	0%
Nozzle Configuration:	7 - 0.007
Rail Pressure:	1500 psi
Fuel Delivery:	54 mm^3

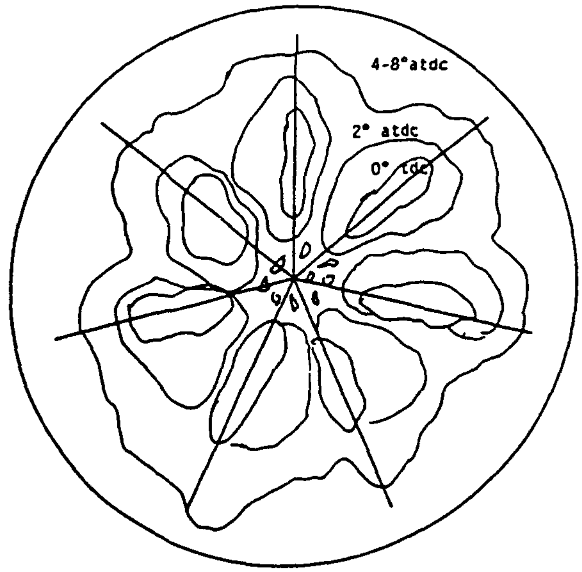

Run 4 is the higher load condition of Run 3. Here ignition occurs within the fuel spray lobe at top dead center and burns outward as expected. Swirl has a small effect initially, but as combustion develops, swirl assists the main combustion event to spread throughout the chamber. The entire chamber is combusting at 4-8 degrees after top dead center. Small droplets do appear, as in Run 3, due to fuel dripping from the nozzle.

Run:	**5**
Nozzle Model:	303
Rate Shaping:	10%
Nozzle Configuration:	6 - 0.006
Rail Pressure:	800 psi
Fuel Delivery:	34 mm^3

In Run 5, ignition occurs within the lobe of the fuel spray along the access and appears to burn inward as in Run 4. Combustion is obviously taking place around the circumference of the cylinder walls and ignition may occur there as well, perhaps due to fuel wetting of the cylinder walls. Combustion is relatively late in the cycle, first observed at 8 degrees after top dead center and then at 12 degrees after top dead center the complete fuels spray appears to be engulfed in flames. Most of the combustion occurs near the cylinder walls, far away from the center of the combustion chamber.

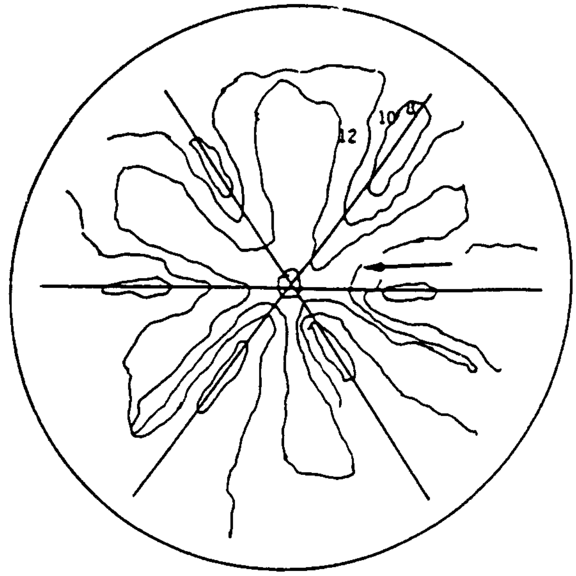

Run:	**6**
Nozzle Model:	303
Rate Shaping:	10%
Nozzle Configuration:	6 - 0.006
Rail Pressure:	1500 psi
Fuel Delivery:	54 mm^3

Run 6 is the higher load of Run 5. Here, the phenomena observed in Run 3 are significantly enhanced. Combustion is first observed at about 3 degrees after top dead center and burns quite rapidly within three degrees the entire combustion chamber is engulfed in flame. There appears to be no movement of the charge due to air motion, probably due to the rapid combustion. There is some nozzle dripping which combusts later on in the cycle, approximately 8 degrees after top dead center.

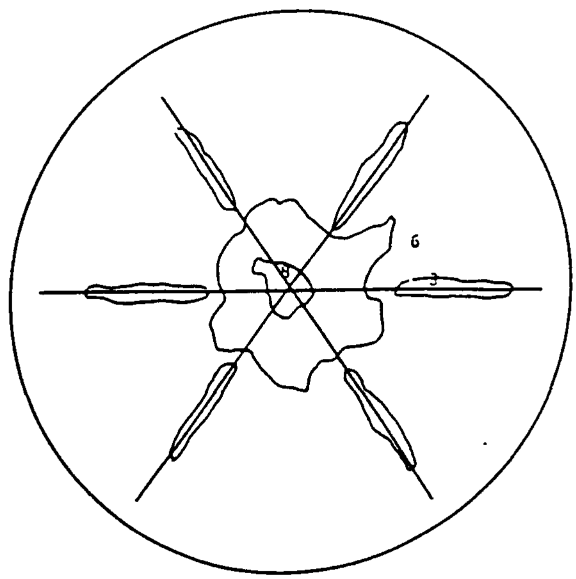

Run:	**7**
Nozzle Model:	304
Rate Shaping:	15%
Nozzle Configuration:	7 - 0.007
Rail Pressure:	800 psi
Fuel Delivery:	34 mm^3

In Run 7, combustion begins near the center of the combustion chamber, relatively early when compared with the previous runs. Combustion initiates at approximately 0 degrees top dead center on the axis of the fuel lobe, close to the combustion chamber center. It then progresses in a normal outwardly fashion. Flame movement appears to move from the center outward, with some small swirl effect. Combustion appears to be thorough and spreads throughout the chamber in a fairly organized manner.

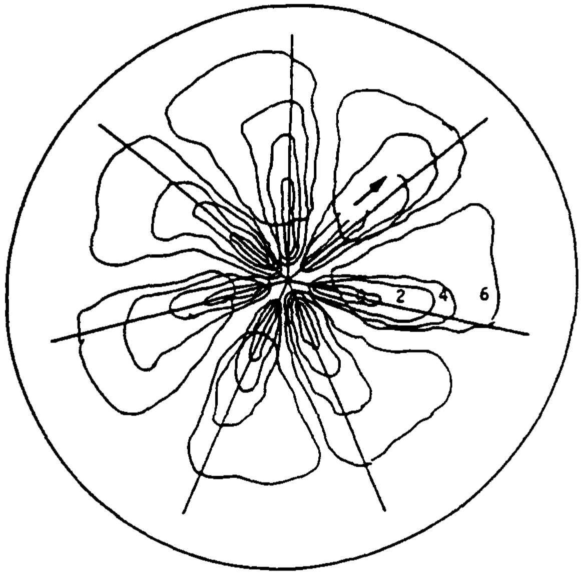

Run:	**8**
Nozzle Model:	304
Rate Shaping:	15%
Nozzle Configuration:	7 - 0.007
Rail Pressure:	1500 psi
Fuel Delivery:	54 mm^3

Run 8 appears very similar to Run 7 in that combustion initiates near the center of the combustion chamber along the axis of the fuel lobe and then spreads outward to fill the chamber. There is some affect due to the air swirl in the combustion chamber. However, like Run 7, combustion appears to occur in a relatively organized manner. There is no fuel wetting of the cylinder wall.

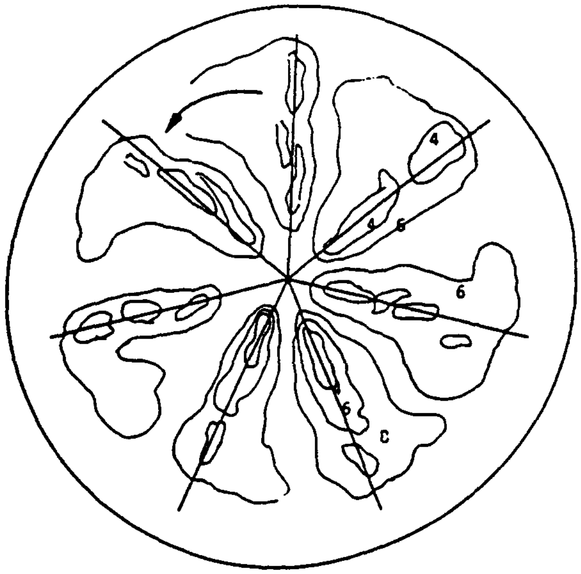

Run:	**9**
Nozzle Model:	304
Rate Shaping:	15%
Nozzle Configuration:	8 - 0.006 with 0.002 prelift
Rail Pressure:	800 psi
Fuel Delivery:	34 mm^3

In Run 9, combustion begins along the axis close to the center, but further out from the center than the previous two runs. Combustion initiates along a greater length of the axis lobe, observed at approximately 3 degrees before top dead center and then moving out through the combustion chamber at 5 degrees after top dead center combustion appears to fill the entire chamber. This is a relatively slower burning process when compared to previous runs. Swirl does have an effect on the spread of the flames throughout the combustion chamber.

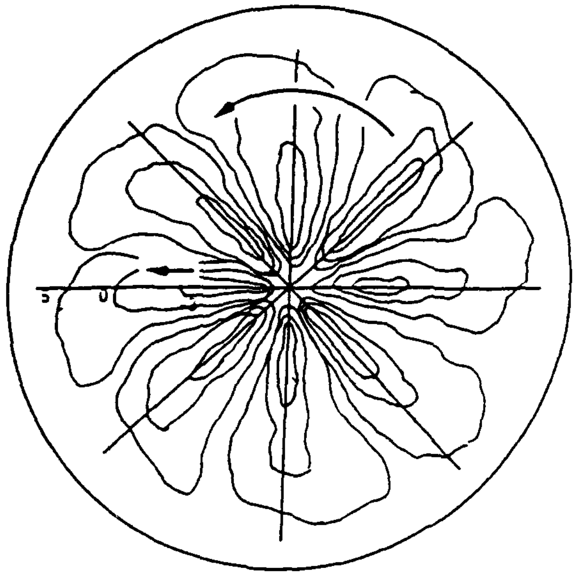

Run:	**10**
Nozzle Model:	304
Rate Shaping:	15%
Nozzle Configuration:	8 - 0.006 with 0.002 prelift
Rail Pressure:	1500psi
Fuel Delivery:	54 mm^3

In Run 10, combustion clearly begins at the cylinder walls, probably due to fuel wetting, although it is difficult to observe because combustion initiates quite rapidly and the ignition process is caught between frames of the camera. At -5 degrees before top dead center, flame is observed and combustion continues rapidly. At -1 degree before top dead center, the entire chamber is engulfed in flames. Flame movement appears to move from the outward circumference of the chamber inward.

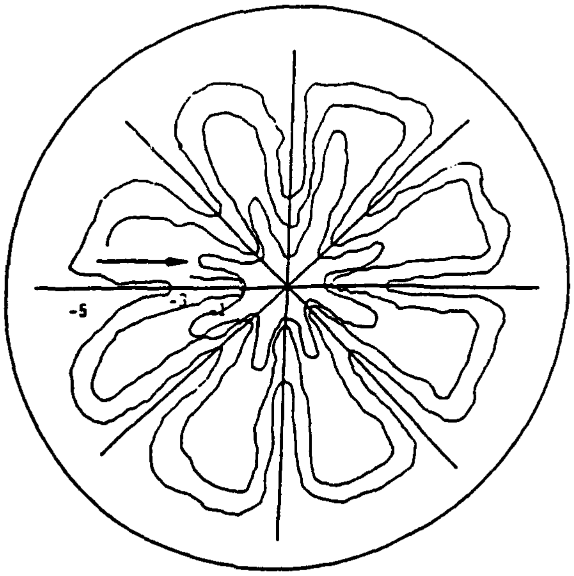

Run: 11
Nozzle Model: 303
Rate Shaping: 0%
Nozzle Configuration: 6 - 0.006
Rail Pressure: 800 psi
Fuel Delivery: 34 mm^3

Run 11, like Run 10, fuel wetting is observed on the cylinder walls. Combustion occurs relatively early at -5 degrees before top dead center. Flame is observed at 2 degrees before top dead center and is moving inward at 0 degrees, or top dead center, the entire combustion chamber is engulfed in flame. Swirl does not appear to have an effect on the flame spread.

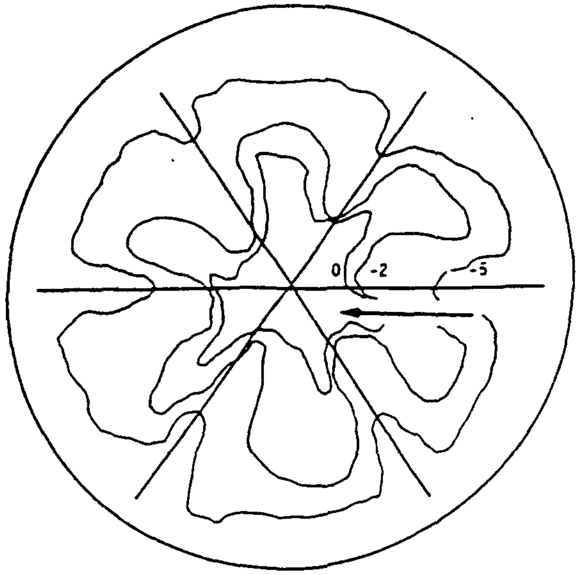

Run: 12
Nozzle Model: 303
Rate Shaping: 0%
Nozzle Configuration: 6 - 0.006
Rail Pressure: 1500 psi
Fuel Delivery: 54 mm^3

In Run 12 combustion again begins at the circumference of the cylinder walls. It appears that ignition is relatively early in the cycle at approximately 0 degrees, or top dead center, and the flame throughout the chamber is observed at 3 degrees after top dead center moving inward. At 5 degrees after top dead center, it appears the entire charge is ignited. There is some nozzle dripping occurring in this cycle which is combusting. Combustion occurs around 3 degrees after top dead center. Swirl does not seem to have an effect on the combustion process. The driving force in flame spread appears to be the movement from the combustion front at the cylinder walls moving inward toward the center.

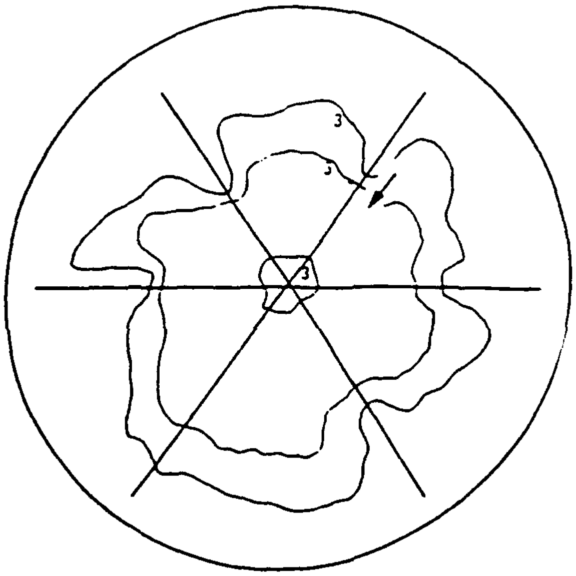

Comparison of Runs:

Combustion pressure data for the injectors is shown in Figure 2 (800 psi rail pressure) and in Figure 3 (1500 psi). At 800 psi rail pressure, the 8 x 0.006 and 6 x 0.006 injectors generate the greatest amount of cylinder pressure, 7.5 MPA and 7 MPa respectively, while the 6 x 0.006 with prelift and 7 x 0.007 are roughly equal at about 5 MPa. Peak cylinder pressure occurs between 3 and 8.5 crankangle degrees. The 7 x 0.007 and 6 x 0.006 with prelift show the most pronounced injection delay. The other injectors show a smoother transition period between injection and combustion.

At 1500 psi rail, the 8 x 0.006 with prelift generates 9 MPa of cylinder pressure and the other injectors have a value of roughly 7 MPa. Peak pressure occurs between 2.75 and 14 crankangle degrees at this injection pressure. As was the case at 800 psi rail, the 7 x 0.007 and 6 x 0.006 with prelift show the most injection delay.

Rate of heat release is the rate chemical energy is released during the combustion process. A non-spatial thermodynamic model from Heywood (5) was used to calculate heat release from pressure and volume data. This equation was incorporated into a computer program called DAYDISP (6) that allowed manipulation of the data gathered from the engine. After the data was manipulated within DAYDISP, it was exported to Lotus and converted into graphics.

The rate of heat release of all injectors operating at 800 psi rail pressure is shown in Figure 4. The different nozzle configurations show very different characteristics. The most interesting feature of this graph is that the 6 x 0.006 with prelift released approximately 1300 kilo joules of heat. This is almost six times the heat release of the other injectors. The reason for this anomaly is not known. It could be explained by faulty injector operation or an instrumentation error.

Injector 303 8 x 0.006 had the highest rate of heat release of roughly 200 kilo joules. The 6 x 0.006 and 8 x 0.006 with prelift nozzles had heat release levels of approximately 165 kilo joules. The 7 x 0.007 injector shows the lowest rate of heat release at 75 kilo joules. In the experiments that were run, the maximum rate of heat release occurred between 2.5 and +10 crankangle degrees for all of the injectors.

Rate of heat release for four of the injectors operating at a system pressure of 1500 psi is shown in Figure 5. At this injection pressure, three of the injectors show very similar results with a rate of heat release of 400 kilo joules. The 7 x 0.007 shows the lowest heat release at 200 kilo joules which occurs at 8.61 degrees. This value is approximately 50% less than the other three injectors and occurs the latest. The maximum rate of heat release at this rail pressure occurs between -2.5 and +8.61 crankangle degrees for all of the injectors. The first injector tested (Run 2) is not included here because a system pressure of 1150 psi was used during that run and the data cannot be compared.

Cumulative heat release for the injectors at a system pressure of 800 psi is shown in Figure 6. The 8 x 0.006 showed a cumulative heat release of approximately 2300 kilo joules. This value is 75% greater than the next injector. The result for this injector suggests that an injector with more holes releases greater cumulative heat than an injector with fewer holes. The 8 x 0.006 with prelift showed a cumulative heat release of almost 1300 kilo joules. The 6 x 0.006 nozzle was next with a cumulative heat release of 700 kilo joules. The last two injectors, 6 x 0.006 with prelift and 7 x 0.007 showed the lowest results at roughly 400 kilo joules. Cumulative heat release occurs between 11 and 20 crankangle degrees.

Cumulative heat release for four of the injectors at the higher system pressure of 1500 psi is shown in Figure 7. The results of cumulative heat release at this injection pressure show that the two injectors with prelift show the poorest results. Injector 304 7 x 0.007 and 303 6 x 0.006 each had a cumulative heat release of nearly 1700 kilo joules, while injector 303 6 x 0.006 with prelift and 304 8 x 0.006 with prelift show cumulative heat release of 900 and 1100 kilo joules respectively. This would indicate that at high pressures an injector with prelift is not desirable. The injectors had a range of 9.3 to 24.5 crankangle degrees for the maximum cumulative heat release at this injection pressure.

Smokemeter Results:

Smokemeter measurements are shown in Figure 8. The 8 x .006 nozzle, without prelift, displayed the highest smokemeter readings and the 6 x .006 nozzle, without prelift, the lowest reading. No clear correlation was demonstrated between nozzle configuration or pre lift and the resulting smoke. There was considerable wall wetting, particularly at the higher rail pressure. This wall wetting was evidenced by ignition beginning from the periphery of the chamber and combustion progressing inward. This pattern can be seen in the films.

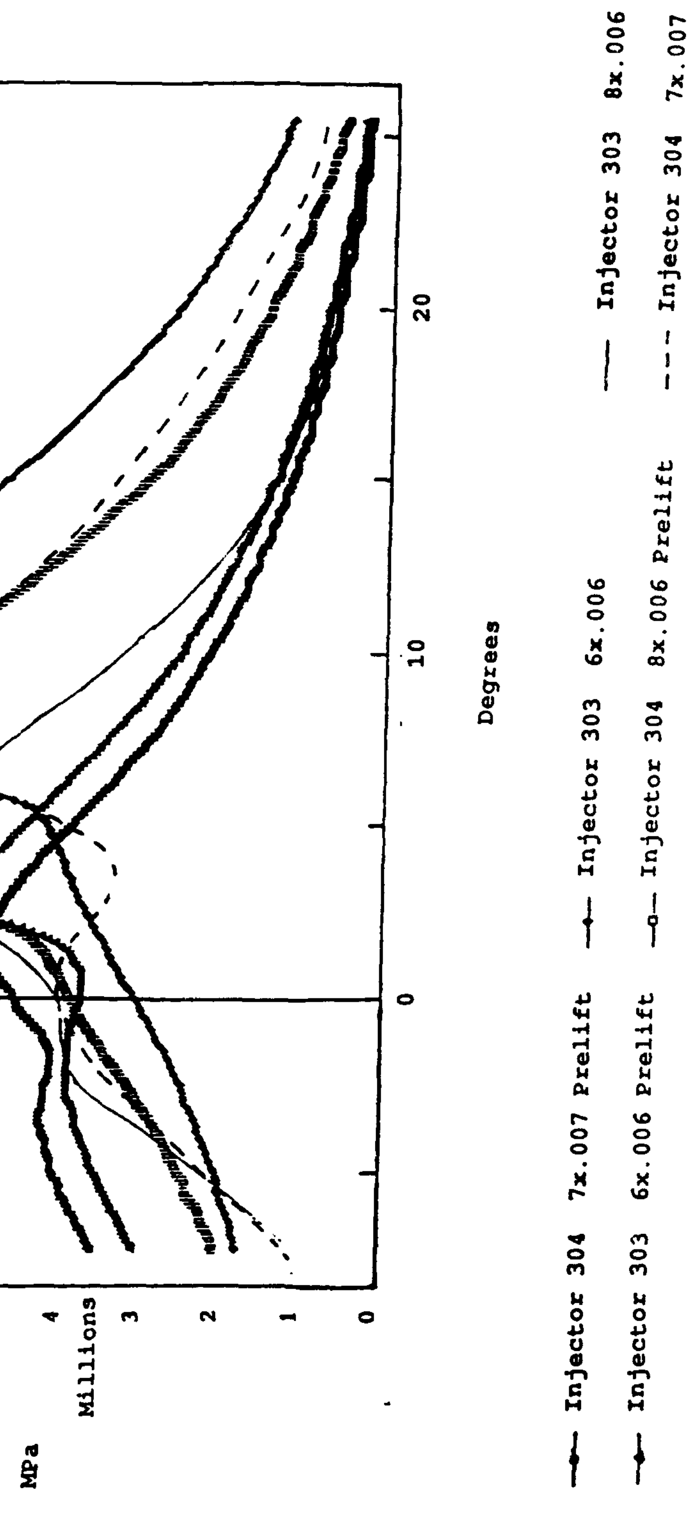

Figure 2. Pressure data at low load (system pressure of 800 psi).

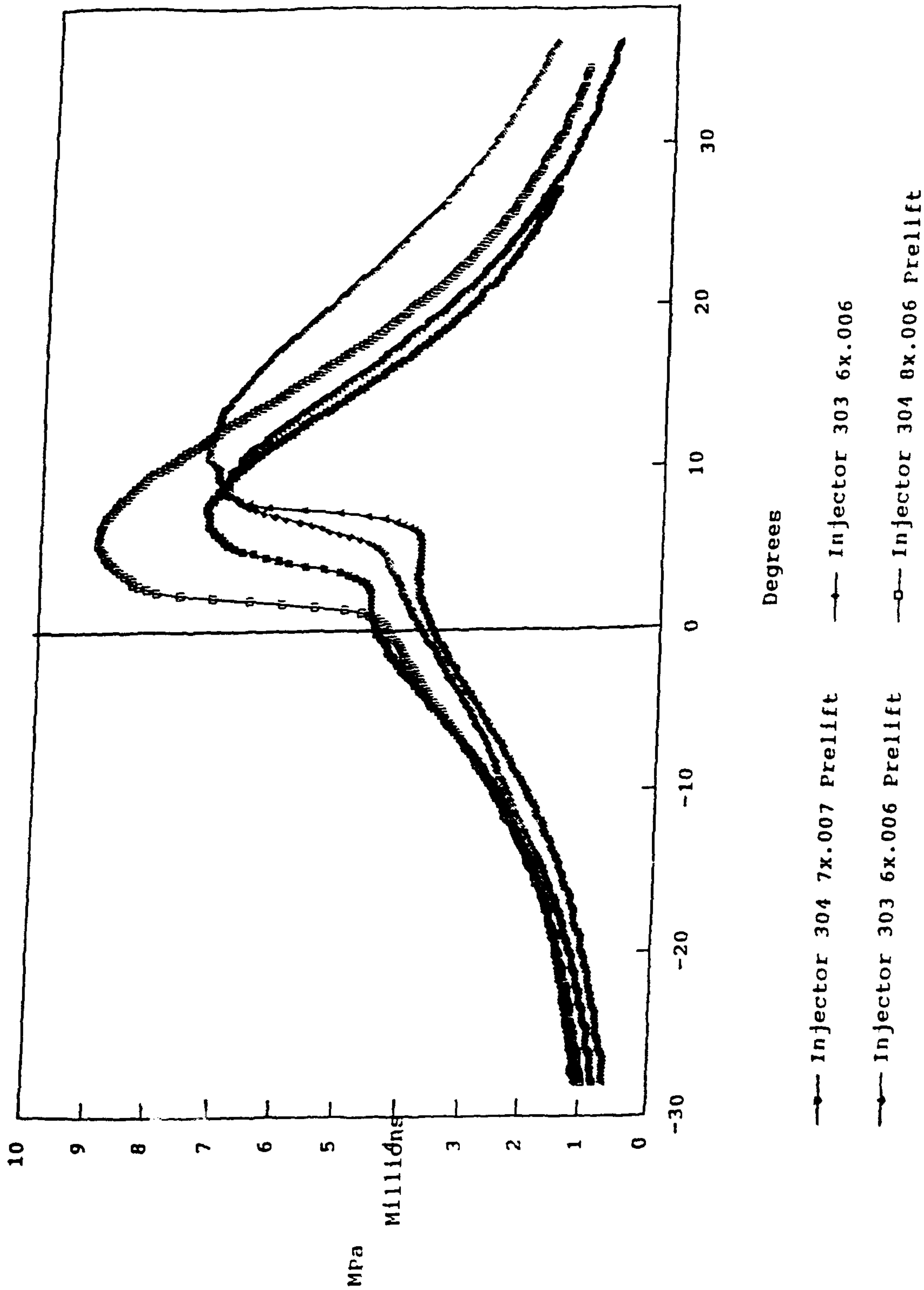

Figure 3. Pressure data at high load (system pressure of 1500 psi).

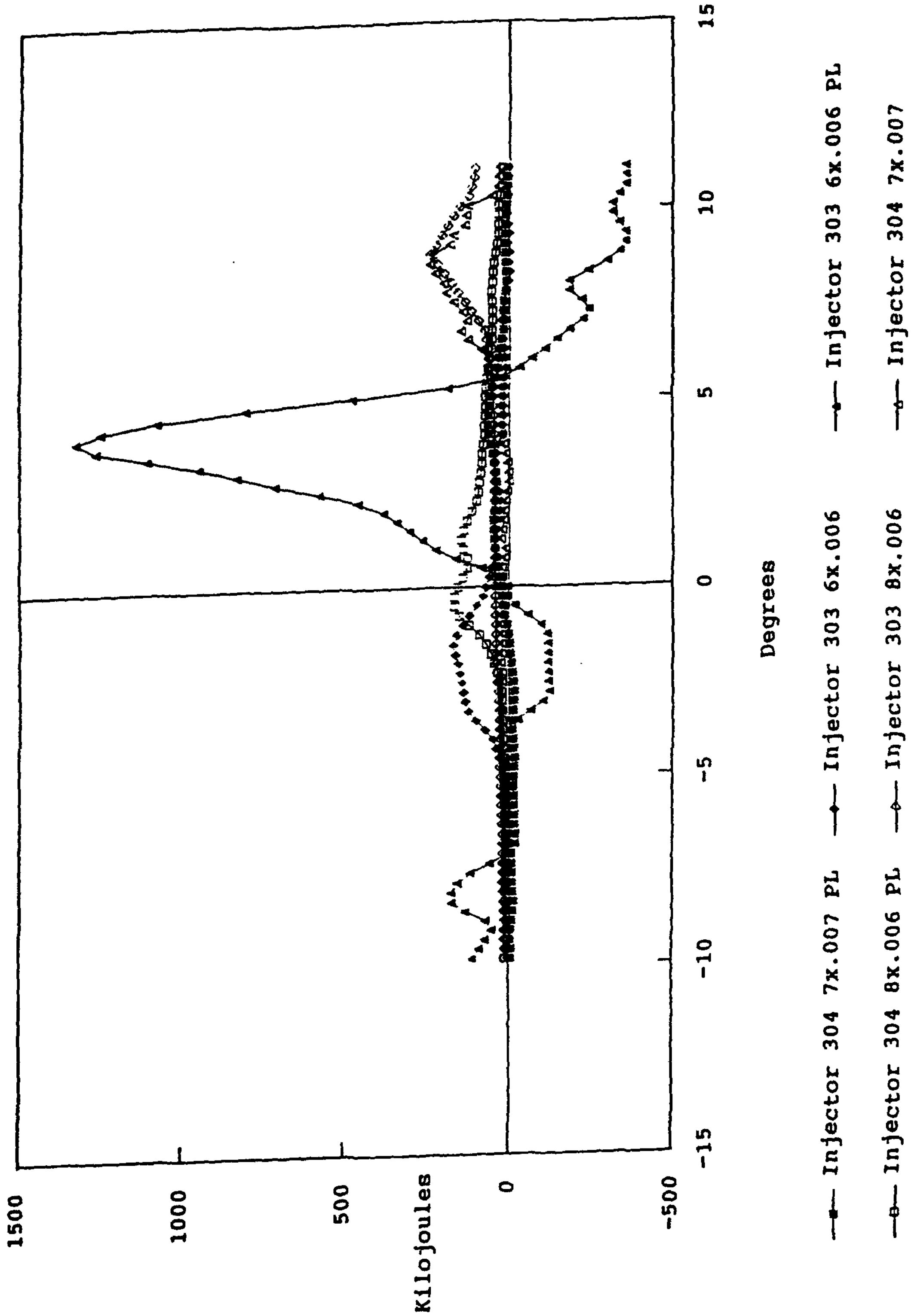

Figure 4. Heat release calculations at low load (system pressure of 800 psi).

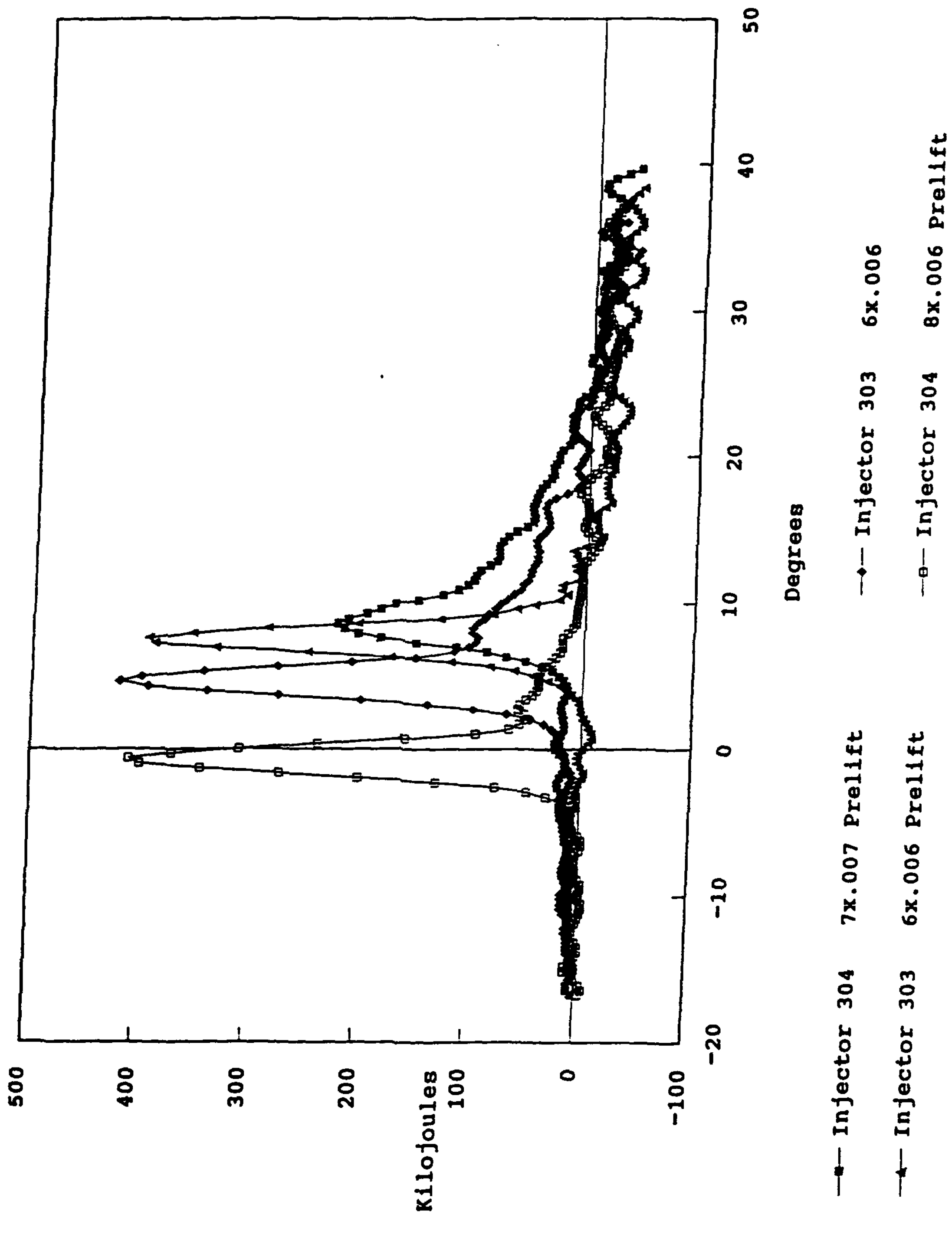

Figure 5. Heat release calculations at high load (system pressure of 1500 psi).

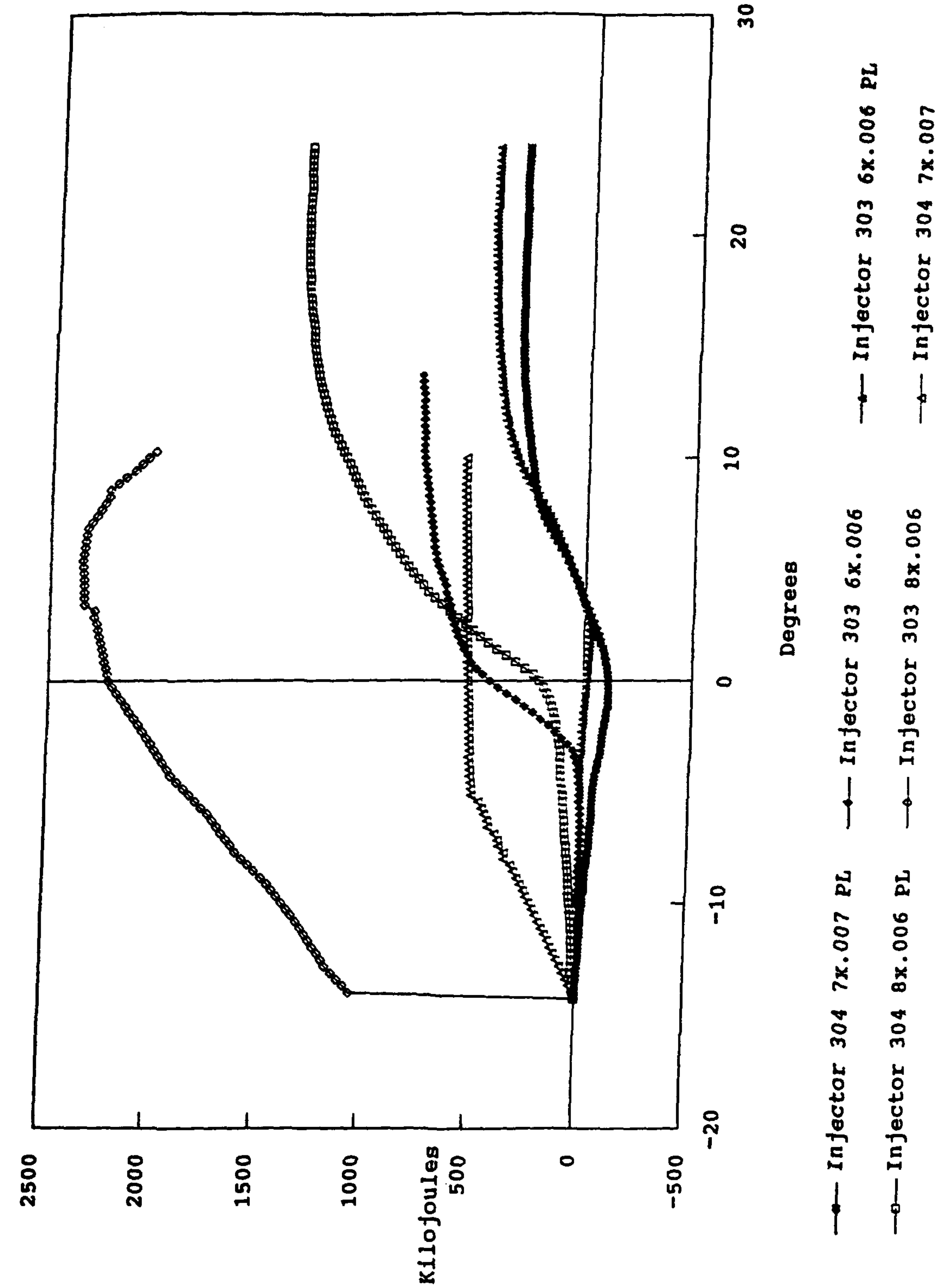

Figure 6. Cumulative heat release calculations at low load (system pressure of 800 psi).

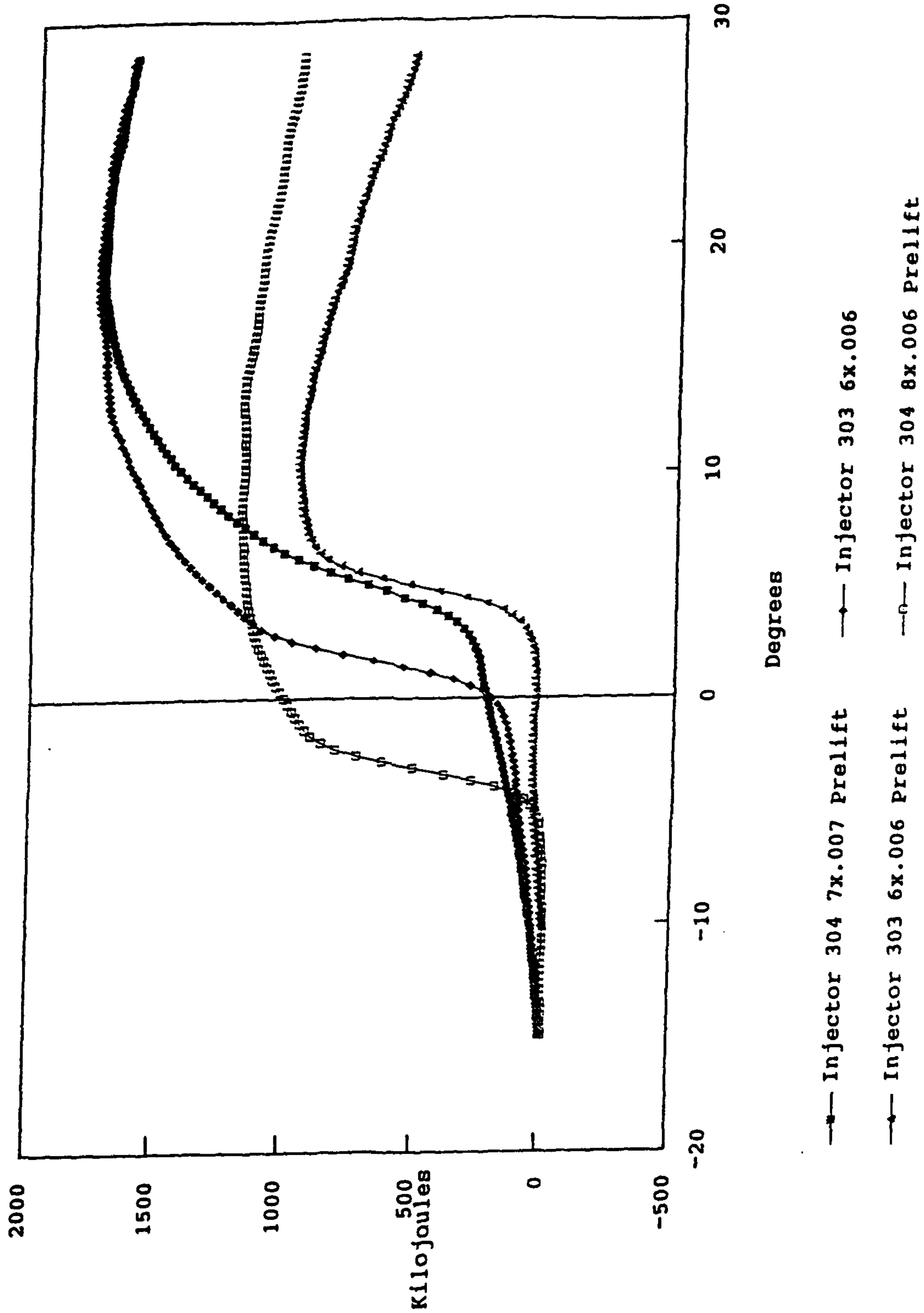

Figure 7. Cumulative heat release calculations at high load (system pressure of 1500 psi).

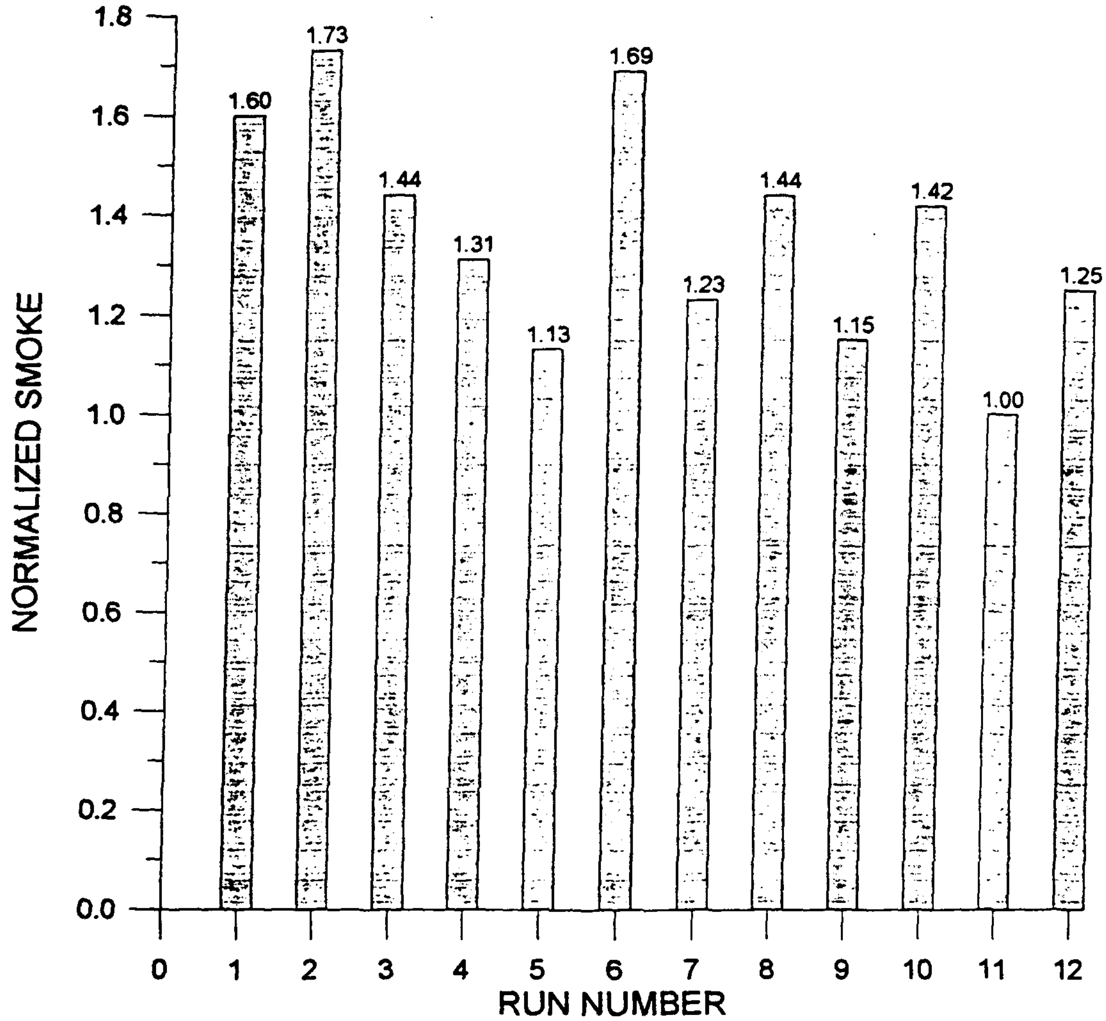

Figure 8. Normalized Smokemeter measurements

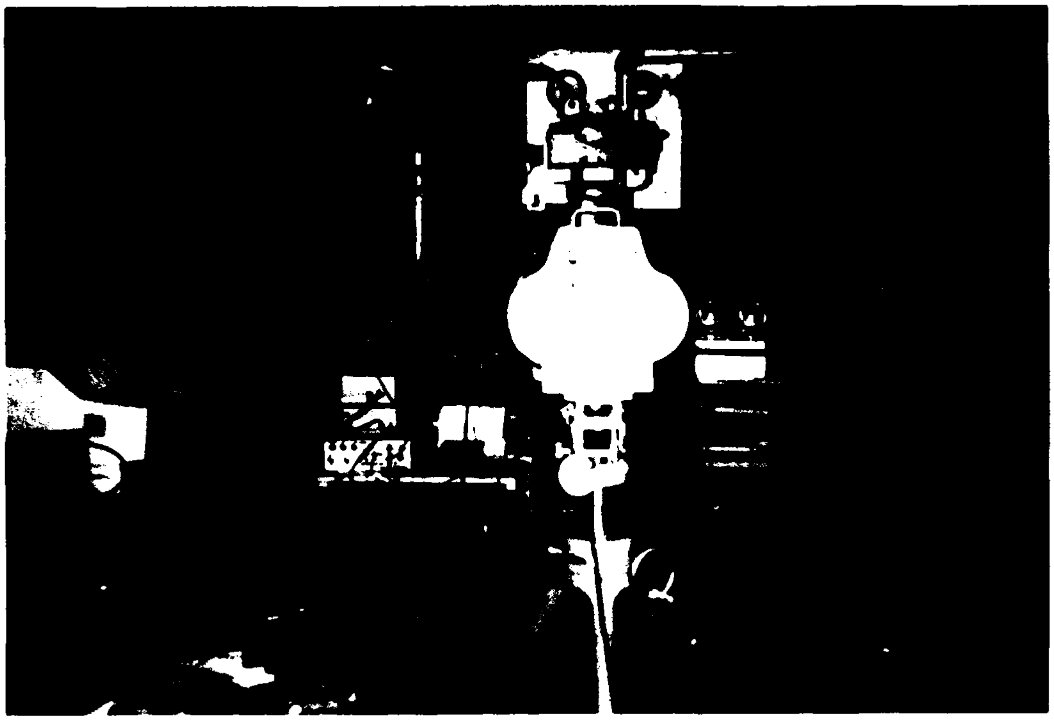

Photograph 1. Experimental Setup

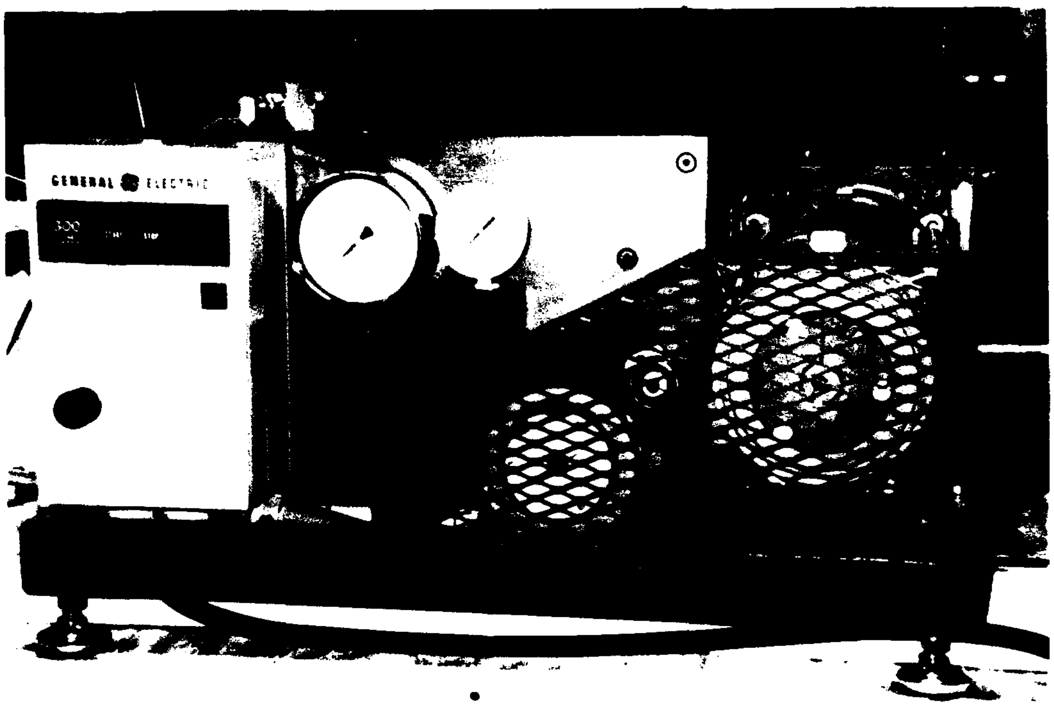

Photograph 2. BKM High Pressure Injection System

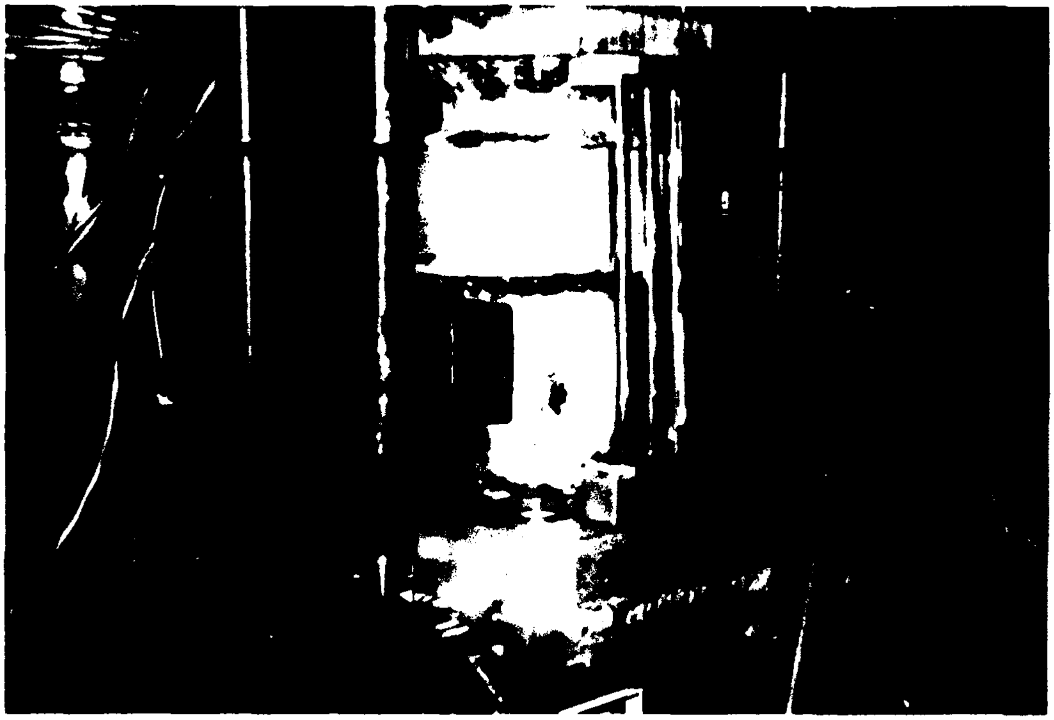

Photograph 3. Engine Detail showing Cylinder Head Extension

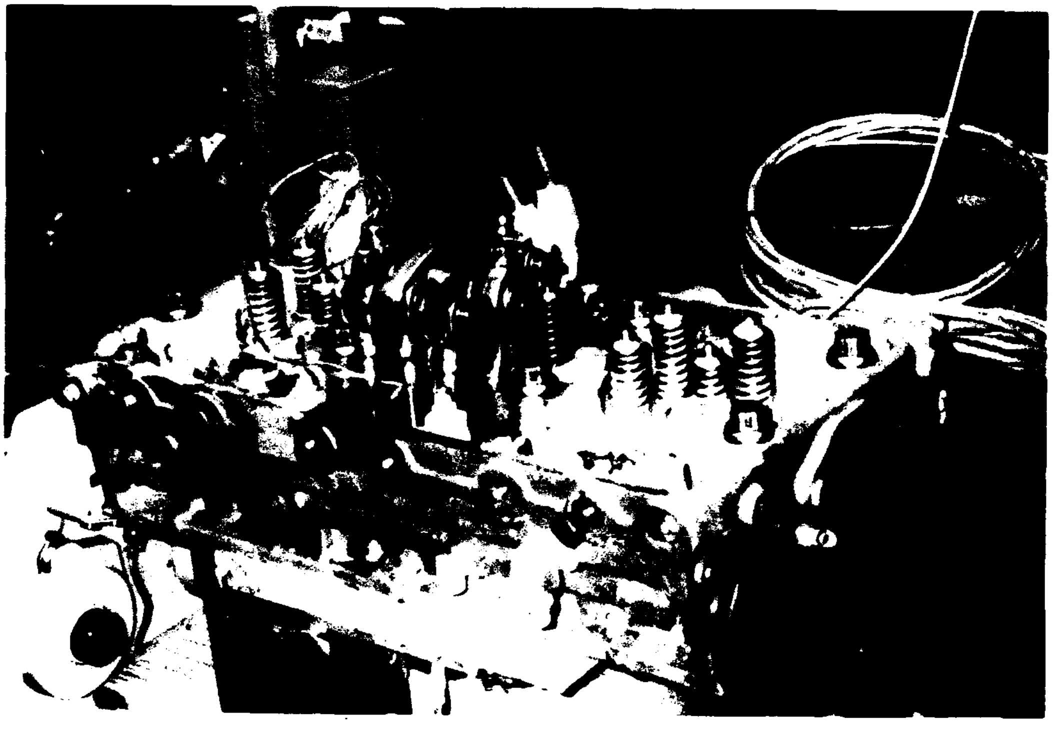

Photograph 4. Cylinder Head with High Pressure Injector

4. Bibliography

1. Stroia, B.J., Abata, D.L., "An Investigation of Injection Rate Controlled Heat Release of Low Cetane Fuels in a Direct Injected Diesel Engine," SAE Paper No. 902061.

2. Abata, D.L., D. Masterson, "Analysis of the Combustion of Four Alternative Fuels in a Two-Stroke Direct Injection Diesel Engine Using High Speed Photography," Final report to Martin Marietta on Award/Order No. 19X-91333V, June 1988.

3. John, J.R., D.L. Abata, "Visualization of the Ignition of Methanol in a Diesel Engine: A Comparison of Ignition Techniques," International Symposium of Alcohol Fuels, Florence, Italy, 1991.

4. Stroia, B.J., D.L. Abata, "Flame Speeds of Low Cetane Fuels in a Diesel Engine," American Society of Mechanical Engineers, No. 91-ICE-14, 1991.

5. Heywood, J., *Internal Combustion Engine Fundamentals*, McGraw-Hill Book Company, New York, 1988.

6. DAYDISP, software available from Rapid Systems, Inc., manufacturers of high speed analog to digital equipment for IBM data acquisition system applications.

7. Beck, N.J., et. al., "Direct Digital Control of Electronic Unit Injectors," SAE Paper No. 840273, 1984.

8. Dent, J.C., "Basis for the Comparison of Various Experimental Methods for Studying Penetration," SAE Paper No. 710571, 1971.

9. Savery, C.W., et. al., "Injection Characteristics of High Pressure Accumulator Type Fuel Injectors," SAE Paper No. 890266, 1989.

10. Bower, G.R., Foster, D.E., "Investigation of the Characteristics of a High Pressure Injector," SAE Paper No. 892101, 1989.

11. Abata, D.L., Stroia, B.J., Beck, N.J., Roach, A.R., "Diesel Engine Flame Photographs with High Pressure Injection," SAE Paper No. 880298, 1988.

MR-941
To: NJ Beck
Fr: DC Steinmeyer
Dt: 6 May 1993
Re: Turbocompound cooling system test - preliminary results

The first test of the TCS was conducted at Golden West College on 4 May 1993. The TCS was placed downstream of the stock single turbocharger on the Cummins VTA-903 engine. The TCS wastegate was locked closed during the test.

Attached is the temperature and pressure data collected during that test. Note that the maximum speed attainable with the TCS fan was 17,700. We had intended to test to 30,000 RPM but the exhaust back pressure due to the TCS limited the power output of the VTA-903. Different combinations of engine speed and load were attempted without success.

Also attached is a plot of the pressure data for 17,700 RPM to show the various trends for different exit restrictions (simulated heat exchanger). Note that the 100% exit opening area is 400 square inches (20 x 20).

The first four data points were run on 28 APR 1993. Upon increasing fan speed beyond 7000 rpm, the magnetic pickup contacted the fan hub, damaging the pickup. The fan was removed and returned to BKM for replacement of the pickup and modification of the mounting system. No other serious problems occurred during the test.

A diagram of the TCS is attached that identifies the locations of the instrumentation points. P8 & T8 were located in the air inlet flow nozzle, upstream from the fan air inlet at P1 & T1.

Note that all pressures are inches of water (gauge) except P6 and P7 which are inches of mercury (gauge). The ambient barometric pressure was 30.10 inches of mercury.

Please forward your comments and conclusions to me. I will pass these results on to TACOM after we have reviewed them with Bill Woollenweber.

cc: RL Barkhimer
MA Calkins

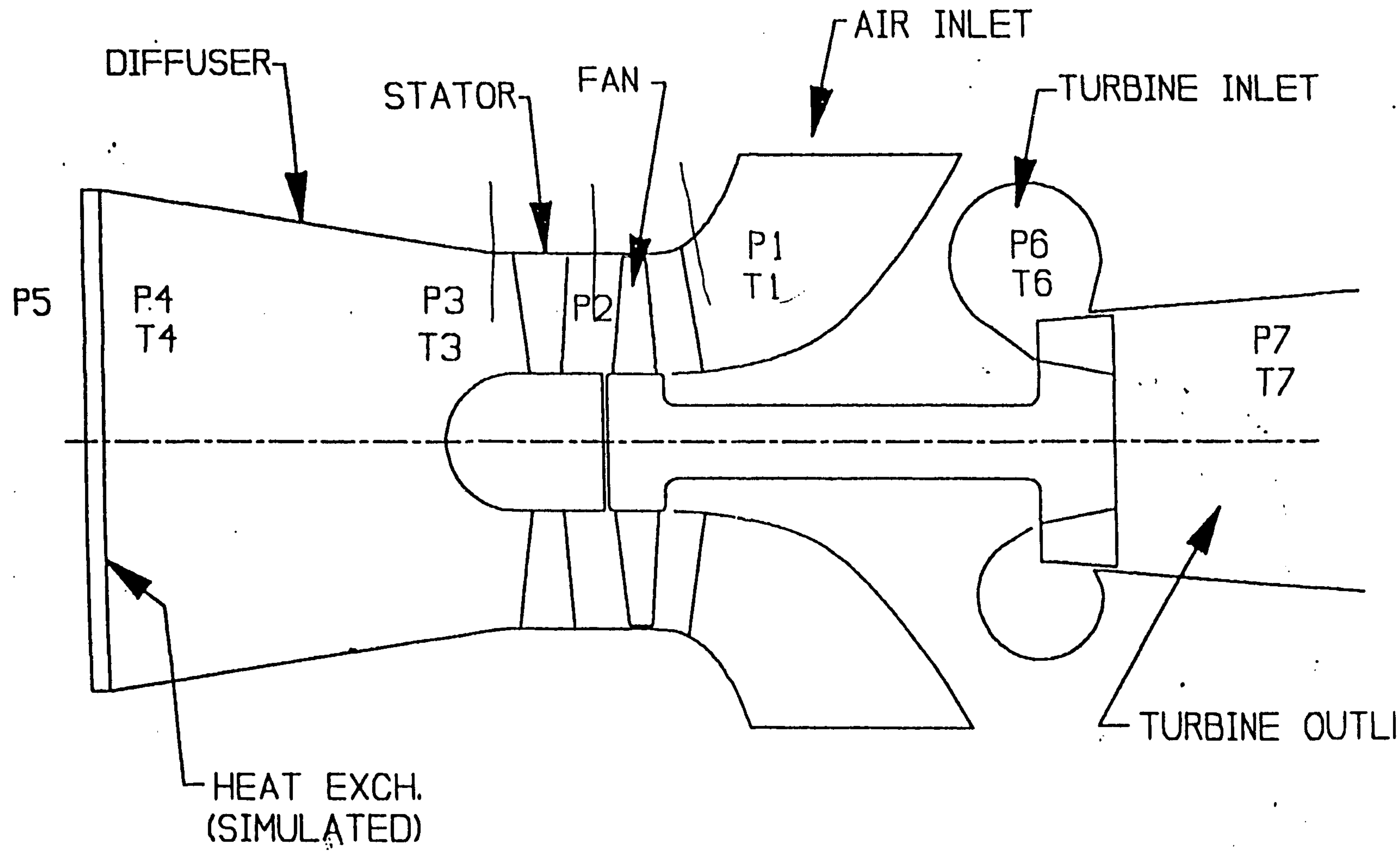

FIGURE 1 - TCS INSTRUMENTATION POINTS

TURBOCOMPOUND COOLING SYSTEM TEST RESULTS

3-May-93

CALCULATED ENGINE AIR ... AT T/C = .80

DCS

TEST POINT	ENGINE		FAN								TURBINE			
	(RPM)	(HP)	FAN SPEED (RPM)	EXIT OPENING (%)	PRES RATIO (P4/BARO)	FLOWRATE (LB/SEC)	TEMP T1(in) (DEG F)	TEMP T2(out) (DEG F)	TEMP T3(out) (DEG F)	TEMP T4(out) (DEG F)	PRES RATIO (P6/P7)	FLOWRATE Ne=.80 (LB/SEC)	TEMP T6(in) (DEG F)	TEMP T7(out) (DEG F)
1	1160	46.8	5000	100	1.000	0.22	76	77	76	76	1.047	0.303	398	380
2	1160	46.8	5000	75	1.000	0.22	78	79	78	78	1.047	0.303	415	400
3	1160	46.8	5000	50	1.000	0.22	78	79	78	78	1.047	0.303	419	405
4	1160	46.8	5000	25	1.000	0.21	81	82	80	79	1.045	0.303	423	409
5	1155	60	5000	25	1.000	0.21	80	81	80	81	1.043	0.302	473	455
6	1155	60	5000	5	1.002	0.13	81	84	83	83	1.043	0.302	498	481
7	1155	60	5000	2.5	1.003	0.09	86	86	85	84	1.047	0.302	518	501
8	1300	86.6	6000	25	1.000	0.27	89	89	86	84	1.063	0.340	572	549
9	1300	86.6	6000	5	1.003	0.16	86	87	87	86	1.063	0.340	600	578
10	1300	86.6	6000	2.5	1.005	0.12	88	89	89	89	1.063	0.340	606	586
11	1385	102.8	7000	25	1.000	0.30	92	92	90	87	1.076	0.362	641	619
12	1385	102.8	7000	5	1.004	0.18	94	93	91	90	1.076	0.362	655	634
13	1385	102.8	7000	2.5	1.007	0.14	91	94	93	93	1.088	0.362	690	667
14	1660	196.9	10000	50	1.000	0.45	95	99	96	93	1.141	0.434	888	845
15	1660	196.9	10000	25	1.001	0.43	102	105	100	97	1.113	0.434	938	898
16	1660	196.9	10000	5	1.004	0.36	106	108	104	101	1.113	0.434	957	919
17	1660	196.9	10000	2.5	1.010	0.29	105	109	106	105	1.116	0.434	975	936
18	1835	321	15000	50	1.000	0.65	99	105	101	100	1.310	0.479	1257	1157
19	1835	321	15000	25	1.002	0.77	-	116	112	110	1.310	0.479	1315	1222
20	1835	321	15000	15	1.010	0.52	115	126	125	122	1.314	0.479	1350	1255
21	1835	321	15000	10	1.005	0.59	-	127	125	119	1.310	0.479	1327	1237
22	2280	369	17700	50	1.000	0.75	128	136	131	130	1.418	0.596	1394	1297
23	2280	369	17700	25	1.002	0.70	109	117	116	115	1.385	0.596	1218	1126
24	2280	369	17700	15	1.007	0.66	110	120	119	114	1.418	0.596	1231	1105
25	2280	369	17700	10	1.013	0.63	113	127	129	125	1.426	0.596	1269	1168
28	2280	369	17700	5	1.028	0.46	113	130	127	125	1.420	0.596	1270	1177

cc: NJB
RLB
MAC

Tacom Cooling Fan Speed 17700

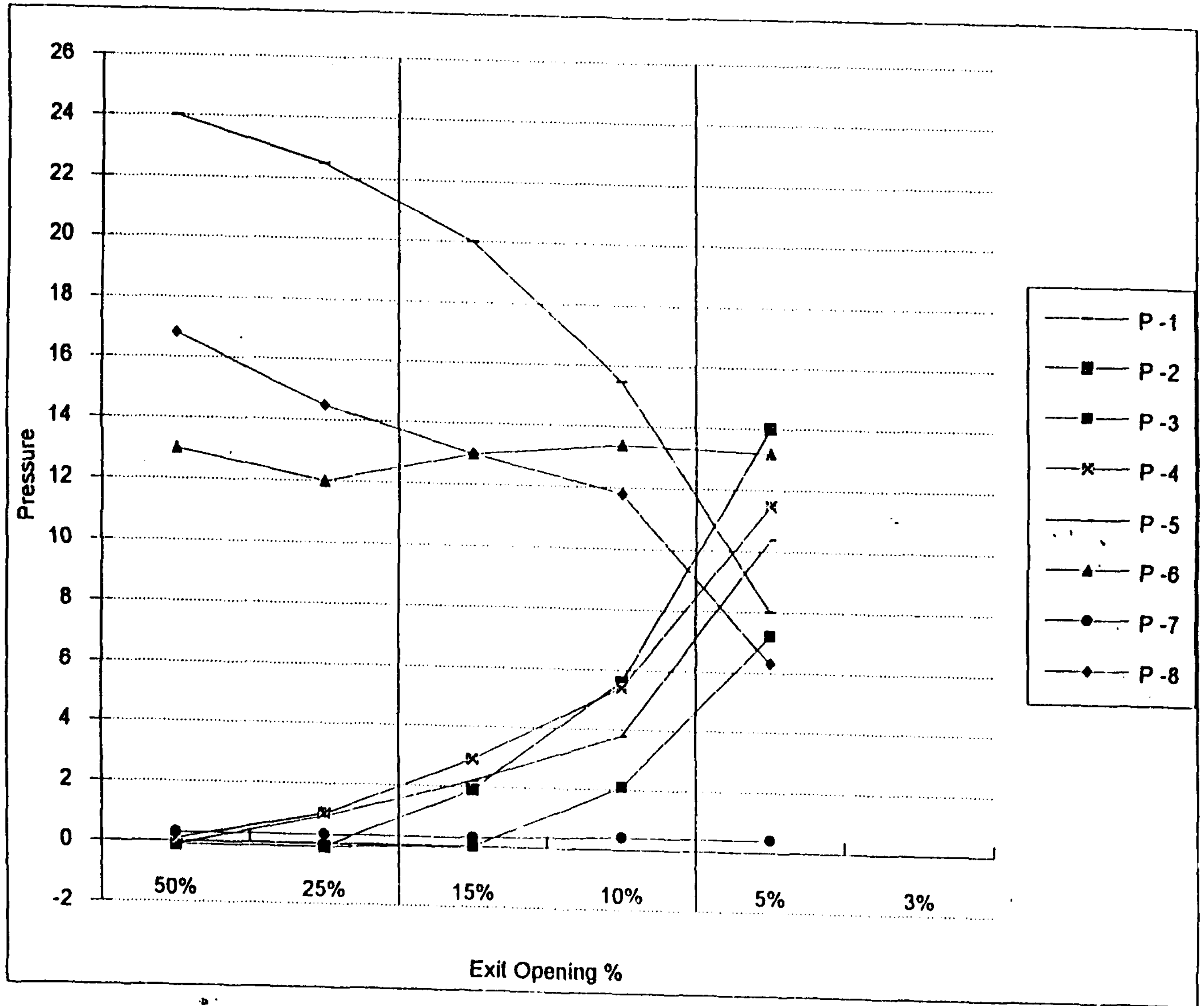

TCS AIRFLOW (FAN)

Exit Opening = 25%

5-12-93

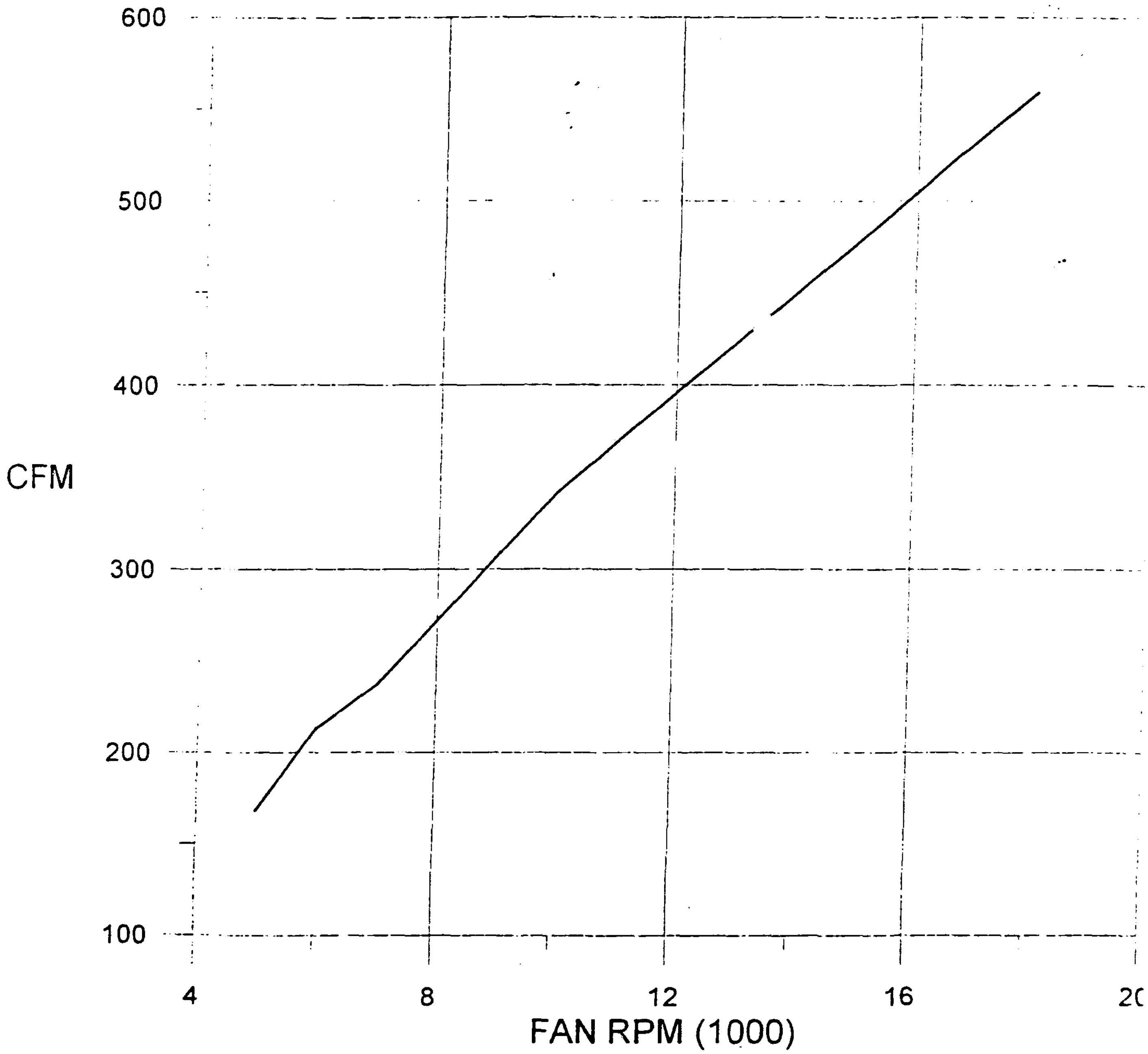

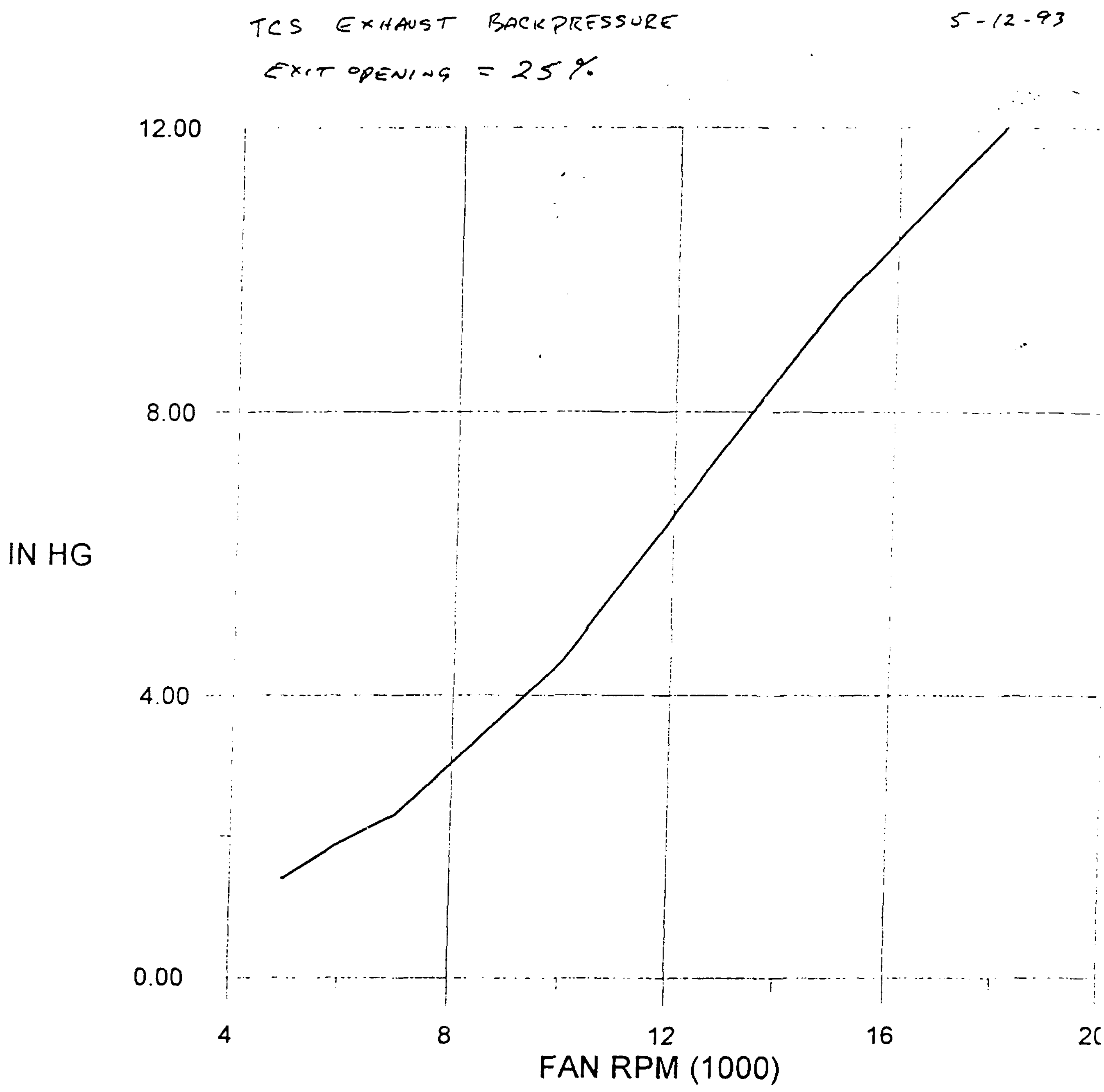
TCS EXHAUST BACKPRESSURE
5-12-93
EXIT OPENING = 25%
12.00
8.00
4.00
0.00
IN HG
4
8
12
16
20
FAN RPM (1000)

940842

Turbo-Compound Cooling Systems for Heavy-Duty Diesel Engines

W. E. Woollenweber
Turbo Design, Inc.

ABSTRACT

Fan-radiator cooling systems for diesel engines have experienced only minor changes in basic design since their inception. However, the increase in power output over decades of development of the engine has forced the cooling system to become larger, more complex and more expensive. Problems of fan noise, low system efficiency, durability and safety persist. The thermodynamic basis for the design of a new cooling system for heavy-duty diesel engines is presented in this paper. The new system consists of an exhaust gas turbine driving a high-speed ducted fan to provide cooling air for engine and vehicle heat exchangers. Since the turbo-fan is not mechanically connected to the engine, the components can be located in more convenient places that favor vehicle aerodynamics, operator visibility and operational safety.

I. INTRODUCTION

The compression ignition engine has undergone a century of development since its invention in Britain in 1890 and its improvement in the 1890's by Rudolf Diesel in Germany [1]. The diesel engine, as it is known today, has evolved as the most efficient prime mover, when turbocharged and aftercooled, for powering heavy-duty equipment of various types all over the world.

Even though the turbocharged, aftercooled diesel engine is highly efficient, it still rejects a large portion of its thermal energy to the cooling system and exhaust. The turbocharger turbine recovers a portion of the available exhaust energy and it is possible to recover an additional amount by adding a second turbine in series with the turbocharger turbine, called turbo-compounding, and returning the power generated by the second turbine to the engine crankshaft through gearing and a fluid coupling.

Tests of a turbo-compound engine in a highway truck show improvement in fuel economy and a reduction in noise level compared with the same type engine not equipped with a second exhaust gas turbine in the exhaust system [2] [3].

Commercial acceptance of the turbo-compound diesel engine has been hampered by its cost and mechanical complication. The turbo-compound gear train usually consists of a high speed gear box, a low speed gear box and a fluid coupling for the purpose of protecting the gearing from engine torsional vibration transmitted from the crankshaft. The power turbine imposes an additional back pressure on the engine; however, this parasitic loss is more than offset by the power developed by the turbine, resulting in a net gain in horsepower output from the turbo-compound power plant.

The mechanical complication of a turbo-compound engine can be simplified if the power output of the low pressure turbine is used for driving an engine accessory. Since the cooling system fan usually absorbs a significant percentage of the engine power, it follows that a low pressure power turbine might be coupled with a high speed, ducted fan for the purpose of supplying cooling air for engine and vehicle heat exchangers. Driving a high speed, ducted fan with a turbine should provide a less costly means of turbo-compounding, since there is no mechanical connection to the engine.

II. BACKGROUND

The location of the fan and radiator at the front of the engine forces compromises in the design of vehicles that are to be driven by the engine. The types of equipment that demand high horsepower output, such as earth movers and military vehicles, must be provided with large fans and radiators to dissipate the large amount of heat that must be transferred from the engine coolant when the engine is operating under load. Large fans and radiators interfere with operator visibility in earth moving equipment. They also cause problems in fitting them into military vehicles where space is limited and where they must be completely protected from damage from projectiles [4]. The aerodynamic shape of highway trucks is adversely affected by the need to mount the fan and radiator in the front of the vehicle. Trucks also suffer a loss in horsepower due to the aerodynamic resistance of the radiator and other heat exchangers being forced through the air at high speeds during on-highway operation.

Due to installation constraints in a variety of applications, fans are consistently forced to run at reasonably low efficiency levels. The radiator is usually solidly mounted on the vehicle frame whereas the engine, which carries the fan, must be flexibly mounted to the frame. Thus, there can be appreciable relative movement between the fan and radiator during operation of the vehicle. A large clearance between the fan blade tips and fan shroud must often be allowed to prevent the blades from contacting the shroud during operation. This large running clearance is detrimental to fan efficiency. Finally, the engine and accessory profile present a large obstruction to airflow leaving the fan, and the leaving velocity of the air is an irrecoverable energy loss. In summary, the efficiency of fan-radiator systems installed in vehicles is usually well below 50 percent.

Another major problem associated with current cooling systems is the noise generated by the fan. In heavy-duty equipment, the fan noise is aggravating to operators who must endure the noise for eight-hour work shifts. To reduce noise, designers have lowered the speed of fans but, in turn, must make them larger in diameter to generate sufficient cooling airflow. This expediency causes the use of heavier fans which puts higher rotational inertia on the engine mass-elastic system and can result in more exhaust emissions due to longer acceleration periods when operating under load.

The safety aspect of the fan on the front of an engine is another very important consideration. The rotating fan blades are nearly invisible to the eye when the engine is running and present a significant hazard to personnel. Also, much time and effort is expended by manufacturers in analyzing the environment in which the fan must operate in order to locate exciting forces that can cause metal fan blades to vibrate at their natural frequencies [5]. The fan must be designed to withstand the exciting forces found to exist in each application without failing from metal fatigue due to resonant vibration.

Thus, there are a number of serious problems associated with the conventional fan-radiator cooling systems in use today. Fans are still rather inefficient, some are noisy and dangerous and have grown in size and weight in consort with the increase in cooling requirements demanded by modern, high horsepower, turbocharged power plants. A new approach to diesel engine cooling that circumvents these problems and allows versatility in future vehicle and equipment design should be welcomed by vehicle and mechanical equipment manufacturers.

In contrast with current fan-radiation systems, a small, turbine-driven fan can be installed in a duct where tip clearance can be minimized and where airflow entering and leaving the fan can be closely controlled. Stator vanes downstream of the fan rotor can straighten the exit flow so that an efficient diffuser can be utilized to recover a high percentage of the leaving velocity energy. Thus, the efficiency of a ducted fan system can be expected to reach values exceeding 50 percent, which is substantially higher than many fan-radiator systems in current use today.

The duct work surrounding a ducted fan can act as a barrier to noise transmission to the surroundings. If necessary or desirable, the duct work can be insulated to further reduce noise transmission. This type of noise suppression is not possible with current fan systems where the fan runs in free air on the front of an engine. In addition, for the sake of system safety, the duct work enclosing the ducted fan can be designed to contain fragments in case a fan failure occurs at any time during operation of the vehicle in which the engine is installed.

In contrast with conventional systems, ducted fan blades are not exposed when operating; hence, personnel cannot inadvertently insert body parts into the moving blades. The inherent safety of a ducted fan cooling system is considered an important improvement over the hazards encountered with the use of free-running fans on current heavy-duty engines.

III. DESCRIPTION OF THE COOLING SYSTEM

The main component of the new cooling system consists of a radial inflow, exhaust gas turbine driving a high-speed, ducted fan mounted on a common shaft. The mechanical construction of the turbo-fan unit can be similar to that of a conventional turbocharger. A cross section assembly of one embodiment of a turbo-fan unit is shown in Figure 1.

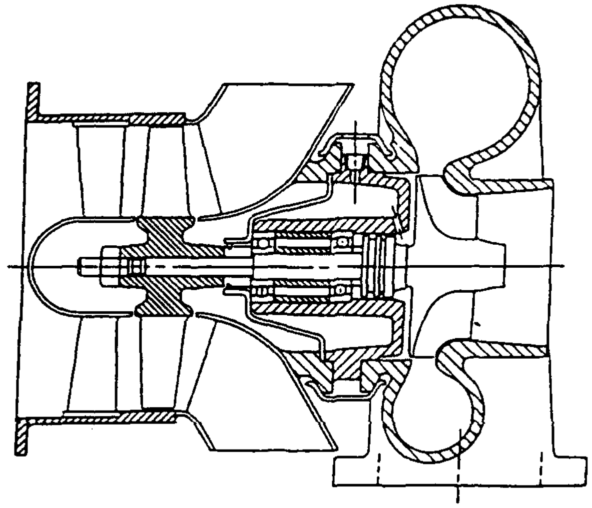

Figure 1. **Turbo-Fan Mechanical Construction**

One turbo-cooling system arrangement with downstream heat exchangers is diagrammatically illustrated in Figure 2. Atmospheric air is drawn in through an inlet screen and accelerated to the fan inlet. The cooling air leaves the fan at relatively high velocity and is decelerated in a diffusing section to an appropriate velocity for entering heat exchangers. The cooling air leaves the heat exchangers to be discharged back into the atmosphere, or used for some other purpose such as cab heating or exhaust gas dilution.

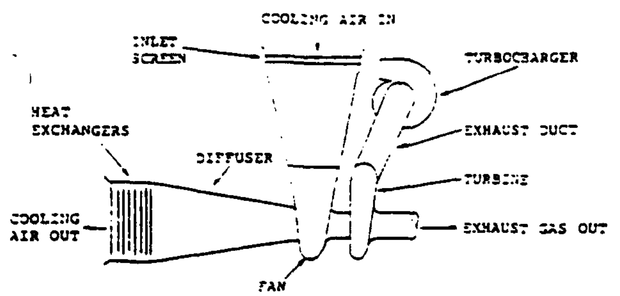

Figure 2. **Turbo-Cooling System with Downstream Heat Exchangers**

An alternate arrangement of the system is illustrated in Figure 3, where the heat exchangers are located upstream of the fan and the cooling air is discharged into the atmosphere directly from the diffuser outlet. Obviously, other arrangements of multiple heat exchangers are possible where they might be divided between upstream and downstream locations.

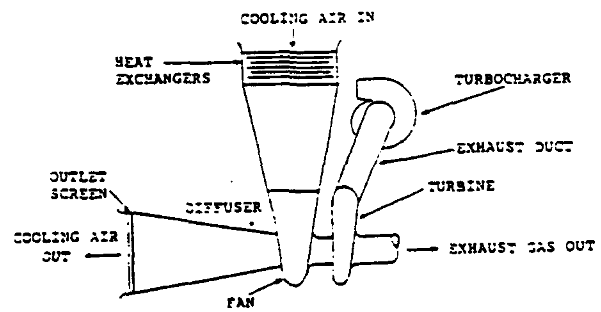

Figure 3. **Turbo-Cooling System with Upstream Heat Exchangers**

In the system analysis, the fan is treated as a low pressure ratio, axial flow compressor, followed by a conical or annular diffusing section. The turbine is a single stage, radial inflow or mixed flow type with an undivided volute casing providing full admission to the turbine wheel.

The compression process in the fan and the expansion process in the turbine are modelled using the Gas Turbine Gas Charts, U.S. Navy Research Memorandum No. 6-44, dated December 1944. These charts were prepared as an aid in making gas turbine performance calculations and facilitate rapid and accurate evaluation of gas property changes in the compression and expansion processes occurring in turbo-machinery. The charts are for pure, dry air and express the relationship between temperature, enthalpy, and a relative pressure function. The relative pressure function magnitudes corresponding to a temperature change for an isentropic process are proportional to the respective terminal pressures of the process.

In the first part of the analysis, the basic thermodynamic feasibility of the system has been investigated without reference to any specific engine applications. Since the system comprises well known, steady flow processes of compression, expansion and diffusion, these can be modelled by selecting specific state points at the beginning and end of each process and calculating values of temperature and pressure after assuming appropriate values for component efficiencies.

The level of back pressure needed to operate the turbo-fan is an important evaluation criteria in the determination of feasibility. In turbo-compounding, the added back pressure imposed by the power turbine can be as high as 18"Hg. It follows that back pressure imposed by the turbo-fan turbine should be less than 18"Hg for the system to be considered feasible.

The most important, independent variable in the system analysis is the amount of cooling air (W_{CA}) needed to satisfy various vehicle cooling conditions. The range of W_{CA} will extend from the amount required by a simple air-to-air charge air cooler to the amount required to fully cool a heavy-duty diesel engine in a modern, off-highway vehicle. Test data available from the literature and from equipment manufacturers has shown the range of W_{CA} to extend up to fifteen times the amount of engine air consumption (15xW_E).

To make the preliminary analysis independent from any given engine type or size, the amount of engine air consumption can be related to engine horsepower output by assuming that most modern engines have achieved a similar state of technical development and that they all consume nearly the same amount of air per horsepower output. This has been confirmed by surveying the air consumption data of a large number of engines, and a value of 2.5 CFM per rated horsepower output has been established as a good average value to use in preliminary calculations of cooling system air flow and fan horsepower.

The horsepower needed to drive the fan is dependent upon the air weight flow, the pressure loses in the system, and the fan efficiency. Practical experience has shown that heat exchanger resistance values (ΔP_{HE}) will be below [illegible]"H_2O for maximum cooling loads at full power output. Using this range of system resistance, the fan pressure ratio can be established and the power required to drive the fan can be calculated.

The engine exhaust gas flow is found by adding the weight flow of fuel used in the combustion process to the known values of engine air consumption. Horsepower output of the exhaust gas turbine is then determined by assuming various levels of exhaust gas temperature, pressure and turbine efficiency. By equating the values of fan power required with values of turbine power available, a power balance is established at various levels of exhaust gas back pressure. Any level of back pressure below the turbo-compound criteria of 18"Hg maximum establishes the preliminary feasibility of the new system. After the preliminary feasibility of the system has been established, the analysis proceeds to evaluate a typical commercial application of the turbo-compound cooling principle.

IV. POWER BALANCE ANALYSIS

The location of important system state points are shown on Figure 4 and defined in Table 1.

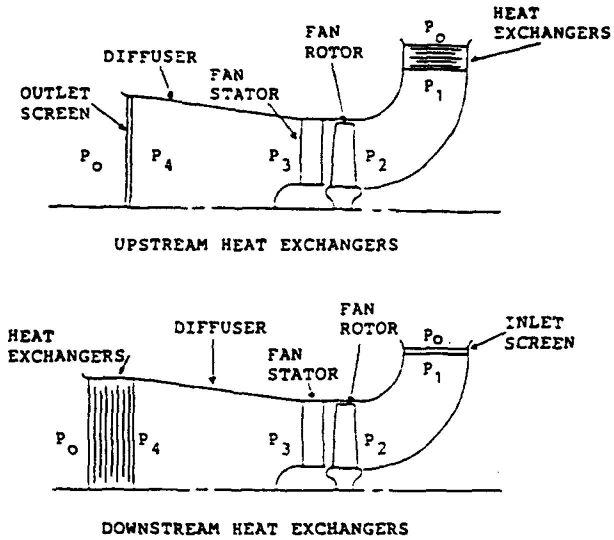

Figure 4. System State Point Locations

Table 1. Definition of System State Points

Point	Definition
P_0	Ambient Pressure
P_1	Pressure after upstream resistance
P_2	Pressure at fan inlet
P_3	Pressure at fan outlet
P_4	Pressure at diffuser outlet
P_5	Turbine inlet pressure
P_6	Turbine outlet pressure
T_0	Ambient temperature
T_1	Temperature after upstream resistance
T_2	Temperature at fan inlet
T_3	Temperature at fan outlet
T_4	Temperature at diffuser outlet
T_5	Temperature at turbine inlet
T_6	Temperature at turbine outlet

Calculation of Fan Power

The calculation of the power required to drive the fan to supply cooling air flow of 10xW_E for an engine ra[illegible] 400 BHP is outlined in detail below. The assumed operating conditions are given as follows:

Heat exchangers located upstream of fan.
Heat exchanger pressure drop, ΔP_{HE} = 3.0"H_2O
Fan inlet velocity, V_2 = 350'/sec
Engine air consumption, Q_E = 2.5 CFM/HP
Diffuser efficiency, η_D = .80
Fan efficiency, η_F = .70

$Q_E = 2.5 \times 400 = 1000$ CFM

$Q_{CA} = 10 \times 1000 = 10{,}000$ CFM

$P_o = 29.61$ "Hg

$T_o = 77°F = 537°R$

$\gamma_o = 1.326 \times \frac{29.61}{537} = .0731$ #/ft^3

$C_P = .242$ BTU/#-°F

$P_1 = 29.61 - .2206 = 29.3894$ "Hg

Assume an engine fuel consumption of .360 #/BHP-HR:

$W_F = .360 \times \frac{400}{60} = 2.40$ #/min

$H_F = 2.4 \times 18{,}500 = 44{,}400$ BTU/min

Assume 21% of input heat is rejected to coolant:

$H_R = .21 \times 44{,}400 = 9324$ BTU/min

$W_{CA} = .0731 \times 10{,}000 = 731$ #/min

$\Delta T_{HE} = \frac{9324}{.242 \times 731} = 52.7°$

$T_1 = 537 + 52.7 = 589.7°R$

$\Delta T_V = \frac{(350)^2}{64.4 \times 778 \times .242} = 10.1°$

$T_2 = 589.7 - 10.1 = 579.6°R$

Assume ΔP_{1-2} = 1.704 "Hg

$P_2 = 29.3894 - 1.704 = 27.6854$ "Hg

$\gamma_2 = \frac{27.6854}{579.6} = .0633$ #/ft^3

Actual $\Delta P_{1-2} = \frac{.0633(350)^2}{4553.33} = 1.704$ "Hg

Assume 80% pressure recovery in the diffuser.

$\Delta P_R = .80 \times 1.704 = 1.3632$ "Hg

$P_3 = 29.61 - 1.3632 = 28.2468$ "Hg

$\rho_F = \frac{28.2468}{27.6854} = 1.0203$

From Gas Charts:

$T_2 = 579.6°R$; $H_2 = 43.12$ BTU/#

$Pr_2 = 3.662$

$Pr_3 = 1.0203 \times 3.662 = 3.736$

$H_{3IS} = 43.88$ BTU/#

$\Delta H_{IS} = 43.88 - 43.12 = .76$ BTU/#

$\Delta H_{ACT} = \frac{.76}{.70} = 1.086$ BTU/#

$HP_F = \frac{778}{550} \times 1.086 \times 12.18 = \underline{18.72}$ HP

To establish the range of fan power required for higher heat exchanger pressure drops, the calculation has been repeated for ΔP_{HE} of 6.0 and 9.0"H_2O.

To establish the sensitivity of fan power requirements to changes in fan efficiency and diffuser efficiency, the calculation has been repeated for η_F of .60 and .80, and η_D of .60 and .70. The results of these calculations are summarized in Tables 2, 3 and 4.

Table 2. **Fan Power.** η_D = .80

	400 BHP Rating		
ΔP_{HE}	η_F=.60	η_F=.70	η_F=.80
3.0	22.97	18.22	17.23
6.0	31.88	27.32	23.92
9.0	40.50	34.71	30.38

Table 3. **Fan Power.** η_D = **.70**

	400 BHP Rating		
ΔP_{HE}	η_F=.60	η_F=.70	η_F=.80
3.0	29.58	25.36	22.19
6.0	38.78	33.24	29.08
9.0	47.40	40.62	35.55

Table 4. **Fan Power.** η_D = **.60**

	400 BHP Rating		
ΔP_{HE}	η_F=.60	η_F=.70	η_F=.80
3.0	36.19	31.02	27.14
6.0	44.81	38.40	33.61
9.0	54.00	46.29	40.50

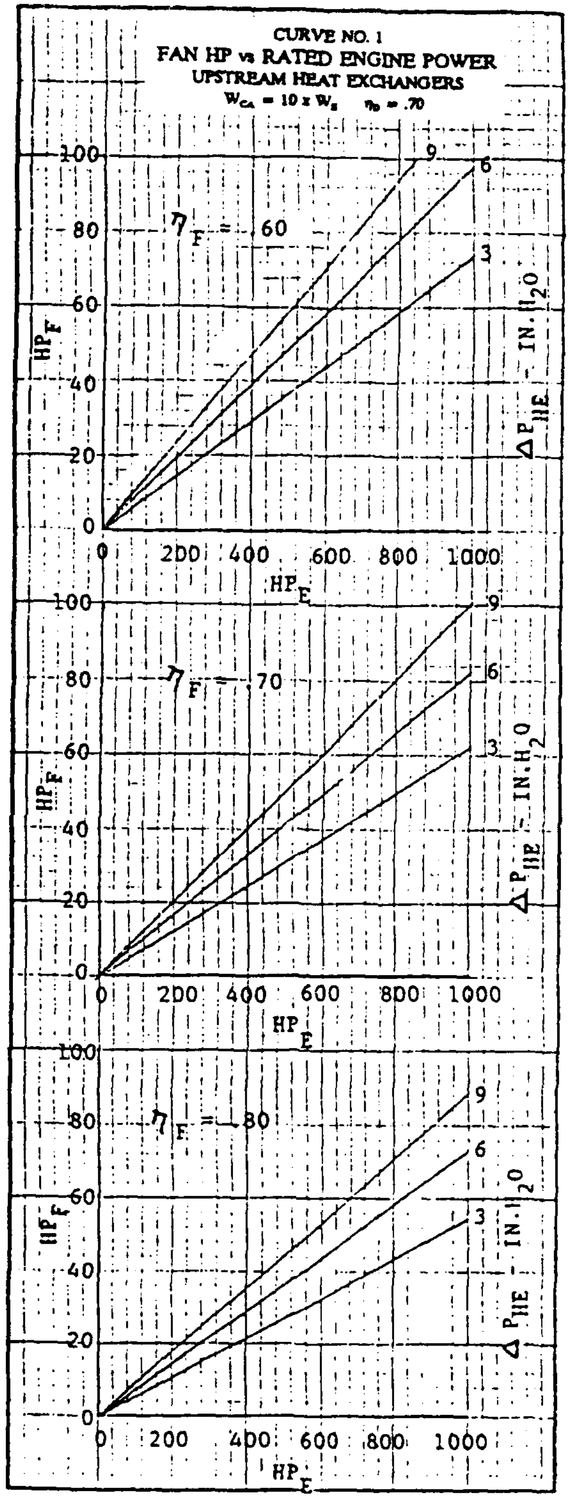

The power to drive the fan versus engine rated power with a diffuser pressure recovery of .70 has been plotted on Curve No. 1 with heat exchanger pressure drop as a parameter and with fan efficiencies of .60, .70 and .80.

The data has been cross plotted on Curve No. 2 to illustrate the sensitivity of fan power to change in fan efficiency. As can be seen on the curve, fan efficiency becomes more important as heat exchanger pressure drop increases.

Curve No. 3 shows the sensitivity of fan power to change in diffuser pressure recovery. The importance of high pressure recovery is evident from the steep slope of the curves at all heat exchanger pressure drop levels.

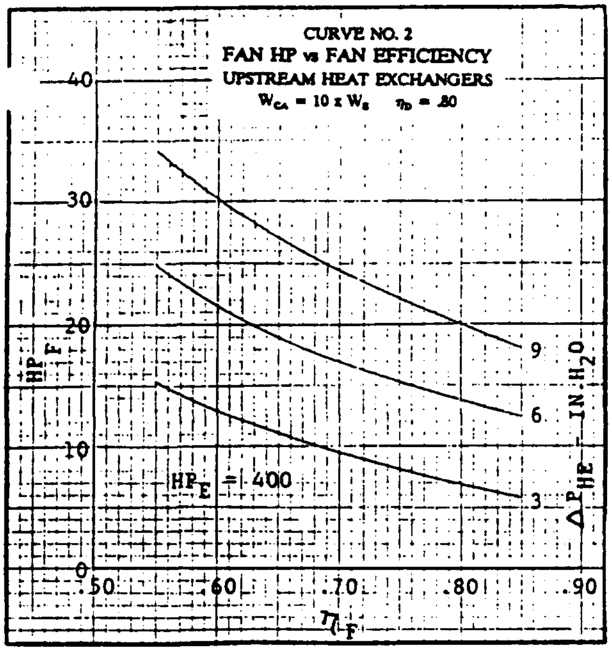

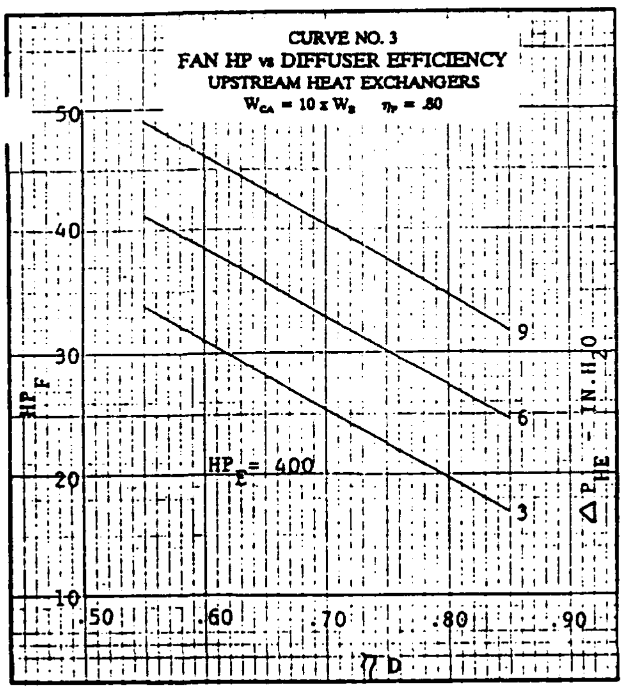

Calculation of Turbine Power

It is assumed that the turbine used to drive the ...d will be mounted in series with a turbocharger turbine that is used for supercharging the engine.

Two turbines in series in an exhaust system have been shown to exhibit a considerable muffling effect [3], so that on an engine so equipped the normal muffler might be reduced in restriction or eliminated entirely. Accordingly, in the following series of preliminary calculations, the turbine exit pressure, P_6, has been assumed to be atmospheric.

By the assumption of various levels of pre-turbine pressure (back pressure), the turbine expansion ratio is established. At a given exhaust gas temperature, the isentropic heat drop across the turbine can be found using the Gas Charts. Then, by assuming reasonable levels of turbine efficiency, the actual heat drop is determined and the turbine power can then be calculated directly.

An example of the turbine power calculation for an engine rating of 400 BHP is given below for a turbine inlet pressure of 2.0"Hg.

$P_5 = 31.61"Hg \qquad P_6 = 29.61"Hg$

$$\rho_T = \frac{31.61}{29.61} = 1.0675$$

$T_5 = 800°F = 1260°R$

From the Gas Charts,

$H_5 = 211.35$ BTU/# $\qquad Pr_5 = 59.61$

$$Pr_6 = \frac{59.61}{1.0675} = 55.84$$

$H_{6IS} = 205.73$ BTU/#

$\Delta H_{IS} = 211.35 - 205.73 = 5.62$ BTU/#

$\eta_T = .60$

$\Delta H_{ACT} = 5\ 62 \times .60 = 3.372$ BTU/#

Assume a fuel consumption of .360 #/BHP-HR

$$W_F = .360 \times \frac{400}{60} = 2.4 \text{ #/min}$$

$$W_{EX} = \frac{73.10 + 2.4}{60} = 1.258 \text{ #/sec}$$

$HP_T = 1.415 \times 3.372 \times 1.258 = \underline{6.00}$ HP

Repeating the preceding calculation for turbine inlet pressures up to 20"Hg.ga. in 2"Hg increments results in establishing the power potential of the turbine under the assumed operating conditions. A summary of the calculated values of turbine power for engine ratings of 400 BHP is given in Table 5 for an exhaust temperature of 800°F, in Table 6 for a temperature of 900°F, and in Table 7 for a temperature of 1000°F.

Table 5. **Turbine Power.** T_{EX} **= 800°F**

P_5	400 BHP Rating		
"Hg.Ga.	η_T=.60	η_T=.70	η_T=.80
2	6.00	6.96	7.96
4	11.57	13.49	15.42
6	16.65	19.42	22.20
8	21.41	24.98	28.55
10	25.88	30.19	34.50
12	30.03	35.04	40.04
14	33.97	39.63	45.30
16	37.67	43.94	50.22
18	41.14	47.99	54.85
20	44.50	51.92	59.34

Table 6. **Turbine Power.** T_{EX} **= 900°F**

P_5	400 BHP Rating		
"Hg.Ga.	η_T=.60	η_T=.70	η_T=.80
2	6.44	7.51	8.59
4	12.32	14.38	16.43
6	17.93	20.92	23.91
8	22.55	27.47	31.40
10	27.85	32.49	37.14
12	32.40	37.80	43.20
14	36.66	42.77	48.88
16	40.65	47.42	54.20
18	44.35	51.75	59.14
20	48.05	56.06	64.04

Table 7. **Turbine Power.** T_{EX} **= 1000°F**

P_5	400 BHP Rating		
"Hg.Ga.	η_T=.60	η_T=.70	η_T=.80
2	6.97	8.14	9.30
4	13.33	15.55	17.77
6	19.28	22.49	25.70
8	24.81	28.94	33.08
10	29.99	34.99	39.98
12	34.78	40.58	46.38
14	39.37	45.93	52.49
16	43.71	51.00	58.28
18	47.73	55.68	63.64
20	51.64	60.24	68.85

The data in Table 6 has been plotted on Curve No. 4 for a fan efficiency of .70 for engine ratings up to 1000 HP.

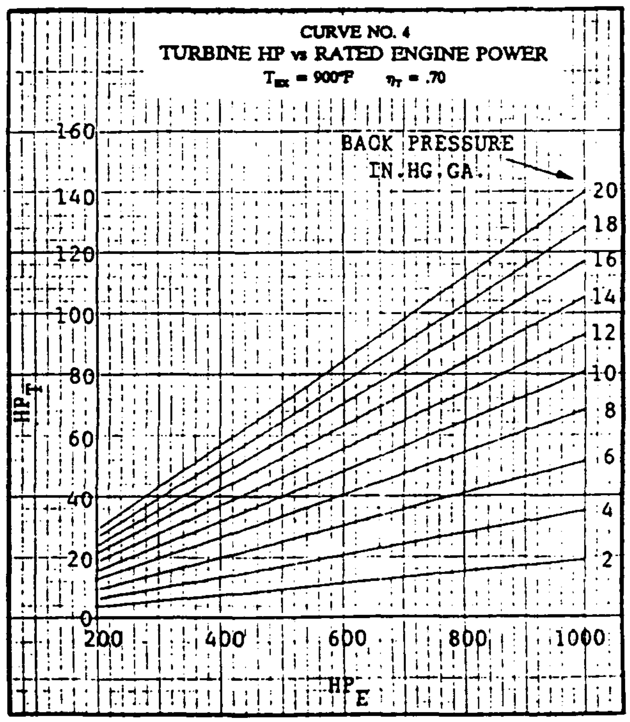

V. PRELIMINARY SIZING OF THE FAN COMPONENT

The size of the fan component is dependent upon the quantity of cooling air to be pumped, the axial velocity of the air entering the fan, and the location of the heat exchangers. In all the foregoing calculations, the air velocity entering the fan has been assumed to be 350'/sec. The effect on the fan size of selecting other air inlet velocity is also investigated in this section.

For an engine rated at 400 BHP and with heat exchangers located downstream of the fan, the cooling air quantity is:

Q_{CA} = 2.5 x 400 x 10 = 10,000 CFM

If V= 350'/sec, the required axial flow area is:

$$A_N = \frac{10,000}{350} \times 2.4 = 68.57 \text{ in}^2$$

Assume a fan diameter of 10.0".

Gross axial flow area,

$A_G = .7854(100) = 78.54 \text{ in}^2$

Area of a 2.6" diam. hub,

$A_H = .7854(2.6)^2 = 5.31 \text{ in}^2$

For a 13 vane fan, the vane blockage area can be approximated by:

$A_V = 13 \times .12 \times 3.7 = 5.77 \text{ in}^2$, where 13 is the number of vanes, .12" is the average vane thickness, and 3.7" is the vane length. A certain amount of clearance over the fan blade tips is necessary which increases the net flow area by a small amount. Assuming a .125" clearance on the diameter, the clearance area is:

$$A_{CL} = .7854\ [(10.125)^2-(10)^2] = 1.98 \text{ in}^2$$

Allowing for a thick boundary layer, the increase in flow area due to the clearance will be estimated as 50% of the geometric area, or approximately 1.0 in². The net axial flow area of a 10.0" diameter fan becomes:

$A_N = 78.54 + 1.0 - 5.31 - 5.77 = \underline{68.46 \text{ in}^2}$

Required net axial area is $\underline{68.57 \text{ in}^2}$

Thus, a 10.0" dia. fan is indicated for an engine rated at 400 BHP and requiring $10xW_E$ cooling air flow.

The selection of a fan inlet air velocity of 350'/sec is a matter of choice. Higher inlet velocity results in a smaller fan size but increases the fan horsepower. Calculations using lower and higher inlet velocity than 350'/sec produced the data listed in Table 8 and this data has been plotted on Curve No. 5.

Table 8. **Preliminary Fan Size, Downstream Heat Exchangers**

	Fan Diameter - Inches		
HP_E	V_2 = 300'/sec	V_2 = 350'/sec	V_2 = 400'/sec
200	7.75	7.20	6.70
400	10.80	10.00	9.40
700	14.35	13.25	12.50
1000	17.10	15.85	14.85

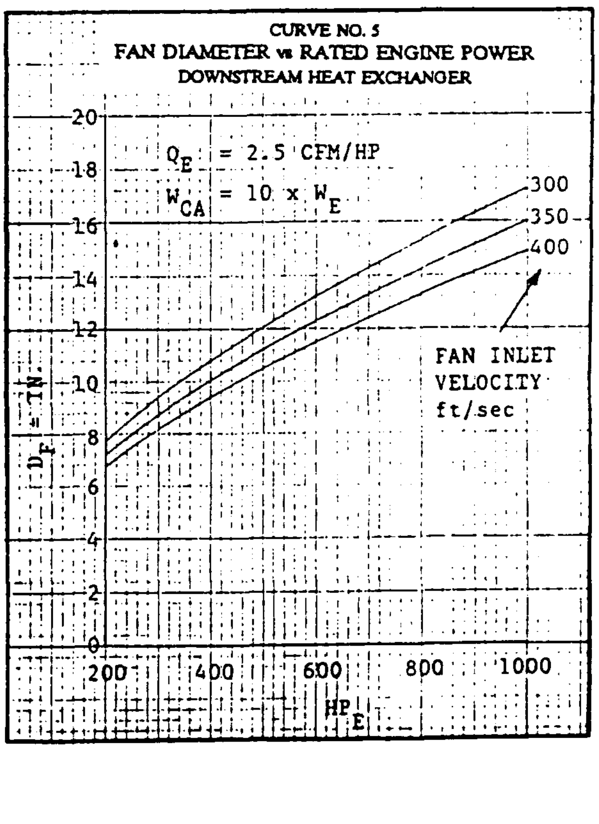

Considering a system with upstream heat exchangers, the volume flow that the fan must pump is increased due to heat added to the air when passing through heat exchangers. For an engine rated at 400 BHP, the temperature rise through the heat exchanger is 52.7°.

Q_{CA} = 10,000 CFM

W_{CA} = 731 #/min

γ_2 = .0633 #/ft^3

$Q_2 = \frac{731}{.0633} = 11{,}548$ CFM

For V_2 = 350'/sec,
the required net area is:

$A_N = \frac{11548}{350} \times 2.4 = \underline{79.19\ in^2}$

For a 10.75" fan,

$A_G = .7852(10.75)^2 = 90.76\ in^2$

Area of a 2.8" hub,

$A_H = .7854(2.8)^2 = 6.16\ in^2$

Vane blockage area,

$A_V = 13 \times .13 \times 3.98 = 6.72\ in^2$

Clearance area,

$A_{CL} = .7854[(10.875)^2 - 10.75)^2]$

$A_{CL} = 2.70\ in^2$

$A_N = 90.76 + 1.35 - 6.16 - 6.72$

$A_N = \underline{79.23\ in^2}$

Thus, locating heat exchangers upstream of the fan results in an increase of .75" in the fan diameter required. However, this increase in diameter may be offset by allowing the fan inlet velocity increase to a higher value than 350'/sec.

The preliminary fan size for use with upstream heat exchangers and a V_2 of 350'/sec is given on Curve No. 6, compared with the fan size required with downstream heat exchangers for engines rated up to 1000 BHP output.

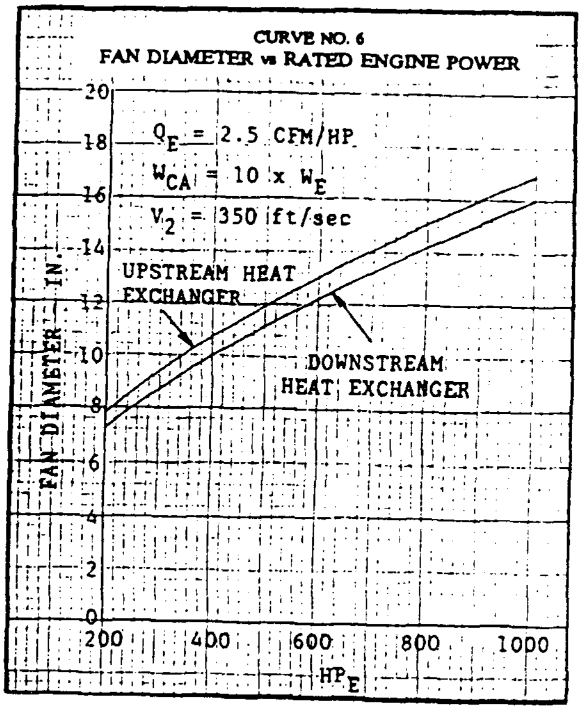

VI. PRELIMINARY SIZING OF THE TURBINE COMPONENT

The size of the turbine wheel is dependent upon the fan power required, the bearing system losses and the speed of rotation of the rotor assembly. It is expected that the speed range of the turbofan will allow the use of grease-lubricated, antifriction bearings that have a mechanical efficiency of close to 99 percent. In this case, the magnitude of the bearing system power absorption will be small enough to be neglected.

For an engine rated at 400 BHP, the following operating conditions are assumed:

$\Delta P_{HE} = 6.0"H_2O;\ \eta_F = .70;\ \eta_D = .70$

$V_2 = 350'/sec;\quad W_E = 73.1$ #/min

$W_F = .360 \times \frac{400}{60} = 2.4$ #/min

$W_{EX} = \frac{73.10 + 2.4}{60} = 1.258$ #/sec

From Curve No. 1, the fan power is found to be 33 HP.

At the design point, the power developed by a radial turbine can be approximated by the expression:

$$H_T = \frac{C_{U1} U_T}{g} \quad \text{where:}$$

C_{U1} = tangential component of the entering gas velocity

U_T = wheel tip speed

g = acceleration of gravity

For a radial inflow turbine, the value of C_{U1}/U_T falls in the range of .85 and the equation for turbine work reduces to:

$$H_T = \frac{.85\ U_T^2}{g}$$

For the 400 BHP engine rating, the required turbine power output to drive the fan is:

$$H_T = \frac{33 \times 550}{1.258} = 14{,}428 \text{ ft \#/\#}$$

The required turbine tip speed to develop the power is:

$$U_T = \sqrt{\frac{14428 \times 32.2}{.85}} = 739\text{'/sec}$$

For a 6.0" diameter turbine, the rotational speed will be:

$$N = \frac{720 \times 739}{\pi \times 6.0} = \underline{28{,}227 \text{ RPM}}$$

Turbine tip speed versus rated engine power has been plotted on Curve No. 7.

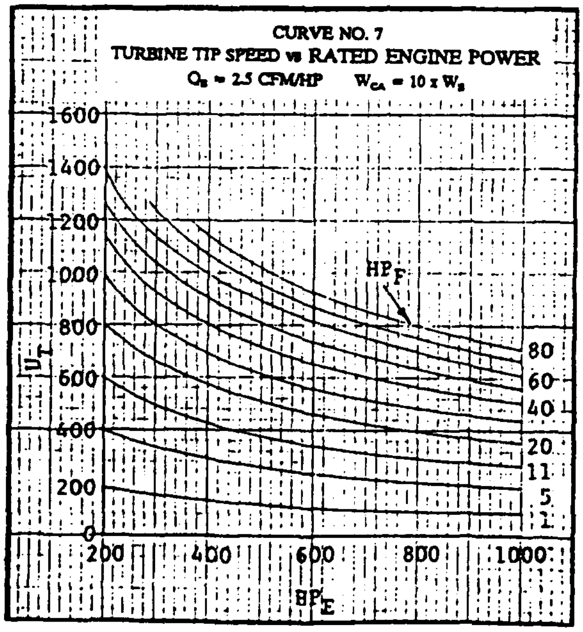

CURVE NO. 7
TURBINE TIP SPEED vs RATED ENGINE POWER
Q_B = 2.5 CFM/HP $\quad W_{CA} = 10 \times W_B$

VII. FEASIBILITY DETERMINATION

For the convenience of determining feasibility and of estimating the size and operating parameters of turbo-cooling systems applicable to diesel engines of up to 1000 HP ratings, Curves No. 8 and 9 have been prepared from a consolidation of the calculated data. Steps to be taken in the use of the charts are as follows:

1. With a cooling air flow of ten times engine air flow, select a pressure drop imposed by heat exchangers sized to adequately cool the engine and auxiliaries.

2. Enter Curve No. 8 with the rated power of the engine and heat exchanger pressure drop to obtain the necessary fan and turbine power.

3. Follow the turbine power value to its intersection with rated engine power to determine the estimated back pressure level. The back pressure value should fall well within the area bounded by the feasibility limit.

4. Enter Curve No. 9 with the fan power value from Curve No. 8 and find the necessary turbine tip speed.

5. Select a turbine wheel diameter and find the rotational speed of the turbo-fan rotor.

6. Decide on the most appropriate location for the heat exchangers and determine the fan size from Curve No. 9.

7. Use the rotational speed and fan size to estimate the tip speed of the fan from Curve No. 9.

8. Use the level of fan tip speed to select the fan material with regard to stress levels that ensure satisfactory durability.

CURVE NO. 8
TURBO-COOLING
FEASIBILITY DETERMINATION CHART

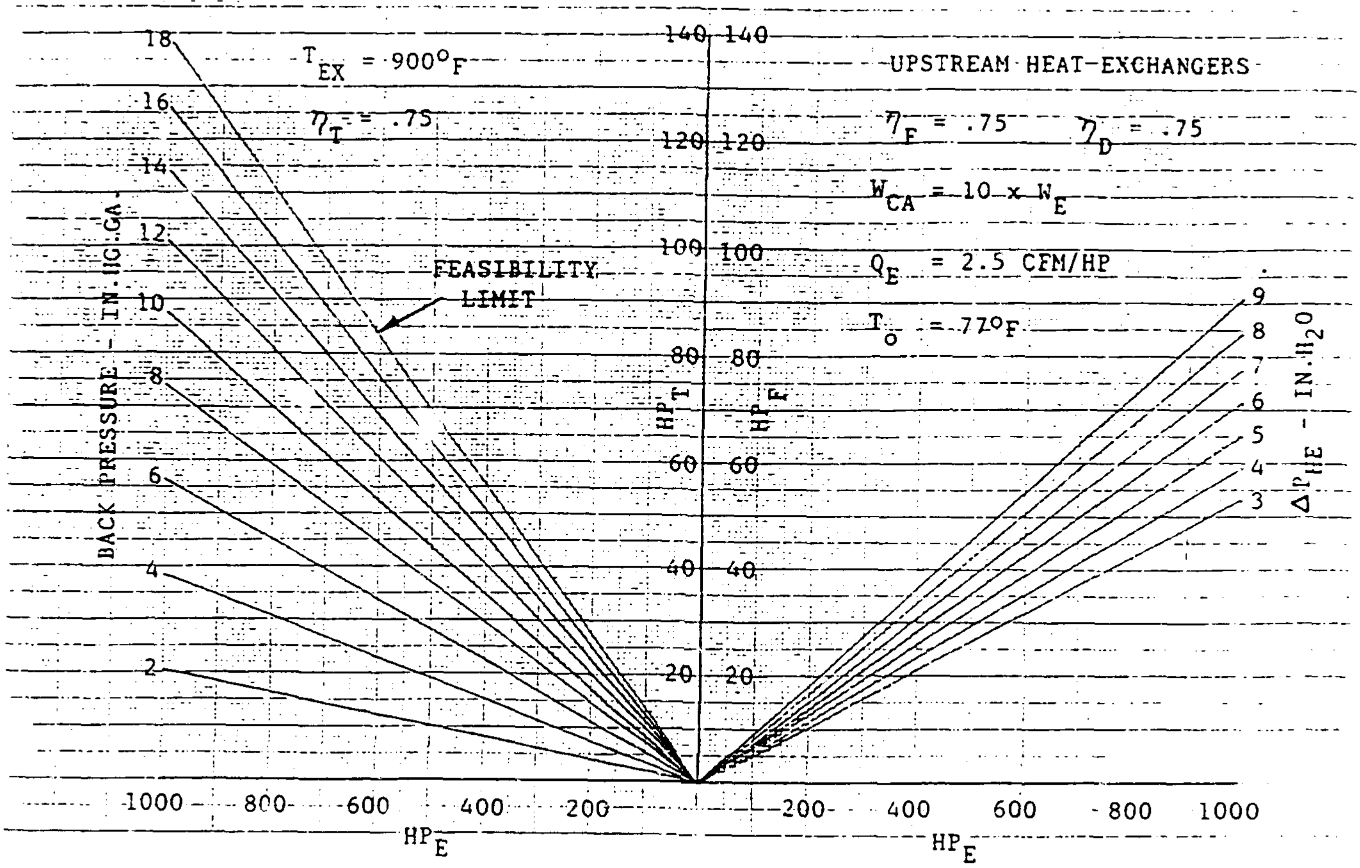

VIII. DETAILED ANALYSES OF TURBO-COOLING SYSTEMS FOR AN 8.0 LITER DIESEL ENGINE USED IN OFF-HIGHWAY EQUIPMENT

The diesel engine and auxiliary equipment used to power some types of off-highway equipment, such as farm machinery and earth movers, usually require the use of four separate heat exchangers. These are the main engine coolant heat exchanger, charge air cooler, a hydraulic oil cooler, and an air conditioning condenser. When considering a new cooling system, the four heat exchangers may be located in a number of different ways since they do not have to be positioned in the conventional manner in front of the engine-driven fan.

If possible, the heat exchangers should be mounted in a parallel configuration either upstream or downstream of the turbo-fan so that the individual resistances are not additive. In this way, the system resistance and fan power requirement are minimized.

In the following analysis, it has been assumed that the heat exchangers are mounted in the preferred parallel arrangement. Also, in the following calculations, the turbo-fan systems being analyzed are identified by the assumed values of the efficiencies of the three main system components. For example, a 70-75-80 system indicates components with a fan efficiency of .70, a turbine efficiency of .75, and a diffuser pressure recovery of .80.

CURVE NO. 9
TURBO-COOLING NOMOGRAM

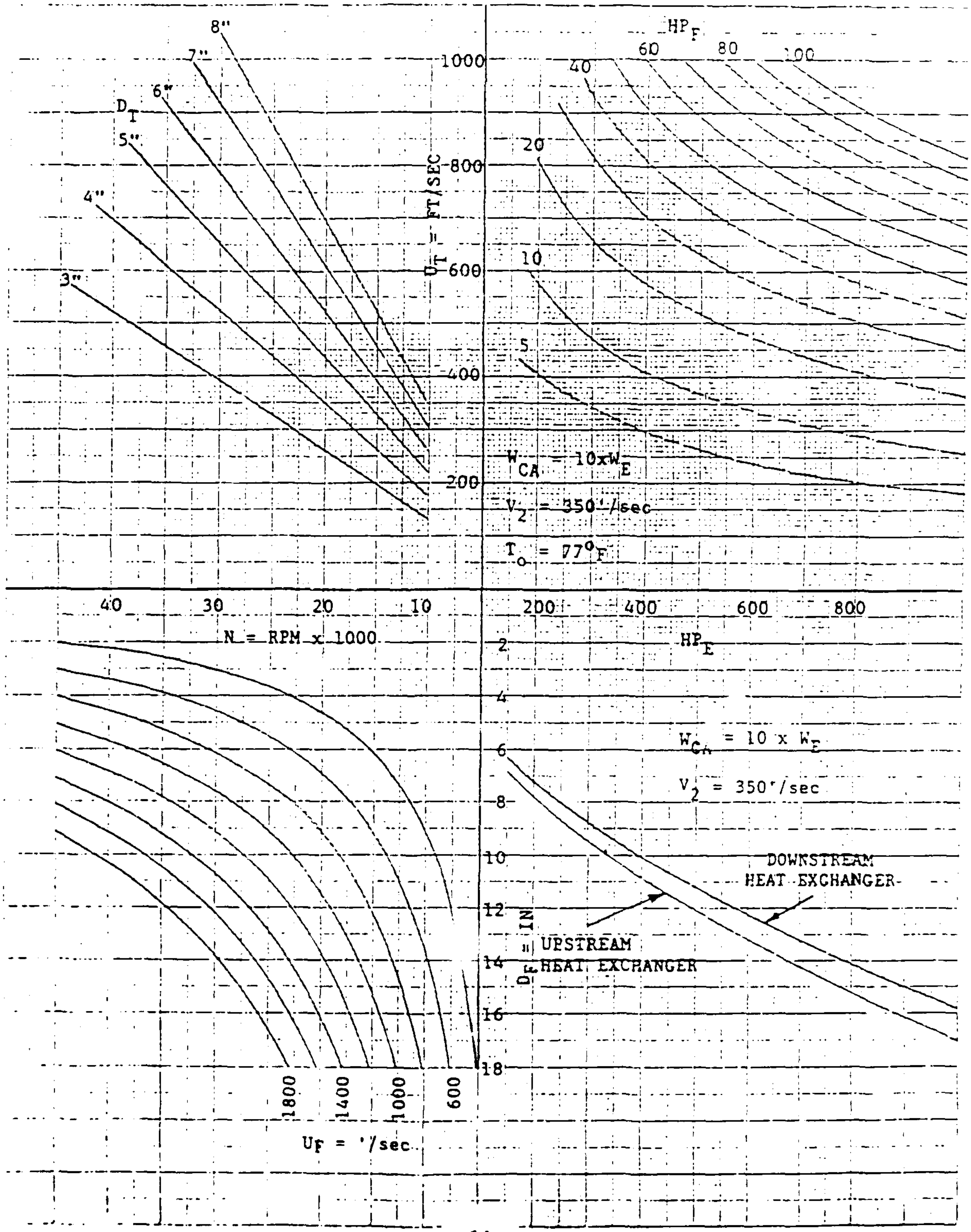

Turbo-Fan System for Charge Air Cooling of 8.0 'ter Engine.

Most modern turbocharged diesel engines are equipped with aftercoolers that remove some of the heat of compression from the charge air before it enters the cylinders. Jacket water has been extensively used as the coolant media; however, changing to air-to-air charge air coolers has become common due to the lower charge air temperatures attainable when using ambient air as the coolant media.[6] The air-to-air heat exchanger is usually mounted in front of the radiator requiring the compressed air from the turbocharger to be piped from the turbocharger mounted on the engine, to the cooler core and then back again to the engine intake manifold.

An alternative to the current system of aftercooling is to use a small turbo-fan to supply cooling air to the air-to-air charge air cooler so that both the turbo-fan and the heat exchanger can be mounted on or near the engine. This rrangement should be more compact than the system that requires the air-to-air heat exchanger to be mounted in front of the radiators. The feasibility of the turbo-fan system for charge air cooling of the 8.0 liter engine has been investigated with and without the use of a diffusing section following the fan. These results are listed in Table 9.

Table 9. **Charge Air Cooling System with and without Diffuser.**

Turbo-Fan	With Diffuser	Without Diffuser
Fan Diameter	5.1"	5.5"
Turbine Diameter	3.5"	4.0"
Speed of Rotation	22,132 RPM	29,048 RPM
Back Pressure	1.73"Hg.ga.	4.0"Hg.ga.
Velocity Ratio	.663	.664
Diffuser Length	49.48"	0

Thus, it appears feasible that for charge air cooling only, a turbo-fan does not need a diffuser to be functional. The mechanical construction of a turbo-fan for charge air cooling would be similar to that shown in Figure 1.

Turbo-Fan System for Full Engine and Auxiliary Cooling of 8.0 Liter Diesel Engine at Rated Load and Speed.

Basic engine data and assumed conditions:

Engine rating: 275 BHP at 2100 RPM

Parallel heat exchanger arrangement upstream of fan.

Assumed system efficiencies: 75-75-75

$\Delta P_{HE} = 5.0"H_2O = .3676"Hg$

$P_o = 29.61"Hg$

$T_o = 110°F$

$\gamma_o = .0689\ \#/ft^3$

Heat rejection:

Engine coolant	H_E	= 4781
Charge air cooler	H_C	= 1616
Hydraulic oil cooler	H_H	= 1098
A/C Condenser	H_{AC}	= 586
Total		8081 BTU/min

Engine air flow, $W_E = 46.93\ \#/min$

Cooling air flow, $W_{CA} = 12xW_E$

$W_{CA} = 12 \times 46.93 = 563.16\ \#/min$

$$Q_{CA} = \frac{563.16}{.0689} = 8174\ CFM$$

The results of the calculations are listed in Table 10.

Since the exact quantity of cooling air flow required can only be estimated at this time, the 8.0 liter engine analysis has been repeated for cooling air flow quantities of 9 times and 15 times engine air flow. The results are included in Table 10 and plotted on Curve 10.

Table 10. Turbo-Cooling System for 8.0 Liter Engine. System Efficiencies 75-75-75

275 BHP at 2100 RPM	9 x W_E	12 x WE	15 x W_E
Fan Power-HP	15.94	20.72	24.57
Fan Diameter-IN.	8.75	9.80	10.90
Turbine Diameter-IN.	5.00	5.50	6.00
Back Pressure-"Hg.ga.	6.75	9.16	11.22
Rotor Speed-RPM	30,206	30,502	30,441
U_T/C_o	.682	.665	.665

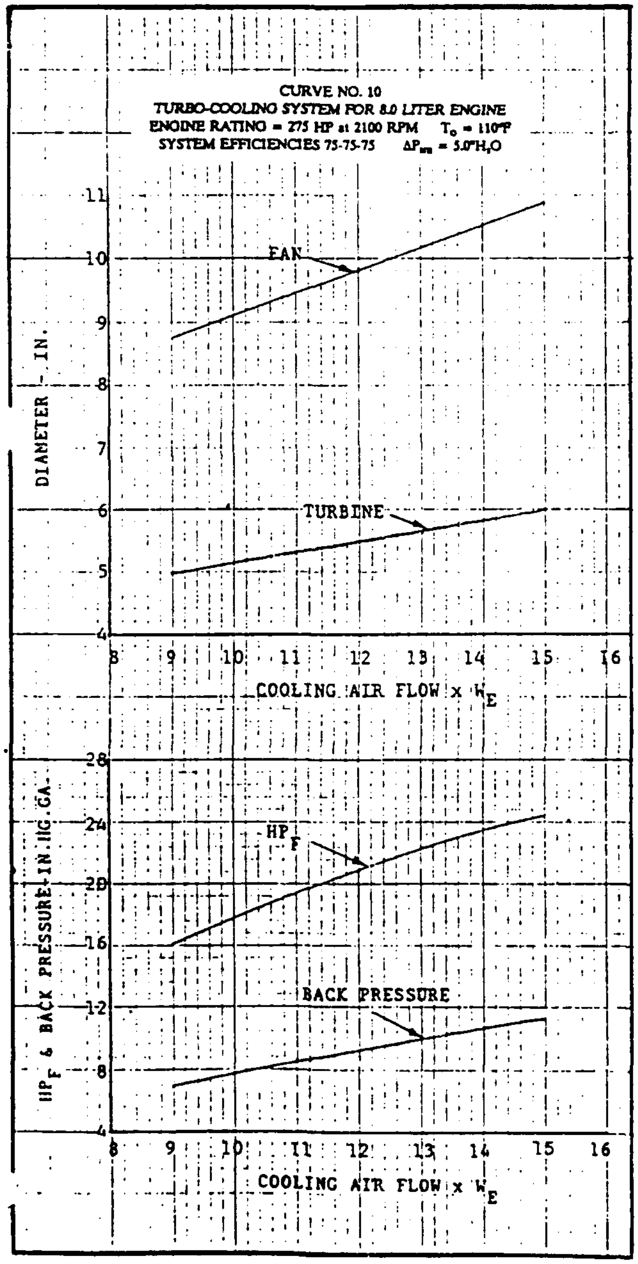

Analysis of Turbo-Fan System for 8.0 Liter Engine at Torque Peak.

The most difficult cooling condition might occur at torque peak and 110°F ambient air temperature. This condition is analyzed as follows:

Basic engine data and assumed conditions:

Torque peak rating:
244 HP at 1400 RPM

Torque rise: 33%

Parallel heat exchangers, upstream of fan.

ΔP_{HE} = 4.0 "H_2O = .2941 "Hg.

Heat rejection at torque peak:

Engine coolant	H_E	= 4491
Charge air cooler	H_C	= 840
Hydraulic oil cooler	H_H	= 734
A/C condenser	H_{AC}	= 398
	Total	6463 BTU/min

System efficiencies: 75-75-75

Engine air flow, W_E = 28.67 #/min
Cooling air flow, W_{CA} = 15 x W_E
W_{CA} = 15 x 28.67 = 430.05 #/min

The results of the analysis of an optimized turbo-cooling system for an 8.0 liter diesel engine at both rated speed and at torque peak are listed in Table 11. The effect of designing a system for operation in 110°F ambient air temperature compared with designing the same system for 77°F ambient temperature can also be found in Table 11.

Table 11. **Optimized Turbo-Cooling System for Liter Engine. Upstream Heat Exchangers**

	Torque Peak	Torque Peak	Rated Speed
Ambient Temp.-°F	77°F	110°F	110°F
Engine Speed-RPM	1400	1400	2100
Cooling Air Flow	$15xW_t$	$15xW_t$	$12xW_t$
System Efficiencies	80-80-80	80-80-80	75-75-75
Fan Power-HP	8.87	9.25	20.72
Fan Diameter-IN	9.60	9.80	9.80
Turbine Diameter-IN	5.50	5.50	5.50
Back Press.-"Hg.ga.	4.74	4.96	9.16
Rotor Speed-RPM	25,293	25,835	30,502
U_t/C_o	.687	.687	.665

<u>Diffuser Design for Optimized Turbo-Cooling System for 8.0 Liter Diesel Engine.</u>

Optimal performance of a turbo-cooling system is dependent upon an efficient diffusion process to convert a large percentage of the exit fan velocity into pressure. The use of stator vanes downstream of the fan rotor can turn the exit air w into a uniform axial flow so that it is possible that it can be effectively diffused. Several well known types of diffusers that can be applied are the conical and the annular. The literature suggests that the maximum pressure recovery that can be expected from a well designed diffuser is 80 percent. This value has been used in the previous calculations of an optimized turbo-cooling system.

Since the effectiveness of the diffuser is of primary importance in achieving optimal performance from the cooling system, an innovative approach to diffuser design is necessary with the objective of reducing the axial length while maintaining a high level of pressure recovery.

The paper by Sovran and Klemp [7] provides information pertaining to pressure recovery coefficients for optimum geometries of rectangular, conical and annular diffusers. The annular type occurs commonly in turbomachinery because fluids must flow around a central shaft and bearing structure. Evidently, the inner surface present in annular diffusers acts to guide the fluid outward resulting in achieving good performance with large wall angles. Since the use of large wall angles results in shortening the axial length required to achieve a specified terminal velocity, the annular diffuser appears to have significant potential for use in a turbo-cooling system.

If the system is optimized for torque peak, the terminal velocity from the diffuser at rated speed can be above the arbitrary figure of 50'/sec used in previous calculations. If the value of V_4 at rated speed is set at 60'/sec, the resulting V_4 at torque peak will be less than 50'/sec. These values appear to be a good compromise for achieving high pressure recovery over the operating speed range of the engine.

For a terminal velocity of 60'/sec at rated speed, the required exit area is:

$$A_4 = \frac{90.79}{60} \times 2.4 = 363 \text{ in}^2$$

If the fan exit air flow is divided by three concentric annular diffusing channels, the diffuser entrance area is divided into thirds.

$$A_3/3 = 72.06/3 = 24.02 \text{ in}^2$$

The exit area of each annulus is:

$$A_4/3 = 363/3 = 121.0 \text{ in}^2$$

The inner annulus dimensions are:

Inlet O.D. = 6.11"; I.D. = 2.6"

Outlet O.D. = 13.0"; I.D. = 3.8"

$\phi_i = 1°$ $\phi_o = 6°$

From the given geometry, L = <u>33.3"</u>

$$\Delta R = \frac{6.11-2.6}{2} = 1.755$$

$$L/\Delta R = \frac{33.3}{1.755} = 18.87$$

$$AR\text{-}1 = \frac{121}{24.02} - 1 = 4.04$$

With these values of $L/\Delta R$ = 18.97 and AR-1 = 4.04, the predicted pressure recovery coefficient ($\overline{C}_P$) from reference [5], Figure 15, Page 289 is over .80.

The middle annulus dimensions are:

Inlet O.D. = 8.24" I.D. = 6.11"

Outlet O.D. = 16.1" I.D. = 10.3"

$\phi_i = 6°$ $\phi_o = 11°$

From the given geometry, L = 20.7"

$$\Delta R = \frac{8.24 - 6.11}{2} = .8425$$

$$L/\Delta R = \frac{20.7}{1.065} = 19.44$$

The outer annulus dimensions are:

Inlet O.D. = 9.925 I.D. = 8.24"

Outlet O.D. = 18.95 I.D. = 14.3"

$\phi_i = 11°$ $\phi_o = 16°$

From the given geometry, L = 15.8"

$$\Delta R = \frac{9.925 - 8.24}{2} = .8425$$

$$L/\Delta R = \frac{15.8}{.8425} = 18.75$$

AR-1 = 4.04

Pressure recovery coefficient, $\overline{C}_P$ = >.80

The value selected for the diffuser terminal velocity has a major effect on the overall length. Overall length of a concentric annular diffuser versus terminal velocity has been plotted on Curve No. 11. A concentric annular diffuser designed for the 8.0 liter engine with a terminal velocity of 60'/sec is illustrated in Figure 5.

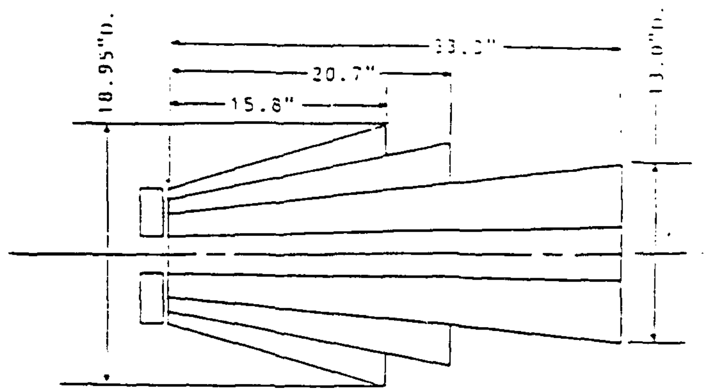

Figure 5. Concentric Annular Diffuser for 8.0 Liter Engine

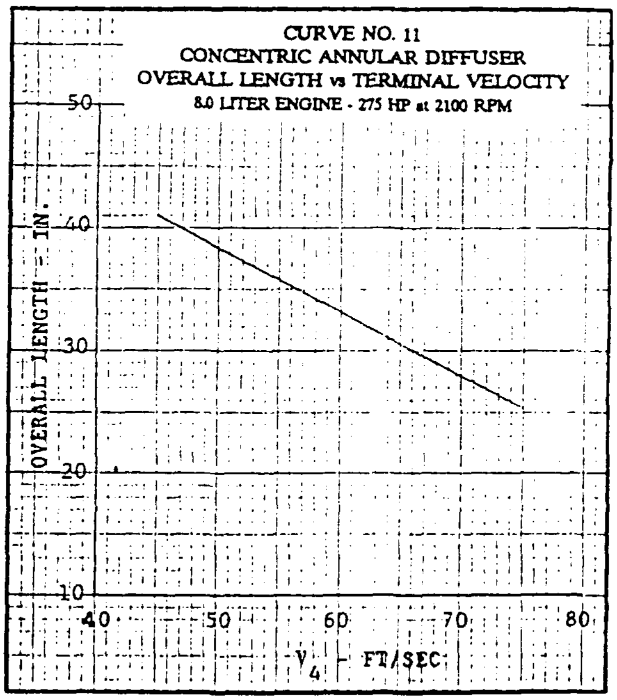

With the dimensions of the diffuser approximately determined, a complete turbo-cooling system for the 8.0 liter engine can be constructed.

If the concentric annular diffuser and fan component are surrounded by a plenum chamber, the fan can be provided with a uniform peripheral air inlet. Uniform air inlet conditions are essential for achieving high fan efficiency. The heat exchangers can be located upstream of the fan in the plenum chamber walls in a parallel arrangement to ensure lowest possible system resistance. The plenum chamber shape can be round to accommodate round heat exchangers, or rectangular as dictated by the most desirable heat exchanger arrangement. The turbine and bearing housing structure of the turbo-fan unit is external from the plenum chamber to ensure a convenient attachment to the engine exhaust gas piping. The volume of the plenum chamber needs to be developed in conjunction with the system heat exchanger size so that the air velocity induced through the heat exchangers by the action of the fan is maintained at a proper level when the maximum cooling load is encountered. One possible configuration of a turbo-cooling system module for the 8.0 liter engine is illustrated in Figure 6. The installation of the complete cooling module in a vehicle might be made where the plenum chamber walls conform to, or are part of, the vehicle structure.

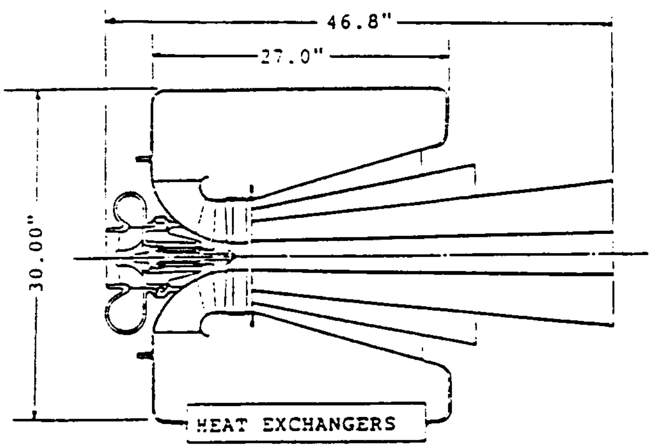

Figure 6. **Turbo-Cooling Module for 8.0 Liter Diesel Engine**

__Estimated Effect of Turbo-Cooling System on Performance of 8.0 Liter Diesel Engine.__

The added back pressure imposed on the engine by the turbo-fan turbine causes a power loss. However, this loss can be offset by the removal of the power absorption of the standard engine-driven fan.

Figure 10 in Reference [2] shows the effect of increasing back pressure on a typical diesel engine. The net power developed from a turbo-compound engine reaches a maximum at some value of power turbine expansion ratio.

Engine tests have been run to simulate turbo-compound performance effects by imposing a variable restriction on the engine exhaust. As the restriction is increased, the expansion ratio across the turbocharger turbine will decrease causing a drop in boost pressure, air flow and trapped air/fuel ratio. The turbocharger must then be re-matched to restore the loss in boost pressure.

The effect of restricting the exhaust of a typical 8.0 liter diesel engine is illustrated on Curve No. 12. Boost pressure of the unrestricted engine is 46"Hg. The standard turbocharger unrestricted boost level has been increased to offset the loss when restriction is applied. It can be seen on the curve that restriction of the exhaust can reach 10.2"Hg before the turbocharger boost level falls to the normal value of 46"Hg.

The fuel consumption values shown are without the standard fan power absorption. If the engine requires a standard fan absorbing 12 HP, there is a net gain in fuel consumption up to a back pressure of 11.2"Hg. If the standard fan absorbs 16 HP, there is a net gain in fuel consumption until the back pressure reaches 13.0"Hg.

The optimized turbo-cooling system for the 8.0 liter engine imposes a 9.1"Hg back pressure on the engine at rated speed. Thus, if the 16 HP fan is replaced by an optimized turbo-cooling system, a net gain in fuel consumption of .010 #/BHP-HR is indicated.

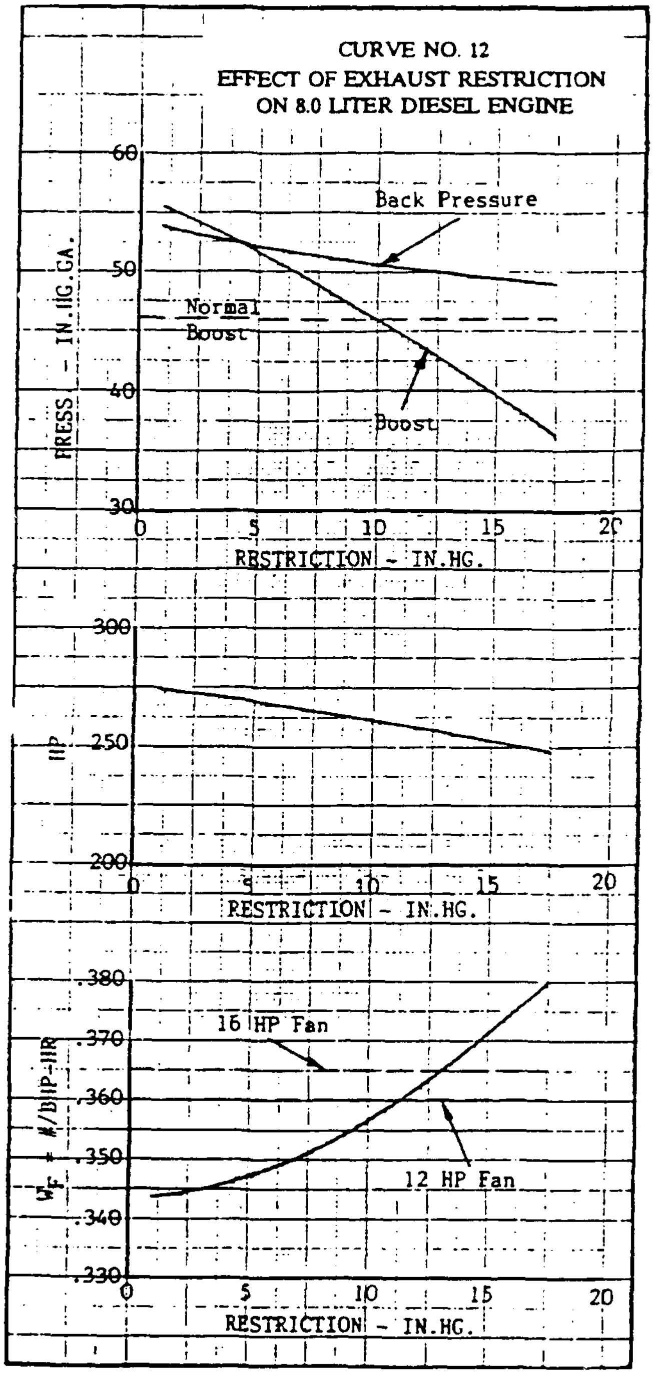

IX. CONCLUSIONS

The calculated results indicated that a sound thermodynamic basis exists for considering turbo-cooling systems for use in heavy-duty, diesel engine powered equipment.

In the small turbocharger field, radial turbines with undivided turbine casings have reached efficiencies of 80 percent at the low expansion ratios needed by turbo-cooling systems. Data published by NASA on the design and testing of low pressure fan stages indicates efficiencies of 85 percent have been achieved in laboratory tests.[8] The mechanical efficiencies of ball bearing systems used in small turbochargers are known to be over 98 percent. Since the overall efficiency of a turbo-fan comprises the product of the efficiencies of the fan, turbine and bearing systems, the achievable level of overall efficiency should exceed 60 percent. It is evident from the literature and from practical experience that most fans used in conventional fan-radiator cooling systems operate with efficiencies less than 50 percent. Thus, there is potential for thermal efficiency improvement in a power plant where a fan-radiator is replaced by an optimized turbo-cooling system.

Assuming that the concentric annular diffuser shown in Figure 5 performs in accordance with theory, then the compact cooling module shown in Figure 6 presents a convenient, versatile cooling system that can be applied to a variety of heavy-duty equipment by adapting the plenum walls to a variety of structural configurations.

Since the turbo-cooling system comprises several discrete components, each one can be designed and developed separately before being combined to form a total system. Organizations that design and manufacture small turbochargers have laboratory facilities ideally suited for this type of component development. A turbocharger development test stand can be used to evaluate prototype fan designs and can also be used to evaluate diffuser designs by mounting the diffuser on the fan outlet and instrumenting it to measure pressure recovery. The turbo-fan turbine is essentially identical to radial or mixed-flow turbines used in small turbochargers and previous extensive development work carried out on this component is directly applicable. Heat exchanger design technology is well known and does not require component development to reach high effectiveness with reasonably low flow resistance.

Thus, no new technology is required to successfully develop turbo-cooling systems. Reasonably high component efficiencies can be expected from the design process and optimal efficiencies can be expected from implementing component development programs using standard laboratory equipment and test techniques.

REFERENCES

1. Diesel, Eugen. Die Geschichte des Diesel Personenwagens. Published by Deutsche Verlags-Anstalt GmbH, Stuttgart, Germany, 1955.

2. Tennant, D.W.H. and Walsham, B.E. The Turbocompound Diesel Engine. SAE Paper No. 89047, February 1989.

3. An Update on Turbo-Compound and Adiabatic Engine Programs. Diesel Progress North American, July 1981.

4. Chiou, J.P. Engine Cooling System of Military Combat/Tactical Vehicles. SAE Paper No. 750030, February 1975.

5. SAE Recommended Practice. Engine Cooling Fan Structural Analysis. SAE J1390, April 1982.

6. Haggh, B. and Holmer, E. Air-to-Air Charge Air Cooling for Truck Engines. SAE Paper No. 790770, August 1982.

7. Sovran, Gino and Klemp, Edward D. Experimentally Determined Optimum Geometries for Rectilinear Diffusers with Rectangular, Conical or Annular Cross-Section. Symposium on the Fluid Mechanics of Internal Flow, Elsevier, Amsterdam, 1967.

8. Osborn, W.M. and Steinke, R.J. Performance of a 1.15 Pressure Ratio Axial Flow Fan Stage With a Blade Tip Solidity of 0.5. NASA TM Y-3052, August 1974.

ISSN 0148-7191

Printed in USA

90-1203C/PG

F-521

TACOM TURBOCHARGER DEVELOPMENT AND TEST PROGRAM

Jurgen Amtmann
BKM, Inc.
5141 Santa Fe Street
San Diego, CA 92109

November 8, 1990

Interim Report for First Quarter 1990
Contract Number DAAE07-87-C-R106

Distribution Unclassified/Unlimited

Prepared for:

U.S. Army TACOM
Warren, MI 48397-5000

File Report F-521
Subject: TACOM Turbocharger Development and Test Program
Date: 8 Nov. 1990

1.0 INTRODUCTION

As part of the original TACOM contract # DAAE07-87-C-R106 to develop a fuel system for the Cummins VTA-903 engine, a variable area turbocharger (VAT) was developed. In addition to the VAT system, the turbocharger incorporates a low friction bearing system for improved mechanical efficiency and a high flow turbine utilizing combination flow. Tooling was built for all major components, and small quantities of parts were cast and machined to build prototype units for test purposes. A test program was conducted consisting of dynamic stability, performance mapping and burst and containment tests. This report covers the development and test results of the basic turbocharger and preliminary results of the variable area system.

2. TECHNICAL DISCUSSION

The objectives of the program were to design an efficient and flexible turbocharger system using the latest developments in turbine, compressor and bearing design to optimize its use on Cummins NTC and VT-903 engines.

2.1 VARIABLE AREA DESIGN

By utilizing a combination axial and radial flow turbine in a twin volute housing, a simple and effective two stage variable area concept was developed. A sliding element in the turbine exducer and a diverter valve ahead of the turbine inlet serve to divert exhaust flow from all cylinders to a single volute, Figures 1 and 2, Appendix C. The increased flow velocity through the turbine thus can be utilized to increase the boost at low engine RPM. At higher engine speeds the slider and diverter valve return to their normal positions and engine exhaust flows to both volutes. During testing, the operation of the slider and diverter valve were separated to determine if a large enough portion of the gain can be attributed to the division of gases by the diverter valve alone to eliminate the complication of the sliding element.

2.2 TURBINE AND COMPRESSOR DESIGN

Turbine design is tailored to take advantage of the low exhaust temperatures encountered in todays high efficiency 4-stroke diesel engines by providing large expansion ratio per pound of exhaust. Turbine efficiency is enhanced by smoother gas flow from the volutes through the turbine wheel, and elimination of leakage flow around the back of the wheel as in purely radial flow turbines. The large exit area provided by the combination flow turbine makes for high flow capacity in small overall size and reduces leaving losses to a minimum.

Compressor design follows the latest technology of chevron, bent tip wheel with vaneless diffuser for minimal smoke on acceleration and the broad range required by todays high torque rise engines which must maintain power to 12000 ft. altitude.

2.3 BEARING SYSTEM DESIGN

To improve mechanical efficiency with minimal risk, a combination ball bearing and journal bearing system was designed. Fig. 3 Appendix C. The ball bearing is mounted in a rotating sleeve at the cooler, compressor end of the turbo with the conventional bronze sleeve bearing providing support at the turbine end. Similar ball bearing systems have undergone extensive laboratory and field tests and have been shown to operate satisfactorily in diesel truck environments. The rotating sleeve is supported by an outer oil film which largely dampens compressor imbalance loads and transfers predominantly thrust loads to the ball bearing. Catalog B10 bearing life using predicted loads and speeds exceed 2130 hours of operation running at constant speed and load, however, a more elaborate EHD film analysis based on oil film thickness to bearing surface roughness ratio predicts almost unlimited life of the ball bearing. The bearing system should be less sensitive to cold starts because a ball bearing can operate on marginal lubrication for longer periods of time than plain thrust bearings of current designs, while the low oil flow required by a ball bearing should eliminate oil leakage at the compressor.

2.4 MECHANICAL CONSTRUCTION

Several unique features distinguish this turbocharger design to facilitate manufacture and assembly.

a. The compressor end oil seal has been improved to eliminate the requirement for machining a groove into the shaft. One side of the groove is formed by the compressor wheel, the other by the slinger sleeve, eliminating the requirement to expand the piston ring over an edge.

b. To eliminate the shaft twisting forces associated with tightening the compressor end nut, the usual socket wrench projection on the turbine has been eliminated and tightening reactions are taken at two flats on the compressor end of the shaft. The shaft end of the turbine has a cavity cast into it calculated to limit burst speed to a containable value. Burst and containment tests results will determine the final configuration and size of this cavity.

c. Both turbine and compressor housings were designed for minimum weight and casting costs which allows low cost adapters to be used to mate the turbo to any engine manifold as required.

The elimination of external cores required to cast clamping flanges on the turbine housing reduces the pattern cost as well as the casting piece price. Adapters can be low cost spinnings or stampings which can be shrunk or clamped to the turbine and compressor housings.

3. PERFORMANCE TESTING

All testing of the turbocharger was done at Roto-Master, an aftermarket turbocharger manufacturer, using a fully instrumented standard gas stand for performance testing. Burst and containment tests were done in a cell specifically constructed for that purpose. The test program was conducted in stages designed to reveal any weakness in the design without putting the test units at risk of damage. Therefore, testing was performed in the following order:

3.1 DYNAMIC STABILITY

Dynamic stability testing of the bearing system was performed according to Caterpillar test procedure ET-48 "Turbocharger Shaft Motion Evaluation", the industry accepted test standard for this type of test. For the tests, the min. and max. size of bearing housing ID and bearing carrier OD were assembled in combinations to represent the four corners of the production size matrix. Rotating components were balanced to maximum production imbalance and assembled in phase to represent worst case balance of a production unit. Each of the four assembly combinations was then run from 40K to 90K RPM in 10K increments and shaft motion and deflection monitored with a spectrum analyzer and recorded. All tests were done at 200 degree F oil inlet temp. and 1200 degree F turbine temp. at 60 PSI and 30 PSI oil pressure. For the test a special extended shaft motion nut was used. Two proximity sensors were installed at 90 degrees to each other in the housing inlet to sense radial motion of the shaft at the compressor end. Signal analysis was via a Hewlett-Packard HP 3561A Dynamic Signal Analyzer and Krohn-Hite 3202 Active Filter plotted to show sensor output vs. frequency. Rotational speed was measured by a coil placed around the housing inlet sensing a magnetized impeller nut. Plots of shaft motion vs. turbine speed were reduced from the Signal Analyzer Data and are included in Appendix A. Total shaft motion as sensed by the instrumentation will be due to a variety of factors such as shaft and wheel eccentricities as well as out of balance conditions. Eccentricities will record as first order (synchronous) signals, while other influences will generate higher order signals. The sum of all signals will represent total shaft motion. Acceptable limits as per ET-48 are shown as dotted lines. Maximum allowable limits of total shaft motion are defined as 45% of maximum radial shaft play (conical) up to 50% rated speed. At speeds over 50% of rated, allowable total shaft motion is 30% of total radial shaft play. Maximum allowable synchronous shaft motion is 16% of maximum radial shaft play. As the plots show, total and synchronous shaft motion were below the allowable limits in all cases and at all speeds.

3.2 COMPRESSOR PERFORMANCE

Compressor maps were generated for 5 compressor trim points starting with the trim calculated for highest efficiency, and bracketing this to determine the best efficiency, width of map, position of surge line and possible areas of instability. Trim points were varied by changing the inducer diameter and the diffuser width of the compressor wheel with matching changes in the housing. Increasing the inducer diameter tilts the map at the top increasing max flow at choke, at the same time tilting the surge line towards higher flow. Changing the diffuser width tends to be an optimization exercise, a narrower diffuser tends to broaden the flow range and raise efficiency, up to a point. The compressor map for the design point trim (-4 configuration) shows that a large island of 76% efficiency exists around the design point. Analysis of the test data shows further that at the design point of pressure ratio = 2.0 and Q = 707 CFM, the efficiency is close to 77%. Compressor Performance Data Sheets (-4 config. only) and Performance Maps (all configs.) are included in Appendix B.

3.3 BURST AND CONTAINMENT TESTS

The principal reason for performing containment tests on a new turbocharger design is to assure that the turbine and compressor housings will contain any shrapnel in case of failure of the rotating components. By tailoring the size and shape of a cavity designed into the hub of the turbine wheel, the natural burst speed of the turbine can be limited to a factor of 2 times the energy at design speed (1.4 times design speed), assuring an adequate safety factor without excessive weight penalties of the housing for containment. The natural burst speed of the compressor wheel is normally higher than that of the turbine, however a failure such as a casting flaw could cause it to fail at a lower speed. To simulate this, a wheel is artificially flawed by drilling or sawing at the hub to cause it to fail approximately 20% over design speed. Two turbines were tested and burst at 161900 RPM and 151400 RPM, both speeds well above the required 140000 - 145000 RPM. Neither burst was contained. Design changes were made to bring the natural burst speed into the required range, and to reinforce the housing to contain at that speed. One compressor was modified and burst at 118100 RPM without containing. Design changes were subsequently made to reinforce the compressor housing in the area of damage. Although the required design changes have been made, no new parts have been manufactured incorporating those changes.

3.4 ENGINE AND VEHICLE TESTS

Engine testing on the Cummins VT-903 has not been done to date, but 3 installations (without VA hardware) have been made on road vehicles equipped with Cummins 855 engines. Of the three installations, one failed after being operated for 2100 miles on a NTA-400 with 420+HP operating short haul, due to inadequate turbine to housing clearance.

As a result, subsequent units were constructed with increased clearance on the turbine OD. The second unit failed after operating 8745 miles on a 400 HP Engine operating long haul of about 700 miles per day including long grades. The ball bearing had failed catastrophically, but it could not be determined if this was the primary cause of failure. The third unit was installed on a NTC-350 equipped tractor making deliveries operating 2 shifts, 7 days. This unit operated for approximately 37000 miles before being removed from service when the engine required an overhaul. Upon examination, the unit showed no discernible wear.

3.5 VARIABLE AREA TESTS

A performance map was generated for the WS-90 turbine operating on the radial inlet only and is compared with the characteristics of operation on both inlets in Figs. 4 and 5, Appendix C. Although peak turbine efficiency drops to 56% from 68%, the radial inlet (only) turbine develops an expansion ratio of 2.4 at a specific flow of almost 42 against a specific flow of 72 at 2.4 for the combination turbine. The variable area associated hardware has not been run on the TACOM VTA-903 engine, however, engine acceleration tests and boost pressure comparisons between radial and axial volutes and slider in and out have been made on a Cummins NTC-400 engine.

3.5.1 ENGINE ACCELERATION TESTS

Baseline acceleration runs were made with a stock Holset BHT-3B and with the WS-90, then exhaust was diverted in both units and acceleration again measured. In the WS-90, exhaust was diverted to both the axial as well as the radial volutes for comparison. The results of several runs were averaged for each condition and plotted in Fig. 6, Appendix C. Acceleration runs were made using the following procedure:

1. Dynamometer load set to 300 HP at 1800 RPM 2. Engine speed reduced to idle 3. Quick throttle opening 4. Measure time to accelerate to 1800 RPM under Load 5. Record boost at 1800 RPM Only the final boost at 1800 RPM was recorded because of instrumentation limitations, however, the results show the trend of increasing engine acceleration with exhaust diversion. For the WS-90, two conditions were investigated, exhaust diverted to the radial volute without closing the axial volute, and exhaust diverted to the axial volute with the sliding tailpipe closing the radial passage. Although engine acceleration is greater with flow in the axial volute, final boost is lower, which may be due to the boost history during acceleration. A performance map was also generated for a WS-90 turbine operating on the radial inlet alone driving a Holset compressor. Fig. 5, Appendix C.

3.5.2 BOOST PRESSURE TESTS

A series of dynamometer runs were made with the same NTC engine at 1100, 1300 and 1500 RPM at power settings up to 350 HP to measure differential pressure at different diverter settings and slider positions. Figs. 7, 8 and 9 in Appendix C show exhaust back pressure and boost pressure for the engine with exhaust diverted to the axial volute for tail pipe in and out, as well as diverted to the radial volute. Boost differential is highest in all cases for diversion to the axial volute with tailpipe in. Although boost pressures were higher with the flow diverted to the radial volute, boost differential was less indicating the lower turbine efficiency while operating in this mode. Fig. 10, Appendix C shows a comparison between the Holset BHT-3B and the WS-90 with VA operating on a 365 HP NTC engine indicating the additional boost available for acceleration below 1500 RPM.

APPENDIX A

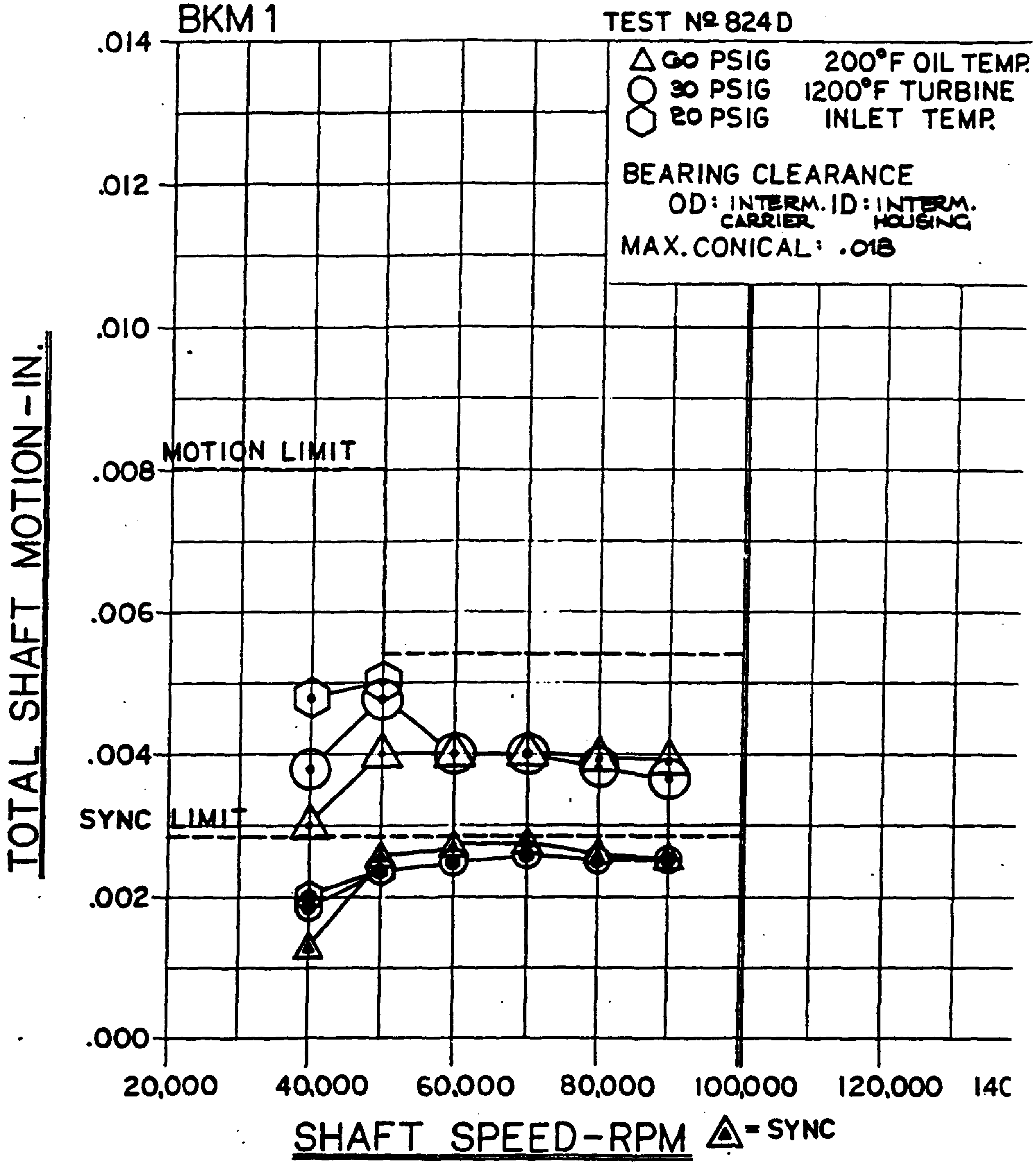

ROTO — MASTER INC.

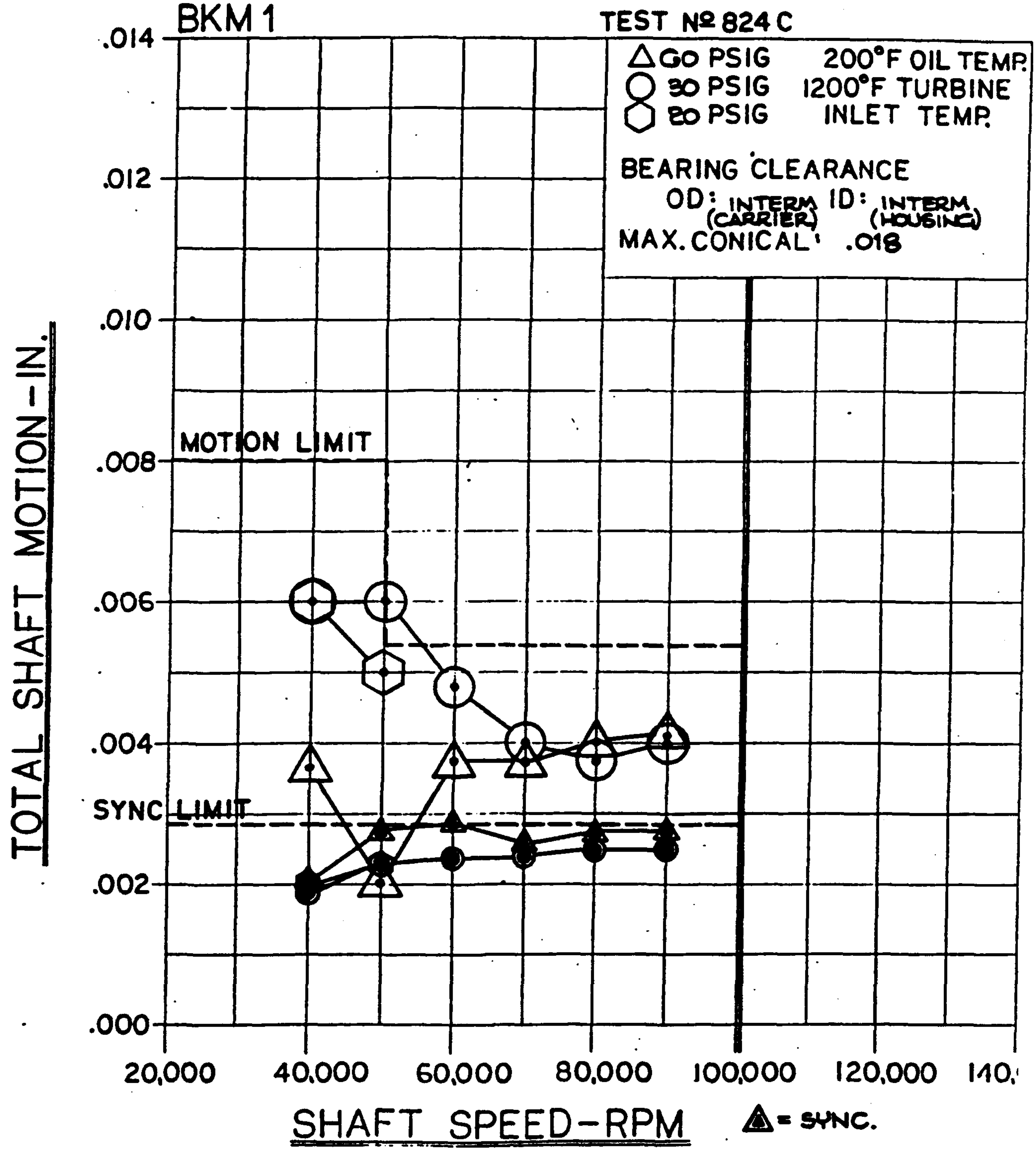

ROTO — MASTER INC.

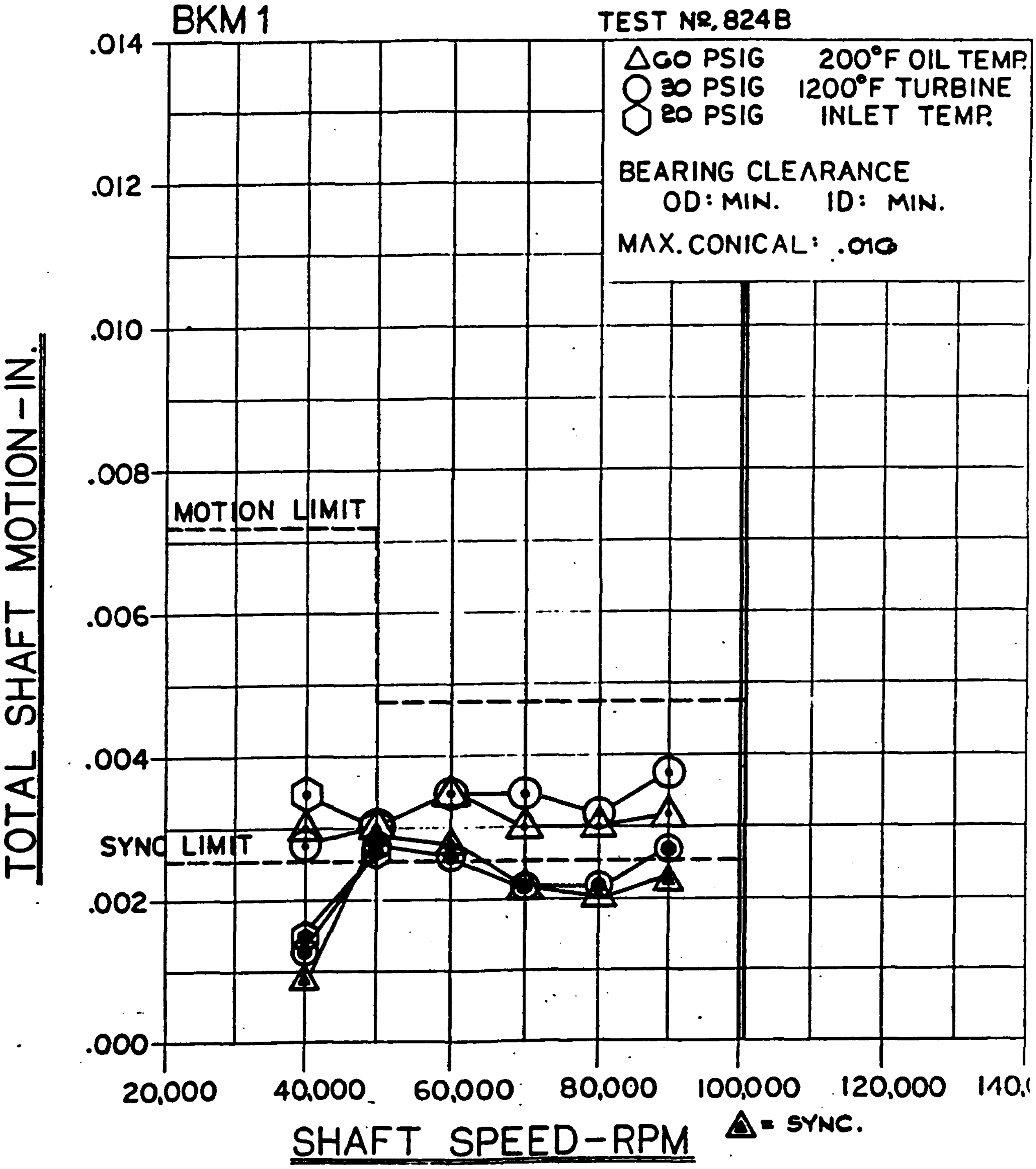

ROTO — MASTER INC.

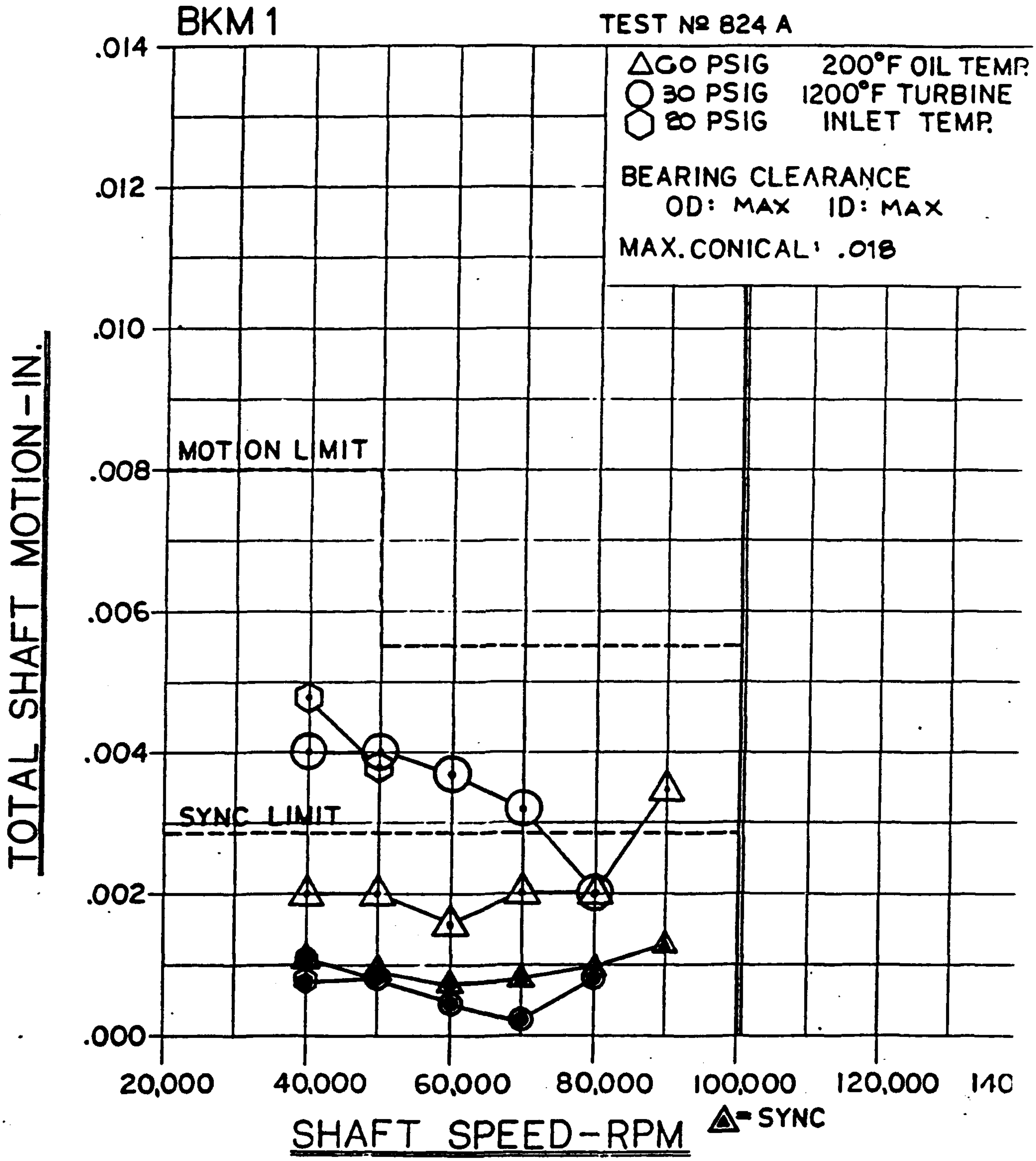

ROTO — MASTER INC.

APPENDIX B

ROTO-MASTER ENGINEERING

EST No. 823 40 K RPM

COMPRESSOR PERFORMANCE TEST DATA SHEET TEST DATE 10-20-88

IMP. P/N BKM (-4) BAROMETER 29.19 PROJECT #BKM
HSG P/N BKM (-4) TRIM BKM TEST NO. 823
OUT DUCT DIA 2.923 IN DUCT DIA 4.502 OPERATOR HDA
OUT DUCT AREA .046 IN DCT AREA .11 ORIFICE DIA. 2.75

CFM and Lb/min CORRECTED TO SAE STANDARD 28.4 IN HgA & 545 DEG. R COMP. INLET COND.

FIRST RUN ON BKM PROTOTYPE

DATA							CALCULATIONS			
P ORIF	DEL P	P1C	P2C	T ORIF	T1C	T2C	CFM	P RATIO	EFF	Lb/min
3.3	20.00	2.5	3.8	110	74	114	530	1.15	.527	36.62
5.0	15.35	2.0	5.3	112	74	117	475	1.20	.645	32.85
6.4	11.17	1.6	6.6	114	74	121	413	1.24	.714	28.52
7.5	7.62	1.1	7.6	115	74	124	345	1.27	.741	23.87
8.1	4.93	.7	8.2	118	75	128	280	1.29	.735	19.33
8.4	2.88	.4	8.4	119	75	134	214	1.29	.683	14.80
8.3	1.30	.2	8.4	122	75	142	144	1.29	.595	9.92

ROTO-MASTER ENGINEERING

TEST No. 823 50 K RPM

COMPRESSOR PERFORMANCE TEST DATA SHEET TEST DATE 10-21-88

IMP P/N BKM 1	BAROMETER 29.29	PROJECT #7067
HSG P/N BKM 1	TRIM BKM 1	TEST NO. 823
OUT DUCT DIA 2.923	IN DUCT DIA 4.502	OPERATOR D.A.
OUT DUCT AREA .046	IN DCT AREA .11	ORIFICE DIA. 2.75

CFM and Lb/min CORRECTED TO SAE STANDARD 28.4 IN HgA & 545 DEG. R COMP. INLET COND.

PERFORMANCE TEST BKM 1

DATA							CALCULATIONS			
P ORIF	DEL P	P1C	P2C	T ORIF	T1C	T2C	CFM	P RATIO	EFF	Lb/min
6.1	30.70	4.0	6.7	122	71	134	676	1.26	.573	46.68
8.5	23.70	3.3	8.9	130	71	139	609	1.33	.660	42.06
10.4	18.07	2.7	10.8	132	71	143	544	1.39	.724	37.56
12.2	12.82	2.0	12.4	136	72	148	467	1.44	.757	32.23
13.3	8.55	1.4	13.4	138	72	153	385	1.47	.756	26.58
13.6	5.20	.8	13.7	141	72	160	300	1.47	.704	20.75
13.6	2.90	.5	13.7	143	72	168	224	1.47	.642	15.48

ROTO-MASTER ENGINEERING

EST No. 823 60 K RPM

COMPRESSOR PERFORMANCE TEST DATA SHEET TEST DATE 10-20-88

IMP P/N BKM BAROMETER 29.15 PROJECT #BKM
HSG P/N BKM TRIM BKM TEST NO. 823
OUT DUCT DIA 2.923 IN DUCT DIA 4.502 OPERATOR HDA
OUT DUCT AREA .046 IN DCT AREA .11 ORIFICE DIA. 2.75

CFM and Lb/min CORRECTED TO SAE STANDARD 28.4 IN HgA & 545 DEG. R COMP. INLET COND.

FIRST RUN ON BKM PROTOTYPE

DATA							CALCULATIONS			
P ORIF	DEL P	P1C	P2C	T ORIF	T1C	T2C	CFM	P RATIO	EFF	Lb/min
11.1	41.80	5.8	11.8	162	76	174	823	1.45	.609	56.84
15.1	31.35	4.8	15.6	168	76	180	742	1.57	.705	51.30
18.6	22.90	3.8	19.0	175	77	190	655	1.68	.751	45.27
20.6	15.80	2.7	20.9	178	77	195	553	1.74	.769	38.23
21.7	10.40	1.9	21.8	182	77	203	452	1.76	.743	31.25
21.4	6.55	1.2	21.6	186	77	212	357	1.75	.683	24.64

ROTO-MASTER ENGINEERING

TEST No. 823 70 K RPM

COMPRESSOR PERFORMANCE TEST DATA SHEET TEST DATE 10-21-88

IMP P/N BKM 1 BAROMETER 29.29 PROJECT #7067
HSG P/N BKM 1 TRIM BKM 1 TEST NO. 823
OUT DUCT DIA 2.923 IN DUCT DIA 4.502 OPERATOR D.A.
OUT DUCT AREA .046 IN DCT AREA .11 ORIFICE DIA. 2.75

CFM and Lb/min CORRECTED TO SAE STANDARD 28.4 IN HgA & 545 DEG. R COMP. INLET COND.

PERFORMANCE TEST BKM 1

DATA							CALCULATIONS			
P ORIF	DEL P	P1C	P2C	T ORIF	T1C	T2C	CFM	P RATIO	EFF	Lb/min
13.6	59.40	8.1	14.6	188	72	201	985	1.57	.559	68.09
17.8	48.70	7.5	18.6	192	72	205	931	1.69	.642	64.31
21.3	39.30	6.6	22.3	196	72	210	866	1.81	.704	59.84
24.8	30.62	5.5	25.4	200	72	216	785	1.91	.741	54.27
27.8	22.95	4.3	28.3	204	72	223	696	2.00	.765	48.06
28.9	16.35	3.2	29.3	207	72	229	591	2.02	.746	40.82
29.4	11.35	2.2	29.6	211	72	238	492	2.03	.710	34.01

ROTO-MASTER ENGINEERING

TEST No. 823 80 K RPM

COMPRESSOR PERFORMANCE TEST DATA SHEET TEST DATE 10-20-88

IMP P/N BKM 1	BAROMETER 29.13	PROJECT #7067
HSG P/N BKM 1	TRIM BKM 1	TEST NO. 823
OUT DUCT DIA 2.923	IN DUCT DIA 4.502	OPERATOR D.A.
OUT DUCT AREA .046	IN DCT AREA .11	ORIFICE DIA. 2.75

CFM and Lb/min CORRECTED TO SAE STANDARD 28.4 IN HgA & 545 DEG. R COMP. INLET COND.

BKM 1 PERFORMANCE.

DATA							CALCULATIONS			
P ORIF	DEL P	P1C	P2C	T ORIF	T1C	T2C	CFM	P RATIO	EFF	Lb/min
21.3	66.30	10.3	22.3	238	77	255	1101	1.85	.573	76.07
26.5	55.70	9.6	27.4	244	77	258	1056	2.01	.649	72.93
31.3	46.20	8.7	32.2	246	77	262	999	2.17	.709	69.06
34.9	37.40	7.5	35.7	249	77	268	923	2.28	.738	63.75
38.1	29.80	6.3	38.8	254	77	275	840	2.38	.755	58.06
40.5	23.00	5.0	41.0	258	77	283	748	2.44	.751	51.68
40.4	17.40	3.7	41.0	263	78	291	647	2.43	.723	44.73

:OTO-MASTER ENGINEERING

TEST No. 823 90 K RPM

COMPRESSOR PERFORMANCE TEST DATA SHEET TEST DATE 1-5-89

IMP P/N BKM 1	BAROMETER 29.45	PROJECT #7067
HSG P/N BKM 1	TRIM BKM 1	TEST NO. 823
OUT DUCT DIA 2.923	IN DUCT DIA 4.502	OPERATOR D.A.
OUT DUCT AREA .046	IN DCT AREA .11	ORIFICE DIA. 2.75

CFM and Lb/min CORRECTED TO SAE STANDARD 28.4 IN HgA & 545 DEG. R COMP. INLET COND.

PERFORMANCE TEST BKM 1

DATA							CALCULATIONS			
P ORIF	DEL P	P1C	P2C	T ORIF	T1C	T2C	CFM	P RATIO	EFF	Lb/m
28.1	70.80	11.7	29.2	262	70	300	1176	2.08	.530	81
35.4	61.00	11.5	36.5	278	69	304	1145	2.32	.608	79
42.2	51.70	10.7	43.3	283	69	306	1104	2.55	.675	76
47.3	43.10	9.6	48.2	286	69	311	1040	2.71	.710	71
51.7	35.53	8.4	52.4	292	69	318	966	2.84	.729	66
54.6	28.50	6.9	55.2	297	71	327	877	2.92	.733	60
55.5	23.80	5.8	56.1	302	72	335	803	2.95	.724	55

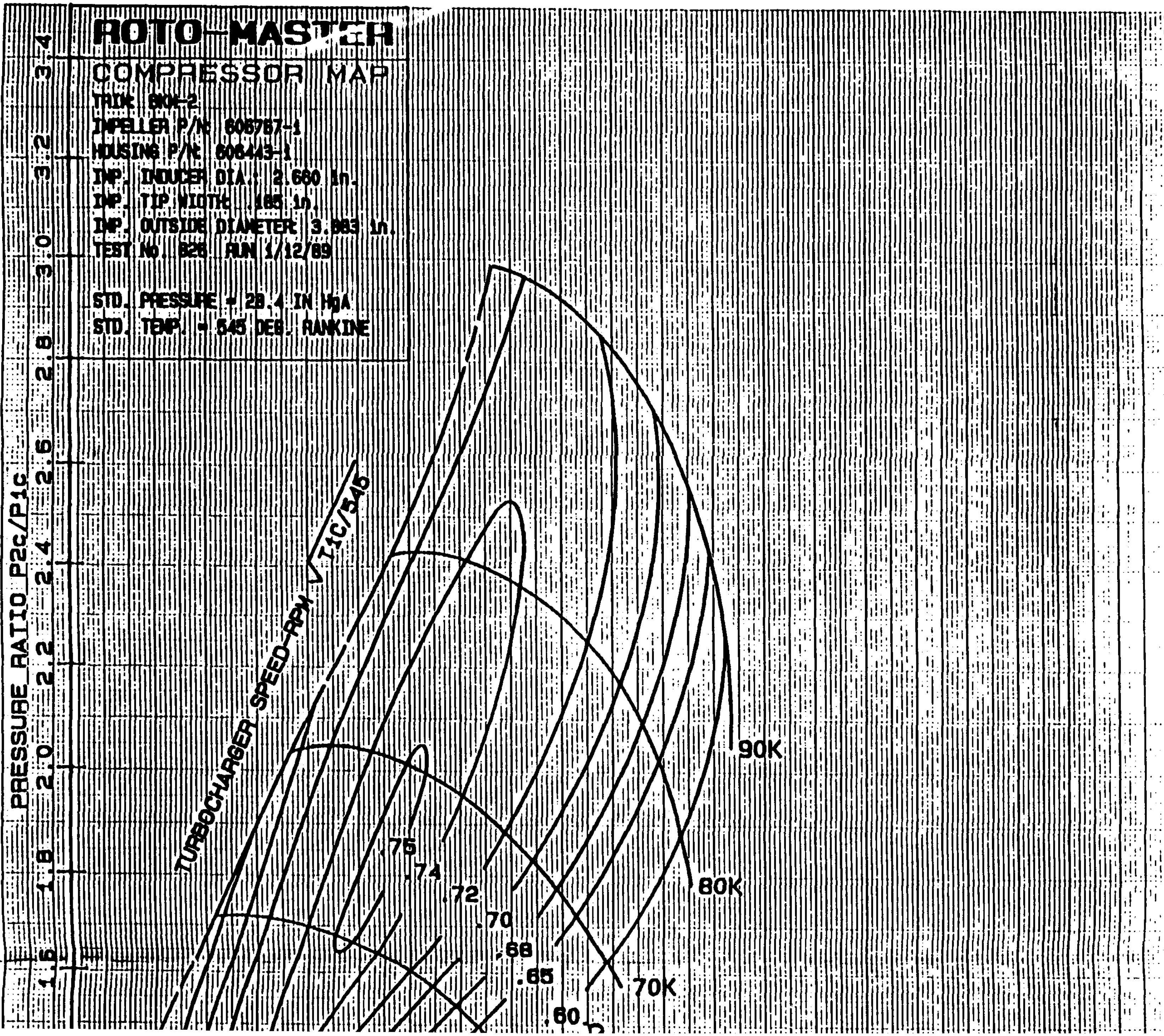
ROTO-MASTER
COMPRESSOR MAP
TRIM: 9KK-2
IMPELLER P/N: 606767-1
HOUSING P/N: 606443-1
IMP. INDUCER DIA.: 2.660 in.
IMP. TIP WIDTH: .185 in.
IMP. OUTSIDE DIAMETER: 3.883 in.
TEST NO. 826 RUN 1/12/89
STD. PRESSURE = 28.4 IN HgA
STD. TEMP. = 545 DEG. RANKINE
PRESSURE RATIO P2c/P1c
3.4
3.2
3.0
2.8
2.6
2.4
2.2
2.0
1.8
1.6
TURBOCHARGER SPEED-RPM √T1C/545
90K
80K
70K
.75
.74
.72
.70
.68
.65
.60

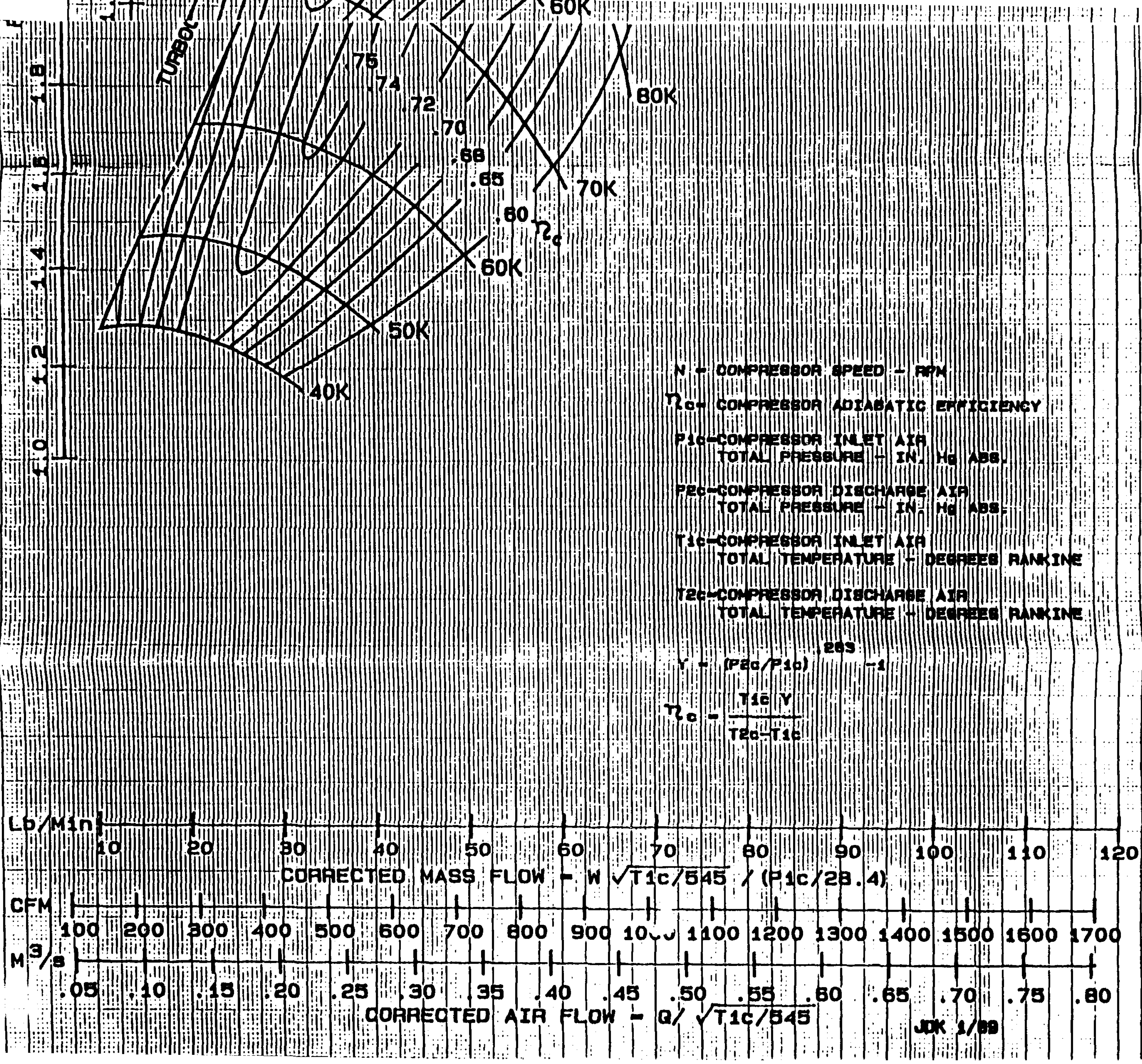

TURBOC
1.8
1.6
1.4
1.2
1.0
.75
.74
.72
.70
.68
.65
.60
η_c
80K
70K
60K
50K
40K
N - COMPRESSOR SPEED - RPM
η_c - COMPRESSOR ADIABATIC EFFICIENCY
P1c-COMPRESSOR INLET AIR TOTAL PRESSURE - IN. Hg ABS.
P2c-COMPRESSOR DISCHARGE AIR TOTAL PRESSURE - IN. Hg ABS.
T1c-COMPRESSOR INLET AIR TOTAL TEMPERATURE - DEGREES RANKINE
T2c-COMPRESSOR DISCHARGE AIR TOTAL TEMPERATURE - DEGREES RANKINE
$Y = (P2c/P1c)^{.283} - 1$
$\eta_c = \frac{T1c\ Y}{T2c - T1c}$
Lb/Min
10 20 30 40 50 60 70 80 90 100 110 120
CORRECTED MASS FLOW - $W \sqrt{T1c/545}$ / (P1c/28.4)
CFM
100 200 300 400 500 600 700 800 900 1100 1200 1300 1400 1500 1600 1700
M^3/s
.05 .10 .15 .20 .25 .30 .35 .40 .45 .50 .55 .60 .65 .70 .75 .80
CORRECTED AIR FLOW - $Q/\sqrt{T1c/545}$
JDK 1/89

(2)

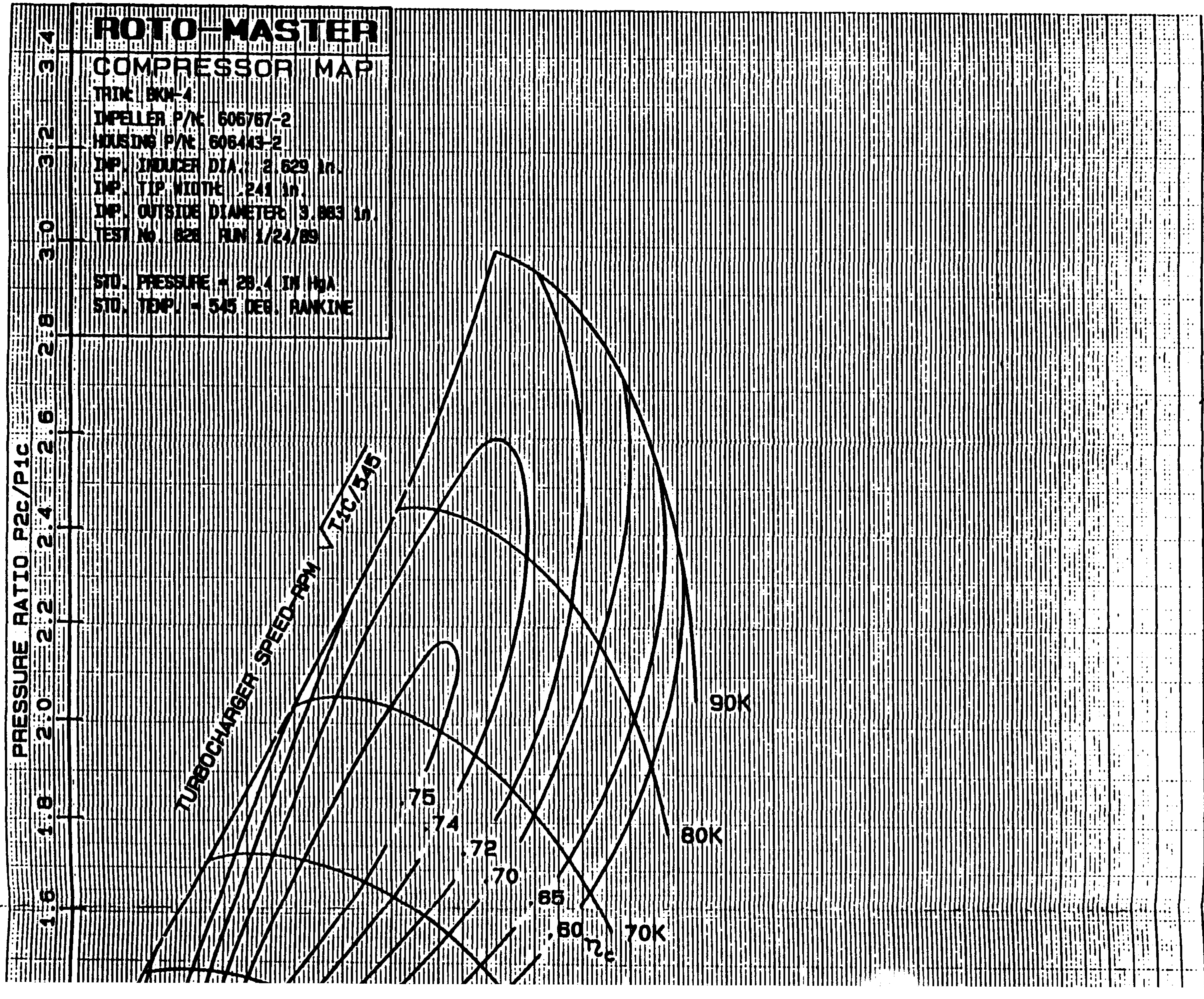
ROTO-MASTER
COMPRESSOR MAP
TRIM: BKM-4
IMPELLER P/N: 606767-2
HOUSING P/N: 606443-2
IMP. INDUCER DIA.: 2.629 in.
IMP. TIP WIDTH: .241 in.
IMP. OUTSIDE DIAMETER: 3.863 in.
TEST No. 828 RUN 1/24/89
STD. PRESSURE = 28.4 IN HgA
STD. TEMP. = 545 DEG. RANKINE
PRESSURE RATIO P2c/P1c
3.4
3.2
3.0
2.8
2.6
2.4
2.2
2.0
1.8
1.6
TURBOCHARGER SPEED-RPM √T1C/545
90K
80K
70K
.75
.74
.72
.70
.65
.60
ηc

(1)

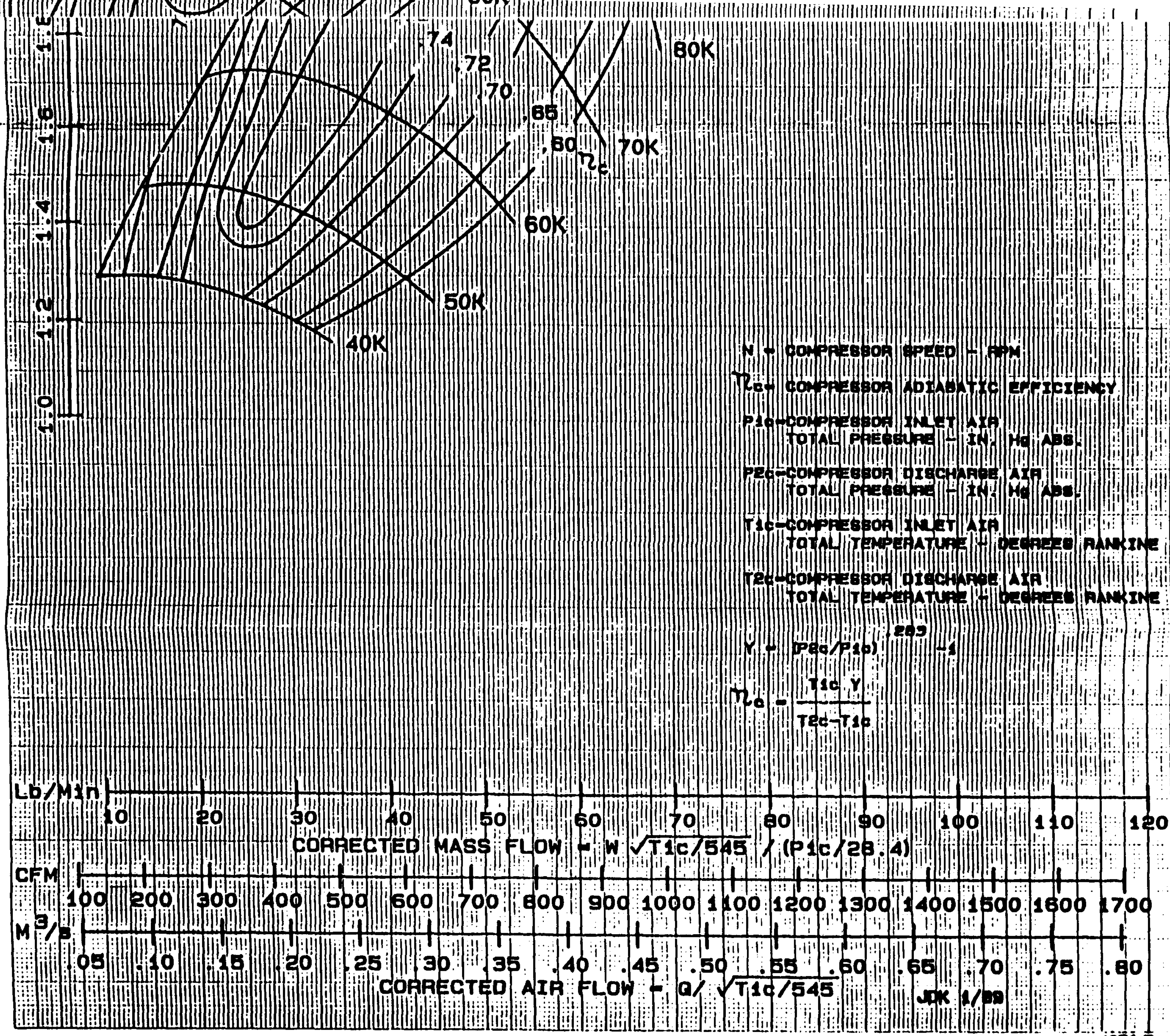

1.0
1.2
1.4
1.6
1.8
.74
.72
.70
.65
.60
η_c
40K
50K
60K
70K
80K
N = COMPRESSOR SPEED - RPM
η_c = COMPRESSOR ADIABATIC EFFICIENCY
P1c=COMPRESSOR INLET AIR TOTAL PRESSURE - IN. Hg ABS.
P2c=COMPRESSOR DISCHARGE AIR TOTAL PRESSURE - IN. Hg ABS.
T1c=COMPRESSOR INLET AIR TOTAL TEMPERATURE - DEGREES RANKINE
T2c=COMPRESSOR DISCHARGE AIR TOTAL TEMPERATURE - DEGREES RANKINE
$Y = (P2c/P1c)^{.283} - 1$
$\eta_c = \frac{T1c\ Y}{T2c - T1c}$
Lb/Min
10 20 30 40 50 60 70 80 90 100 110 120
CORRECTED MASS FLOW = W $\sqrt{T1c/545}$ / (P1c/28.4)
CFM
100 200 300 400 500 600 700 800 900 1000 1100 1200 1300 1400 1500 1600 1700
M^3/s
.05 .10 .15 .20 .25 .30 .35 .40 .45 .50 .55 .60 .65 .70 .75 .80
CORRECTED AIR FLOW = Q/ $\sqrt{T1c/545}$
JDK 1/89
1321 C

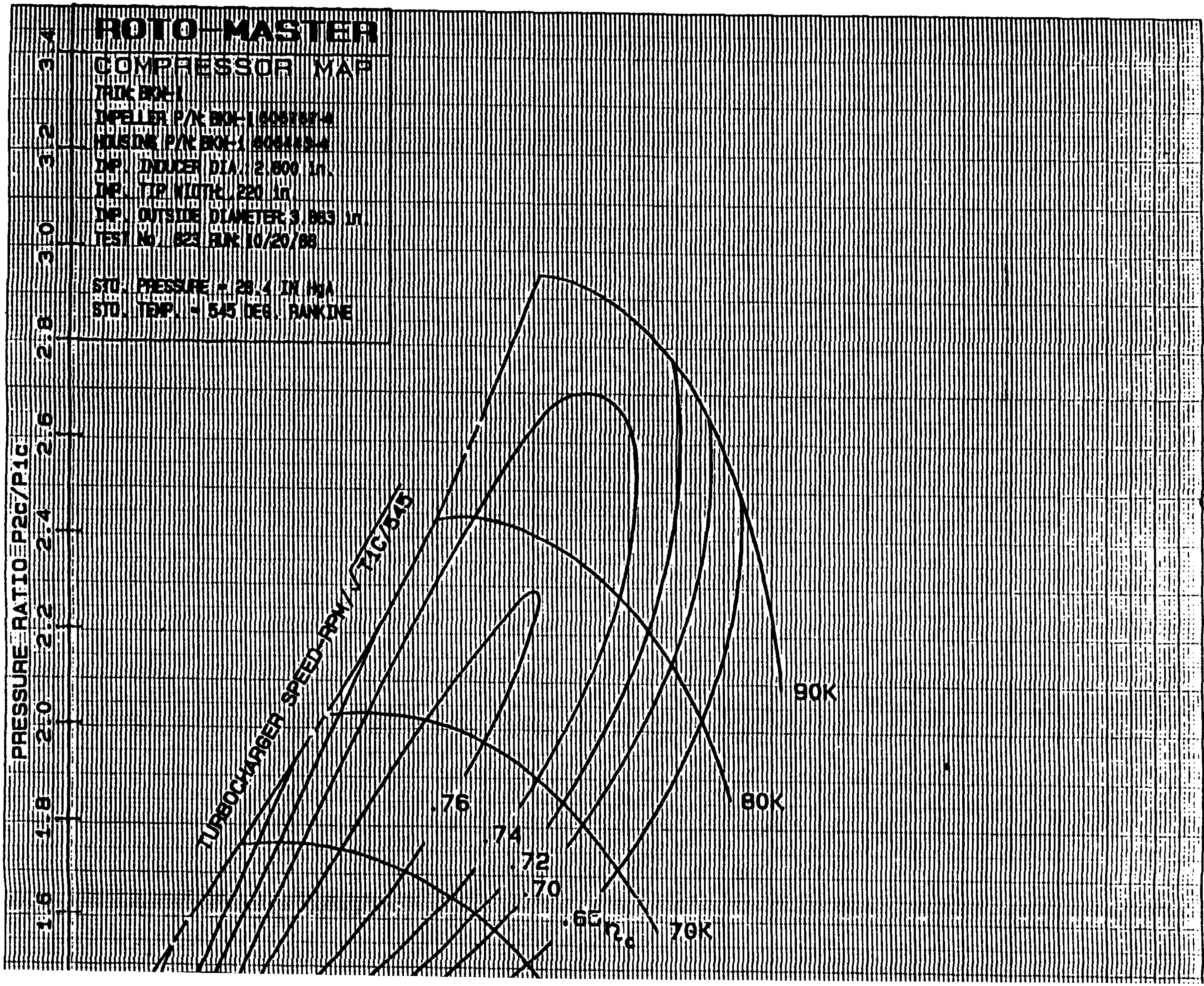
ROTO-MASTER
COMPRESSOR MAP
IMP. INDUCER DIA. 2.800 in.
IMP. OUTSIDE DIAMETER 3.863 in.
STD. PRESSURE = 28.4 IN HgA
STD. TEMP. = 545 DEG. RANKINE
PRESSURE RATIO P2C/P1C
3.4
3.2
3.0
2.8
2.6
2.4
2.2
2.0
1.8
1.6
TURBOCHARGER SPEED-RPM/√T1C/545
.76
.74
.72
.70
.66
η_c
90K
80K
70K

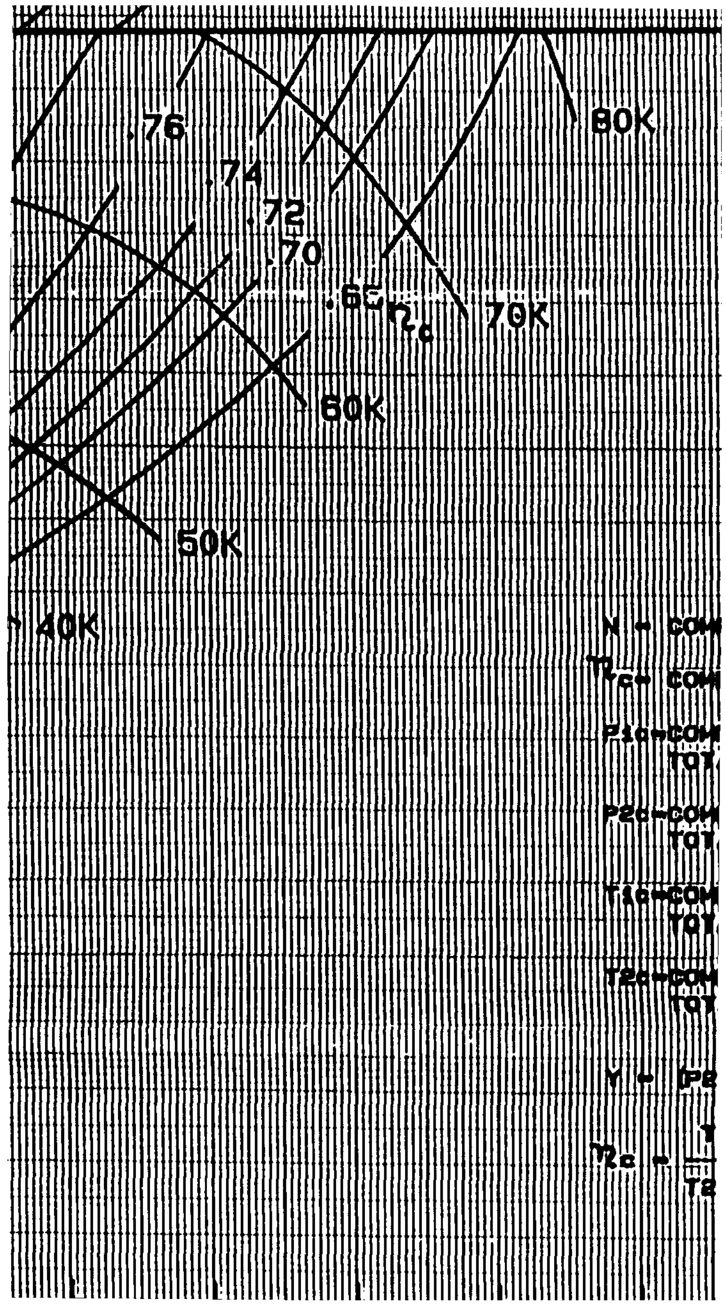

80K
70K
60K
50K
40K
.76
.74
.72
.70
.68
η_c
N = COM
η_c = COM
P1c=COM
TOT
P2c=COM
TOT
T1c=COM
TOT
T2c=COM
TOT
Y = [P2
η_c = T / T2

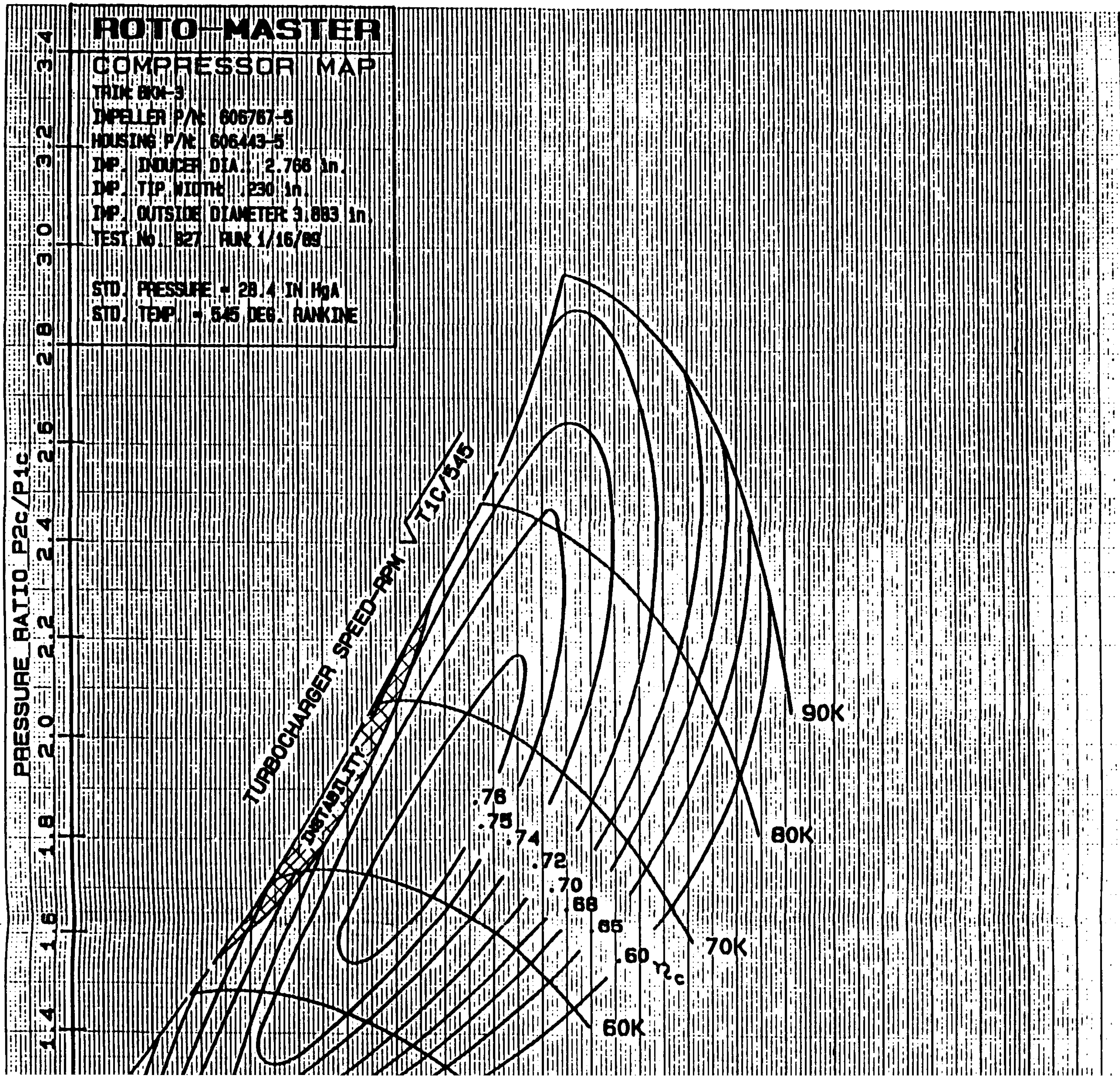
ROTO-MASTER
COMPRESSOR MAP
TRIM: BKM-3
IMPELLER P/N: 606767-5
HOUSING P/N: 606443-5
IMP. INDUCER DIA.: 2.766 in.
IMP. TIP WIDTH: .230 in.
IMP. OUTSIDE DIAMETER: 3.883 in.
TEST No. 827 RUN: 1/16/89
STD. PRESSURE = 28.4 IN HgA
STD. TEMP. = 545 DEG. RANKINE
PRESSURE RATIO P2c/P1c
1.4
1.6
1.8
2.0
2.2
2.4
2.6
2.8
3.0
3.2
3.4
TURBOCHARGER SPEED-RPM $\sqrt{T1C/545}$
INSTABILITY
90K
80K
70K
60K
.76
.75
.74
.72
.70
.68
.65
.60
η_c

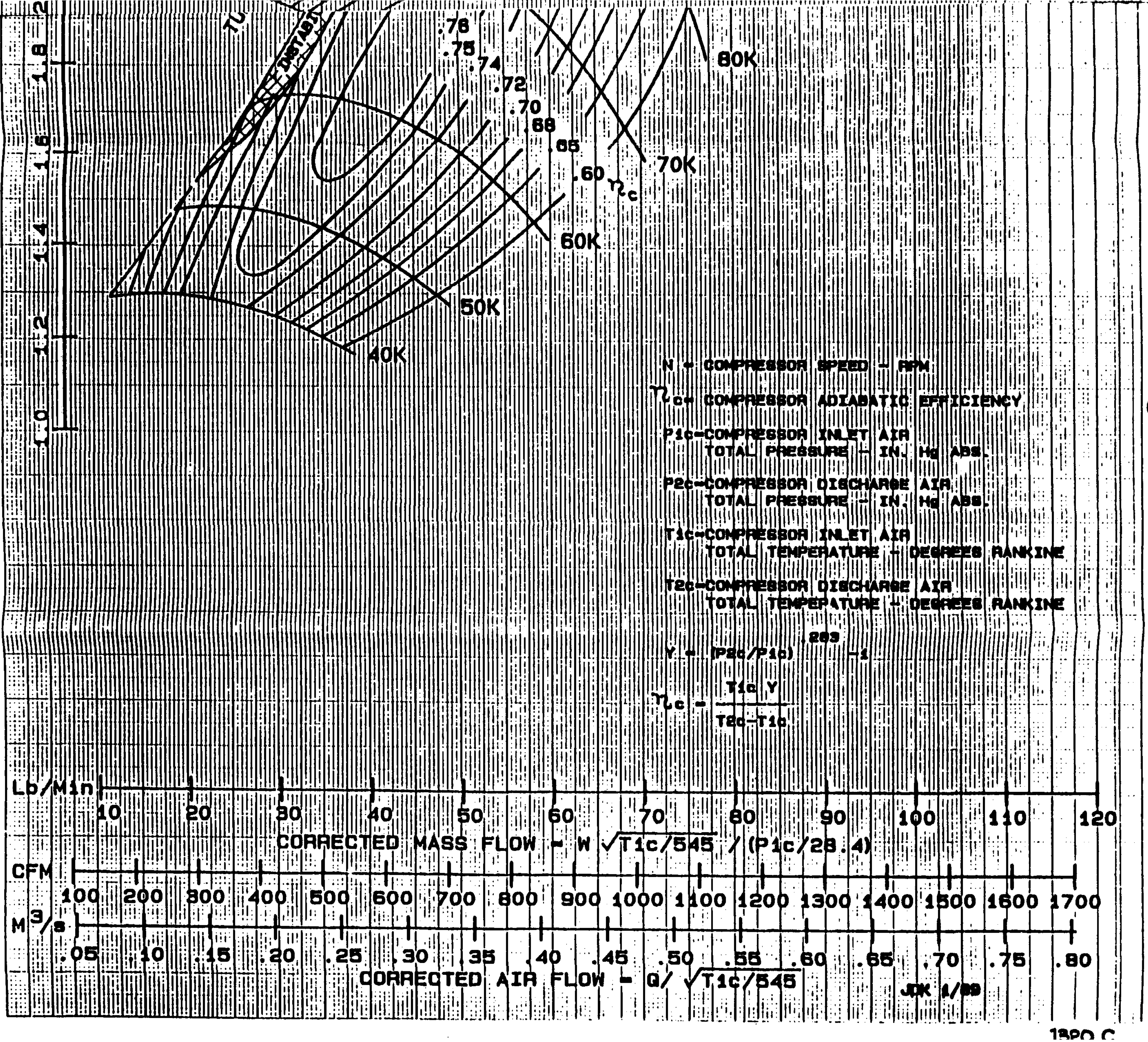

1.0
1.2
1.4
1.6
1.8
2
.76
.75
.74
.72
.70
.68
.65
.60 η_c
40K
50K
60K
70K
80K
N = COMPRESSOR SPEED - RPM
η_c = COMPRESSOR ADIABATIC EFFICIENCY
P1c=COMPRESSOR INLET AIR TOTAL PRESSURE - IN. Hg ABS.
P2c=COMPRESSOR DISCHARGE AIR TOTAL PRESSURE - IN. Hg ABS.
T1c=COMPRESSOR INLET AIR TOTAL TEMPERATURE - DEGREES RANKINE
T2c=COMPRESSOR DISCHARGE AIR TOTAL TEMPERATURE - DEGREES RANKINE
$Y = (P2c/P1c)^{.283} - 1$
$\eta_c = \frac{T1c\ Y}{T2c - T1c}$
Lb/Min
10 20 30 40 50 60 70 80 90 100 110 120
CORRECTED MASS FLOW - $W \sqrt{T1c/545}$ / (P1c/28.4)
CFM
100 200 300 400 500 600 700 800 900 1000 1100 1200 1300 1400 1500 1600 1700
M^3/s
.05 .10 .15 .20 .25 .30 .35 .40 .45 .50 .55 .60 .65 .70 .75 .80
CORRECTED AIR FLOW - $Q/\sqrt{T1c/545}$
JDK 1/89

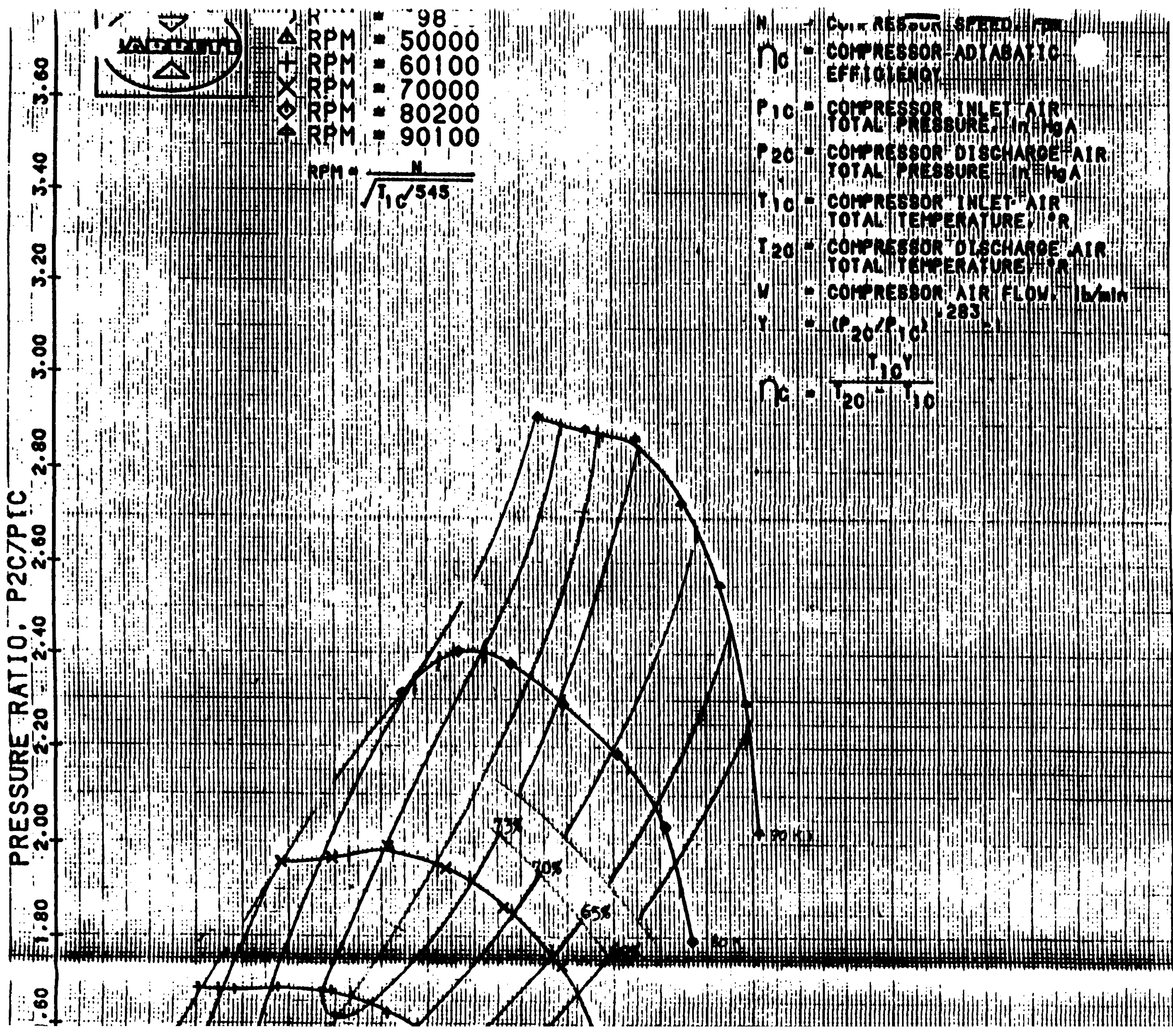
R = 98
RPM = 50000
RPM = 60100
RPM = 70000
RPM = 80200
RPM = 90100
RPM = N / √(T1C/545)
N = COMPRESSOR SPEED, RPM
ηC = COMPRESSOR ADIABATIC EFFICIENCY
P1C = COMPRESSOR INLET AIR TOTAL PRESSURE, in HgA
P2C = COMPRESSOR DISCHARGE AIR TOTAL PRESSURE, in HgA
T1C = COMPRESSOR INLET AIR TOTAL TEMPERATURE, °R
T2C = COMPRESSOR DISCHARGE AIR TOTAL TEMPERATURE, °R
W = COMPRESSOR AIR FLOW, lb/min
Y = (P2C/P1C)^.283 - 1
ηC = T1C Y / (T2C - T1C)
PRESSURE RATIO, P2C/P1C
3.60
3.40
3.20
3.00
2.80
2.60
2.40
2.20
2.00
1.80
1.60
75%
70%
65%

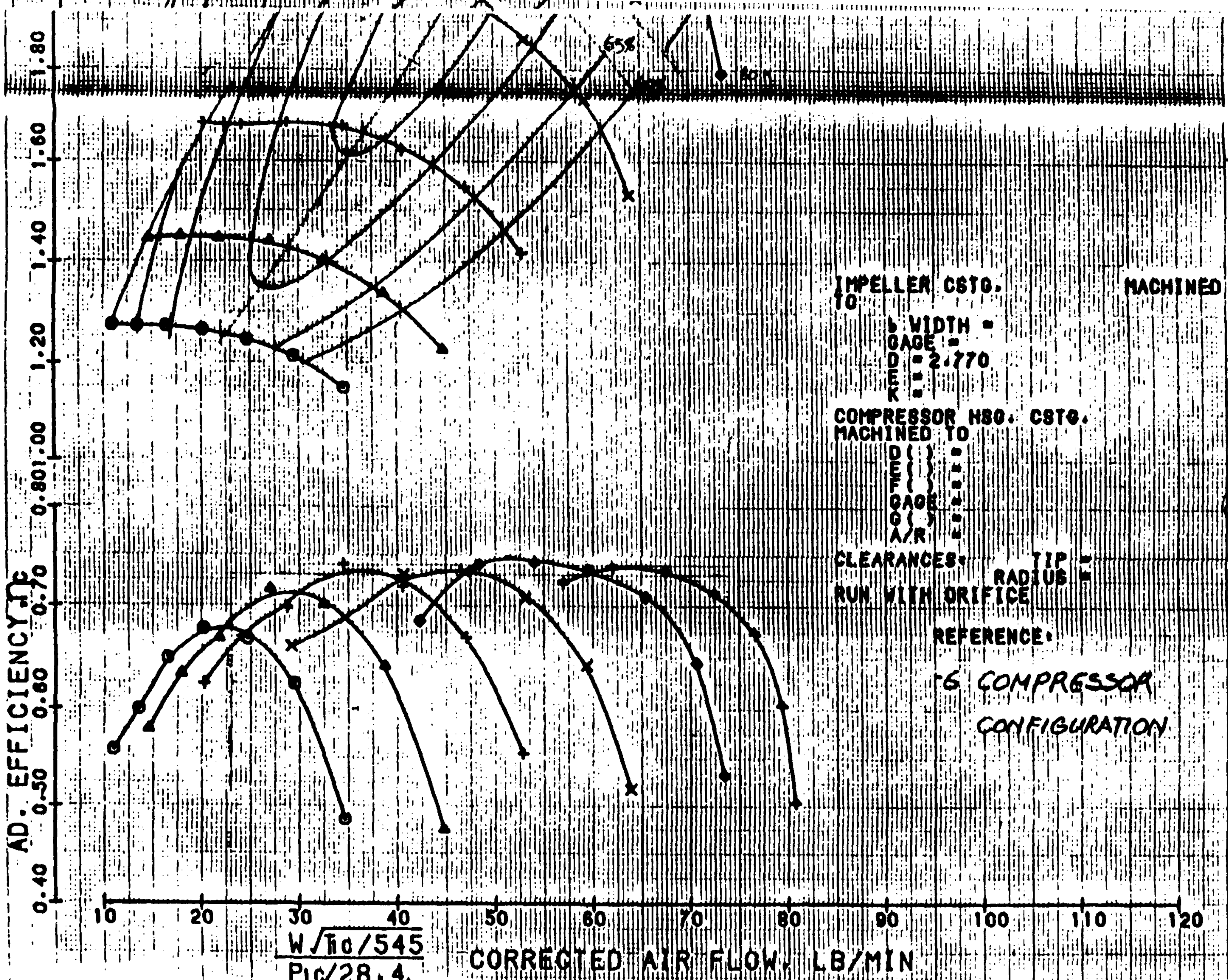

CALCULATED BY	IBM		BKM -2 TURBO
TRACED BY	LJM	6-23-69	
CHECKED BY		2-17-69	COMPRESSOR PERFORMANCE
APPROVED BY			AIRESEARCH INDUSTRIAL DIVISION

1E528

APPENDIX C

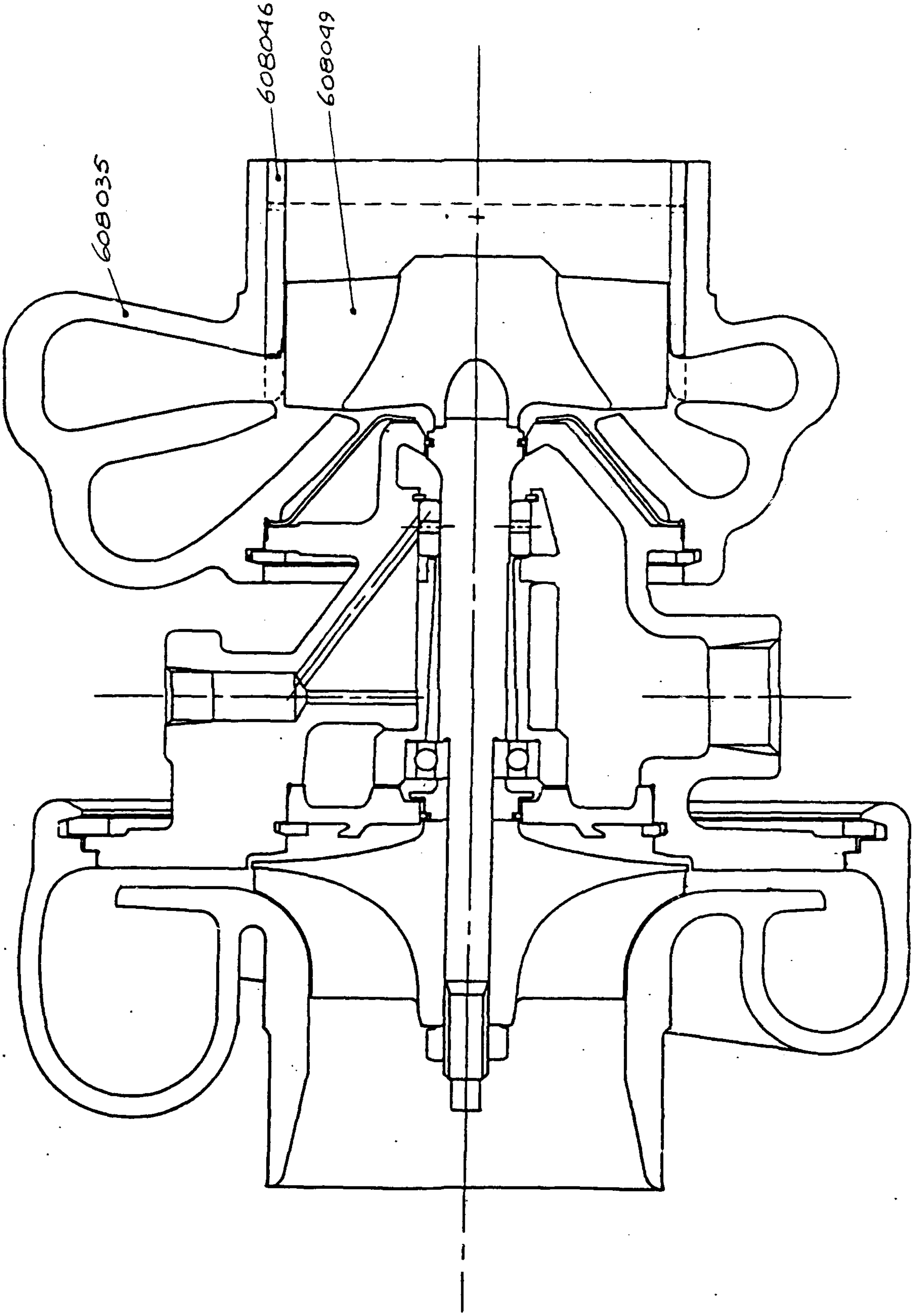

TACOM. MAN. ADJUST
VA TURBOCHARGER
SCALE: NONE

FIG. 1

SERVOJET WS TURBOCHARGER

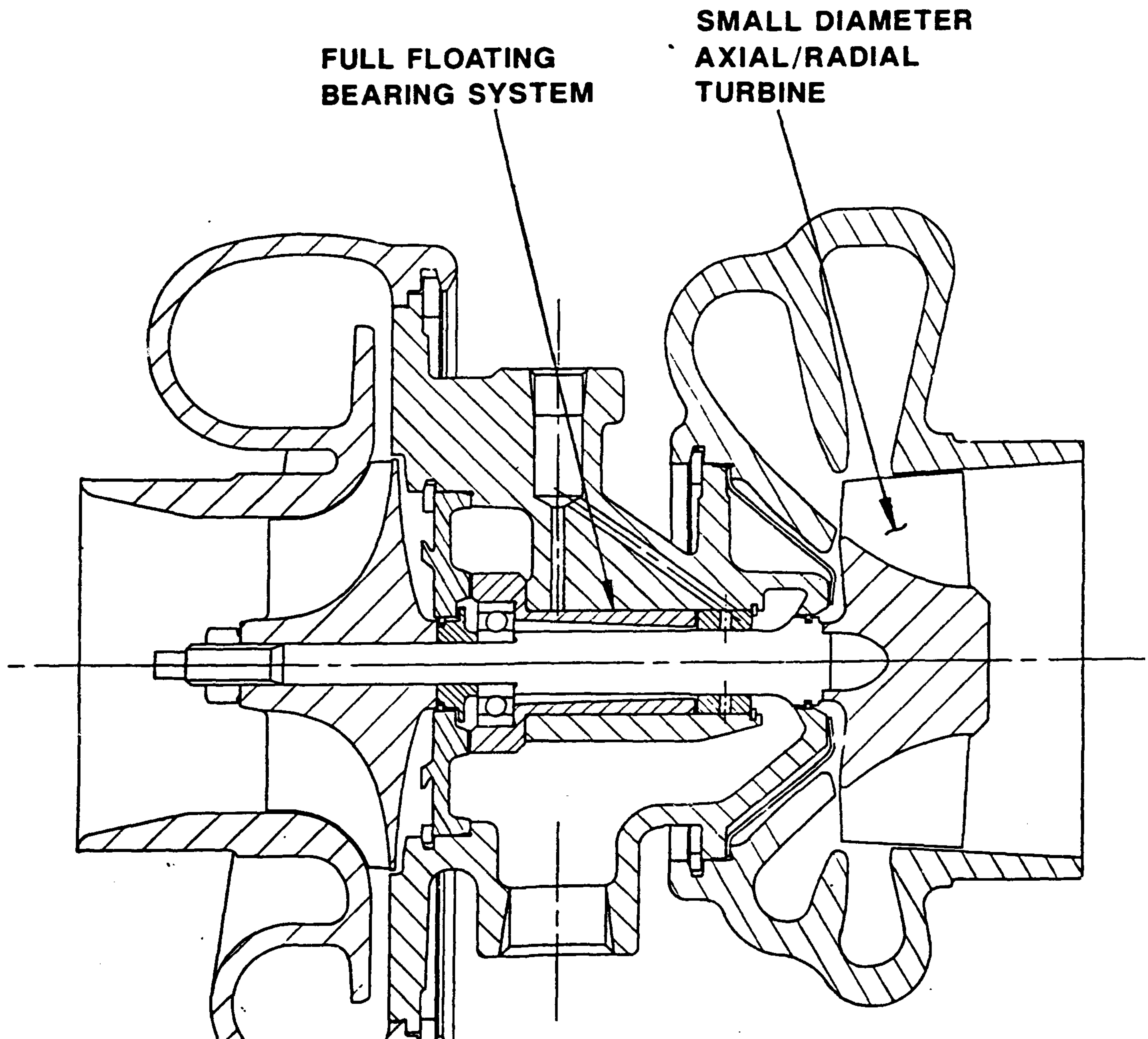

FIG. 3

60571

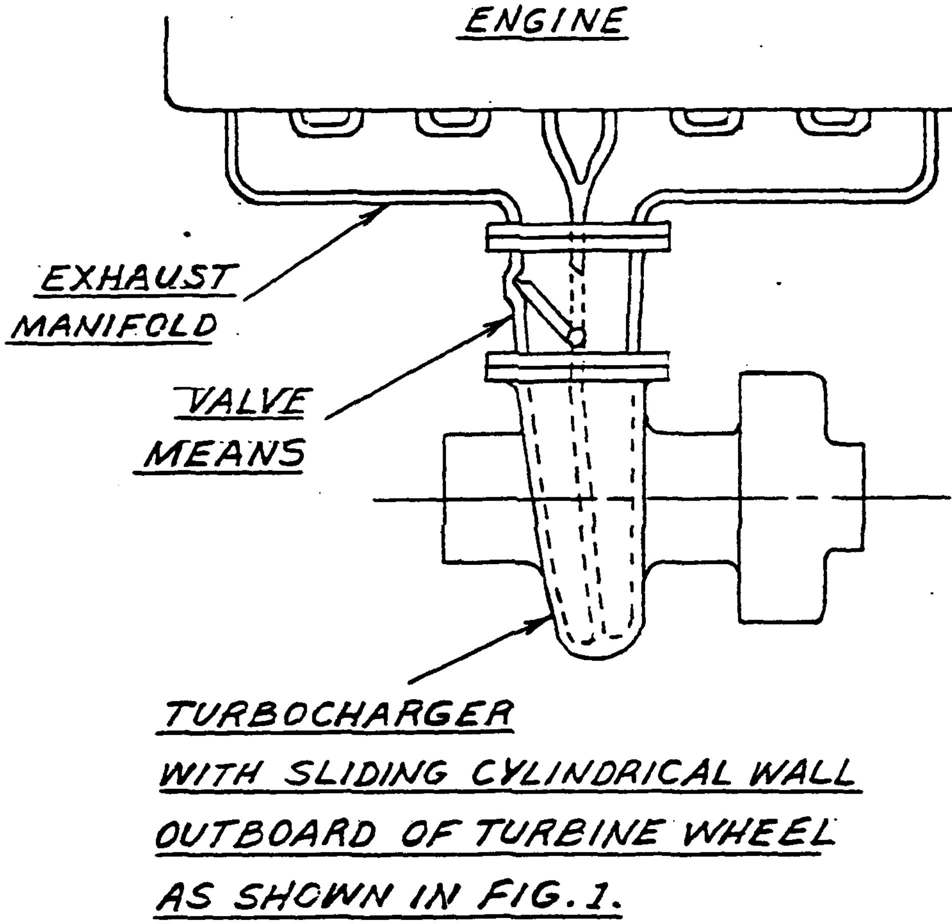

FIG. 2

3-2-87
W. E. W.

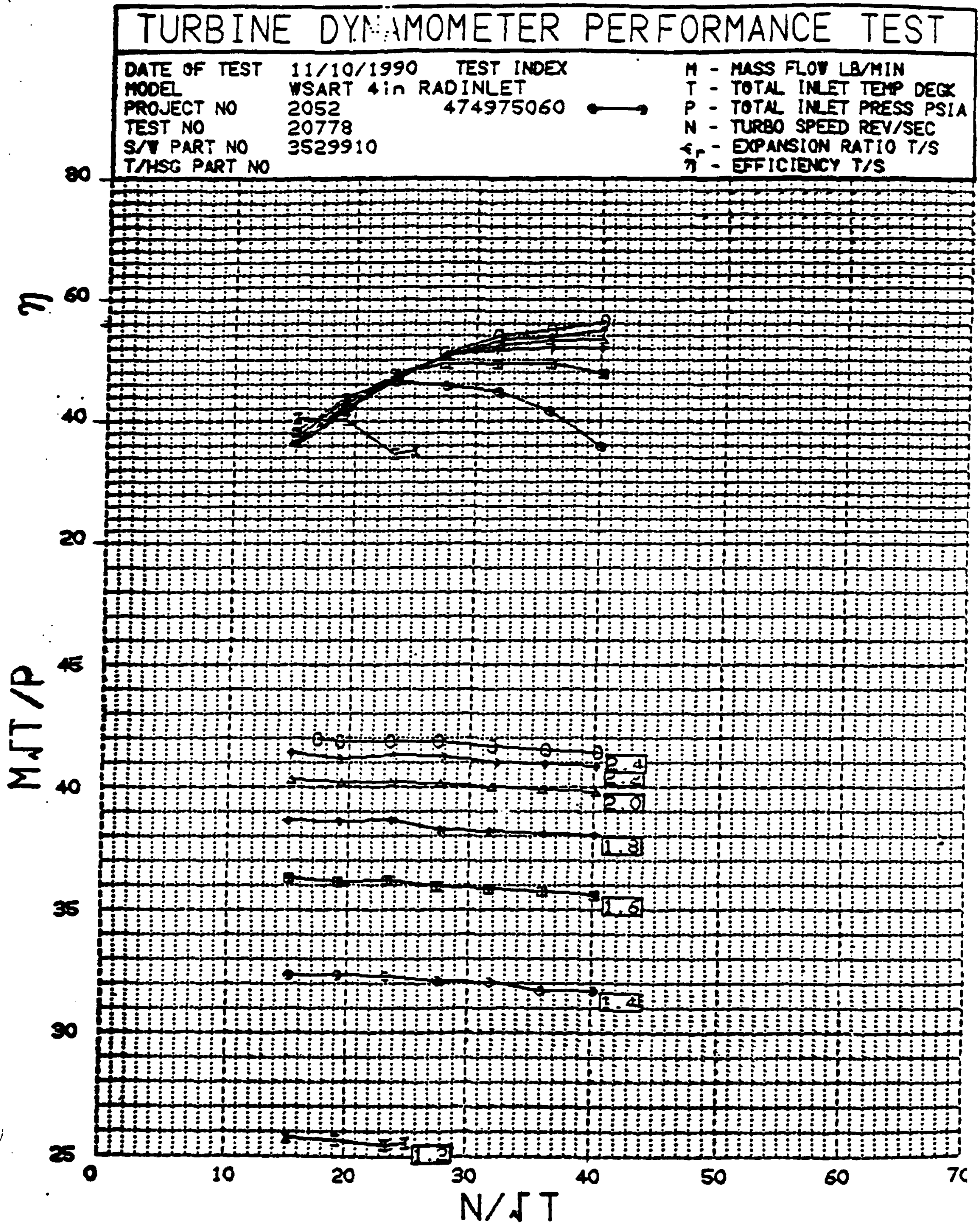
TURBINE DYNAMOMETER PERFORMANCE TEST
DATE OF TEST 11/10/1990 TEST INDEX
MODEL WSART 4in RADINLET
PROJECT NO 2052 474975060
TEST NO 20778
S/W PART NO 3529910
T/HSG PART NO
M - MASS FLOW LB/MIN
T - TOTAL INLET TEMP DEGK
P - TOTAL INLET PRESS PSIA
N - TURBO SPEED REV/SEC
ϵ_r - EXPANSION RATIO T/S
η - EFFICIENCY T/S
η
80
60
40
20
45
40
35
30
25
$M\sqrt{T}/P$
2.4
2.2
2.0
1.8
1.6
1.4
1.2
0
10
20
30
40
50
60
70
$N/\sqrt{T}$

FIG. 4

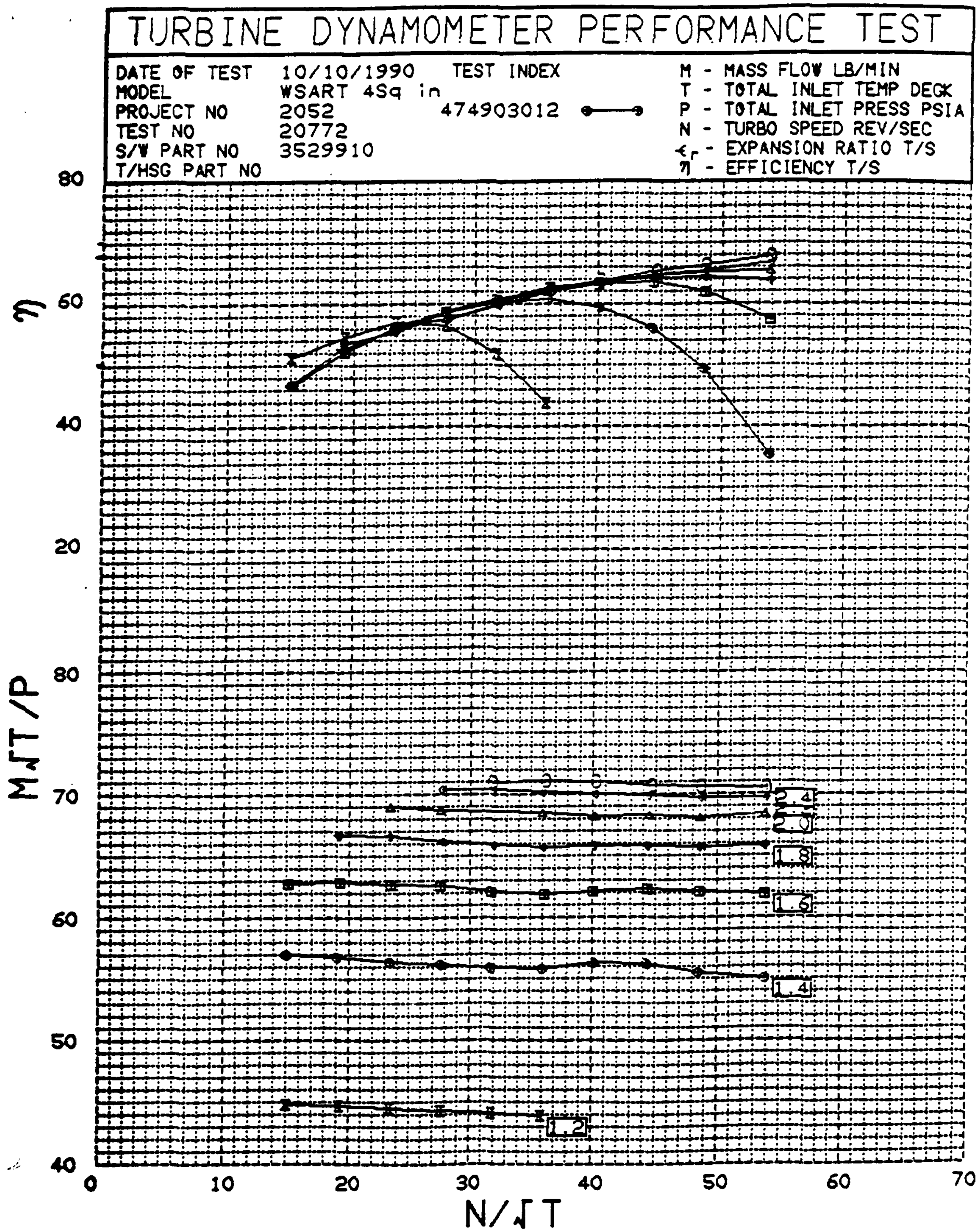

TURBINE DYNAMOMETER PERFORMANCE TEST
DATE OF TEST 10/10/1990
TEST INDEX
MODEL WSART 4Sq in
PROJECT NO 2052
474903012
TEST NO 20772
S/W PART NO 3529910
T/HSG PART NO
M - MASS FLOW LB/MIN
T - TOTAL INLET TEMP DEGK
P - TOTAL INLET PRESS PSIA
N - TURBO SPEED REV/SEC
ϵ_r - EXPANSION RATIO T/S
η - EFFICIENCY T/S
η
M√T/P
N/√T
2.4
2.0
1.8
1.6
1.4
1.2
80
60
40
20
80
70
60
50
40
0
10
20
30
40
50
60
70

FIG. 5

ACCELERATION COMPARISON
WS-90 vs BHT-3B

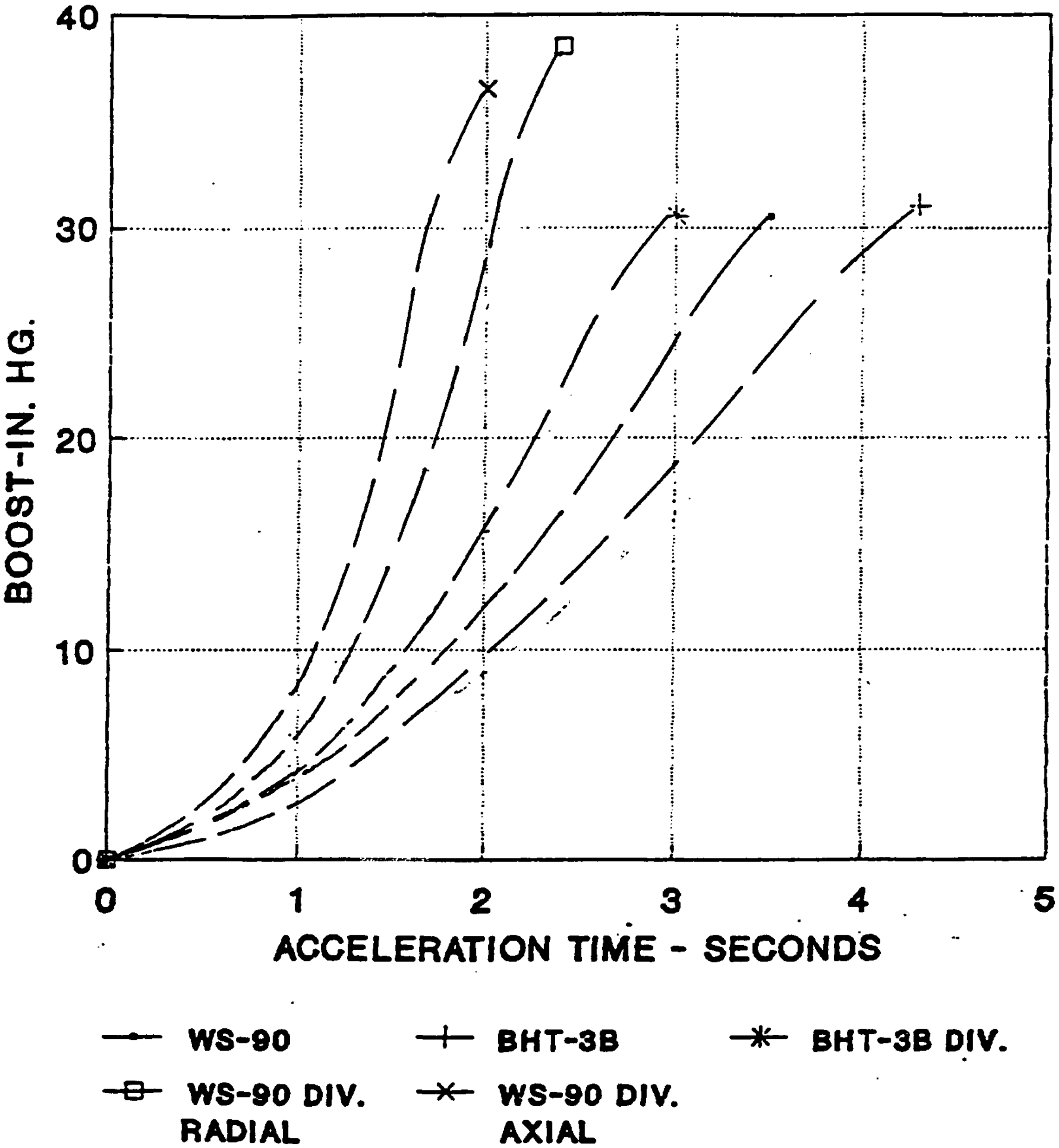

ACC 12/07/90

FIG. 6

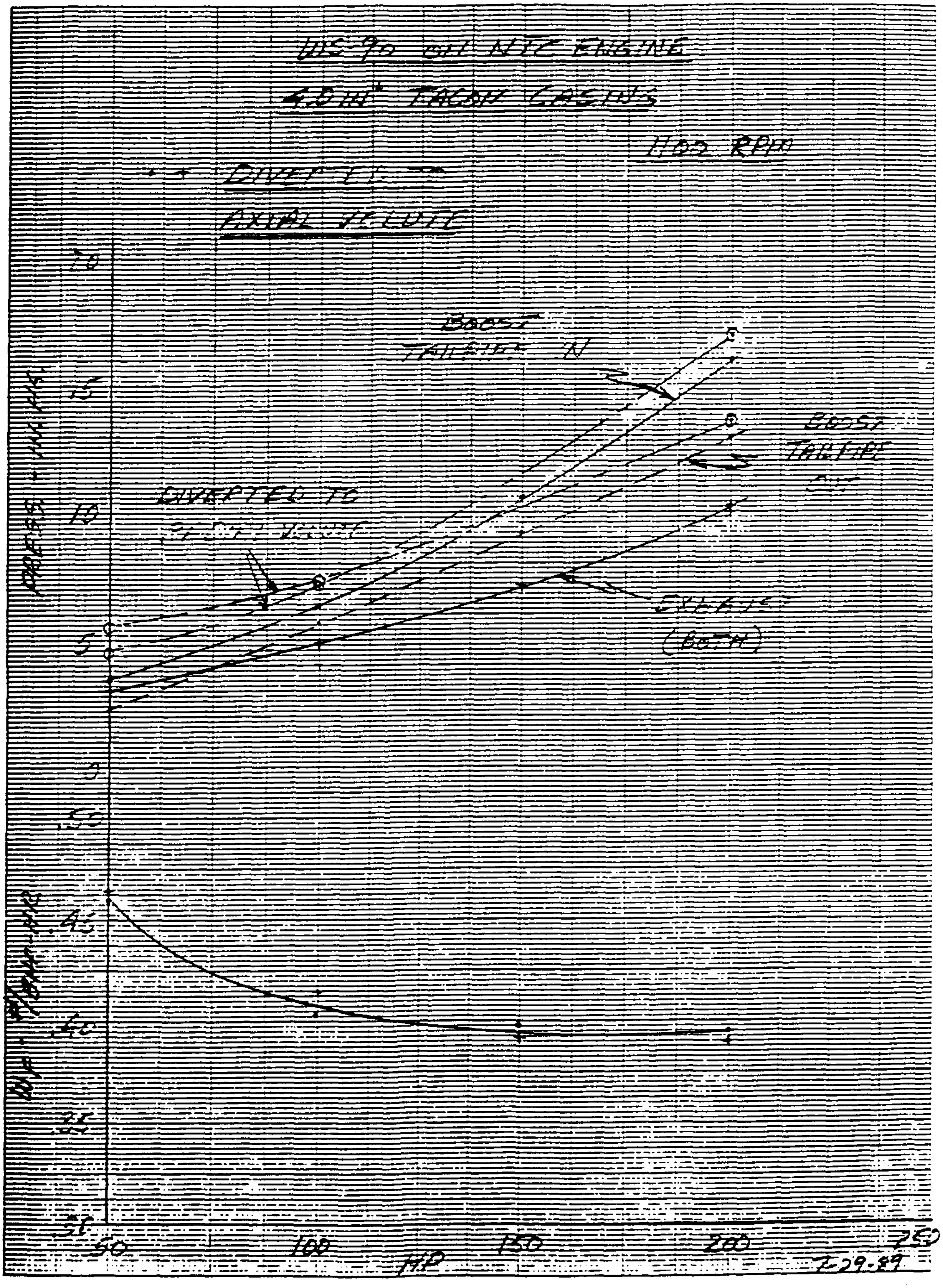
WS-90 OIL NTC ENGINE
4.5 IN² TACOM CASING
1100 RPM
DIVERTED
AXIAL VOLUTE
BOOST
BOOST
DIVERTED TO
(BOTH)
20
15
10
5
0
.55
.45
.40
.35
.30
50
100
150
200
250
HP
7-29-89

FIG. 7 C-7

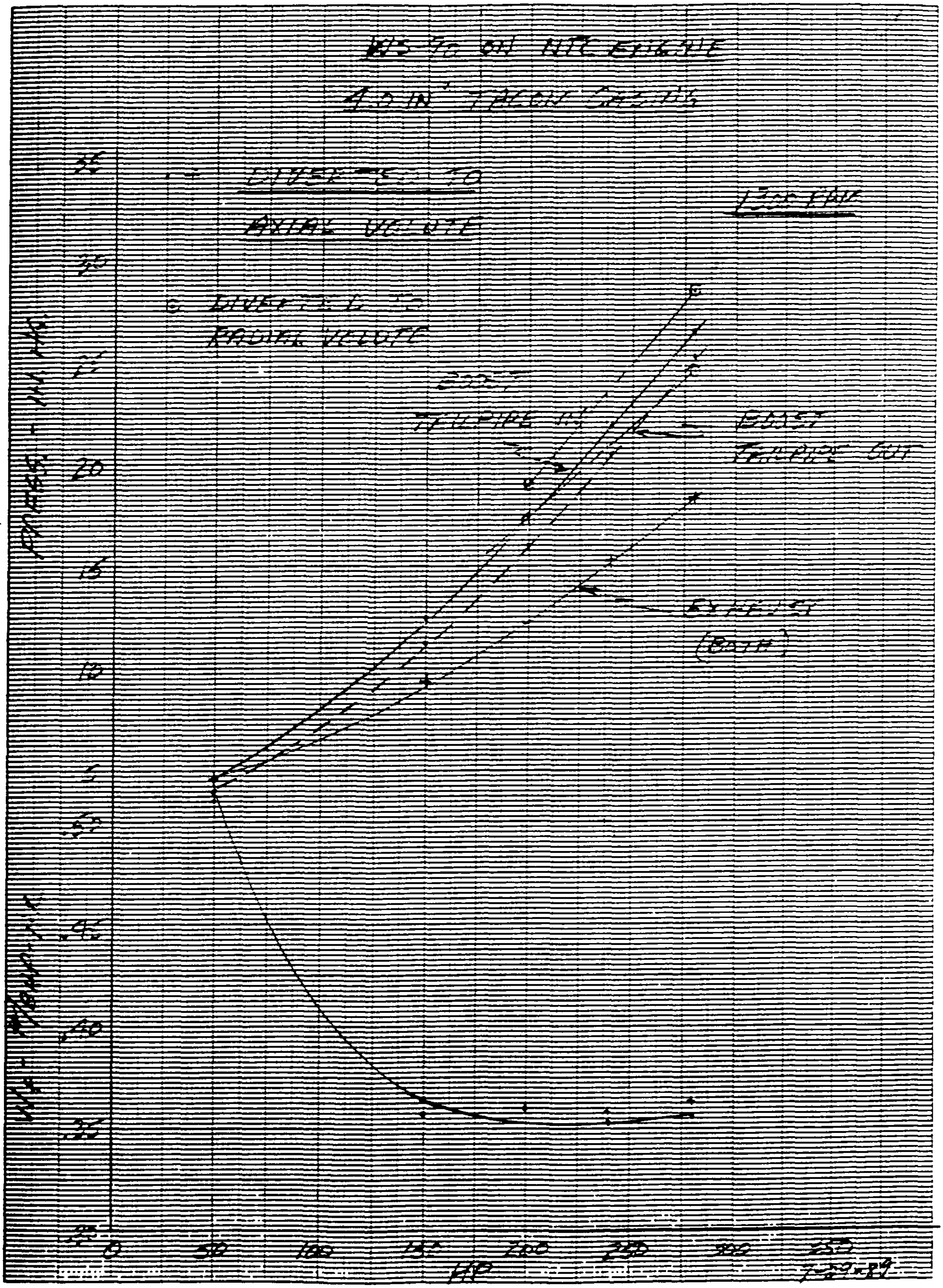

FIG 8 C-8

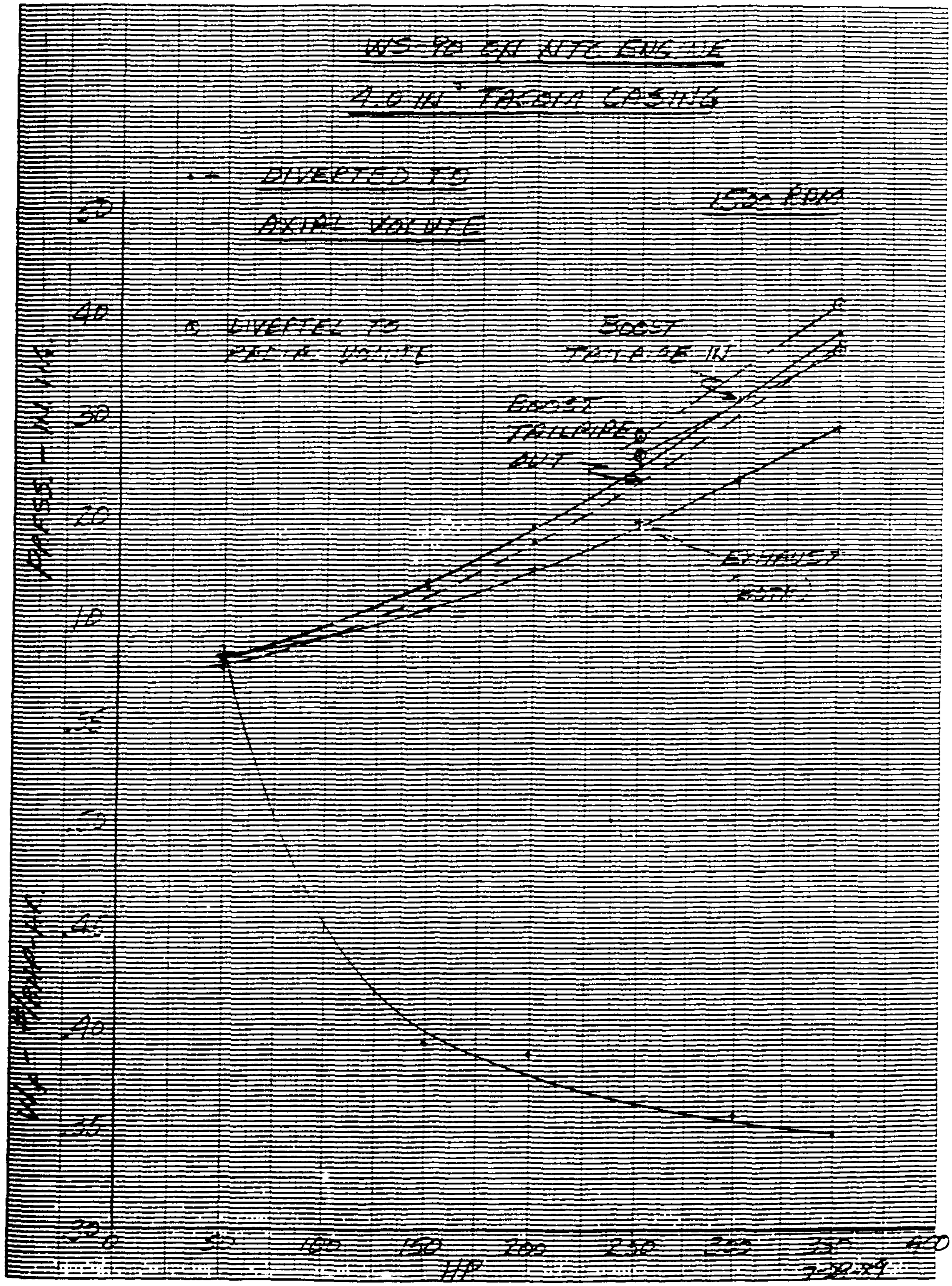

K+E 10 X 10 TO THE CENTIMETER 18 X 25 CM.
KEUFFEL & ESSER CO. MADE IN U.S.A.
46 1510

FIG. 9

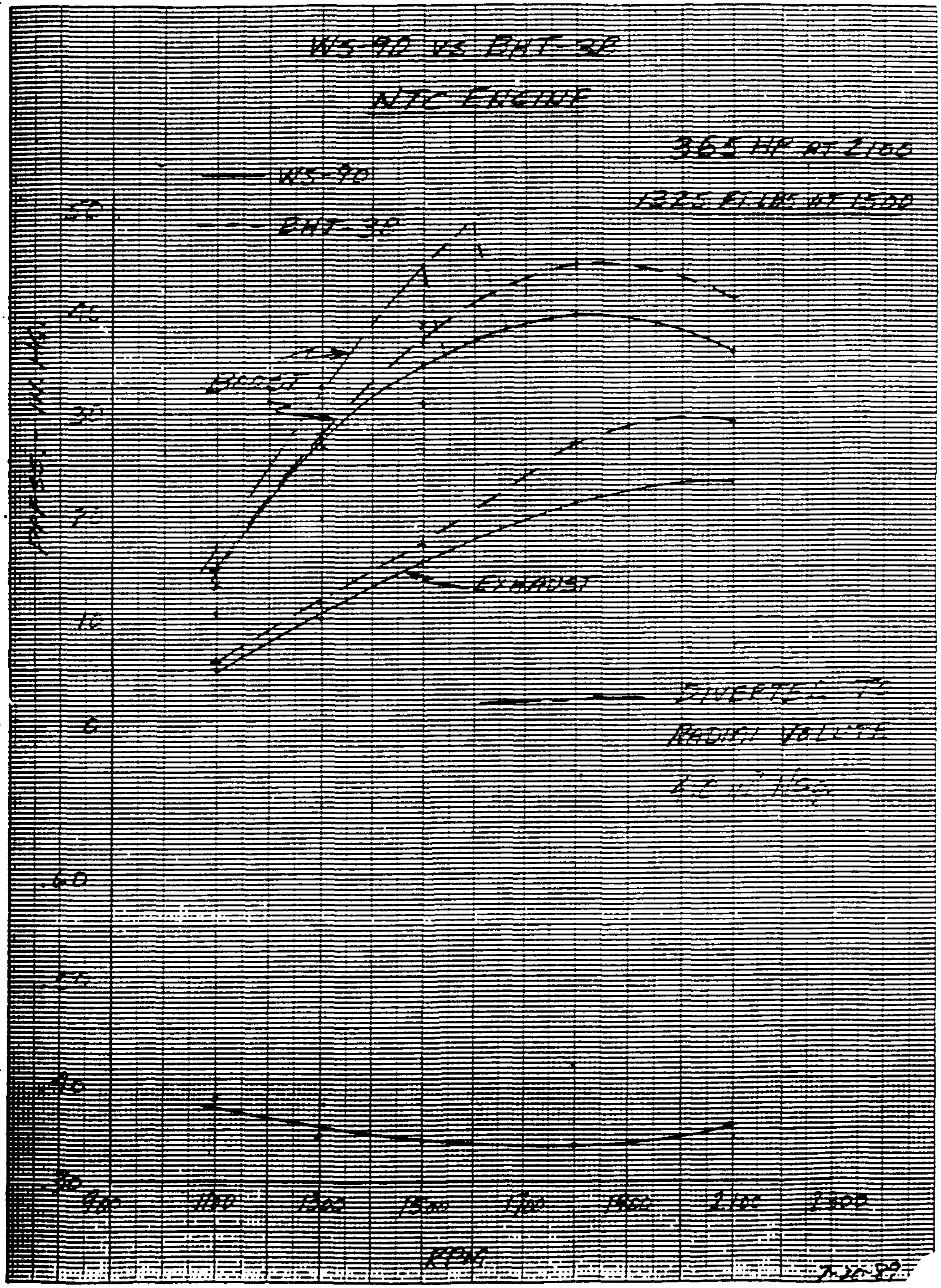
WS-90 vs BHT-32
NTC ENGINE
365 HP AT 2100
WS-90
BHT-32
BOOST
EXHAUST
900
1100
1300
1500
1700
1900
2100
2300
RPM

FIG. 10 C-10

Bibliography

1. N.J. Beck, Et Al, High Pressure Fuel Injection - A Rational Approach to Diesel Engine Efficiency, Emissions, and Economics. SAE paper 830863.

2. D.L. Abata, B.J. Stroia, N.J. Beck, A.R. Roach, Diesel Engine Flame Photographs With High Pressure Injection. SAE paper 880298.

3. W.E. Weseloh, EEC IV Full Authority Diesel Fuel Injection Control. SAE paper 861098.

4. N.J. Beck, Et Al, Direct Digital Control of Electronic Unit Injectors. SAE paper 840273.

5. N.J. Beck, O.A. Uyehara, Factors That Affect BSFC and Emissions for Diesel Engines - Part I. SAE paper 870343.

6. N.J. Beck, O.A. Uyehara, Factors That Affect BSFC and Emissions for Diesel Engines - Part II. SAE paper 870344.

Glossary

ACT	Air Charge Temperature
BHP	Brake Horsepower
BSFC	Brake Specific Fuel Consumption
ECU	Electronic Control Unit
EEC-IV	Electronic Engine Controller (Ford Motor Co.)
EPR	Electronic Pressure Regulator
ET	Energize Time
GWC	Golden West College
HSV	High-Speed Solenoid Valve
IBM-PC	International Business Machines - Personal Computer
MAP	Manifold Air Pressure
PHSV	Proportional High-Speed Solenoid Valve
PIP	Position Input Pulse (Crankshaft position)
RPM	Revolutions per Minute
RPX	Rail Pressure Transducer
SPI	Servojet Products International
TCS	Turbocompound Cooling System
MTU	Michigan Technological University (Houghton, MI)